



UNIVERSITY OF LEEDS

Efficient and robust estimation of non-classical effects in quantum devices

Matthew James Girling

Submitted in accordance with the requirements for the degree of
Doctor of Philosophy

The University of Leeds
School of Physics and Astronomy

October, 2023

Intellectual Property Statement

The candidate confirms that the work submitted is his own, except where work which has formed part of jointly authored publications has been included. The contribution of the candidate and the other authors to this work has been explicitly indicated below. The candidate confirms that appropriate credit has been given within the thesis where reference has been made to the work of others.

Chapters 3 and 4 are based on:

M. Girling, C. Cîrstoiu, and D. Jennings. “Estimation of correlations and nonseparability in quantum channels via unitarity benchmarking”. *Physical Review Research*, 4(2), 023041 (2022).

Chapters 2 and 5 are based on:

M. Girling, C. Cîrstoiu, and D. Jennings. “A simple formulation of no-cloning and no-hiding that admits efficient and robust verification”. *arXiv preprint*, arXiv:2303.02662 (2023).

For both these papers the bulk of the research was undertaken by me with advice and guidance from David and Cristina. Both of my co-authors gave input on the analytical results, while any numerical calculations or computer simulations were completed solely by myself. The manuscripts for both papers above were written by me and then edited jointly.

This copy has been supplied on the understanding that it is copyright material and that no quotation from the thesis may be published without proper acknowledgement.

The right of Matthew James Girling to be identified as Author of this work has been asserted by him in accordance with the Copyright, Designs and Patents Act 1988.

Acknowledgements

First and foremost, I would like to thank my supervisor, David Jennings, for his constant support throughout the last years. He has taught me how to think about research, how to do research, and how to present research. Throughout, he has helped guide my work always with detailed and thoughtful feedback. I am grateful for his advice on all aspects of the PhD, especially during the disruptions associated with the pandemic. The mantra of the simplest non-trivial example are indeed words to live by.

I am also very grateful to have collaborated with Cristina Cîrstoiu on the two papers which form the majority of this thesis. It was a pleasure to work with her and she has given brilliant advice and assistance with thorny mathematical problems. She has also helped me to develop as researcher, such as by teaching me how to restructure results into a narrative.

I want to thank Roger Colbeck for useful discussions on perfect hiding in quantum theory and Robin Harper for helpfully explaining some practicalities when benchmarking quantum devices. Both Matty Hoban and Daniel Mills gave productive feedback on an early draft of my second paper.

On a personal level, I first thank my fellow amateur dendrologists Si and Rhea. I am very grateful to have met them. The two Toms, who have been with me all the way, thank you. I owe a debt to Sarah for keeping me sane throughout and reminding me that any situation can be improved with the addition of humour.

Finally and above all, I thank my mum, dad and sister for their love and support.

Abstract

The ability to transfer quantum information between systems is a fundamental component of quantum technologies, and can generate correlations. However correlations in quantum channels are less well studied than those in quantum states. Motivated by recent techniques in randomized benchmarking (RB), we develop a range of results for efficient estimation of correlations in channels. We extend the notion of unitarity - an average figure of merit that captures the coherence of a quantum channel - to substructures within a bipartite quantum channel. We define a correlation unitarity and prove that it provides a witness of nonseparability - a strictly non-classical effect. We find that this measure can be estimated with robustness to errors in state preparation and measurements (SPAM) for any separable or Pauli quantum channel, and we show that a benchmarking/tomography protocol with mid-circuit resets can reliably witness nonseparability for sufficiently small reset errors. Related experimental techniques, that we develop, can be used to study quantum incompatibility. Incompatibility is a feature of quantum theory that sets it apart from classical theory, and the inability to clone an unknown quantum state is one of the most fundamental instances. We extend the definition of unitarity to general physical theories. Then, we introduce the notion of compatible unitarity pair (CUP) sets, that correspond to the allowed values of unitarities for compatible channels in the theory. We show that a CUP-set constitutes a simple ‘fingerprint’ of a physical theory, and that incompatibility can be studied through them. We analytically prove quantum CUP-sets encode both the no-cloning/broadcasting and no-hiding theorems of quantum theory. We then develop RB protocols that efficiently estimate quantum CUP-sets and provide simulations using IBMQ of the simplest instance. Finally, we discuss ways in which the above methods provide independent benchmarking information and test the limits of quantum theory on devices.

This thesis is dedicated to the memory of Zubair Majeed.

Contents

Intellectual Property Statement	i
Acknowledgements	iii
Abstract	v
Contents	ix
List of Figures	xiii
List of Tables	xvii
List of Protocols	xix
1 Introduction	1
1.1 Quantum theory and quantum devices	1
1.2 Mathematical preliminaries	4
1.2.1 Systems, states and quantum channels	4
1.2.2 Benchmarking of quantum channels	7
1.2.3 Unitarity of quantum channels	9
1.3 Overview of thesis	11
1.3.1 Quantum incompatibility	11
1.3.2 Overview of Chapters 2 and 5	12
1.3.3 Quantifying coherent correlations	15
1.3.4 Overview of Chapters 3 and 4	16
2 A simple formulation of the no-cloning and no-hiding theorems	19
2.1 CUP-sets and incompatibility	20
2.1.1 Unitarity of a channel	20
2.1.2 Defining cloning and hiding	22
2.1.3 Compatible unitarity pairs of a theory	23
2.1.4 No-cloning and no-hiding through the CUP-set	25
2.2 Classical CUP-sets	26
2.2.1 Unitarity of classical channels	26
2.2.2 Cloning and hiding in classical theory	26
2.2.3 The simplest classical CUP-set	27
2.2.4 Reversible classical CUP-set	27
2.2.5 Full classical CUP-set	28

2.3	Quantum CUP-sets	29
2.3.1	Incompatibility and hiding via trade-off relations on CUP-sets	29
2.3.2	The simplest quantum CUP-set	32
2.3.3	Reversible quantum CUP-set	33
2.3.4	Upper bound for reversible CUP-sets	34
2.3.5	Full quantum CUP-set	37
2.4	Generalized incompatibility and reversibility	37
2.4.1	Unitarity of GPT channels	37
2.4.2	Channel compatibility in general theories	38
2.4.3	Properties of unitarity for GPT channels	39
2.4.4	Proofs for purity in classical and quantum theory	41
2.5	Conclusions	42
2.5.1	The long arm of purity	42
2.5.2	Overview	43
3	Quantifying local and correlated coherence in quantum channels	45
3.1	Operational subunitarities of quantum channels	45
3.1.1	Elementary subunitarities of a channel	46
3.1.2	Subunitarity formulation of information-disturbance	48
3.1.3	The Liouville representation of quantum channels	50
3.1.4	Unitarity in the Liouville representation	52
3.2	Generalized subunitarities of bipartite quantum channels	53
3.2.1	Liouville decomposition of bipartite quantum channels	53
3.2.2	General subunitarities with the Liouville representation	54
3.2.3	The subunitarities of product channels	56
3.3	Correlation unitarity of bipartite quantum channels	57
3.3.1	Witness of non-separability	60
3.3.2	Properties of correlation and sub-unitarity for Pauli channels	69
3.3.3	Further interpretations of the correlation unitarity	72
3.4	Conclusions	73
4	Estimation of coherent correlations and non-separability via benchmarking protocols	75
4.1	Randomized Benchmarking Protocols	76
4.2	Unitary 2-designs & Unitarity Benchmarking Protocols	77
4.3	Bipartite channel subunitarities via local twirls	83
4.3.1	Local twirls of a bipartite system	83
4.3.2	The matrix of subunitarities for local twirls	84
4.3.3	The matrix components for separable channels	87
4.3.4	Jordan decomposition for arbitrary bipartite channels	88
4.3.5	Analysis of a local twirl unitarity benchmarking protocol	90
4.4	SPAM robust estimation of subunitarities for device noise	93
4.4.1	Estimation of subunitarities through local & global protocols	94
4.4.2	Black box noise estimation with randomized compiling	97
4.5	Estimation of local subunitarities with resetting errors	97
4.5.1	Estimation while utilizing the maximally mixed state	98
4.5.2	Estimation while utilizing computational basis states	101

4.5.3	Benchmarking non-local subunitarities directly	103
4.6	Conclusions	103
4.6.1	Comparison with addressability of qubits	103
4.6.2	Overview	105
5	Efficient and robust verification of quantum no-go theorems	107
5.1	Initial considerations	108
5.1.1	Decomposition with device gatesets	108
5.1.2	Effects of noise	109
5.2	Direct CUP-set estimation through state purity measurements	110
5.2.1	Estimation through complementarity formulation	110
5.2.2	Estimation through Choi state formulation	111
5.2.3	Preparation of the maximally mixed state and experimental results	112
5.2.4	Discussion of direct methods	113
5.3	SPAM robust CUP-set estimation through RB	114
5.3.1	Estimation through randomized benchmarking	114
5.3.2	Interleaved unitarity protocol for $(\mathcal{E}, \bar{\mathcal{E}})$ without noise	116
5.3.3	Interleaved unitarity protocol for $(\mathcal{E}, \bar{\mathcal{E}})$ with noise	117
5.3.4	Efficient implementation of protocols	119
5.3.5	Discussion of SPAM robust methods	119
5.3.6	Comparison with direct methods	120
5.4	Estimation through spectral methods	121
5.4.1	Unitarity and channel eigenvalues	121
5.4.2	Estimation of CUP-set through spectral tomography	123
5.5	Conclusions	124
6	Concluding remarks	127
6.1	Summary of results	128
6.2	Outlook	129
A	Material related to CUP-sets	131
A.1	Convexity of unitarity	131
A.2	Analytical form for quantum CUP-set surfaces	132
A.2.1	Upper surface ($SWAP^\alpha$)	132
A.2.2	Lower right surface ($CNOT_{AB}^\alpha$)	134
A.2.3	Lower left surface ($CNOT_{BA}^\alpha \circ CNOT_{AB}$)	135
A.3	Compatible fidelity pairs	136
A.4	Interpretation of unitarity and reversibility	138
B	Material related to subunitarities and correlation unitarity	141
B.1	Review of notation	141
B.2	General definition of separability	142
B.3	Properties of the subunitarities of product channels	142
B.4	Properties of the subunitarities of separable channels	143
B.5	Comparison of correlation unitarity with norm measures	144
B.6	Expression for correlation unitarity using an operational function	145
	Bibliography	147

List of Figures

1.1	Interplay between the key concepts of this thesis. Three areas within quantum technologies research are shown. Each arrow represents a line of inquiry towards a goal or a research question that could be asked. For example, (e) could be “How do structural features of quantum theory limit the performance of quantum devices?”. Some of these arrows have been better studied than others. One direction that has been less well studied is (b), which is the primary focus of this work. By connecting benchmarking tools to fundamental features of quantum theory, we obtain results that apply to the rest of the diagram including (d), (e), and (f).	2
1.2	Robust and efficient verification of quantum incompatibility. In classical theory we have the ability to perfectly clone and perfectly hide classical information. In contrast, quantum theory has fundamental incompatibility that prohibits the same behaviour. This is captured by defining CUP-sets, and shown here is the estimation of the simplest quantum CUP-set \mathcal{C} . The reversible CUP-set for classical theory corresponds to the full boundary of the unit square $[0, 1]^2$, and allows perfect cloning (the point $(1, 1)$) and perfect hiding (the point $(0, 0)$). Using benchmarking techniques we estimate \mathcal{C} , shown here, on an IBM Q device and find that it saturates the general quantum bounds we derive in Theorem 2.1. Verifying such fundamental bounds provides a means to test the performance of emerging quantum computers.	14
2.1	Quantum CUP-sets. The simplest isometric and reversible CUP-sets under quantum theory, with their analytical bounds ($d_X = d_A = d_B = 2$). The isometric CUP-set \mathcal{C} generated by global isometries is the central boomerang-shaped region (blue). Extending this to reversible operations \mathcal{C}_r increases the set in the direction of $(0, 0)$ to the boundary with the Hiding Zone (yellow). The two diagonal red lines are obtained from the general analytic upper and lower bounds for CUP-sets in quantum theory. In contrast, for classical theory we have that \mathcal{C}_r is the border of the unit square, while \mathcal{C} is the triple of points $(1, 1), (1, 0), (0, 1)$	33
2.2	Circuit decomposition for generic 2 qubit isometry $\mathcal{V}(\alpha, \beta, \gamma)$. For $d_X = d_A = d_B = 2$, all isometries can be expressed in the above form, where $0 \leq \alpha, \beta, \gamma \leq \pi$ [1]. The complementary channels $\mathcal{E} = \text{tr}_B \circ \mathcal{V}$ & $\bar{\mathcal{E}} = \text{tr}_A \circ \mathcal{V}$ are shown, by ranging over α, β, γ we can generate the isometric CUP-set \mathcal{C} for 1 to 2 qubits.	34

2.3 **Sufficient circuit decomposition for 2 qubit isometry $\mathcal{V}(\alpha, \beta)$.** For $d_X = d_A = d_B = 2$, the above isometry is sufficient to generate all points (u, \bar{u}) of the isometric CUP-set \mathcal{C} for 1 to 2 qubits with $0 \leq \alpha, \beta \leq \pi$. This follows from the general decomposition given in Figure 2.2, observing that the initial two gates do not change the state of the system, and the invariance of unitarity under local unitaries. 34

3.1 **Distribution of u_c for 2-qubit unitaries.** We plot the histogram of values of $u_c(\mathcal{U}_{\text{sim}})$ for 20,000 random 2 qubit unitaries, \mathcal{U}_{sim} . The correlation unitarities lie between 0 and 1, and must take the value $u_c(\mathcal{E}_A \otimes \mathcal{E}_B) = 0$ for product channels, and $u_c(\text{SWAP}) = 1$ for the *SWAP* channel. The value of u_c is invariant under local unitary changes of basis. The upper bound for 2 qubit separable channels is $u_c^{\text{sep}} \leq 7/12$, and is also shown on the plot. We sampled using the methods of [2] and simulated using QuTip [3]. 58

4.1 **SPAM error robust estimation of u_c for generic quantum channels.** The convergence of the values of correlation unitarity and C as gate noise takes a product form, for a 2 qubit simulation. We show $|u_c - C|$ over p , where $\mathcal{F} = p\mathcal{E}_A \otimes \mathcal{E}_B + (1 - p)\mathcal{G}$. The channels $\mathcal{E}_A, \mathcal{E}_B$ and \mathcal{G} are sampled using the methods of [2] and simulated using QuTip [3]. 96

4.2 **Subunitarity estimation with reset error.** Shown is a simulation of Protocol 2 to estimate the subunitarity $u_A \equiv u_{A \rightarrow A}(\mathcal{E}_{AB})$, modelling the reset error associated B as in equation (4.75). This reset error is shown for different levels of depolarization p , including $p = 0$ i.e. no reset. The channel \mathcal{E}_{AB} in this case has a theoretical value of $u_{A \rightarrow A}(\mathcal{E}_{AB}) = 0.261$. The protocol returns an estimate of the subunitarity accurate to $\sim 90\%$ for reset errors up to $\sim 20\%$ 99

4.3 **Witnessing channel non-separability.** Given a quantum channel \mathcal{E}_{AB} we consider the ability to efficiently witness its non-separability via correlation unitarity in the presence of resetting noise. This could be realized, for example, in the context of robust tomography using randomized benchmarking [4]. We consider a 1-parameter family of 2-qubit channels obtained from a convex combination of the maximally non-separable *SWAP* channel and the identity channel (a product channel). The contour plot compares the true value of correlation unitarity $u_c(\mathcal{E}_{AB})$ with the correlation measure $C_{\text{sim}} \approx C$ estimating equation (4.68) in the presence of reset errors. For two qubits, non-separability occurs if $u_c(\mathcal{E}_{AB}) > 7/12$. We simulate both Protocol 1 and 2, and we find that for a wide range of reset errors we may witness non-separability for $p, q \gtrsim 0.5$. The region of green where $p, q \geq 1/2$ is an artifact of our particular method, and with a more refined algorithm we expect detection of non-separability also in this region. 100

4.4	Correlation unitarity vs. addressability. Correlation unitarity is largely independent from existing addressability measures, while Kraus rank is a better indicator of the the value of u_c , which is consistent with it capturing the non-separable correlations between subsystems. This suggests the measure might be suitable for benchmarking 2-qubit gates where the unitary transfer of quantum information between subsystems is required. The above plot is for random channels of different ranks from the distributions of Bruzda <i>et al.</i> and simulated using QuTip [2, 3].	104
5.1	Circuit decomposition in IBM gateset for lower right isometric CUP-set surface. Circuit for 2 qubit isometry $CNOT_{AB}^\alpha(\rho \otimes 0\rangle\langle 0)$, and complementary channels \mathcal{E} & $\bar{\mathcal{E}}$ for the lower right surface of the CUP-set are shown. The final R_Z rotation is optional but aids in the estimation of CUPs through spectral techniques.	108
5.2	Circuit decomposition in IBM gateset for lower left isometric CUP-set surface. Circuit for 2 qubit isometry $CNOT_{BA}^\alpha \circ CNOT_{AB}(\rho \otimes 0\rangle\langle 0)$, and complementary channels \mathcal{E} & $\bar{\mathcal{E}}$ for the lower left surface of the CUP-set are shown.	109
5.3	CUP-set deformation through depolarization. The simplest quantum CUP-set \mathcal{C} is shown when one output is depolarized, $(u(\mathcal{D}_p \circ \mathcal{E}), u(\bar{\mathcal{E}}))$ for different values of p	110
5.4	Unitarity estimation with state purities. Circuits for estimation of unitarity $u(\mathcal{E})$ of single qubit channel \mathcal{E} through SWAP test and state purity relations.	111
5.5	Direct estimation of quantum CUP-sets. The two simplest quantum CUP-sets are experimentally estimated directly through SWAP test schemes. A best fit depolarising noise model has been applied to each surface (see Table 5.2).	113
5.6	SPAM robust estimation of quantum CUP-sets. The simplest quantum CUP-sets are experimentally estimated through an interleaved unitarity randomized benchmarking scheme. A best fit depolarising noise model has been fitted to each surface (see Table 5.2), where each surface is produced from 9 pairs of experimental values.	120
5.7	Bound on CUP-set through random unitaries. For two surfaces of the isometric CUP-set \mathcal{C} (for a range of 50 discrete values of $0 \leq \alpha \leq 1$) we can test how quickly the lower bound given in Lemma 5.1 converges towards the actual unitarity given in Theorem 5.1. Roughly, we observe, for bound within 1% of the unitarity we need 1 random setting if $u > 2/3$, and at most 100 random settings for lower values.	121
A.1	Compatible Fidelity Pairs. The simplest non-trivial set, \mathcal{C} , of compatible average gate fidelity pairs, $(f(\mathcal{E}), f(\bar{\mathcal{E}}))$, are shown. The bound given in equation (A.32) constrains the set to within the unit circle.	137

List of Tables

5.1	Operational overhead of CUP-set estimation. Comparison of total number of experiments undertaken for the estimation of a point on the CUP distribution. For each technique, an experimental scheme was run on a simulation of a quantum device, with device noise imported from IBM Q via qiskit.	125
5.2	Depolarization fits for noisy CUP-sets. For each experimental estimation of the quantum CUP-sets \mathcal{C} & \mathcal{C}_r we fit a depolarising noise model $(u_N, \bar{u}_N) = ((1 - p_A)^2 u, (1 - p_B)^2 \bar{u})$ to each surface (see Section 5.1.2). Best fit values for (p_A, p_B) are tabulated here.	126

List of Protocols

1	SPAM robust subunitarity estimation ($\mathcal{C} \times \mathcal{C}$)	90
2	SPAM effected subunitarity estimation ($\mathcal{C} \times 1$)	98
3	Interleaved unitarity RB for marginal channel $\mathcal{E}(\rho) := \text{tr}_B \circ \mathcal{U}_{AB}(\rho \otimes 0\rangle\langle 0)$	115
4	Efficient interleaved unitarity RB for single qubit channel \mathcal{E} , adapted from [5].	119

Abbreviations

Any abbreviations or acronyms used throughout this work are summarized in the following table.

CPTP	Completely Positive Trace-Preserving
CUP	Compatible Unitarity Pair
CUP-set	Set of Compatible Unitarity Pairs
LOCC	Local Operations and Classical Communication
GPT	Generalized Probability Theory
LOSR	Local Operations with Shared Randomness
NISQ	Noisy Intermediate Scale Quantum
POVM	Positive Operator-Valued Measure
RB	Randomized Benchmarking
SPAM	State Preparation And Measurement

Notation

Notational conventions used throughout this work are summarized in the following table.

X, Y, A, B, \dots	Systems or subsystems
\mathcal{H}_X	Hilbert space associated with quantum system X
$\mathcal{B}(\mathcal{H}_X)$	Bounded space of operators on \mathcal{H}_X
$\rho, \sigma, \omega, \dots$	Quantum states
$\psi, \varphi, \phi, \dots$	Pure quantum states
$ \text{vec}(\rho)\rangle, \boldsymbol{\rho}\rangle$	Vectorization of ρ
x, y, z, \dots	Classical states
$\{x_i\}$	Pure classical states
$\mathcal{E}, \mathcal{F}, \mathcal{G}, \dots$	Quantum or classical channels
\mathcal{V}	Isometric channel
\mathcal{R}	Reversible channel
\mathcal{D}	Depolarizing channel
$u(\mathcal{E})$	Unitarity of \mathcal{E}
\mathcal{U}	Unitary quantum channel
$\mathcal{J}(\mathcal{E})$	Choi-Jamiołkowski state for \mathcal{E}
$\mathcal{L}(\mathcal{E}), \boldsymbol{\mathcal{E}}$	Liouville representation of \mathcal{E}

Introduction

Everything is a quantum operation.

Irish folklore

Unknown

1.1 Quantum theory and quantum devices

Efficiently certifying and benchmarking non-classical features in quantum theory will be central to the development of quantum technologies [6–12], which require precise control and manipulation of quantum systems. High-fidelity quantum gates and circuits are essential for scalable quantum computing so it is important to benchmark the effects of physical noise on how accurately a target unitary is realized on the quantum device. For example, noise due to unwanted coherent correlations or leakage can detrimentally affect error rate thresholds required for fault tolerant quantum computing [13–15]. Therefore, the detection and quantification of non-classical effects not only impacts Noisy Intermediate Scale Quantum (NISQ) devices [16] leading to improved circuit fidelities and error mitigation, but also goes beyond our current era by providing necessary tools to test the physical assumptions of quantum error correction.

On a high level, in the above we are considering how quantum theory can be used to test quantum devices. However the opposite direction is also interesting. By quantifying and measuring non-classical effects on quantum devices we can test the limits of quantum theory using existing technology.

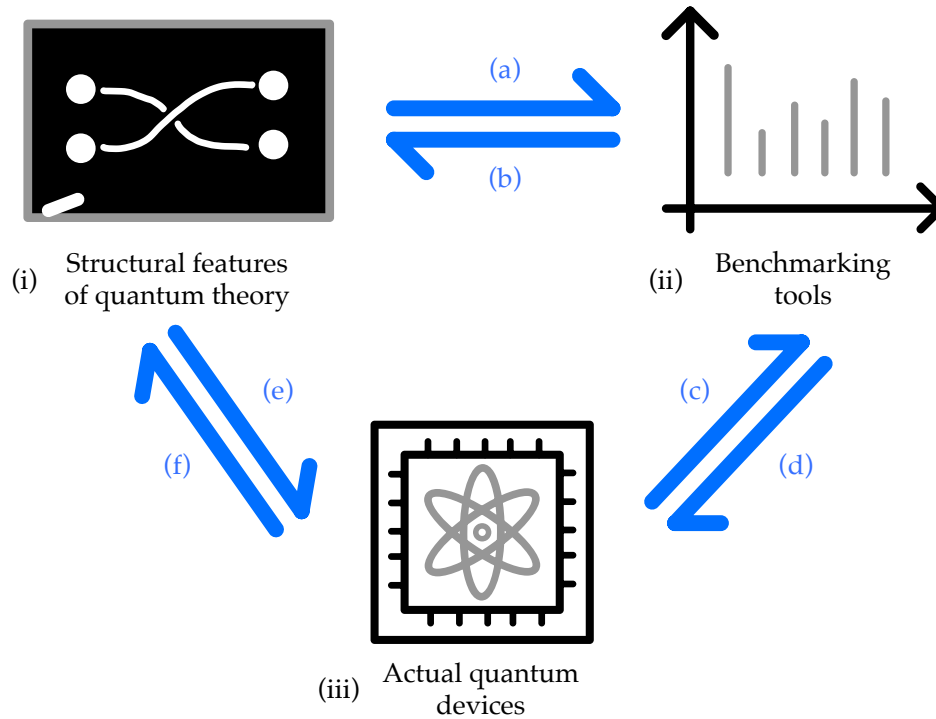


Figure 1.1: **Interplay between the key concepts of this thesis.** Three areas within quantum technologies research are shown. Each arrow represents a line of inquiry towards a goal or a research question that could be asked. For example, (e) could be “How do structural features of quantum theory limit the performance of quantum devices?”. Some of these arrows have been better studied than others. One direction that has been less well studied is (b), which is the primary focus of this work. By connecting benchmarking tools to fundamental features of quantum theory, we obtain results that apply to the rest of the diagram including (d), (e), and (f).

Quantum physics places much stronger limits on how we can transform information, compared to classical physics. These limits can be captured by the notion of incompatibility, that encapsulates fundamental impossibility results in quantum theory [17–20]. The most commonly encountered form of incompatibility refers to measurements – position and momentum cannot be simultaneously measured with the same precision – leading to formulations of no information without disturbance [21]. However, incompatibility can be described far more generally [22–24]. Two local processes on systems A and B are said to be compatible if there exists a *global* process that can produce both. The no-broadcasting theorem, an extension of the famous no-cloning theorem, can be cast as the incompatibility of local identity channels at A and B [20]. It is readily seen that if a physical theory admits perfect cloning, such as classical theory, then the theory cannot have any form of incompatibility.

Quantum technologies open new directions to experimentally test foundational aspects of quantum theory such as incompatibility [25–29]. However, current devices are inher-

ently noisy [16, 30–32]. Errors in State Preparation and Measurement (SPAM) can have an outsized effect on performance compared to errors in operations to evolve the system [33]. This presents a challenge in developing tests for foundational properties in a way that is robust to errors arising from the implementation of the experiment itself. Existing measures of quantum incompatibility typically assume full access to the processes involved and are therefore not SPAM robust [22]. Such foundational tests can also produce valuable benchmarks of errors [34], as they have clear operational significance rooted in fundamental properties of quantum mechanics.

Finally, we have a consideration of efficiency. Direct process tomography [35, 36] of a quantum process – that is, measuring all inputs and outputs – has a complexity that is known to scale exponentially with system size. Therefore to evaluate such processes we need average measures, that give less detail but that can be estimated efficiently in terms of system size. Within the area of device benchmarking, techniques have been developed such as gate-set tomography and randomized benchmarking (RB), which allow for efficient estimation of average measures [37]. Further, these measures are robust against initial and final SPAM errors.

Putting this together, in this work, our primary research question is as follows:

Can we use benchmarking tools to capture fundamental features of quantum theory?

This question is indicated by (b) in Figure 1.1. We undertake this question for the following three goals, which each are of interest independently and are indicated by (f), (d), and (e) in Figure 1.1, respectively.

General goals

- (1) To test the limits of quantum theory using current noisy quantum devices.
- (2) To gain independent information about the nature of device noise.
- (3) To provide efficient and robust certification of non-classical effects.

Within this thesis each chapter focuses on either mathematical results relating to quantum theory or on deriving experimental methods to apply these results to quantum devices. Therefore we setup a mathematical framework to tackle (1) within Chapter 2. However this framework requires a fairly complex experimental set-up, and so in Chapters 3 and 4 we focus on (2) and (3) which require simpler – but related – experimental methods. Having gained some experience and intuition we return to the experimental methods for (1) in Chapter 5.

We will shortly give a more precise version of each of these goals with the details of how we approach them. However, before we can give this overview, we must introduce some key

concepts used throughout this work.

1.2 Mathematical preliminaries

We now introduce some mathematical concepts used throughout this work, before we can give an overview of the technical content of each chapter. We assume the reader has some familiarity with quantum mechanical fundamentals including linear algebra, Dirac notation, and the quantum circuit model of quantum computation. For a complete introduction to the mathematical tools of quantum information science we suggest: Nielsen & Chuang's iconic textbook [32], the excellent book of John Watrous [38], and the lecture notes from John Preskill's course on Quantum Computation [39]. A critical reference for the author has been the lecture notes from David Jennings' course on Advanced Quantum Information [40].

1.2.1 Systems, states and quantum channels

Much of this work is framed around quantum devices where the smallest subsystems are qubits and we characterize the device as a multi-qubit open quantum system. However, except where explicitly stated, the results given here apply to any quantum system and do not require the particular tensor product structure of a multi-qubit system.

The following notation is consistently used throughout this work. Consider an open quantum system, X . We give it the dimension d_X , and we denote the associated Hilbert space \mathcal{H}_X . A valid quantum state, ρ , for this system is any $d_X \times d_X$ Hermitian matrix with non-negative eigenvalues, $\text{eigs}(\rho) \geq 0$, and normalized such that $\text{tr}[\rho] = 1$. We will use lower-case Greek letters for quantum states i.e. ρ, σ, τ .

With this definition, a pure quantum state is then any state we can write in the form $\rho = |\psi\rangle\langle\psi|$, where $|\psi\rangle$ is a vector of length one in the Hilbert space associated with the system. Pure states represent maximal knowledge of the state of the system. Mixed states can always be written as a probabilistic convex combination of pure states, $\rho = \sum_i^r p_i |\psi_i\rangle\langle\psi_i|$, for $\sum_i^r p_i = 1$ with $p_i \geq 0$. Therefore mixed states can be thought of as ambiguity in the state of the system. The degree to which a state is mixed is captured by its *purity*. This is an important concept in this work and defined in the following way.

Definition 1.1. For any quantum state, ρ , the **purity**, $\gamma(\rho)$, is defined as

$$\gamma(\rho) := \text{tr}[\rho^2]. \quad (1.1)$$

The purity has the following elementary properties that make it a useful measure of the noisiness of a quantum state.

Lemma 1.1 (Properties of purity). *Consider the purity, γ , of any quantum state ρ in a system with dimension d_X . We have the bounds $\frac{1}{d_X} \leq \gamma(\rho) \leq 1$ with $\gamma(\rho) = 1$ if and only if ρ is a pure state. The purity is lower bounded by $\gamma(\rho) = \frac{1}{d_X}$ for the maximally mixed state given by $\rho = \mathbb{1}/d_X$ where $\mathbb{1}$ is the $d_X \times d_X$ identity matrix.*

Proofs for these properties can be found in [38] and essentially follow from considering the decomposition $\rho = \sum_i^r p_i |\psi_i\rangle\langle\psi_i|$ for any quantum state. The maximally mixed state represents no knowledge as to the state of the system and gives the lower bound of the purity, while the upper bound is given for a pure state representing complete knowledge.

Summary

The purity, $\gamma(\rho)$, of a quantum state, ρ , is a measure of the level of knowledge we have about the state of the system. Therefore it quantifies how noisy the state is.

Key parts of our work can be framed as generalizing the concept of purity to describe more and more of the behaviour of quantum systems – and finally describe the limits of quantum theory itself.

For any quantum system we will also want to perform measurements. Any quantum measurement, M , with k outcomes on a d_X dimensional system can be described by a set of $d_X \times d_X$ matrices, $M = \{M_0, M_1, \dots, M_{k-1}\}$, with non-negative eigenvalues, $\text{eigs}(M_j) \geq 0$, and normalized such that $\sum_i^k M_i = \mathbb{1}$, where $\mathbb{1}$ is the $d_X \times d_X$ identity matrix. Further, given a quantum state, ρ , the probability of the j^{th} outcome of the measurement is $p(j) = \text{tr}[M_j \rho]$. Mathematically, the above conditions ensure quantum measurements are restricted to the set of Positive Operator-Valued Measures (POVMs).

Now we describe the behaviour of quantum systems, the main focus of this work.

Definition 1.2. *A quantum channel, \mathcal{E} , is any linear transformation $\rho \rightarrow \mathcal{E}(\rho)$ such that $\sigma = \mathcal{E}(\rho)$ is a valid quantum state for all possible states ρ of the input system.*

This definition is simple, but very powerful. Mathematically the definition above restricts quantum channels to Completely Positive Trace-Preserving (CPTP) maps. More formally, any quantum channel $\mathcal{E} : \mathcal{B}(\mathcal{H}_X) \rightarrow \mathcal{B}(\mathcal{H}_Y)$ will be a map from the bound space of operators on the Hilbert space associated with the input system, say \mathcal{H}_X , to the bound space of operators on the Hilbert space associated with the output system, say \mathcal{H}_Y . We will only give these details when it is necessary to clarify how a channel acts. In general we will use upper-case calligraphic Latin letters for quantum channels i.e. $\mathcal{E}, \mathcal{F}, \mathcal{G}$.

Of particular importance is the unitary channel, $\mathcal{U}(\rho) := U\rho U^\dagger$, for a unitary matrix $UU^\dagger = U^\dagger U = \mathbb{1}$. Unitary channels describe the evolution of closed quantum systems. The identity channel, id , is the particular unitary channel that leaves a system unchanged, such that $id(\rho) := \rho$ for all states ρ . However, the output system of a quantum channel need not

be the same system as the input – therefore we can use channels to describe a wide range of behaviour.

In fact, state preparation can be cast as a channel from the trivial one-dimensional system to a fixed state in a larger system, $1 \rightarrow \rho$. Similarly, discarding part of (or all of) a system is a channel – as it is a process that always sends valid states to valid states. This channel is the partial trace, $\text{tr}_B(\rho_{AB}) = \rho_A$ for an arbitrary bipartite system AB . In fact, we can use quantum channels to describe all the main aspects of quantum theory including the preparation of states, their evolution, discarding subsystems through the partial trace, and measurement updates.

Sometimes, it is important to clarify the input and output systems of channel. Under such circumstances we will use subscripts for the systems, such that a channel from a system X to a system Y is written $\mathcal{E}_{X \rightarrow Y}$.

Quantum channels allow for a few different representations – ways of mathematically writing down how the acts – which we will introduce when they are first used. The linearity of quantum mechanics means that convex combinations of quantum channels are also quantum channels, such as $p\mathcal{E} + (1 - p)\mathcal{F}$ for two quantum channels \mathcal{E} and \mathcal{F} . Quantum channels can also be applied in sequence, provided the output system dimension of first channel matches the input system dimension of the second channel. For sequential channels we write $\mathcal{F} \circ \mathcal{E}$ for the application of \mathcal{E} followed by \mathcal{F} . Note that $\mathcal{F} \circ \mathcal{E}$ is also a quantum channel.

Summary

Quantum channels, $\mathcal{E}, \mathcal{F}, \mathcal{G}$, describe the behaviour of quantum systems. They are highly flexible and can express all the main elements of quantum theory.

As channels are so versatile, they are the natural tool to use to describe the dynamics of quantum devices. For any algorithm (or any target process) we will want to: prepare some pure state, evolve the state unitarily,¹ perform a measurement on the final state. Further, the total desired evolution must be broken up into the individual native operations that form the device gateset, $\Gamma = \{\mathcal{U}_i\}$. Therefore we might have a circuit similar to

$$|\psi\rangle\langle\psi| \text{ --- } \boxed{\mathcal{U}_3} \text{ --- } \boxed{\mathcal{U}_2} \text{ --- } \boxed{\mathcal{U}_3} \text{ --- } \boxed{\mathcal{U}_1} \text{ --- } \boxed{\mathcal{U}_2} \text{ --- } \boxed{\mathcal{U}_4} \text{ --- } M \quad (1.2)$$

with time flowing from left to right.

In reality, all these operations will be noisy – unintended interactions with the environment and imprecise control mean the device will not act as a closed quantum system. We can use quantum channels to describe this noise. There will be some quantum channels describing the initial error is state preparation, $|\psi\rangle\langle\psi| \rightarrow \rho$, and the error in the final measurement, $M \rightarrow \tilde{M}$. These are the aforementioned SPAM errors. The unitary evolution will also be noisy so we replace each idealised operation with a channel, $\tilde{\mathcal{U}}_i$. Putting this together we

¹We will assume the desired evolution here is unitary, for simplicity, however some important processes such as error correction are inherently non-unitary.

have a circuit similar to

$$\rho \text{ --- } \boxed{\tilde{U}_3} \text{ --- } \boxed{\tilde{U}_2} \text{ --- } \boxed{\tilde{U}_3} \text{ --- } \boxed{\tilde{U}_1} \text{ --- } \boxed{\tilde{U}_2} \text{ --- } \boxed{\tilde{U}_4} \text{ --- } \tilde{M} \quad (1.3)$$

for the real world device.

We now turn to quantifying how ‘far’ the circuit in equation (1.3) is from the idealised circuit in equation (1.2). This is called benchmarking, and the tools that have been developed in this area are crucial to our approach.

1.2.2 Benchmarking of quantum channels

The first obstacle when assessing the performance of a device is scalability. Naively, to learn an unknown channel we have to see how the channel transforms each element of a complete basis for the system. For a single qubit, this means preparing each of the 6 Pauli eigenstates, performing the target operation, and measuring each of the 3 traceless Pauli observables. This gives 18 parameters to estimate. For n qubits, this implies $(2^{2n} - 1)^2$ variables, and so is exponentially difficult as we scale up the number of qubits. State-of-the-art tomographic techniques reduce this to 2^{2n} and this cannot be improved upon [41]. Therefore rather than completely learning a channel, it is desirable to have techniques that give less detailed (but still useful) information and require fewer experiments to be completed. Such techniques are said to be *efficient*.

A second consideration is which errors in the circuit shown in equation (1.3) are the ones which limit the performance of the device. For current devices, the SPAM errors – the errors for initially preparing states and the final measuring the system – can be an order of magnitude larger than the errors on individual elements of the gateset [33]. Further, to use quantum error correction the required error threshold to reach is on the errors in the gateset and not on SPAM errors [38, 42, 43]. Therefore techniques that can assess gateset errors independently from SPAM errors are critical. For a more detailed discussion of SPAM errors, see Chapter 4. Such methods that separate out the errors in a target process from SPAM errors are said to be *SPAM robust*.

Summary

As quantum devices continue to grow in system size and quality, it will be important to develop further methods that can assess the performance of a device. Two important considerations are favourable scaling and isolating the limiting errors.

Putting this together, techniques that are efficient and SPAM robust would be advantageous if they can be connected to meaningful information about the channel we want to probe. One such family of methods are randomized benchmarking (RB) protocols which exploit properties of Clifford group to average a noise channel down to a simple one parameter model which can be readily estimated.

For the noisy computational gateset, $\tilde{\Gamma} = \{\tilde{\mathcal{U}}_i\}$, we can write $\tilde{\mathcal{U}}_i = \mathcal{E}_i \circ \mathcal{U}_i$ for each idealised target unitary followed by a error channel, \mathcal{E}_i . This assumes that the error is Markovian and independent of where in the circuit the gate is placed [6]. A further assumption that greatly simplifies analysis is that there is an error channel associated with the gateset that is constant across the gateset, such that $\tilde{\mathcal{U}}_i = \mathcal{E} \circ \mathcal{U}_i$. We discuss this assumption of gate-independence in Chapter 4 and note that RB protocols have been shown to return accurate estimates for an effective noise channel \mathcal{E} even for highly gate-dependent noise [44, 45].

In the simplest instance, an RB protocol returns an estimate of the *average gate infidelity*, $r(\mathcal{E})$, of an effective noise channel \mathcal{E} associated with a noisy computational gateset – the Clifford group [32, 38, 46, 47]. For any quantum channel, \mathcal{E} , the average gate infidelity is defined as

$$r(\mathcal{E}) := 1 - \int d\psi \langle \psi | \mathcal{E}(|\psi\rangle\langle\psi|) | \psi \rangle, \quad (1.4)$$

where integration is over pure states and with respect to the Haar measure. We have $r(\mathcal{E}) = 0$ if and only if $\mathcal{E} = id$ for the identity channel, $id(\rho) := \rho$ for all states ρ [48]. Therefore this infidelity measure captures the Haar-average deviation of \mathcal{E} from the identity channel, which corresponds to perfect preservation of the state of the system. In this way, the infidelity is the first-order moment (or mean value) for the channel.

Summary

The average gate infidelity, $r(\mathcal{E})$, of a quantum channel, \mathcal{E} , is simple measure that quantifies the average deviation of the channel from the identity, $id(\rho) = \rho$.

The average gate infidelity for the effective noise channel \mathcal{E} associated with a gateset can be used to bound the worst-case error rate for the gateset, which is defined in terms of the diamond norm [49]. This is the relevant quantity in the context of fault-tolerant computation [50, 51]. We have the following best known bounds [43] in terms of infidelity:

$$\frac{d}{d+1} r(\mathcal{E}) \leq \frac{1}{2} \|id - \mathcal{E}\|_{\diamond} \leq \sqrt{d(d+1)r(\mathcal{E})}, \quad (1.5)$$

where $\|id - \mathcal{E}\|_{\diamond}$ is the diamond norm distance (see equation (4.1)) of the channel \mathcal{E} to the identity channel [38]. We discuss why the diamond norm cannot be directly estimated efficiently in Chapter 4. However, the above bounds are weak for highly coherent noise (i.e. unintended unitary rotations) [43]. Therefore obtaining additional information about the noise is vital.

Recent work has extended the core benchmarking toolkit, for example through higher-order moment analysis [52], character benchmarking techniques [53], the extension to benchmarking of logical qubits [54] and analogue regimes [55]. Simultaneous randomized benchmarking [56] has also been developed as a means to quantify the addressability of a subsystem in a device and thus provide a basic assessment of the presence of cross-talk and correlation errors.

1.2.3 Unitarity of quantum channels

Our work exploits recent techniques from randomized benchmarking theory [5, 57–59] that were originally introduced to provide additional information beyond the average gate infidelity, $r(\mathcal{E})$, for noise channels. Specifically, if infidelity is the first order moment of a channel as discussed above, then we can gain additional independent information by considering the second-order moment (or variance) of the channel. This variance is captured by the *unitarity*, of a quantum channel, $u(\mathcal{E})$, a measure of the coherence maintained by the channel. The unitarity is of interest outside of benchmarking – and is a central quantity in this work. Therefore we will spend some time introducing the definition of unitarity and then exploring its key properties.

The most natural way to define the unitarity, $u(\mathcal{E})$, of a quantum channel, \mathcal{E} , is given by an average of the purity of the channel across all input states, with the contribution from the maximally mixed state, $\rho = \mathbb{1}/d_X$, subtracted off. This allows us to see that the unitarity is strictly a generalization from considering the purity of states to the purity of quantum channels.

Definition 1.3. For any quantum channel, \mathcal{E} , the **unitarity** $u(\mathcal{E})$ is defined as

$$u(\mathcal{E}) := \frac{d_X}{d_X - 1} \left(\int d\psi \operatorname{tr}[\mathcal{E}(\psi)^2] - \operatorname{tr}[\mathcal{E}(\mathbb{1}/d_X)^2] \right), \quad (1.6)$$

where $\psi = |\psi\rangle\langle\psi|$ and the integration is with respect to the Haar measure over pure states of a d_X -dimensional input system [57].

The unitarity can be formulated as a variance of the channel in the following way. We can define notation for integration of a variable over the Haar measure as $\langle X \rangle = \int d\psi X$ for any X dependent of ψ . We have that $\langle \psi \rangle = \int d\psi \psi = \mathbb{1}/d_X$ as the Haar-average over all states is simply the maximally mixed state, $\mathbb{1}/d_X$. Further, due to the linearity of quantum channels, we have $\langle \mathcal{E}(\psi) \rangle = \int d\psi \mathcal{E}(\psi) = \mathcal{E}(\int d\psi \psi) = \mathcal{E}(\mathbb{1}/d_X)$. Putting this together, as noted in [60], the unitarity can be formulated as

$$u(\mathcal{E}) = \frac{d_X}{d_X - 1} \operatorname{tr}[\operatorname{var}(\mathcal{E})] = \frac{d_X}{d_X - 1} \operatorname{tr}[\langle \mathcal{E}(\psi)^2 \rangle - \langle \mathcal{E}(\psi) \rangle^2]. \quad (1.7)$$

Due to the linearity of the trace, we can easily show that this variance formulation of unitarity is equivalent to the definition given in equation (1.6).

The unitarity obeys natural limits which make it useful for quantifying how noisy a quantum channel is. Specifically, unitarity takes its extremal values if and only if the corresponding channel is of a particular form. We now introduce these two important classes of channels.

Firstly, we have completely depolarizing channels, \mathcal{D} , where no information about the input system is retained after the channel. These take the form $\mathcal{D}(\rho) := \sigma$ for any input state

ρ and some fixed output state σ , potentially in a completely different system. A simple example of completely depolarizing channel is $\mathcal{D}(\rho) = |0\rangle\langle 0|$ which discards any input state ρ and returns the single qubit computational basis state $|0\rangle\langle 0|$. Note that, in theory, ρ can be state of any system (i.e. the state of the whole universe) and the output system will still be a single qubit pure state. This illustrates the versatility of working with quantum channels. Completely depolarizing channels are of paramount importance in this work as they correspond to the most noisy processes possible – all information is lost.

Secondly, we have isometric channels, \mathcal{V} , which perfectly preserve all the information about the input system. Isometries take the form $\mathcal{V}(\rho) := V\rho V^\dagger$ where $V^\dagger V = \mathbb{1}$ for identity matrix on the input system. Isometries are generalizations of unitaries where the output system dimension can be larger than the input. Isometries are completely reversible, like unitaries, with $\mathcal{V}^\dagger \circ \mathcal{V}(\rho) = \rho$. A simple example of an isometry would be $\mathcal{V}(\rho) = \rho \otimes |0\rangle\langle 0|$, where for any input state ρ we output ρ within a larger system.

We summarize how these key channels relate to the unitarity in the following lemma.

Lemma 1.2 (Properties of unitarity). *Consider the unitarity, $u(\mathcal{E})$, of any quantum channel \mathcal{E} . The unitarity obeys the bounds $0 \leq u(\mathcal{E}) \leq 1$ with $u(\mathcal{E}) = 1$ if and only if $\mathcal{E} = \mathcal{V}$, for an isometry \mathcal{V} . The unitarity is lower bounded with $u(\mathcal{E}) = 0$ if and only if $\mathcal{E} = \mathcal{D}$, for a completely depolarizing channel. Further, the unitarity is invariant under local changes of basis such that $u(\mathcal{V} \circ \mathcal{E} \circ \mathcal{U}) = u(\mathcal{E})$ for any initial unitary \mathcal{U} and final isometry \mathcal{V} .*

Proofs for these properties are non-trivial, and we will derive them in Chapter 2 when we discuss generalizations of unitarity to other probability theories. They also appear in the literature within [57] and [61]. The unitarity attains its extremal values if and only if the channel completely retains all information about the input system, for a isometry \mathcal{V} , or loses all information about the input system, for a completely depolarizing channel, \mathcal{D} . We also have that unitarity remains constant under final unitary rotations, e.g. changes of basis. This is similar to how the purity, $\gamma(\rho)$, of a state, ρ , is invariant under unitary rotations, $\gamma(\mathcal{U}(\rho)) = \gamma(\rho)$.

The above properties make unitarity a good measure of how well the channel transfers quantum information and maintains the coherence of any input state. Further, we will show that it is well suited as a tool for examining fundamental elements of quantum theory.

Summary

The unitarity, $u(\mathcal{E})$, of a quantum channel, \mathcal{E} , is a simple measure which quantifies how well the channel preserves quantum information on average.

Crucially, the unitarity can be estimated for effective noise channels on quantum devices, with an efficient and SPAM-robust RB protocol – similar to the infidelity. It provides improved bounds on the diamond norm compared to infidelity, from (equation (32), [62]) we

have:

$$\frac{K}{\sqrt{2}} \leq \frac{1}{2} \|id - \mathcal{E}\|_{\diamond} \leq \sqrt{\frac{d^3 K^2}{4} + \frac{(d+1)^2 r(\mathcal{E})^2}{2}} \quad (1.8)$$

where $K^2 = \frac{d^2-1}{d^2}(u(\mathcal{E}) + \frac{2d}{d-1}r(\mathcal{E}) - 1)$. When the channel \mathcal{E} is unitary ($u(\mathcal{E}) = 1$) both bounds scale as $\mathcal{O}(\sqrt{r(\mathcal{E})})$ which tightens the lower bound of equation (1.5). For a purely stochastic channel, where the unitarity is directly related to the infidelity, both bounds scale as $\mathcal{O}(r(\mathcal{E}))$, thereby tightening the upper bound of equation (1.5). While measures like the diamond norm have clear operational significance, such as for single-shot channel discrimination, they are in general neither efficiently estimatable nor robust to SPAM-errors, in contrast to the unitarity.

Throughout this work we will show that the unitarity of a quantum channel is versatile tool, that we can utilize for our aims of connecting benchmarking techniques with foundational features of quantum theory.

1.3 Overview of thesis

With the essential mathematical tools and concepts for this work established, we now give an overview of the content of each chapter. This includes establishing additional motivations aside from novel benchmarking of noise, and highlighting our key results.

1.3.1 Quantum incompatibility

Within benchmarking theory broadly we are considering how fundamentals from quantum theory can be used to test the performance of quantum devices. However, we can also consider the opposite direction – treating noise quantum devices as tools to probe the limits of quantum theory. This was the first goal we introduced for this work.

The fact that unitarity is a measure of coherence for a channel suggests that it would be good at capturing situations where quantum theory places limitations on the coherence of channels. A famous example is the no-cloning theorem [17] which forbids a channel that would produce copies of the unknown input state to two output systems. We will show that the no-cloning theorem can be expressed in a simple manner using unitarity.

A broad range of behaviour is captured by quantum incompatibility and with this in mind, initially we have the following aim:

Specific goal

- (1) Formulate measures of quantum incompatibility that can be robustly and efficiently estimated on quantum devices.

Existing criteria to decide the compatibility of quantum channels can be formulated generally in terms of semidefinite programming and by introducing witnesses of incompatibility

[63, 64]. The task has also been shown to be equivalent to the quantum state marginal problem [65]. Other formulations rely on the Fisher metric [66] or on the diamond norm [67] to capture information-disturbance trade-offs. Another approach is via robustness measures [68, 69]. Evaluating these different figures of merit for incompatibility requires extensive optimisations that typically require a full description of the (quantum) processes involved.

The inability to clone a quantum state [17] can be shown to be an extremal case of incompatibility [22], and the ability to “hide” data in correlations can be viewed as being dual to cloning. This problem arises in the black-hole information paradox [70–72], and the no-hiding theorem was established to prove the impossibility of hiding a qubit state in the quantum correlations of a closed system [70]. This has the implication that black hole information must have some degree of spatial localization, either within the black hole interior or in the external region to the black hole [70–72].

No-cloning and no-hiding can also be related to other quantum impossibility results such as no-masking [73, 74] and no-deleting [75]. There have been some recent experimental tests of the no-hiding theorem [28] including the utilization of small scale quantum computers [76]. No-cloning has also been tested in the context of information-disturbance [29]. However, here we develop a broader framework that exploits recent theoretical ideas that arise in the analysis of quantum technologies.

Our approach to this problem is motivated by ideas from randomized benchmarking theory [11, 37]. Recall that such methods produce estimates of average channel properties (fidelity, unitarity etc.) in a way that is robust to state preparation and measurement errors and does not require exponentially difficult process tomography. In particular, we will argue that the unitarity of a quantum channel, as a measure of coherence [5, 48, 57], is a natural means to *simultaneously* describe both no-cloning and no-hiding. We will show how quantum incompatibility, and therefore the above no-go results, can be captured by unitarity within a single inequality.

At a high-level, our work can be viewed as extending the simple concept of the purity of a state, which is a measure of disorder², to what can be viewed as a purity-measure of the physical theory itself. This extension serves as a simple and intuitive 2-dimensional “fingerprint” of the theory. An example for quantum theory is shown in Figure 1.2.

1.3.2 Overview of Chapters 2 and 5

Our main focus is to simultaneously handle both classical and quantum theories under a unifying umbrella using average channel properties that can be robustly estimated on quantum devices.

²In quantum theory, this is $\gamma(\rho) := \text{tr}[\rho^2]$ for any state ρ .

We start in Chapter 2, where we develop a generalization of the *unitarity* $u(\mathcal{E})$ of a quantum channel, that allows extensions of our work to more general physical theories [77–79]. We show that this generalized unitarity has key properties that make it well suited to capturing compatibility, compared to other average measures such as fidelities [80, 81].

We briefly summarize the framework we develop to capture incompatibility of a theory in Section 2.1. For any theory we consider a global process, $\mathcal{G}_{X \rightarrow AB}$, from a system X into systems AB , and where the subscript simply indicates the input and output systems of the channel. Then we define *marginal channels*

$$\begin{aligned}\mathcal{E} &:= \mathcal{E}_{X \rightarrow A} = \text{tr}_B \circ \mathcal{G}_{X \rightarrow AB}, \\ \bar{\mathcal{E}} &:= \mathcal{E}_{X \rightarrow B} = \text{tr}_A \circ \mathcal{G}_{X \rightarrow AB},\end{aligned}\tag{1.9}$$

by tracing out A or B . Therefore \mathcal{E} and $\bar{\mathcal{E}}$ are obtained by discarding either part of the bipartite output state. This means \mathcal{E} quantifies only the information that is transferred from $X \rightarrow A$ and $\bar{\mathcal{E}}$ only the information that is transferred from $X \rightarrow B$. These channels let us define *compatible unitarity pairs* (CUPs), which we write as

$$(u(\mathcal{E}), u(\bar{\mathcal{E}})) \equiv (u, \bar{u}).\tag{1.10}$$

If we restrict $\mathcal{G}_{X \rightarrow AB}$ to certain classes for channels, then range over all channels of that type, we obtain a *CUP-set* – which depends only on the underlying physical theory, properties of the given family of channels and the dimensions of the systems d_X, d_A & d_B . In Section 2.1, we show that CUP-sets allow us to compare and contrast fundamental aspects of different physical theories, including incompatibility. Then in Section 2.2, we establish that classical physics has a CUP-set exactly on the boundary of the unit square, while in stark contrast the simplest CUP-set in quantum theory is described by a non-trivial shape in the (u, \bar{u}) plane (see Figure 1.2).

We explain why the shape of CUP-sets encode quantum incompatibility and we prove (see Theorem 2.1) the following result when $\mathcal{G}_{X \rightarrow AB}$ is restricted to the set of isometric channels:

Result (Incompatibility bound on isometric quantum CUP-set) *Any point (u, \bar{u}) in an isometric quantum CUP-set lies in the band defined by*

$$\frac{d_X}{d_X + 1} \left(\frac{1}{d_A} + \frac{1}{d_B} \right) \leq u + \bar{u} \leq 1\tag{1.11}$$

where d_X is the shared input system dimension, and d_A & d_B are the respective output dimensions.

This provides a general constraint on any isometric quantum CUP-set, which will still be a non-trivial shape within this band. In Section 2.3, we relate this result to the no-cloning theorem and the impossibility of perfect hiding of quantum information under unitary evolution, to which there is no classical equivalent. The above bounds are tight under general

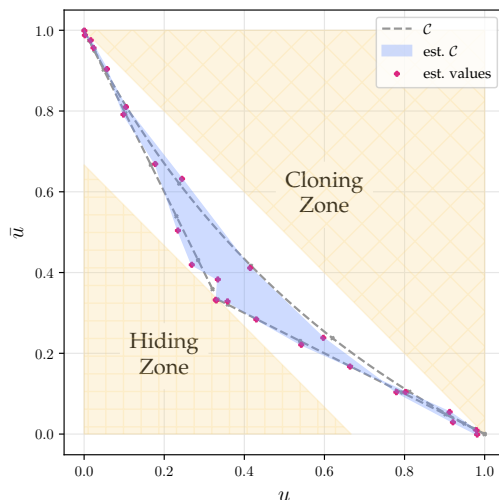


Figure 1.2: **Robust and efficient verification of quantum incompatibility.** In classical theory we have the ability to perfectly clone and perfectly hide classical information. In contrast, quantum theory has fundamental incompatibility that prohibits the same behaviour. This is captured by defining CUP-sets, and shown here is the estimation of the simplest quantum CUP-set \mathcal{C} . The reversible CUP-set for classical theory corresponds to the full boundary of the unit square $[0, 1]^2$, and allows perfect cloning (the point $(1, 1)$) and perfect hiding (the point $(0, 0)$). Using benchmarking techniques we estimate \mathcal{C} , shown here, on an IBM Q device and find that it saturates the general quantum bounds we derive in Theorem 2.1. Verifying such fundamental bounds provides a means to test the performance of emerging quantum computers.

conditions that we discuss. Further, we show that when $d_X = d_A = d_B$, these CUP-sets are further constrained in a manner that captures the no-hiding theorem exactly (see Theorem 2.2).

With this framework for incompatibility established we must turn to the estimation of CUP-sets on quantum devices to complete our goal. However, to estimate CUP-sets reliably we require techniques from device benchmarking [57, 82, 83]. Specifically, the benchmarking methods that we extend for estimating CUPs are more complex than those we define in the remainder of this thesis. Therefore we leave this discussion of experimental CUP-sets until Chapter 5 after we consider more straightforward randomized benchmarking procedures within Chapter 4.

In Chapter 5, we take a very direct approach by estimating a range of CUPs using the SWAP test [84]. These methods are detailed in Section 5.2. Secondly, we consider how techniques including randomized benchmarking, can be used to estimate CUPs in a SPAM-robust way, see Sections 5.3.1 & 5.4. We show that – with some assumptions – quantum CUP-sets can be estimated SPAM robustly on current devices (see Figure 1.2).

In the final part of Chapter 5, we discuss how the direct and robust methods compare, and to what degree we can infer that current devices obey the limits of quantum theory en-

capsulated by quantum incompatibility.

1.3.3 Quantifying coherent correlations

In Chapter 3, we extend of the core unitarity framework to build measures of the coherence in and between subsystems and the coherence of correlations within a channel. Then, in Chapter 4, we give an introduction to randomized benchmarking and show our new measures are accessible through RB protocols that allow for independent information about the nature of device to be obtained beyond existing techniques. However, beyond noise analysis in quantum technologies, there are other motivations why one would like to be able to efficiently assess correlative structures within quantum channels.

For example, consider a bipartite quantum channel $\mathcal{E}_{AB} : \mathcal{B}(\mathcal{H}_A \otimes \mathcal{H}_B) \rightarrow \mathcal{B}(\mathcal{H}_A \otimes \mathcal{H}_B)$ from a bipartite quantum system AB to itself with A and B being subsystems. Correlations within the channel are required for the transfer of a quantum state prepared on the first subsystem A to the second subsystem B : for example to transform the input pure states $|\psi\rangle_A \otimes |\phi\rangle_B$ to $|\phi\rangle_A \otimes |\psi\rangle_B$ via the SWAP unitary. This transformation is impossible under product channels of the form $\mathcal{E}_{AB} = \mathcal{E}_A \otimes \mathcal{E}_B$, with \mathcal{E}_A being a channel from A to A and \mathcal{E}_B being a channel from B to B , and so non-product channels are clearly required. However, quantifying these channel correlations is a distinct problem from measuring the correlation-generating abilities of a quantum channel. The SWAP unitary perfectly transfers a quantum state on A to B , however it has zero correlation generating abilities as it sends the set of product states $\rho_A \otimes \sigma_B$ to itself. In contrast the channel that sends all quantum states on AB to a Bell state is maximal in generating correlations, however it clearly transmits zero information from A to B .

Intermediate between these two extremal channels are *separable* channels that are defined as a convex combination of product channels.

Definition 1.4. *A separable channel, \mathcal{E}_{AB} , from a bipartite quantum system AB to itself can be written in the form*

$$\mathcal{E}_{AB} = \sum_i p_i \mathcal{E}_{A,i} \otimes \mathcal{E}_{B,i} \quad (1.12)$$

for some probability distribution p_i of product channels $\mathcal{E}_{A,i} \otimes \mathcal{E}_{B,i}$ which act independently on subsystems A and B .

Separable channels can only create classical correlations between A and B , but it is clear they do not transfer any quantum information from A to B .

Definition 1.5. *A non-separable channel, \mathcal{E}_{AB} , from a bipartite quantum system AB to itself is a channel which cannot be written in the separable form given above.*

Channels that generate non-classical correlations through the transfer quantum information from A to B must be non-separable. This includes the *SWAP* channel which transfers the maximum amount of information between the subsystems.

Further, connections between non-classical channel correlations and correlations within quantum states do exist. Specifically, the set of separable channels play a central role in the resource theory of Local Operations and Shared Randomness (LOSR) [85–94], for the study of non-classicality in quantum theory. It has recently been argued that this framework is the appropriate setting in which to properly analyse Bell non-locality and the self-testing of quantum states [91, 92]. Therefore a non-separable quantum channel requires the consumption of state correlations, and an ability to efficiently and robustly certify non-separability in a general quantum channel \mathcal{E}_{AB} implies the use of non-local quantum resources.

More broadly, since process tomography is exponentially hard, one can ask what non-classical features of quantum channels [95, 96] can be accessed in practice. We know that actual physical systems only probe a very small region of the set of all possible quantum states, dubbed the “physical corner of Hilbert space” [97, 98], and so a similar question for quantum channels can be addressed by drawing on recent developments in randomized benchmarking theory.

1.3.4 Overview of Chapters 3 and 4

We now describe how, within Chapters 3 and 4, we address two more of the goals we gave for this work. Firstly, to achieve of our goal of gaining independent information about the nature of device noise, we will aim to:

Specific goal

- (2) Enable novel benchmarking of the performance of quantum computers at the level of subsystems.

Secondly, for our goal of providing robust certification of non-classical effects, we separate out the following aims:

Specific goals

- (3a) Quantify the degree to which a quantum channel deviates from being separable in a form that can be estimated efficiently and robustly.
- (3b) Demonstrate an application of this approach by deriving an information-disturbance relation that can be efficiently and robustly verified.

We shall show that the unitarity of a quantum channel is well-suited to aims (2), (3a) and (3b), and suggests a route to analysing similar structural questions about bipartite quantum

channels in a form that is amenable to efficient and SPAM-robust experiments.

We will show that for a bipartite quantum system AB the concept of unitarity naturally extends to a collection of *subunitarities* $u_{X \rightarrow Y}(\mathcal{E})$ of a quantum channel \mathcal{E} on a bipartite system AB . The subscripts denote the input and output subsystems under consideration. For example, the subunitarity $u_{A \rightarrow A}$ describes how much coherence is maintained within the A subsystem by a channel; while the subunitarity $u_{A \rightarrow B}$ captures the information transferred by a channel from A into B .

Each of these subunitarities gives finer information about how the channel acts on the quantum systems A and B , and transfers information between subsystems. This allows us to address both (2) and (3b) above. However we find that only non-trivial combinations of subunitarities are estimatable in a SPAM-robust protocol, and so this forces us to develop methods to estimate channel correlations for aim (3a).

Objective (3a) turns out to be substantially more challenging than (3b), and we begin in Chapter 3 with the problem of quantifying channel correlations. In Section 3.1, recalling that the unitarity of a channel can be reformulated as a variance estimate, we construct a correlation measure $u_c(\mathcal{E}_{AB})$ that parallels the covariance between two classical random variables. Assembling this correlation measure leads to defining the subunitarities in Section 3.2.

In Section 3.1.2, we show that the simplest subunitarities can be related to the unitarity of marginal channels. This links to our general results in Chapter 2 on quantum incompatibility and leads to a novel form of the information-disturbance relation in terms of subunitarities. For a bipartite unitary, \mathcal{U}_{AB} , we have

$$u_{A \rightarrow A}(\mathcal{U}_{AB}) + u_{A \rightarrow B}(\mathcal{U}_{AB}) \leq 1, \quad (1.13)$$

where \mathcal{U}_{AB} is a bipartite channel describing unitary evolution of the joint system. What the above captures is the inherent limits quantum theory places on transferring information from one subsystem into others. For example, if the unitary is structured such that all the information from subsystem A stays in subsystem A , then *necessarily* no information goes from A to the other output subsystem, B . The above upper bound on the corresponding subunitarities captures this exactly, as if $u_{A \rightarrow A}(\mathcal{U}_{AB}) = 1$ then necessarily $u_{A \rightarrow B}(\mathcal{U}_{AB}) = 0$.

In the final part of Chapter 3 given by Section 3.3, we prove that the measure $u_c(\mathcal{E}_{AB})$ certifies non-classical features of a channel. More precisely, we prove that over the set of separable quantum channels (i.e. convex combinations of product channels) it is strictly bounded away from the global maximum, and thus provides a witness of non-separability for quantum channels.

In Chapter 4 we address the problem of efficiently estimating the correlated unitarity of effective noise channels in a benchmarking scenario. We begin with an exploration of randomized benchmarking in Section 4.1. We then show how existing protocols use properties of a unitary 2-design to estimate the unitarity of gateset noise within Section 4.2.

We then turn to our original protocols. For this we follow a similar approach to simultaneous randomized benchmarking in which one employs local 2-designs on each subsystem. This is of relevance for quantifying cross-talk errors in quantum devices. In Sections 4.3 and 4.4, we show that for bipartite separable channels the correlated unitarity can be obtained efficiently in a SPAM-robust protocol. For more general non-separable channels, we show in Section 4.5 that for weak reset errors that this can still be estimated and within a natural model demonstrate explicitly that the protocols can witness non-separability over a substantial range of reset errors.

We end the chapter by discussing the relation between our work and simultaneous randomized benchmarking and show that our protocols provide additional, independent information on cross-talk and correlative errors.

A simple formulation of the no-cloning and no-hiding theorems

“I do not know of any grottos,” replied Jacopo.
The cold sweat sprang forth on Dantès’ brow.
“What, are there no grottos at Monte Cristo?” he asked.
“None.”

The Count of Monte Cristo
Alexandre Dumas

The impossibility of cloning an unknown quantum state is one of the most famous instances of incompatibility, and is captured by the no-cloning theorem [17, 22]. The no-hiding theorem is another such instance, and can be viewed as being dual to no-cloning [70]. Such quantum features will play a key role in the development of quantum devices, and underlie why quantum error correction must be intrinsically different from classical error correction [32]. Both extremes of quantum incompatibility can be described in a unified way using quantum channels.

In this chapter, we develop a novel formulation of incompatibility that unifies both no-cloning and no-hiding. Our approach is to consider how the unitarity of quantum channels, a tool from device benchmarking, may be generalized for channels within other probability theories – such as classical probability theory. We will use this generalized definition of unitarity to establish a framework to measure the range of (in)compatibility allowed in a theory, based around the unitarity of compatible channels under a theory.

We then derive bounds which strongly constrain the quantum case. Moreover, we show that these bounds encode no-cloning and no-hiding exactly. We examine how our frame-

work allows for a detailed comparison with classical probability theory – where both perfect copying and perfect hiding are permitted.

Finally, we analytically explore the simplest non-trivial cases for both quantum and classical theory. These minimal examples of our general framework exhibit all the main features and are simple enough to allow for testing on current devices. Critically, compared to existing measures of incompatibility, our methods allow for efficient and robust estimation on quantum devices. However the techniques required are fairly involved. So we relate the discussion of estimation to Chapter 5 after we introduced more elementary benchmarking protocols within Chapter 4.

2.1 CUP-sets and incompatibility

We now construct a framework to study fundamental incompatibilities of a physical theory in a form that is sufficiently simple to allow for efficient and robust estimation. The analysis in this chapter focuses on quantum and classical theory, but we can extend it to any general probabilistic theory as described in Section 2.4.

2.1.1 Unitarity of a channel

We first introduce a measure – the unitarity – that quantifies how noisy a channel is. This is generalization of the unitarity defined for quantum channels (see equation (1.6)). This measure can also be viewed as the variance of the channel [60].

For both quantum and classical theory, we have the notion of a physical state x of a system, which may be mixed or pure¹. For example, in classical statistical mechanics a pure state is a microstate, while a macrostate is a mixed state. The most general evolutions of states are called channels, and a channel \mathcal{E} , is simply any map that takes valid states to states. For example, the identity channel $id(x) := x$ for all states x . We next need a couple of additional concepts in order to define the unitarity of a channel.

Firstly, for both classical and quantum theory, we have a notion of geometry that arises for the states. In quantum theory we have the Hilbert-Schmidt inner product. For two Hermitian operators A and B this inner product is defined as $\langle A, B \rangle := \text{tr}[AB]$, and leads to the definition of the *purity* of a quantum state ρ given by $\gamma := \langle \rho, \rho \rangle = \text{tr}[\rho^2]$. The same features exist in classical theory, and for a given probability distribution (p_k) describing a classical state of a system we have its associated purity given by $\gamma(p) := \langle p, p \rangle := \sum_k p_k^2$. Therefore, in either classical or quantum theory, we can define the purity of a state x as given by $\gamma(x) := \langle x, x \rangle$ for the appropriate inner product. The purity provides a measure of the noisiness of a given state, and for example can be associated to the minimal collision entropy over

¹More precisely a pure state is an extremal point in the set of all states, such as $|\psi\rangle\langle\psi|$ in quantum theory, while a mixed state is obtained from probabilistic mixtures of pure states.

discriminating measurements in the theory [100]. Moreover, this quadratic-order measure can be readily estimated for either classical or quantum theory.

Secondly, for both quantum and classical theory we have a preferred measure $d\mu(x)$ which is non-zero over the set $\partial\mathcal{S}$ of pure states of the theory. For quantum theory this is the Haar measure, while for finite-dimensional classical systems it is the uniform measure over the discrete pure states.

We can now define a generalised unitarity, that captures how well a channel in quantum or classical theory preserves information.

Definition 2.1. *The **unitarity** of a channel, \mathcal{E} , under either quantum or classical theory is given by*

$$u(\mathcal{E}) := \alpha \int_{\partial\mathcal{S}} d\mu(x) \gamma(\mathcal{E}(x) - \mathcal{E}(\eta)) \quad (2.1)$$

where $\eta := \int_{\partial\mathcal{S}} d\mu(x) x$ is the maximally mixed state under the theory, and where $\gamma(x)$ is the purity of a state x , defined as $\gamma(x) := \langle x, x \rangle$ given an inner product in the space of states. The normalizing constant α is chosen such that $u(\text{id}) = 1$.

This unitarity measure has a range of nice properties, which we will prove within the setting of generalized probability theories given in Section 2.4. For example, in Lemma 2.3, we prove that $u(\mathcal{E}) = 0$ if and only if \mathcal{E} is a completely depolarizing channel that acts as $\mathcal{E}(x) = y$ for any state x and some fixed state y . Such a channel can be viewed as erasing all information in the input state of the system. Additionally, for any theory in which $\gamma(x) = \langle x, x \rangle$ (i.e. quantum and classical theory), the unitarity is bounded between 0 and 1, and $u(\mathcal{V}) = 1$ for all isometries \mathcal{V} , which we prove in Corollary 2.2. Isometries are transformations that perfectly preserve all information in the input state x . Similarly, for such theories, the unitarity is invariant under changes of basis $u(\mathcal{V} \circ \mathcal{E}) = u(\mathcal{E})$ for any channel \mathcal{E} and isometry \mathcal{V} (see Lemma 2.5), and extension of the invariance of the unitarity of quantum channels under unitaries given in [57].

Summary

The generalised unitarity, $u(\mathcal{E})$, captures the degree to which a channel, \mathcal{E} , preserves information – in classical, quantum, or some other theory of physics. It is maximized for channels that perfectly preserve information about the input state and minimized for channels that completely discard the input state.

These attributes make this generalized unitarity a natural tool for capturing the incompatibility of channels.

2.1.2 Defining cloning and hiding

Given a channel \mathcal{G} from a subsystem X to subsystems AB we define the *marginal channels* as

$$\mathrm{tr}_B \circ \mathcal{G}(x), \quad (2.2)$$

$$\mathrm{tr}_A \circ \mathcal{G}(x), \quad (2.3)$$

where tr_A denotes the action of discarding the subsystem A , and similarly tr_B denotes discarding B . This is similar to the marginals of a bipartite quantum state, ρ_{AB} , where we have $\rho_A = \mathrm{tr}_B[\rho_{AB}]$. With the concept of a marginal channel, we can define what it means to clone or hide a state in a theory. The ability to perfectly clone/broadcast a state within a theory can be defined as the existence of a channel \mathcal{G} from an input system X to two output systems A and B , such that

$$\mathrm{tr}_B(\mathcal{G}(x)) = \mathrm{id}(x) = x, \quad (2.4)$$

$$\mathrm{tr}_A(\mathcal{G}(x)) = \mathrm{id}(x) = x, \quad (2.5)$$

for all states x . In other words the input state is perfectly copied to both outputs, and A and B are copies of X as spaces. Note that broadcasting is where one allows correlations between the two output systems, while cloning does not have correlations and is normally considered for pure states only. This distinction is not important here since we focus on the marginal outputs only, and henceforth we refer to the above process as cloning. The no-cloning theorem [17] can therefore be cast as a statement that, under quantum theory, there is no channel \mathcal{G} such that equations (2.4) and (2.5) both hold for all states x .

The no-hiding theorem in its original formulation [70] says that if a quantum state $|\psi\rangle$ evolves unitarily such that the output on one subsystem is a constant state – namely a completely depolarizing channel – then the state $|\psi\rangle$ can be perfectly recovered from the remaining environment subsystem. We can formulate the no-hiding theorem in terms of the above channel marginals in the following way. For a closed quantum system under unitary evolution (e.g. when $\mathcal{G} = \mathcal{V}$), if $\mathrm{tr}_B(\mathcal{V}(x)) = y$ for some fixed state y , then necessarily x must be completely recoverable at $\mathrm{tr}_A(\mathcal{V}(x))$. Therefore the no-hiding theorem requires that $\mathrm{tr}_C \circ \mathrm{tr}_A(\mathcal{V}(x)) = x$, up to final change of basis, and where the additional partial trace (tr_C) may be required to match the dimension of the input system.

Channel marginals can also capture a more general notion of hiding in any theory. More precisely, we say that we can perform *perfect* hiding in a theory if there is a channel \mathcal{G} from an input system X to two output systems A and B such that for all input states x we have

$$\mathrm{tr}_B(\mathcal{G}(x)) = \mathcal{D}_1(x) = y_1 \quad (2.6)$$

$$\mathrm{tr}_A(\mathcal{G}(x)) = \mathcal{D}_2(x) = y_2, \quad (2.7)$$

where \mathcal{D}_1 and \mathcal{D}_2 are completely depolarizing channels that send all input states to the fixed states y_1 and y_2 respectively. In other words the marginal channels of \mathcal{G} fully erase any information encoded in x . However, this is not everything. We also require that x is genuinely encoded in the global correlations between A and B . Therefore, we additionally require that \mathcal{G} is a reversible transformation, $\mathcal{G} = \mathcal{R}$, which means there is another channel \mathcal{F} from A and B to X such that $\mathcal{F} \circ \mathcal{G}(x) = id(x) = x$. This defines perfect hiding, but it might be possible to have partial hiding of a state, in the same way as it is possible to partially clone a quantum state.

Summary

The no-cloning and no-hiding theorems are two extremes of quantum incompatibility. We have shown that they both can be formulated in a concise manner using marginal channels, $\text{tr}_A \circ \mathcal{G}$ and $\text{tr}_B \circ \mathcal{G}$ for a global process \mathcal{G} from $X \rightarrow AB$. To capture no-hiding we should consider isometries, $\mathcal{G} = \mathcal{V}$, for perfect hiding we should consider reversible channels, $\mathcal{G} = \mathcal{R}$, while for no-cloning we should consider the marginals of any channel.

We next turn to quantifying how well a theory (classical, quantum or a more general theory) can both clone and hide. To completely capture hiding our framework should reproduce both quantum theory's no-hiding theorem, as well as identify perfect hiding. We do this through the above focus on marginal channels, and use the unitarity to quantify how well these local channels preserve information.

2.1.3 Compatible unitarity pairs of a theory

We now label the two marginal channels defined in equation (2.2), which gives us the notation to proceed with our framework for incompatibility within channels.

Definition 2.2. For any channel, \mathcal{G} , from an input system X to a joint system AB with marginal systems A and B , we define the marginal channels

$$\mathcal{E}(x) := \text{tr}_B \circ \mathcal{G}(x), \quad (2.8)$$

$$\bar{\mathcal{E}}(x) := \text{tr}_A \circ \mathcal{G}(x). \quad (2.9)$$

We name the tuple of the unitarities of these channels a **compatible unitarity pair (CUP)** and use the notation:

$$(u(\mathcal{E}), u(\bar{\mathcal{E}})) \equiv (u, \bar{u}). \quad (2.10)$$

From the previous discussion of cloning and hiding we found that the set of global channels, \mathcal{G} , that we consider matters. For hiding, we must consider the set of isometric channels to capture quantum theory's no-hiding theorem – as well as the set of *reversible* channels for perfect hiding in classical and quantum theory [101]. In contrast, for cloning we are free to range over all possible channels within a theory.

CUPs, (u, \bar{u}) , capture how a channel splits up information between two parties. Channels under different theories will have different limits on how this can be done.

It is possible to describe a general process on a open system in terms of reversible channels on (larger) closed systems for both quantum and classical theory [102, 103]. In quantum theory, global isometries suffice (captured by a Stinespring dilation [38]), however classical theory requires the use of auxiliary randomness [103]. As discussed in Section 2.3.3, the *reversible channels* are defined as those channels, \mathcal{R} , for which we have

$$\langle \mathcal{R}(x), \mathcal{R}(y) \rangle = c \langle x, y \rangle \quad (2.11)$$

for all states x, y and a constant $0 < c \leq 1$, and where the inner product is usual one given in Section 2.1.1 for quantum and classical theory. The *isometric channels* are a proper subset of reversible channels for both classical and quantum theory. Any isometric channel \mathcal{V} is a reversible channel for which $c = 1$. The smaller set of isometry channels are the traditional set considered for incompatibility in quantum theory, due to the Stinespring dilation theorem.

When $\mathcal{G} \in \mathcal{V}$, the set of isometric channels, and \mathcal{E} & $\bar{\mathcal{E}}$ are its marginal channels – as defined in equations (2.8) & (2.9) – then we write $\mathcal{E} \sim \bar{\mathcal{E}}$ and say that these channels are isometrically compatible. In this case, for quantum theory, the channels \mathcal{E} & $\bar{\mathcal{E}}$ are complementary to each other.

Similarly if $\mathcal{G} \in \mathcal{R}$, the set of reversible channels, then we write $\mathcal{E} \sim_r \bar{\mathcal{E}}$. Finally, when we consider \mathcal{G} to be the set of *all* channels in a theory, we write $\mathcal{E} \sim_* \bar{\mathcal{E}}$ such that \mathcal{E} and $\bar{\mathcal{E}}$ are marginals of any valid channel \mathcal{G} from X to AB . This notation is just to simplify definitions, and does not suggest an equivalence relation.

We are now ready to define the central quantity through which we examine the (in)compatibility allowed in physical theories.

Definition 2.3. We define the *isometric Compatible Unitarity Pair set* (hereafter called the *isometric CUP-set*) as

$$\mathcal{C}^{X \rightarrow AB} := \{(u(\mathcal{E}), u(\bar{\mathcal{E}})) \in \mathbb{R}^2 : \mathcal{E} \sim \bar{\mathcal{E}}\} \quad (2.12)$$

which is determined by both the dimensions of the particular state spaces and where $\mathcal{E} \sim_r \bar{\mathcal{E}}$ are the marginals of any the admissible isometry channels in the theory.

In a similar way, we define the *reversible CUP-set*, $\mathcal{C}_r^{X \rightarrow AB}$, when $\mathcal{E} \sim_r \bar{\mathcal{E}}$ for the marginals of any reversible channel. Finally, we define the *full CUP-set*, $\mathcal{C}_*^{X \rightarrow AB}$, for the marginals of any valid channel, when $\mathcal{E} \sim_* \bar{\mathcal{E}}$. For the remainder of this work we shall drop the superscripts specifying the subsystems and just write \mathcal{C} , \mathcal{C}_r and \mathcal{C}_* for the CUP-sets.

These abstract definitions are required to address quantum theory and classical theory in a unified way. However we show that, in practice, for each theory CUP-sets are simple

shapes in the 2-dimensional plane. These shapes encode the incompatibility of the theory in intuitive geometrical way.

Summary

CUP-sets, \mathcal{C} , \mathcal{C}_r and \mathcal{C}_* , capture *all* the ways information can be split up between two parties with a quantum/classical channel. Therefore CUP-sets measure the level of (in)compatibility allowed in the theory itself.

Since the unitarity is bounded between 0 and 1, we have the following series of inclusions

$$\mathcal{C} \subseteq \mathcal{C}_r \subseteq \mathcal{C}_* \subseteq [0, 1]^2. \quad (2.13)$$

It turns out that CUP-sets can also be defined for general probabilistic theories, and we discuss this in Section 2.4. Note that for any theory we have $(0, 0) \in \mathcal{C}_*$, since we are always free to discard the input state and prepare an arbitrary constant state on the output systems (for which the unitarity vanishes). Likewise, since the identity channel is in any theory, and we are free to swap/relabel subsystems (which is an isometric process) so that $(1, 0)$ and $(0, 1)$ lie in \mathcal{C} . These are common points for CUP-sets across different physical theories.

2.1.4 No-cloning and no-hiding through the CUP-set

No-cloning and no-hiding fit into this framework as follows. Firstly, if the physical theory admits perfect cloning then this implies that $(1, 1) \in \mathcal{C}_*$ since $u(\mathcal{E}) = 1$ if and only if $\mathcal{E} = id$ up to a final isometry [61]. We also note that it has been shown [19, 77] that broadcasting is possible in a physical theory if and only if the theory has a simplex state space of perfectly distinguishable states, and so essentially only classical theory has $(1, 1)$ in its CUP-sets. The no-cloning theorem can be cast compactly as a statement that – for quantum theory, the full CUP-sets \mathcal{C}_* (and therefore all CUP-sets) exclude the point $(1, 1)$.

Secondly, from Section 2.1.2, the no-hiding theorem given in terms of marginal channels states that – for quantum theory under isometric evolution — if $\mathcal{E} = \mathcal{D}$ (a completely depolarizing channel) then necessarily the input state can be completely recovered in the other subsystem. In the case $d_X = d_A = d_B$, this implies $\bar{\mathcal{E}} = \mathcal{V}$, an isometry. We will show (see Section 2.3) that this statement of the no-hiding theorem is captured exactly by the isometric quantum CUP-set \mathcal{C} , as for the point $(0, x)$ in \mathcal{C} then $x = 1$ only. Additionally in the case of unequal subsystems, the no-hiding theorem and the impossibility of perfect hiding implies the point $(0, 0)$ must still be strictly excluded from the isometric CUP-set \mathcal{C} . We prove this also holds in Section 2.3.

We also consider whether a theory admits perfect hiding with the addition of auxiliary randomness. This is captured by the reversible CUP-sets, \mathcal{C}_r . If the theory admits perfect hiding with auxiliary randomness then we have $\mathcal{D}_1 \sim_r \mathcal{D}_2$ for some completely depolarizing channels \mathcal{D}_1 and \mathcal{D}_2 . However, as we prove in Section 2.4, this statement is equivalent to the existence of the origin in the reversible CUP-set, $(0, 0) \in \mathcal{C}_r$. We will show that the reversible

CUP-sets of classical probability theory always contain $(0, 0)$ whereas the quantum reversible CUP-sets only contain $(0, 0)$ under certain dimensional restrictions related to mixed state purification.

Finally, for both quantum and classical theory we examine the case with the smallest non-trivial dimensions in detail. Since quantum physics neither admits perfect cloning, nor perfect hiding under unitary evolution, the simplest quantum CUP-sets form non-trivial subsets of the unit square $[0, 1]^2$, which we discuss shortly. In contrast, both $(0, 0)$ and $(1, 1)$ always lie within the classical (reversible) CUP-sets, as we shall show shortly.

2.2 Classical CUP-sets

We now explore how a classical CUP-set captures the compatibility allowed in classical probability theory. We shall see that the CUP-sets of classical theory are radically different from quantum theory, and so are a simple and vivid way to contrast the two theories.

2.2.1 Unitarity of classical channels

For a classical probability distribution on a d dimensional system, the pure states correspond exactly to the d extremal points $\{x_i\}_{i=1}^d$ of the state space. Therefore, for classical theory, the unitarity given in equation (2.1) reduces to

$$u(\mathcal{E}) = \frac{d}{d-1} \sum_{i=0}^{d-1} \gamma(\mathcal{E}(x_i) - \mathcal{E}(\eta)), \quad (2.14)$$

where $\eta = \frac{1}{d} \sum_{i=0}^{d-1} x_i$ is the maximally mixed state.

The only isometric operations with input and output systems of the same dimensions are those that permute the pure states. Recall that for any isometry we have $u = 1$ (see Corollary 2.2). Furthermore, reversible classical channels are fully generated by the set of isometries and auxiliary classical randomness [103–105], as they correspond to injective Boolean functions. This allows us to characterise CUP-sets for classical theory.

The state space of a single probabilistic classical bit is a $d = 2$ system with two possible pure states $x_0 := (1, 0)$ and $x_1 := (0, 1)$ in \mathbb{R}^2 . Any pure state x_i encodes the bit $m \in \{0, 1\}$. There are only two single-bit isometries: the identity channel id and NOT operation for which $NOT(x_0) = x_1$ & $NOT(x_1) = x_0$. For a two-bit system $d = 4$, we can define the pure states through the tensor product of the single bit pure states e.g. $x_{ab} := x_a \otimes x_b$ for $a, b \in \{0, 1\}$.

2.2.2 Cloning and hiding in classical theory

To clone/broadcast a classical mixed state bit in a state, $x := (p, 1 - p)$ with $0 \leq p \leq 1$, one simply brings in an auxiliary bit in the pure state $x_0 = (1, 0)$ and then performs a controlled-

not (CNOT) gate, controlled on the state x with the auxiliary bit as the target. The marginal distributions are then both given by x ; the input information was perfectly copied to the marginals. In terms of channels, the protocol is simply given by

$$\mathcal{V}(x) = CNOT(x \otimes x_0), \quad (2.15)$$

which outputs a 2-bit state.

Hiding of a classical (deterministic) bit involves encoding a bit, $x = (1, 0)$ or $x = (0, 1)$, entirely in correlations so that the marginal bit states are $\eta = (1/2, 1/2)$, the maximally disordered state. However, we also require that the bit is still perfectly recoverable from the total state. This can be done as follows: we introduce a single auxiliary bit in the state η , which is viewed as an unknown key bit, and we perform a controlled-not gate on x that is controlled on η . Equivalently we get

$$\mathcal{R}_{\text{hide},1/2}(x) = CNOT(\eta \otimes x), \quad (2.16)$$

which is a correlated 2-bit state. It has marginals η and also since $CNOT \circ CNOT = id$ we can perfectly recover the bit from the joint 2-bit state. This is the classical one-time pad protocol for encryption and the operation performs perfect hiding in classical theory [106].

2.2.3 The simplest classical CUP-set

Returning to a classical mixed state bit in a state, $x := (p, 1 - p)$ with $0 \leq p \leq 1$, the most general isometries from a single bit into two bits take the form of $\mathcal{V}(x) := \pi_{AB}(x \otimes x_0)$ where π_{AB} is a permutation on the four basis states. There will be 6 such different isometric operations, however they produce the same 3 points on the CUP diagram as follows. As the unitarity of the marginal channels \mathcal{E} and $\bar{\mathcal{E}}$ are invariant under local isometries at A and B , then separable operations $\pi_{AB} = \pi_A \otimes \pi_B$ will give the point $(u, \bar{u}) = (1, 0)$, corresponding to $\mathcal{E} = id$ and $\bar{\mathcal{E}} = \mathcal{D}$. The swap operation permuting the two systems will produce the point $(u, \bar{u}) = (0, 1)$. Finally, if the permutation corresponds to the $CNOT$ operation with control on system A , then on the CUP-set diagram this gives the point $(u, \bar{u}) = (1, 1)$, as $\mathcal{E} = \bar{\mathcal{E}} = id$. We therefore have that

$$\mathcal{C} = \{(1, 0), (0, 1), \text{ and } (1, 1)\}, \quad (2.17)$$

for the simplest non-trivial isometric CUP-set in classical theory.

2.2.4 Reversible classical CUP-set

We now consider the classical CUP-set produced by the set of reversible global operations \mathcal{R} . The following class of operations

$$\mathcal{R}_p(x) = x \otimes (px_0 + (1 - p)x_1) \quad (2.18)$$

introduces an auxiliary system B prepared in a fixed probabilistic state. This is not isometric, but satisfies $tr_B \circ \mathcal{R}_p(x) = x$, and is therefore reversible. All such channels \mathcal{R}_p correspond to point $(u, \bar{u}) = (1, 0)$ of the CUP-sets. Generally, reversible operations are given by

$$\mathcal{R} := \pi_{AB} \circ \mathcal{R}_p \quad (2.19)$$

where π_{AB} is again the permutation of the four basis states.

Motivated by the single-bit hiding protocol in Section 2.2.2, we consider $\pi_{AB} = CNOT_{AB}$, the controlled-not with A as the control and with B as the target, that generates the following family of reversible maps

$$\mathcal{R}_{hide,p} := CNOT_{AB} \circ \mathcal{R}_p. \quad (2.20)$$

These are partially-hiding channels with the perfect-hiding channel occurring for $p = 1/2$, corresponding to the point $(u, \bar{u}) = (0, 0)$. For general $p \in [0, 1]$ we have $(u, \bar{u}) = (1, p')$ with $p' = (1 - 2p)^2$. Since we can swap output subsystems we also get $(u, \bar{u}) = (p', 1)$. The remaining reversible channels are obtained from

$$\mathcal{R}_{broad,p} := CNOT_{BA} \circ \mathcal{R}_p \quad (2.21)$$

which gives the points $(u, \bar{u}) = (0, p')$ with $p' = (1 - 2p)^2$ and similarly, $(u, \bar{u}) = (p', 0)$ if we swap the output subsystems. We therefore have that

$$\mathcal{C}_r = \{(t, 0), (0, t), (t, 1), \text{ and } (1, t) \text{ for all } t \in [0, 1]\}. \quad (2.22)$$

In other words the reversible CUP-set \mathcal{C}_r is simply the border of the unit square $[0, 1]^2$.

2.2.5 Full classical CUP-set

Finally, we consider the full 1 to 2 bit CUP-set, \mathcal{C}_* , obtained by ranging over all single-bit to two-bit systems. It can be shown (see Corollary 2.1) that if a global channel \mathcal{E} from X to AB gives a point (u, \bar{u}) in any CUP-set and \mathcal{D} is any global, completely depolarizing channel, then the set of convex combinations $p\mathcal{E} + (1 - p)\mathcal{D}$ give the line segment joining (u, \bar{u}) to $(0, 0)$. This automatically implies that for classical theory we have

$$\mathcal{C}_* = [0, 1]^2, \quad (2.23)$$

since we can take convex combinations of reversible channels with a completely depolarizing channel and the resulting line segments fill the unit square.

The classical full CUP-set fills the unit square, capturing that there is no incompatibility between marginals. This follows from the existence of classical cloning $(u, \bar{u}) = (1, 1)$ as we can always disregard information to obtain any other point within the unit square.

2.3 Quantum CUP-sets

Quantum CUP-sets are much more tightly constrained in the unit square $[0, 1]^2$ than their classical counterparts, and we relate this to quantum no-go theorems. In this section we provide evidence for this statement, via tight analytical bounds on the sum of quantum CUPs.

For quantum theory, the general form for the unitarity given in equation (2.1) reduces to familiar form given in Definition 1.3 in Chapter 1. Recall that, within the context of benchmarking quantum devices, the unitarity u of the average noise channel \mathcal{E} associated with a gateset can be estimated using randomized benchmarking [107]. Further there are protocols to estimate the unitarity of noise are efficient and robust against state preparation and measurement (SPAM) errors [5], as we will discuss at length in Chapter 4. We will make use of these properties in Chapter 5 when we estimate CUP-sets on devices.

2.3.1 Incompatibility and hiding via trade-off relations on CUP-sets

We can now establish the following general bounds on the quantum CUP-sets that arise from isometric channels, \mathcal{C} . This gives us a handle on the structure of such sets and in particular how they relate to cloning and hiding.

Theorem 2.1 (General bounds on isometric quantum CUP-set \mathcal{C}). *Consider any input system X of dimension d_X and output systems A and B of dimensions d_A and d_B , with $d_X \leq d_A d_B$. The associated isometric quantum CUP-set $\mathcal{C} \subseteq [0, 1]^2$ is confined to the band in the (u, \bar{u}) -plane defined by*

$$\frac{d_X}{d_X + 1} \left(\frac{1}{d_A} + \frac{1}{d_B} \right) \leq u + \bar{u} \leq 1. \quad (2.24)$$

This bound is tight and the isometric quantum CUP-set \mathcal{C} intersects the bounding lines at $(1, 0)$, $(0, 1)$ and when $d_A = d_B$ it also attains the optimal hiding point $(u, \bar{u}) = \left(\frac{d_X}{d_A(d_X+1)}, \frac{d_X}{d_A(d_X+1)} \right)$.

Proof. It can be shown [61] that the unitarity of a channel can be expressed as

$$u(\mathcal{E}) = \frac{d_X}{d_X^2 - 1} (d_X \operatorname{tr} [\tilde{\mathcal{E}}(\mathbb{1}/d_X)^2] - \operatorname{tr} [\mathcal{E}(\mathbb{1}/d_X)^2]) \quad (2.25)$$

where $\tilde{\mathcal{E}}$ is any complementary channel to \mathcal{E} , which we can choose to be $\bar{\mathcal{E}}$. Applying the above expression to the complementary pair $(\mathcal{E}, \bar{\mathcal{E}})$ we then have that

$$u(\mathcal{E}) + u(\bar{\mathcal{E}}) = \frac{d_X}{d_X + 1} (\operatorname{tr} [\mathcal{E}(\mathbb{1}/d_X)^2] + \operatorname{tr} [\bar{\mathcal{E}}(\mathbb{1}/d_X)^2]). \quad (2.26)$$

For the lower bound, we bound each purity term individually. For any quantum state, ρ , for a system of dimension d we have the purity is lower bounded as $\text{tr}[\rho^2] \geq 1/d$, and therefore

$$u(\mathcal{E}) + u(\bar{\mathcal{E}}) \geq \frac{d_X}{d_X + 1} \left(\frac{1}{d_A} + \frac{1}{d_B} \right). \quad (2.27)$$

For the upper bound, we use the following property of complementary channels. We have that $\mathcal{E} := \text{tr}_B \circ \mathcal{V}_{X \rightarrow AB}$ & $\bar{\mathcal{E}} := \text{tr}_A \circ \mathcal{V}_{X \rightarrow AB}$ for an isometric channel $\mathcal{V}_{X \rightarrow AB}$. Therefore the state $\rho_{AB} = \mathcal{V}_{X \rightarrow AB}(\mathbb{1}/d_X)$ has the marginals $\rho_A = \mathcal{E}(\mathbb{1}/d_X)$ and $\rho_B = \bar{\mathcal{E}}(\mathbb{1}/d_X)$. For a general bipartite quantum state ρ_{AB} we have [108] that

$$\gamma(\rho_A) + \gamma(\rho_B) \leq 1 + \gamma(\rho_{AB}), \quad (2.28)$$

and therefore

$$u(\mathcal{E}) + u(\bar{\mathcal{E}}) \leq \frac{d_X}{d_X + 1} (1 + \gamma(\mathcal{V}_{X \rightarrow AB}(\mathbb{1}/d_X))). \quad (2.29)$$

As $\mathcal{V}_{X \rightarrow AB}$ is an isometry

$$\gamma(\mathcal{V}_{X \rightarrow AB}(\mathbb{1}/d_X)) = \text{tr}[(V(\mathbb{1}/d_X)V^\dagger)^2] = \frac{1}{d_X}. \quad (2.30)$$

Substituting this into the previous inequality we obtain,

$$u(\mathcal{E}) + u(\bar{\mathcal{E}}) \leq 1, \quad (2.31)$$

which completes the proof. \square

These bounds place hard limits on the amount of quantum information that can be hidden in the correlations between systems, and also how it can be shared between local systems. The upper bound can be directly related to the no-cloning theorem, as if $u = 1$ for the identity channel then necessarily $\bar{u} = 0$ for the other marginal being completely depolarizing. The perfect hiding point $(0, 0)$ is always precluded from the isometric CUP-set which is a consequence of the no-hiding theorem. Further, the upper bound is saturated for the identity and swap-channels, while the lower bound can be saturated in the case $d_X = d_A = d_B = d$ via a d^2 dimensional generalization of the Controlled-NOT operation.

Summary

CUP-sets capture the impossibility of perfectly copying unknown quantum information in a simple and geometrical way. Namely, if we have $u = 1$ for complete transfer of information from X to A then *necessarily* we have $\bar{u} = 0$ for no information going from X to B . Therefore cloning is forbidden.

In the case of equal input system and output subsystem dimensions, the isometric quantum CUP-set is further restricted. We now proof that the marginal channels and unitarity of such systems obey a series of equivalence relations. The details of the proof are not essential to narrative here, but will lead to the appearance of another no-go theorem.

Lemma 2.1. Consider an isometry, $\mathcal{V}_{X \rightarrow AB}$, from an input system X and joint output system AB with equal dimensions $d_X = d_A = d_B$. This defines the complementary marginal channels $\mathcal{E} := \text{tr}_B \circ \mathcal{V}_{X \rightarrow AB}$ and $\bar{\mathcal{E}} := \text{tr}_A \circ \mathcal{V}_{X \rightarrow AB}$. The pair \mathcal{E} and $\bar{\mathcal{E}}$ obey the following equivalence relations

$$\begin{array}{ccc} \mathcal{E} = \mathcal{U} & \iff & \bar{\mathcal{E}} = \mathcal{D} \\ \updownarrow & & \updownarrow \\ u(\mathcal{E}) = 1 & \iff & u(\bar{\mathcal{E}}) = 0 \end{array} \quad (2.32)$$

where $\mathcal{D}(\rho) = \sigma$ is a completely depolarizing channel to a fixed state σ .

Proof. We first prove $\mathcal{E} = \mathcal{U} \iff \bar{\mathcal{E}} = \mathcal{D}_\psi$. Note that for any quantum channel \mathcal{F} , its complementary channel $\tilde{\mathcal{F}}$ is unique up to an isometry on the output of $\tilde{\mathcal{F}}$ [109]. Further, we can write any isometry from $n = \log d$ to $2n$ qubits in the form $\mathcal{V}_{X \rightarrow AB}(\rho) = \mathcal{U}_{AB}(\rho \otimes |0\rangle\langle 0|^{\otimes n})$. Therefore it suffices to find any fixed dimension channel $\tilde{\mathcal{E}}$ complementary to \mathcal{E} , and apply a final unitary rotation. The isometry $\mathcal{V}_{X \rightarrow AB} = \mathcal{U}_A \otimes \mathcal{U}_B(\rho \otimes |0\rangle\langle 0|^{\otimes n}) = \mathcal{U}_A(\rho) \otimes \mathcal{U}_B(|0\rangle\langle 0|^{\otimes n})$ where \mathcal{U}_A and \mathcal{U}_B are unitaries on the respective subsystems A and B , gives the required form for \mathcal{E} , and we are free to set $\mathcal{U}_B(|0\rangle\langle 0|) = |\psi\rangle\langle\psi|$ which is the exact form of $\bar{\mathcal{E}}$. Applying the same argument starting from $\bar{\mathcal{E}}$ completes the inverse direction.

We now prove $\mathcal{E} = \mathcal{U} \iff u(\mathcal{E}) = 1$. For any quantum channel, \mathcal{F} , we have $\mathcal{F} = \mathcal{V} \iff u(\mathcal{F}) = 1$ where \mathcal{V} is an isometry [61]. For fixed input and output dimensions the set of isometric channels is equal to the set of unitary channels, and so the relation holds.

Finally, we prove $\bar{\mathcal{E}} = \mathcal{D}_\psi \iff u(\bar{\mathcal{E}}) = 0$. For any quantum channel, \mathcal{F} , we have $\mathcal{F} = \mathcal{D} \iff u(\mathcal{F}) = 0$ for a completely depolarizing channel $\mathcal{D}(\rho) = \sigma$ where σ is a fixed (potentially mixed) state. Given the form of $\mathcal{V}_{X \rightarrow AB}$, the only marginal channel, $\bar{\mathcal{E}}$, that disregards the input state completely is given by $\bar{\mathcal{E}}(\rho) = \text{tr}_A \circ \mathcal{U}_A \otimes \mathcal{U}_B(\rho \otimes |0\rangle\langle 0|^{\otimes n}) = \mathcal{U}_B(|0\rangle\langle 0|^{\otimes n}) = |\psi\rangle\langle\psi|$, for some pure state. Therefore all completely depolarizing channels generated by $\mathcal{V}_{X \rightarrow AB}$ must be to pure states, \mathcal{D}_ψ , and the condition holds. \square

These relations lead to a simple formulation of the no-hiding theorem as a further restriction on the shape of isometric quantum CUP-sets.

Theorem 2.2 (No-hiding bound on isometric quantum CUP-set \mathcal{C}). Consider any input system X and output systems A and B all of equal dimension. The associated quantum CUP-set \mathcal{C} is confined such that for

$$(u, \bar{u}) = (0, x) \Rightarrow x = 1. \quad (2.33)$$

Proof. This follows directly from Lemma 2.1, where we have $u(\bar{\mathcal{E}}) = 1 \iff u(\mathcal{E}) = 0$ and the definitions of u and \bar{u} . \square

This restriction on isometric quantum CUP-sets encapsulates the no-hiding theorem in the following manner. Here the no-hiding theorem states that if one marginal channel contains no information about the input system, then necessarily all the information can be recovered through the other marginal channel [70]. Therefore when $d_X = d_A = d_B$, if $\mathcal{E} = \mathcal{D}$ then necessarily $\bar{\mathcal{E}} = \mathcal{U}$, a unitary. From Theorem 2.2, these quantum CUP-sets capture this geometrically, as for the point $(0, x)$ in \mathcal{C} then $x = 1$ only. Which corresponds exactly (and only) to $\mathcal{E} = \mathcal{D}$ and $\bar{\mathcal{E}} = \mathcal{U}$, thereby capturing the no-hiding theorem. As the unitarity of a quantum channel is a simple measure that can be readily estimated with SPAM robustness for device noise, this opens a path to robust testing of another no-go theorem on current devices.

Summary

CUP-sets capture the impossibility of hiding unknown quantum information through unitary evolution in a simple and geometrical way. Namely, if we have $u = 0$ for no information going from X to A , then *necessarily* we have $\bar{u} = 1$ for complete transfer of all information from X to B . Therefore no information is hid in the correlations.

We have established strong bounds on the shape of isometric quantum CUP-sets in the 2-D plane. Further the bounds encode quantum no-go theorems for arbitrary input and output system sizes. However ultimately we wish to test this framework on actual quantum devices. Towards this end, we should examine in detail the behaviour of a isometric CUP-set when the input and output systems are the smallest non-trivial quantum systems – qubits.

2.3.2 The simplest quantum CUP-set

The simplest isometric quantum CUP-set is also the simplest quantum CUP-set in general due to the series of inclusions in equation (2.13). Further, the smallest non-trivial dimensions will be when $d_X = d_A = d_B = 2$, so we consider this case in detail. From Theorem 2.1, for the isometric CUP-set \mathcal{C} , this gives the following bounds

$$\frac{2}{3} \leq u + \bar{u} \leq 1. \quad (2.34)$$

with the optimal hiding point given by $(u, \bar{u}) = (1/3, 1/3)$.

For isometries mapping single qubit to two qubits, $\mathcal{V}(\rho) := \mathcal{U}_{AB}(\rho \otimes |0\rangle\langle 0|)$, it is sufficient to range over all unitaries \mathcal{U}_{AB} to explore the full parameter space of (u, \bar{u}) for \mathcal{C} . The general form of two qubit unitaries contains at most 3 CNOTs and 3 independently parametrised single qubit rotations [1] (see Figure 2.2). However, the two parameter isometry set with $\mathcal{U}_{AB} = \mathcal{U}_{AB}(\alpha, \beta)$ (for $\alpha, \beta \in \mathbb{R}$) (as in Figure 2.3) generates all possible complementary channel pairs, up to local unitaries [1]. As the CUP-set is invariant under local unitaries, this family suffices to fully describe it.

In Figure 2.1 we plot this simplest CUP-set, where 3 boundary curves can be identified. The families of channels generating the boundary are of interest for structural reasons and

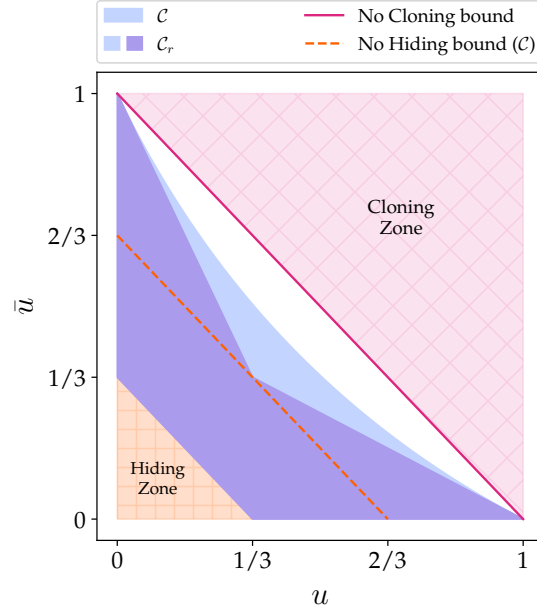


Figure 2.1: **Quantum CUP-sets.** The simplest isometric and reversible CUP-sets under quantum theory, with their analytical bounds ($d_X = d_A = d_B = 2$). The isometric CUP-set \mathcal{C} generated by global isometries is the central boomerang-shaped region (blue). Extending this to reversible operations \mathcal{C}_r increases the set in the direction of $(0, 0)$ to the boundary with the Hiding Zone (yellow). The two diagonal red lines are obtained from the general analytic upper and lower bounds for CUP-sets in quantum theory. In contrast, for classical theory we have that \mathcal{C}_r is the border of the unit square, while \mathcal{C} is the triple of points $(1, 1)$, $(1, 0)$, $(0, 1)$.

will be key to the experimental implementation we devise. The curved upper curve is given by a smooth interpolation between the identity channel and the SWAP channel that simply swaps the outputs on A and B . More precisely it is given by $\mathcal{U}_{AB} = \text{SWAP}^\alpha$ for $0 \leq u \leq 1$ and $0 \leq \alpha \leq 1$. The analytical relationship between u & \bar{u} for the upper curve is

$$(u, \bar{u}) = (u, 3 + u - 2\sqrt{1 + 3u}). \quad (2.35)$$

The analytical relationship between u and \bar{u} for the lower curves is linear, as shown in Figure 2.1. The lower right curve is given by $\mathcal{U}_{AB} = \text{CNOT}_{AB}^\alpha$, over the domain $\frac{1}{3} \leq u \leq 1$. While the left curve is given by $\mathcal{U}_{AB} = \text{CNOT}_{BA}^\alpha \circ \text{CNOT}_{AB}$ over the domain $0 \leq u \leq \frac{1}{3}$. The derivations of the boundary curves are provided in Appendix A.2.

2.3.3 Reversible quantum CUP-set

A general reversible quantum CUP-set \mathcal{C}_r (where d_A , d_B and d_X are not necessarily equal) is given by considering the marginals of the set of globally reversible channels. For $d_X < d_A d_B$ this set will be strictly larger than the set of isometric channels. The set of reversible quantum channels has been fully characterised [101]: \mathcal{E} is a reversible channel if and only if

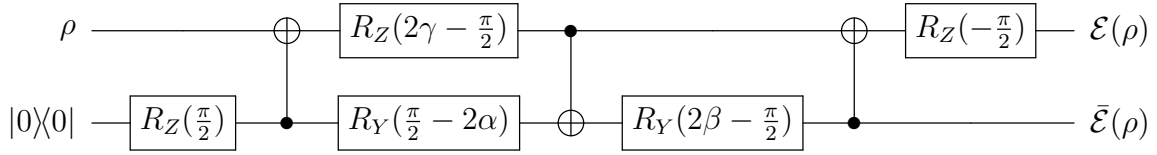


Figure 2.2: **Circuit decomposition for generic 2 qubit isometry** $\mathcal{V}(\alpha, \beta, \gamma)$. For $d_X = d_A = d_B = 2$, all isometries can be expressed in the above form, where $0 \leq \alpha, \beta, \gamma \leq \pi$ [1]. The complementary channels $\mathcal{E} = \text{tr}_B \circ \mathcal{V}$ & $\bar{\mathcal{E}} = \text{tr}_A \circ \mathcal{V}$ are shown, by ranging over α, β, γ we can generate the isometric CUP-set \mathcal{C} for 1 to 2 qubits.

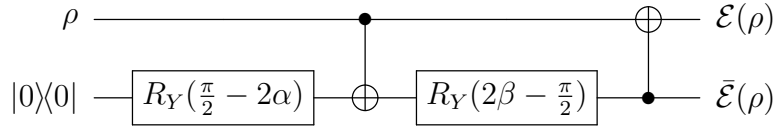


Figure 2.3: **Sufficient circuit decomposition for 2 qubit isometry** $\mathcal{V}(\alpha, \beta)$. For $d_X = d_A = d_B = 2$, the above isometry is sufficient to generate all points (u, \bar{u}) of the isometric CUP-set \mathcal{C} for 1 to 2 qubits with $0 \leq \alpha, \beta \leq \pi$. This follows from the general decomposition given in Figure 2.2, observing that the initial two gates do not change the state of the system, and the invariance of unitarity under local unitaries.

there is a unitary U and a *mixed* state σ

$$\mathcal{E}(\rho) = U(\rho \otimes \sigma)U^\dagger. \quad (2.36)$$

Alternatively, \mathcal{E} is a reversible quantum channel if and only if

$$\langle \mathcal{E}(\rho), \mathcal{E}(\tau) \rangle = c \langle \rho, \tau \rangle \quad (2.37)$$

for all states ρ, τ and some constant $c > 0$. Here the inner product is the Hilbert-Schmidt inner product given by $\langle X, Y \rangle := \text{tr}[X^\dagger Y]$. The latter demonstrates that reversible channels are a natural generalization of isometry channels. In fact, as for classical theory, we can always write any reversible channel \mathcal{R} as the convex combination of isometries $\mathcal{R} = \sum_i^r p_i \mathcal{V}_i$ with $\sum_i^r p_i = 1$ and $p_i \geq 0$ (see Lemma 2.2). Therefore we can think of the reversible CUP-set \mathcal{C}_r as introducing auxiliary classical randomness to the isometric CUP-set \mathcal{C} .

2.3.4 Upper bound for reversible CUP-sets

In the following we establish that the reversible quantum CUP-set, \mathcal{C}_r , shares the same upper boundary as the isometric quantum CUP-set, \mathcal{C} – adding randomness does not increase our ability to clone information. However, the existence of a non-trivial lower bound for \mathcal{C}_r , and therefore the possibility of perfect hiding, will depend on the values of d_A, d_B and d_X .

We now constrain \mathcal{C}_r by showing show that any point (u, \bar{u}) within the set will obey the same upper bound as \mathcal{C} .

Lemma 2.2. *Given any input system X of dimension d_X and output systems A and B of dimensions d_A, d_B , with $d_X \leq d_A d_B$. The associated reversible quantum CUP-set $\mathcal{C}_r \subseteq [0, 1]^2$ is bounded in (u, \bar{u}) -plane by*

$$u + \bar{u} \leq 1. \quad (2.38)$$

Proof. We can always write a reversible channel $\mathcal{R}(\rho) := \mathcal{U}_{AB}(\rho \otimes \sigma)$ with a potentially mixed state σ , as the convex combination of isometries \mathcal{V}_i as

$$\mathcal{R}(\rho) = \mathcal{U}_{AB}(\rho \otimes \sigma) = \mathcal{U}_{AB}(\rho \otimes \sum_i^r p_i \psi_i) = \sum_i^r p_i \mathcal{U}_{AB}(\rho \otimes \psi_i) = \sum_i^r p_i \mathcal{V}_i(\rho) \quad (2.39)$$

for some pure states $\psi_i = |\psi_i\rangle\langle\psi_i|$. We define the marginals $\mathcal{E}_{\mathcal{R}} := \text{tr}_B \circ \mathcal{R}$ and $\bar{\mathcal{E}}_{\mathcal{R}} := \text{tr}_A \circ \mathcal{R}$. Therefore we can write the marginal channel $\mathcal{E}_{\mathcal{R}}$ as

$$\mathcal{E}_{\mathcal{R}} = \text{tr}_B \circ \mathcal{R} = \sum_i^r p_i \text{tr}_B \circ \mathcal{V}_i = \sum_i^r p_i \mathcal{E}_i \quad (2.40)$$

if we define $\mathcal{E}_i := \text{tr}_B \circ \mathcal{V}_i$ and similarly for $\bar{\mathcal{E}}_i$. As the unitarity is convex (see Lemma A.2) we have

$$u(\mathcal{E}_{\mathcal{R}}) = u\left(\sum_i^r p_i \mathcal{E}_i\right) \leq \sum_i^r p_i u(\mathcal{E}_i) \quad (2.41)$$

and similarly for $\bar{\mathcal{E}}_i$. However $u(\mathcal{E}_i) + u(\bar{\mathcal{E}}_i) \leq 1$ for all i from our bound on isometric CUP-sets in Theorem 2.1. Therefore we have

$$u(\mathcal{E}_{\mathcal{R}}) + u(\bar{\mathcal{E}}_{\mathcal{R}}) \leq \sum_i^r p_i (u(\mathcal{E}_i) + u(\bar{\mathcal{E}}_i)) \leq \sum_i^r p_i = 1. \quad (2.42)$$

Which completes the proof, as $(u(\mathcal{E}_{\mathcal{R}}), u(\bar{\mathcal{E}}_{\mathcal{R}})) = (u, \bar{u})$ in the reversible CUP-set. \square

Therefore while the reversible CUP-set, \mathcal{C}_r , may be larger than the isometric CUP-set, \mathcal{C} , it must obey the same upper bound.

Perfect hiding with classical randomness

In the case $d_X = d_A = d$ and $d_B = d^2$, the reversible CUP-set \mathcal{C}_r contains the point $(0, 0)$ and perfect hiding can be achieved. However, as the channel is neither unitary nor isometric, it does not constitute a violation of the no-hiding theorem. The following channel is sometimes called the quantum one-time pad [110] and illustrates a perfect hiding channel when $d = 2$. Further, it can be straightforwardly generalized to higher dimensions.

Labeling the 4 Pauli operators on a single qubit as $\{P_i\} = \{\mathbb{1}, X, Y, Z\}$ we randomly apply an operator to the input state and record which to a classical register, such that

$$\mathcal{R}(\rho) = \frac{1}{4} \sum_i^4 P_i \rho P_i \otimes |i\rangle\langle i|. \quad (2.43)$$

where $\{|i\rangle\langle i|\}$ are the four computational basis states on two qubits. This channel has maximally mixed marginals, $\text{tr}_A[\mathcal{R}(\rho)] = \mathbb{1}/2$ and $\text{tr}_B[\mathcal{R}(\rho)] = \mathbb{1}/4$. Thus $(u, \bar{u}) = (0, 0)$. However there exists a quantum channel, \mathcal{R}' , such that $\mathcal{R}' \circ \mathcal{R}(\rho) = \rho$ for any state ρ . Physically, \mathcal{R}' is implemented by measuring the classical register, B , and applying the corresponding Pauli operator to system A , then discarding the register. The Kraus operators, $\mathcal{R}'(\cdot) = \sum_i R'_i \cdot R'_i^\dagger$, for this channel will be of the form:

$$\{R'_i\} = \{P_i \otimes \langle i|\} \quad (2.44)$$

It is readily seen that $\sum_i R'_i{}^\dagger R'_i = \mathbb{1}$ and therefore that this is a valid quantum channel.

We can connect any channel to a isometric process in a higher dimension through the stinespring dilation. This connects any reversible (or full) CUP-set to a isometric CUP-set with high dimensional output systems. Applied to the above hiding channel, \mathcal{R} , the following isometry

$$V = \frac{1}{4} \sum_i^4 P_i \otimes |i\rangle_B \otimes |i\rangle_C \quad (2.45)$$

gives $\mathcal{R}(\rho) = \text{tr}_C[V\rho V^\dagger]$ where the dimension of subsystem C is $d_C = 4$. However by tracing out the A subsystem, we find ρ can be completely recovered in BC . In fact, any bipartite combination of the subsystems A , B and C defines a pair of marginal channels for the isometric CUP-sets \mathcal{C} with dimensions $(2, 16)$ or $(4, 8)$. The lower bound on isometric CUP-sets given in Theorem 2.1 then guarantees that there is no arrangement of A , B and C such that both marginals are completely depolarising – confirming that quantum information cannot be completely hidden, and can always be recovered fully in the unitary dynamics of the larger system.

Boundaries of the simplest reversible CUP-set

In the case $d_X = d_A = d_B = 2$, the reversible quantum CUP-set \mathcal{C}_r is quite similar to \mathcal{C} . It has exactly the same upper boundary but different lower boundaries which are again straight lines. We have the following analytical bounds for reversible CUPs of these dimensions

$$\frac{1}{3} \leq u + \bar{u} \leq 1. \quad (2.46)$$

Where the lower bound can be found algebraically from the general circuit decomposition of a unitary on two qubits and using the characterisation theorem of reversible channels.

The lower bounding curves are straight lines, and given by considering the marginal unitarities of the reversible channel $\mathcal{R}(\rho) = \mathcal{U}_{AB}(\rho \otimes \frac{\mathbb{1}}{2})$. The right lower surface is given by $\mathcal{U}_{AB} = CNOT_{AB}^\alpha$ over the domain $\frac{1}{3} \leq u \leq 1$. The middle lower surface is $\mathcal{U}_{AB} = CNOT_{BA}^\alpha \circ CNOT_{AB}$ for $0 \leq u \leq \frac{1}{3}$. Finally, the left surface is given by $\mathcal{U}_{AB} = CNOT_{AB}^\alpha \circ CNOT_{BA} \circ CNOT_{AB}$ for $u = 0$.

A similar construction to the lower boundaries of this reversible CUP-set appears in the context of interleaved fidelity randomized benchmarking [111].

2.3.5 Full quantum CUP-set

Finally, the full quantum CUP-set \mathcal{C}_* , is generated by the marginals any quantum channel from $X \rightarrow AB$. For example, in the simplest case, \mathcal{C}_* is given by the marginal unitarities of any 1 to 2 qubit quantum channel. Then the upper boundary is given in equation (2.35), which it shares with both \mathcal{C}_r and \mathcal{C} . More generally, for any system dimensions, any point (u, \bar{u}) below the upper boundary given by \mathcal{C} is part of the full CUP-set. This is readily seen by considering a partially depolarizing channel on each output subsystem, as discussed in Section 5.1.2.

2.4 Generalized incompatibility and reversibility

Generalized probability theories (GPTs), provide a broad framework in which one can compare different physical theories and study their fundamental properties from an abstract, often information-theoretic viewpoint [77]. Our primary aim is to measure the incompatibility of quantum and classical theory in a manner that can be compared, captures no-go theorems, and – at least for quantum theory – can be efficiently computed on devices with robustness to noise. However our work can be framed in a general GPT setting, which we explore in this section. We also prove some properties of unitarity which were given following Definition 2.1. This assures the key properties hold across for quantum theory, classical theory and other theories.

2.4.1 Unitarity of GPT channels

A GPT is defined by a closed, convex set \mathcal{S} of states, and an effects space E , from which the allowed measurements on \mathcal{S} are constructed. The extremal points of \mathcal{S} are called the pure states, and we denote this set by $\partial\mathcal{S}$. We shall further assume that we can embed both the state space \mathcal{S} and effects space E in a Euclidean vector space, with inner product $\langle \cdot, \cdot \rangle$. A measurement \mathcal{M} is given by any tuple of effects $\mathcal{M} = \{m_1, m_2, \dots, m_N\}$ with $m_i \in E$ such that $\sum_k \langle m_k, x \rangle = 1$ for all states x in \mathcal{S} . The probability of getting an outcome m_k on a state x is given by $p(m_k|x) = \langle m_k, x \rangle$. The dimension d of the state space is given by the maximal number of completely distinguishable states $\{x_1, x_2, \dots, x_d\}$ in \mathcal{S} , where a set of states is completely distinguishable if there is a measurement $\mathcal{M}^\# = \{m_1, m_2, \dots, m_d\}$ that unambiguously identifies which of the states was measured through its deterministic outcome. We call $\mathcal{M}^\#$ a *sharp* measurement. Any physical process corresponds to a channel

\mathcal{E} , which is a linear map that sends any valid state x in the input system to another valid state $\mathcal{E}(x)$ in the output system.

For a GPT, we define the following function, the *purity* $\gamma(x)$ of a state x via

$$\gamma(x) := \max_{\mathcal{M}^\sharp} \sum_k \langle m_k, x \rangle^2, \quad (2.47)$$

where the maximization is taken over all sharp measurements $\mathcal{M}^\sharp = \{m_k\}$ in the theory [112]. While this optimization is non-trivial it turns out that the optimal measurements are simply the measurement of the pure states in classical theory (see Lemma 2.6), and in the case of quantum theory a rank-1 projective measurement in the basis the state is diagonal in (see Lemma 2.7). Additionally we can define a generalized maximally mixed state for any GPT obtained by averaging over the pure states $\partial\mathcal{S}$ of the theory

$$\eta := \int_{\partial\mathcal{S}} d\mu(x) x. \quad (2.48)$$

Together equations (2.47) & (2.48) allow for the unitarity of a channel, as given in equation (2.1), to be calculated for theories which do not have an inner product purity $\langle x, x \rangle$. More generally, the constant α in equation (2.1) will depend on the structure of the state space \mathcal{S} and the measure $d\mu(x)$.

2.4.2 Channel compatibility in general theories

While recent works deal with incompatibility of measurements in general theories [23, 24], one can also extend to the notion of (in)compatible channels [113].

The way in which the state space of subsystems relates to the state space of the global system is slightly non-trivial, and the details can be found in [77, 78, 114–116]. For composite systems we also have the notion of tracing-out or discarding of subsystems, that corresponds to the unit effect. We now put subscripts to specify the systems involved, so that x_A is a state for system A and x_{ABC} is a state for a tripartite system ABC . For a state x_{AB} on a bipartite system AB we assume there is channel $x_{AB} \rightarrow \text{tr}_A[x_{AB}] =: x_B$ that outputs a state x_B on B that results from discarding or ignoring system A . This amounts to computing the marginal of a probability distribution. We also define the identity channel as $id(x) = x$ for all $x \in \mathcal{S}$. Given a channel \mathcal{E} from a subsystem X to subsystems AB we can define the *marginal channels* as

$$\text{tr}_B \circ \mathcal{E}(x) \text{ and } \text{tr}_A \circ \mathcal{E}(x). \quad (2.49)$$

Two (or more) channels in a theory are *compatible* if they arise as marginal channels of a valid global channel within the theory.

Given the structure of the perfect-hiding channel in classical theory, we therefore argue that to capture no-go theorems, the appropriate set of global channels to consider in a theory

is the set of reversible channels. In any theory, we say a channel \mathcal{E} is *reversible* precisely if there is a second channel \mathcal{F} in the theory such that $\mathcal{F} \circ \mathcal{E} = id$ such that the total channel is the identity channel. For theories with an inner product between states, a particular subset of reversible channels are *isometry* channels \mathcal{V} , which preserve the inner product structure i.e. for any pair of states y, z it satisfies $\langle y, z \rangle = \langle \mathcal{V}(y), \mathcal{V}(z) \rangle$.

We also note that perfect cloning in classical theory involves an isometry channel, while perfect-hiding in classical theory involves a non-isometric, but reversible channel. Therefore if we restricted to only isometric channels in a theory this would suggest that is impossible to hide a bit in classical theory, which is not true.

In light of this, we say that a theory admits perfect cloning precisely if there is a channel \mathcal{E} from a system X into a bipartite system AB such that the marginal channels are both the identity channel. We also say that the theory admits perfect hiding precisely if there is a reversible channel \mathcal{R} from X into AB with marginals being two completely erasing channels \mathcal{D}_1 from X into A and \mathcal{D}_2 from X into B . Here a channel \mathcal{D} is completely erasing if for all $x \in \mathcal{S}$ we have $\mathcal{D}(x) = y$ for some fixed y .

Putting this together we have all the tools to examine incompatibility in a GPT using compatible unitarity pairs and therefore CUP-sets. However as our primary aim is to compare classical and quantum theory we leave explicit construction of GPT CUP-sets for future analysis.

2.4.3 Properties of unitarity for GPT channels

We now prove some technical details of unitarity within the GPT setting. This gives us a collection of properties that hold for both classical and quantum theory.

Firstly, we show that the unitarity vanishes for channels that completely discard the input state.

Lemma 2.3. *For any GPT in which $d\mu(x)$ is non-zero over all of ∂S we have that $u(\mathcal{E}) = 0$ if and only if $\mathcal{E} = \mathcal{D}$, for a completely depolarizing channel $\mathcal{D}(y) = z$ for all input states y with output state z fixed.*

Proof. A sum of non-negative numbers is zero if and only if each number is identically zero. Therefore we have that $u(\mathcal{E}) = 0$ if and only if $\langle m_k, \mathcal{E}(x) - \mathcal{E}(\eta) \rangle = 0$ for all m_k in the optimal measurement and for all $x \in \partial S$. Since $m_k \neq 0$ for all k this means that $u(\mathcal{E}) = 0$ if and only if $\mathcal{E}(x) - \mathcal{E}(\eta) = 0$ for all x , which is true if and only if $\mathcal{E}(x) = \mathcal{E}(\eta) = y$ for all x and fixed y . \square

For channels that discard the input state with some probability and transform it with another probability, the unitarity also has a simple form.

Lemma 2.4. *For any GPT with an inner product between states and effects, and in which $d\mu(x)$ is non-zero over all of ∂S we have $u(p\mathcal{E} + (1-p)\mathcal{D}) = p^2u(\mathcal{E})$ where \mathcal{E} is any channel, and \mathcal{D} is a completely depolarizing channel $\mathcal{D}(y) = z$ for all states y with z fixed.*

Proof. The proof follows from the expansion of the definition of unitarity under linearity, and that $\mathcal{D}(x) - \mathcal{D}(\eta) = 0$ (from Lemma 2.3). Putting this together

$$\begin{aligned} u(p\mathcal{E} + (1-p)\mathcal{D}) &:= \alpha \int_{\partial S} d\mu(x) \gamma(p(\mathcal{E}(x) - \mathcal{E}(\eta)) + (1-p)(\mathcal{D}(x) - \mathcal{D}(\eta))), \\ &= \alpha \int_{\partial S} d\mu(x) \max_{\mathcal{M}^\#} \sum_k \langle m_k, p(\mathcal{E}(x) - \mathcal{E}(\eta)) \rangle^2, \\ &= p^2 \alpha \int_{\partial S} d\mu(x) \max_{\mathcal{M}^\#} \sum_k \langle m_k, \mathcal{E}(x) - \mathcal{E}(\eta) \rangle^2 = p^2 u(\mathcal{E}). \end{aligned} \tag{2.50}$$

Which is the required form. □

The simple form given above for the unitarity when depolarizing channels are involved can be directly applied to CUP-sets. It allows us to deform the CUP-set according to the level of depolarization we apply.

Corollary 2.1. *For any CUP-set if the global channel \mathcal{G} from $X \rightarrow AB$ gives the point (u, \bar{u}) then the set of convex combinations $p\mathcal{G} + (1-p)\mathcal{D}$ gives the point $(p^2 u, p^2 \bar{u})$, where \mathcal{D} is a global completely depolarizing channel $\mathcal{D}(y) = z$ for all states y with z fixed.*

Proof. This follows from Lemma 2.4 with the observation that the marginals $\text{tr}_A \circ \mathcal{D}$ & $\text{tr}_B \circ \mathcal{D}$ of a completely depolarizing channel are also completely depolarising channels (to a different fixed state). □

Lemma 2.5. *Consider a GPT in which $\gamma(x) = \langle x, x \rangle$. Then for any isometry, \mathcal{V} , and any other channel, \mathcal{E} , we have $u(\mathcal{V} \circ \mathcal{E}) = u(\mathcal{E})$.*

Proof. The proof follows from expansion of the definition of unitarity under linearity, and

that $\langle \mathcal{V}(x), \mathcal{V}(y) \rangle = \langle x, y \rangle$ for all isometries \mathcal{V} and any states x and y . Then

$$\begin{aligned}
u(\mathcal{V} \circ \mathcal{E}) &= \alpha \int_{\partial \mathcal{S}} d\mu(x) \gamma(\mathcal{V} \circ \mathcal{E}(x) - \mathcal{V} \circ \mathcal{E}(\eta)), \\
&= \alpha \int_{\partial \mathcal{S}} d\mu(x) \langle \mathcal{V} \circ \mathcal{E}(x) - \mathcal{V} \circ \mathcal{E}(\eta), \mathcal{V} \circ \mathcal{E}(x) - \mathcal{V} \circ \mathcal{E}(\eta) \rangle, \\
&= \alpha \int_{\partial \mathcal{S}} d\mu(x) \langle \mathcal{V} \circ \mathcal{E}(x), \mathcal{V} \circ \mathcal{E}(x) \rangle \\
&\quad + \langle \mathcal{V} \circ \mathcal{E}(\eta), \mathcal{V} \circ \mathcal{E}(\eta) \rangle \\
&\quad - 2 \langle \mathcal{V} \circ \mathcal{E}(x), \mathcal{V} \circ \mathcal{E}(\eta) \rangle \\
&= \alpha \int_{\partial \mathcal{S}} d\mu(x) \langle \mathcal{E}(x), \mathcal{E}(x) \rangle + \langle \mathcal{E}(\eta), \mathcal{E}(\eta) \rangle - 2 \langle \mathcal{E}(x), \mathcal{E}(\eta) \rangle \\
&= \alpha \int_{\partial \mathcal{S}} d\mu(x) \langle \mathcal{E}(x) - \mathcal{E}(\eta), \mathcal{E}(x) - \mathcal{E}(\eta) \rangle, \\
&= \alpha \int_{\partial \mathcal{S}} d\mu(x) \gamma(\mathcal{E}(x) - \mathcal{E}(\eta)) = u(\mathcal{E}).
\end{aligned} \tag{2.51}$$

□

Corollary 2.2. *Consider a GPT in which $\gamma(x) = \langle x, x \rangle$. Then for any isometry, \mathcal{V} , we have $u(\mathcal{V}) = 1$.*

Proof. This follows directly from Lemma 2.5 with $\mathcal{E} = id$. □

2.4.4 Proofs for purity in classical and quantum theory

The following lemmas serve to illustrate that the general definition of purity for any GPT given in equation (2.47) reduces to the familiar forms for both classical and quantum theory. We first tackle classical theory.

Lemma 2.6. *For any classical state x of dimension d , we have*

$$\gamma(x) := \max_{\mathcal{M}^\sharp} \sum_k \langle m_k, x \rangle^2 = \langle x, x \rangle \tag{2.52}$$

where the maximization is taken over all sharp measurements $\mathcal{M}^\sharp = \{m_k\}$ of dimension d .

Proof. As discussed in Section 2.4, the pure states of classical probability theory are given by the d extremal points $\{x_i\}_{i=1}^d$ of the state space. There is only one measurement that distinguishes d states, namely $\mathcal{M}^\sharp = \{x_i\}_{i=1}^d$ for the set of pure states. Further, for any (mixed) state x , we can write $x = \sum_i^d p_i x_i$ where $\sum_i^d p_i = 1$ and all p_i are non-negative. Putting this together we have

$$\gamma(x) = \sum_k \langle x_k, x \rangle^2 = \sum_{i,j,k} \langle x_k, p_i x_i \rangle \langle x_k, p_j x_j \rangle = \sum_{i,j,k} p_i p_j \delta_{ki} \delta_{ji} = \sum_i p_i^2. \tag{2.53}$$

To complete the proof we observe that $\langle x, x \rangle = \sum_{i,j} p_i p_j \langle x_i, x_j \rangle = \sum_i p_i^2$. □

The same result can be shown for quantum theory.

Lemma 2.7. *For any quantum state ρ of dimension d we have*

$$\gamma(\rho) := \max_{\mathcal{M}^\#} \sum_k \langle m_k, \rho \rangle^2 = \text{tr}[\rho^2], \quad (2.54)$$

where the maximization is taken over all sharp measurements $\mathcal{M}^\# = \{m_k\}$ of dimension d .

Proof. We can write any quantum state in its eigenbasis, $\rho = \sum_i^d \lambda_i |e_i\rangle\langle e_i|$, such that $\text{tr}[\rho]^2 = \sum_i^d \lambda_i^2$. As $\mathcal{M}^\#$ completely distinguishes d states we have

$$\begin{aligned} \max_{\mathcal{M}^\#} \sum_k \langle m_k, \rho \rangle^2 &= \max_{\mathcal{M}^\#} \sum_k \left(\sum_i^d \lambda_i \text{tr} \left[m_k^\dagger |e_i\rangle\langle e_i| \right] \right)^2, \\ &= \max_M \sum_k \left(\sum_i^d \lambda_i M_{ki} \right)^2, \end{aligned} \quad (2.55)$$

where $M_{ki} := \text{tr} \left[m_k^\dagger |e_i\rangle\langle e_i| \right]$, and forms a doubly stochastic matrix given by $\sum_i^d M_{ki} = \sum_k^d M_{ki} = 1$. Expanding the purity

$$\begin{aligned} \max_{\mathcal{M}^\#} \sum_k \langle m_k, \rho \rangle^2 &= \max_M \sum_{i,j,k} \lambda_i \lambda_j M_{ki} M_{kj}, \\ &= \max_M \sum_{i,j} \lambda_i \lambda_j (M^T M)_{ij}. \end{aligned} \quad (2.56)$$

As the product of any two doubly stochastic matrices is doubly stochastic, $\sum_i (M^T M)_{ij} = \sum_j (M^T M)_{ij} = 1$. We then use that the vector $\lambda = (\lambda_1, \lambda_2, \dots, \lambda_d)^T$ majorizes the vector $\mu := M^T M \lambda$. Such that

$$\max_{\mathcal{M}^\#} \sum_k \langle m_k, \rho \rangle^2 = \sum_i \lambda_i \mu_i \leq \sum_i \frac{\lambda_i^2 + \mu_i^2}{2} \leq \sum_i \lambda_i^2. \quad (2.57)$$

Where the last inequality follows the Schur-convexity of $f(x) = x^2$. Equality holds as we can choose the measurement in the eigenbasis, which attains the bound. \square

This completes our discussion of unitarity, incompatibility and CUP-sets within the setting of generalized probability theories.

2.5 Conclusions

2.5.1 The long arm of purity

One way of viewing the approach we have taken here, is that we are starting with the concept of purity and applying it with greater and greater abstraction in the sequence

$$\text{States} \rightarrow \text{Channels} \rightarrow \text{Theories}. \quad (2.58)$$

Let us make this more precise. In any general theory we can begin with an elementary notion of disorder of a state, which can be quantified via the purity $\gamma(x)$. This can now be extended to the channel level for the theory and we obtain the unitarity $u(\mathcal{E})$ which is the natural generalization of purity. Indeed if we view a state x as itself being a preparation *channel* $1 \rightarrow x$ from the trivial system to S then it is readily seen that we have that $u(x) = \gamma(x)$ and the two notions coincide. For more non-trivial channels it can be shown [61] that the unitarity coincides with the conditional purity of the Choi state of \mathcal{E} . The unitarity is a variance-based measure of the disorder of a channel from one input system to one output system.

We next extend this further to consider how order can be shared or distributed amongst subsystems A and B of a theory and unitarity pairs (u, \bar{u}) , and subsets of channels. Again, this is a generalization of the preceding concept since if B is the trivial system then $(u, \bar{u}) = (u(\mathcal{E}), 0)$, which is just the unitarity of a channel. When applied to *sets* of channels this leads to encodings of no-go results of the theory. In this sense CUP-sets are purity measures of a given physical theory within the space of all operational theories.

2.5.2 Overview

We have derived a simple formulation of information-disturbance and incompatibility in quantum theory, given through the set of *compatible unitarity pairs* (CUPs). These pairs of compatible channels can be defined in any generalized probability theory, and they capture key limits of information transformation under the chosen theory.

We undertook a thorough comparison between CUP-sets under quantum theory, where they are tightly bound, and classical theory where the CUP-set lies on the boundary of the unit square. We then explored the CUP-set for quantum theory in detail, including general bounds on these sets, which we related to quantum no-go theorems.

However, to complete our aims we must connect our framework with efficient and robust estimation on quantum devices. However we will find the benchmarking techniques required are more involved than those required for the estimation protocols of other results in Chapter 4. Therefore we leave discussion of experimentally realizing the CUP-set framework to Chapter 5.

Quantifying local and correlated coherence in quantum channels

The 1-norm and the 2-norm [...] these really are God's favourite norms!

Quantum Computing Since Democritus
Scott Aaronson

In this chapter, we establish several novel measures of coherence flow within bipartite quantum channels. We then prove that our measures have a selection of desirable properties and examine how they act on specific families of channels. Specifically, we extend the concept of the unitarity of a channel – a measure of how well a channel preserves coherence – to sub-structures of channels. These *subunitarities* capture the local coherence of a channel. Inspired by the covariance of random variables, we then use the subunitarities to build a measure of correlations in bipartite channels. Crucially, we prove this measure is a witness of non-classical behaviour in channels, in particular non-separability. While these measures are of interest independently, we will show in the following chapter that they appear naturally within the context of randomized benchmarking protocols. This is critical to our approach as we aim to produce measures that can be efficiently and robustly estimated on devices. We discuss the complications that arise during estimation in the Chapter 4.

3.1 Operational subunitarities of quantum channels

We wish to formulate an experimentally accessible measure of correlations in a general bipartite quantum channel. Paralleling the situation with quantum states, we say that a quantum

channel $\mathcal{E}_{AB} : \mathcal{B}(\mathcal{H}_A \otimes \mathcal{H}_B) \rightarrow \mathcal{B}(\mathcal{H}_A \otimes \mathcal{H}_B)$ from a bipartite system AB to itself is *uncorrelated* or alternatively a *product* channel if $\mathcal{E}_{AB} = \mathcal{E}_A \otimes \mathcal{E}_B$ for a channel \mathcal{E}_A from A to itself and \mathcal{E}_B from B to itself. Otherwise it is said to be a *correlated* channel. We shall also consider the set of *separable* channels, which take the form of a statistical mixture of product channels $\mathcal{E}_{AB} = \sum_i p_i \mathcal{E}_A^i \otimes \mathcal{E}_B^i$ for a probability distribution (e.g. $p_i \geq 0$ and $\sum_i p_i = 1$). A quantum channel is said to be *non-separable* if it lies outside the convex set of separable channels. The extension to channels from input systems AB to potentially different output systems $A'B'$ is obvious, but to avoid over-complicating notation we primarily focus on identical input and output systems and only discuss the more general case in Section 3.1.2, where it is required. The general definition is provided in Appendix B.2.

3.1.1 Elementary subunitarities of a channel

Given two classical random variables X and Y a simple and direct method of measuring correlations is to compute the covariance of X and Y . This is given as $\text{cov}(X, Y) := \langle XY \rangle - \langle X \rangle \langle Y \rangle$, where the angle brackets denote taking the expectation value of the random variable. Moreover, we have that $\text{cov}(X, X) = \text{var}(X)$, the variance of the random variable X , which in turn quantifies the noisiness of X . The relevance here is, as discussed in Chapter 1, it has been noted [60] that the unitarity of a channel can be expressed as

$$u(\mathcal{E}) = \frac{d_X}{d_X - 1} \text{tr}[\text{var}(\mathcal{E})] = \frac{d_X}{d_X - 1} \text{tr}[\langle \mathcal{E}(\psi)^2 \rangle - \langle \mathcal{E}(\psi) \rangle^2], \quad (3.1)$$

where $\langle X \rangle = \int d\psi X$ for any X denotes taking the average of an operator-valued random variable with respect to the Haar measure.

As the unitarity can be viewed as the variance of a quantum channel, we can ask if a form of *covariance* for a quantum channel exists similar to the covariance of two random variables in classical statistics. However, while there is a clear notion of a marginal distribution for a joint probability distribution the situation is more complex for a bipartite quantum channel where the reduction to ‘marginal channels’ depends on the structure of the initial state considered [118]. Instead, here we take the basic form of covariance of two random variables as a guide and construct a unitarity-based correlation measure $u_c(\mathcal{E}_{AB})$ for a bipartite quantum channel with certain desirable features.

As we want the measure $u_c(\mathcal{E}_{AB})$ for quantum channels to function like $\text{cov}(X, Y)$ for classical random variables, we must define sensible channel equivalents to $\langle X \rangle$, $\langle Y \rangle$ and $\langle XY \rangle$. In the context of RB protocols on bipartite quantum channels we shall show in Section 4.4 that a natural marginal channel measure $u_{A \rightarrow A}$ emerges that parallels the classical marginal expectation $\langle X \rangle$. This is given by the following *subunitarity* $u_{A \rightarrow A}$ of a bipartite quantum channel.

Definition 3.1. The *subunitarity* $u_{A \rightarrow A}$, of a bipartite channel, \mathcal{E}_{AB} , is defined as

$$u_{A \rightarrow A}(\mathcal{E}_{AB}) := u(\mathcal{E}_A), \quad (3.2)$$

where $\mathcal{E}_A(\rho) := \text{tr}_B[\mathcal{E}_{AB}(\rho \otimes \frac{\mathbb{1}_B}{d_B})]$ for any state ρ of A and where $\frac{\mathbb{1}_B}{d_B}$ is the maximally mixed state on the subsystem B .

The same construction applies for the B subsystem with the associated channel $\mathcal{E}_B(\rho) := \text{tr}_A[\mathcal{E}_{AB}(\frac{\mathbb{1}_A}{d_A} \otimes \rho)]$, with $\frac{\mathbb{1}_A}{d_A}$ as the maximally mixed state on A , giving $u_{B \rightarrow B}(\mathcal{E}_{AB}) := u(\mathcal{E}_B)$. For both these subunitarities prepare the maximally mixed state on the other system – this is logical, as this is the state that is obtained from averaging over all states and represents no knowledge about the subsystem.

It is also clear that we can define two further subunitarities $u_{A \rightarrow B}$ and $u_{B \rightarrow A}$ between the subsystems. These are defined as

$$u_{A \rightarrow B}(\mathcal{E}_{AB}) := u(\mathcal{E}_{A \rightarrow B}) \quad (3.3)$$

where $\mathcal{E}_{A \rightarrow B}(\rho) := \text{tr}_A[\mathcal{E}_{AB}(\rho \otimes \frac{\mathbb{1}_B}{d_B})]$ for any input state ρ of A and where $\frac{\mathbb{1}_B}{d_B}$ is the maximally mixed state on the subsystem B . We can define a similar channel $\mathcal{E}_{B \rightarrow A}$ from B to A such that $u_{B \rightarrow A}(\mathcal{E}_{AB}) := u(\mathcal{E}_{B \rightarrow A})$. Equivalently we could make use of the unitary, *SWAP*, that swaps the subsystems A and B such that $\text{SWAP}(\rho_A \otimes \rho_B) = \rho_B \otimes \rho_A$ for any states ρ_A and ρ_B . Then we have the simple relation

$$u_{A \rightarrow B}(\mathcal{E}_{AB}) = u_{A \rightarrow A}(\text{SWAP} \circ \mathcal{E}_{AB}), \quad (3.4)$$

and similarly for $u_{B \rightarrow A}$.

From these definitions it is clear that the subunitarity $u_{X \rightarrow Y}(\mathcal{E}_{AB})$, with $X, Y = (A, B)$ being subsystems, is based on the situation in which a quantum state ρ is prepared on X with the maximally mixed state on the other subsystem and then evolved under the channel \mathcal{E}_{AB} . The quantity $u_{X \rightarrow Y}(\mathcal{E}_{AB})$ inherits the properties of unitarity and therefore measures how close this global evolution is to being an isometric mapping of the state ρ on X into the output system Y , thereby quantifying information transfer.

Summary

The subunitarity $u_{X \rightarrow Y}(\mathcal{E}_{AB})$ quantifies the amount of quantum information that flows from subsystem X into subsystem Y within a channel \mathcal{E}_{AB} .

The subunitarities $u_{A \rightarrow A}$ and $u_{B \rightarrow B}$ for the bipartite quantum channel have the property that when applied to product channels give

$$\begin{aligned} u_{A \rightarrow A}(\mathcal{E}_A \otimes \mathcal{E}_B) &= u(\mathcal{E}_A) \\ u_{B \rightarrow B}(\mathcal{E}_A \otimes \mathcal{E}_B) &= u(\mathcal{E}_B). \end{aligned} \quad (3.5)$$

These relations imply that *if* we can also construct a subunitarity $u_{AB \rightarrow AB}$ such that

$$u_{AB \rightarrow AB}(\mathcal{E}_A \otimes \mathcal{E}_B) = u(\mathcal{E}_A)u(\mathcal{E}_B), \quad (3.6)$$

then we can define a correlation measure that mirrors covariance in the following way.

Definition 3.2. *The correlation unitarity, $u_c(\mathcal{E}_{AB})$, of a bipartite channel \mathcal{E}_{AB} is defined as*

$$u_c(\mathcal{E}_{AB}) := u_{AB \rightarrow AB}(\mathcal{E}_{AB}) - u_{A \rightarrow A}(\mathcal{E}_{AB})u_{B \rightarrow B}(\mathcal{E}_{AB}), \quad (3.7)$$

where $u_{A \rightarrow A}$, $u_{B \rightarrow B}$ and $u_{AB \rightarrow AB}$ are subunitarities of the channel.

We can in fact construct this measure, however the subunitarity $u_{AB \rightarrow AB}$ is more difficult to define than the local subunitarities $u_{A \rightarrow A}$ and $u_{B \rightarrow B}$ already given. The definition of $u_{AB \rightarrow AB}$ is most easily expressed in the Liouville representation, and is provided in Section 3.2.2, and the justification for the naturalness of these terms is provided in Chapter 4 where we will show that these arise naturally from randomized benchmarking theory. The technical reason for this is that they are the quantities that arise if one considers quadratic order expectations over Haar random states where one includes the bipartite structure explicitly.

However, before deriving the remaining term in our correlation measure, in the next sub-section we show how the above subunitarities lead to a statement of the information-disturbance relation that is amenable to experimental verification.

3.1.2 Subunitarity formulation of information-disturbance

The information-disturbance relation [21] is a fundamental result in quantum theory and can be summarized as saying that if a quantum channel is close to being a unitary – or more generally an isometric channel – then the leakage of quantum information into the environment must be “small”. This trade-off can be expressed in terms of the diamond norm distance of the channel from a unitary channel for the output system, and the diamond norm distance of the complementary channel from a completely depolarizing channel for the environment. However, such quantities can neither be estimated efficiently nor in a SPAM-robust form. Within Chapter 2, we provided an alternative formulation of the information-disturbance relation that does not suffer from these weaknesses. Here we show that we can express this result in the language of subunitarities, where we consider the trade-offs when moving quantum information between subsystems of a bipartite process.

We now make a simplifying assumption¹, we consider the evolution of the bipartite system to be unitary, \mathcal{U}_{AB} . This is a natural assumption to make when considering information-

¹One can numerically verify that this assumption is not required for single qubit subsystems.

disturbance, as we want to include environmental effects within the total system, and therefore expect the total process to be unitary.

For this setting, we now show the following result on subunitarities that provides a statement of quantum incompatibility [21, 22]. To our knowledge the question of efficiently and SPAM-robustly testing such foundational results has not been previously considered, and so such a result opens up this possibility by formulating in terms of quantities native to randomized benchmarking protocols. Given the ability to estimate unitarity in randomized benchmarking protocols we therefore expect that our relation could also be verified efficiently and robustly using existing hardware. We now state and prove the subunitarity-based information-disturbance relation.

Theorem 3.1 (Subunitarity information–disturbance relation). *Consider a bipartite unitary, \mathcal{U}_{AB} , on a joint system AB . Then*

$$u_{A \rightarrow A}(\mathcal{U}_{AB}) + u_{A \rightarrow B}(\mathcal{U}_{AB}) \leq 1, \quad (3.8)$$

where $u_{A \rightarrow A}$ and $u_{A \rightarrow B}$ are subunitarities of the bipartite channel.

Proof. We can prove that the above is a special case of our results for the reversible quantum CUP-set in Chapter 2. From the definition of subunitarities (see Definition 3.1), we have

$$u_{A \rightarrow A}(\mathcal{U}_{AB}) = u(\mathcal{E}_{A \rightarrow A}), \quad (3.9)$$

for a channel $\mathcal{E}_{A \rightarrow A}(\rho) := \text{tr}_B \circ \mathcal{U}_{AB}(\rho \otimes \frac{\mathbb{1}}{d_B})$. Similarly for the other output subsystem we have $u_{A \rightarrow B}(\mathcal{U}_{AB}) = u(\mathcal{E}_{A \rightarrow B})$ for a channel $\mathcal{E}_{A \rightarrow B}(\rho) := \text{tr}_A \circ \mathcal{U}_{AB}(\rho \otimes \frac{\mathbb{1}}{d_B})$. It can be easily checked that the channel $\mathcal{R}(\rho) := \mathcal{U}_{AB}(\rho \otimes \frac{\mathbb{1}}{d_B})$ is a reversible channel, as $\text{tr}_B \circ \mathcal{U}_{AB}^\dagger \circ \mathcal{R}(\rho) = \rho$ for any state ρ . Therefore the channels $\mathcal{E}_{A \rightarrow A}$ and $\mathcal{E}_{A \rightarrow B}$ are the marginal channels of \mathcal{R} such that $\mathcal{E}_{A \rightarrow A} = \text{tr}_B \circ \mathcal{R}$ and $\mathcal{E}_{A \rightarrow B} = \text{tr}_A \circ \mathcal{R}$.

However, for any reversible channel, \mathcal{R}' , from a system X to a joint system AB , we have shown in Lemma 2.2 that the unitarities of the marginals obey the following relation

$$u(\text{tr}_B \circ \mathcal{R}') + u(\text{tr}_A \circ \mathcal{R}') \leq 1. \quad (3.10)$$

Setting $\mathcal{R}' = \mathcal{R}$ for this specific reversible channel, we have

$$\begin{aligned} u(\text{tr}_B \circ \mathcal{R}) + u(\text{tr}_A \circ \mathcal{R}) &\leq 1, \\ u(\mathcal{E}_{A \rightarrow A}) + u(\mathcal{E}_{A \rightarrow B}) &\leq 1, \\ u_{A \rightarrow A}(\mathcal{U}_{AB}) + u_{A \rightarrow B}(\mathcal{U}_{AB}) &\leq 1. \end{aligned} \quad (3.11)$$

Which completes the proof. \square

The above result provides a compact form of information-disturbance [21], in the following way, and can be straightforwardly generalized to case of differing input and output subsystem dimensions. For clarity, in this section, we shall put subscripts on the channels to denote their input and output systems explicitly, and write $\mathcal{E}_{i \rightarrow j}$ to denote a channel from any system i into j . Recall that, from the definition of subunitarities, we have

$$u_{A \rightarrow A}(\mathcal{U}_{AB}) = u(\mathcal{E}_{A \rightarrow A}), \quad (3.12)$$

for $\mathcal{E}_{A \rightarrow A}(\rho) := \text{tr}_B \circ \mathcal{U}_{AB}(\rho \otimes \frac{1}{d_B})$. Similarly for the other output subsystem we must have $u_{A \rightarrow B}(\mathcal{U}_{AB}) = u(\mathcal{E}_{A \rightarrow B})$ for $\mathcal{E}_{A \rightarrow B}(\rho) := \text{tr}_A \circ \mathcal{U}_{AB}(\rho \otimes \frac{1}{d_B})$. With these operational relations, Theorem 3.1 captures the tradeoff of information flow from a single subsystem, A , into either subsystem of the bipartite system AB .

More precisely, we can consider leakage of quantum information from a system into its environment, which is of relevance to, for example, quantum computing in a noisy environment when one wishes to approximate a unitary channel as accurately as possible. We can consider a quantum channel $\mathcal{E}_{A \rightarrow A} \approx \mathcal{U}_{X \rightarrow A}$, which is approximately close to a target unitary, $\mathcal{U}_{A \rightarrow A}$, in terms of unitarity. We quantify this as $u(\mathcal{E}_{A \rightarrow A}) = u(\mathcal{U}_{A \rightarrow A}) - \epsilon$ for some $\epsilon \geq 0$ quantifying the approximation. However the unitarity of a channel equals 1 if and only if it is an isometry [57, 61] and so the monogamy relation of Theorem 3.1 implies that $u(\mathcal{E}_{A \rightarrow B}) \leq \epsilon$. Furthermore it is easily shown (see Chapter 2) that the unitarity vanishes if and only if the channel is a completely depolarizing channel. This in turn implies that the channel $\mathcal{E}_{A \rightarrow B}$ must be ϵ -close in terms of unitarity to a completely depolarizing channel. In other words, the relation implies that the information leaking into the the other subsystem necessarily decreases to zero as the channel $\mathcal{E}_{A \rightarrow A}$ approaches a unitary channel.

Summary

We have shown that subunitarities also express an information-disturbance relation, which is a foundational concept. We have $u_{A \rightarrow A}(\mathcal{U}_{AB}) + u_{A \rightarrow B}(\mathcal{U}_{AB}) \leq 1$ for the subunitarities of a unitary \mathcal{U}_{AB} . Therefore when all information stay in a subsystem, $u_{A \rightarrow A}(\mathcal{U}_{AB}) = 1$, then necessarily the channel produces no correlations and transfers no information to the other subsystem $u_{A \rightarrow B}(\mathcal{U}_{AB}) = 0$. This may open the path to robust testing of information-disturbance on current highly noisy devices.

Information-disturbance is closely related to both the no-cloning and no-broadcasting theorems [17, 20, 119, 120]. We discuss how unitarity can be used to address these quantum no-go theorems in Chapter 2.

3.1.3 The Liouville representation of quantum channels

We now introduce vectorization of quantum states and the Liouville representation of a quantum channel. These mathematical tools will be extremely useful throughout this chapter.

Consider quantum channels $\mathcal{E}: \mathcal{B}(\mathcal{H}_X) \rightarrow \mathcal{B}(\mathcal{H}_X)$, where $\mathcal{B}(\mathcal{H}_X)$ denotes the space of linear operators on the Hilbert space \mathcal{H}_X for a d -dimensional quantum system. We can choose an orthonormal basis of operators $X_0, X_1, \dots, X_{d^2-1}$ for $\mathcal{B}(\mathcal{H}_X)$ with $X_0 = \mathbb{1}/\sqrt{d}$ such that with respect to the Hilbert Schmidt inner product $\langle X_\mu, X_\nu \rangle := \text{tr}[X_\mu^\dagger X_\nu] = \delta_{\mu,\nu}$. In particular, this means that X_1, \dots, X_{d^2-1} are all traceless operators. We shall refer to bases of this kind in the following compact way, $X_\mu = (X_0 = \frac{1}{\sqrt{d}}\mathbb{1}, X_i)$. We highlight that we shall use Greek-labels (μ, ν, \dots) for sums that run over *all* basis operators and Latin-labels (i, j, \dots) notation to run over just the *traceless* basis operators.

We define vectorization of operators via $|\text{vec}(|a\rangle\langle b|)\rangle := |a\rangle \otimes |b\rangle$ for computational basis states [38]. This definition can be extended by linearity to get the mapping $M \rightarrow |\text{vec}(M)\rangle$ for any operator $M \in \mathcal{B}(\mathcal{H}_X)$. Then for any quantum channel $\mathcal{E}: \mathcal{B}(\mathcal{H}_X) \rightarrow \mathcal{B}(\mathcal{H}_X)$ we define its Liouville representation, $\mathcal{L}(\mathcal{E})$, through the relation

$$\mathcal{L}(\mathcal{E})|\text{vec}(M)\rangle = |\text{vec}(\mathcal{E}(M))\rangle, \quad (3.13)$$

for all M . To simplify things going forward, we shall adopt the notation that we denote all vectorized quantities in boldface. This is similar to how a vector is sometimes represented in boldface as $\mathbf{v} = (v_1, v_2, \dots, v_n)$. So we write $|\mathbf{M}\rangle := |\text{vec}(M)\rangle$ and $\mathcal{E} := \mathcal{L}(\mathcal{E})$. Using this boldface notation we can re-express equation (3.13) in the more compact form

$$\mathcal{E}|\rho\rangle = |\mathcal{E}(\rho)\rangle, \quad (3.14)$$

for any state ρ , and any channel \mathcal{E} . Channel conjugation is particularly pleasing in this representation as it becomes matrix multiplication, such that

$$\mathcal{E}\mathcal{F}|\rho\rangle = |\mathcal{E} \circ \mathcal{F}(\rho)\rangle, \quad (3.15)$$

for any state ρ , and any channels \mathcal{E} and \mathcal{F} .

Summary

The Liouville representation, \mathcal{E} , is a way of representing any quantum channel, \mathcal{E} , as a matrix, acting on states, ρ , encoded in vectors, $|\rho\rangle$, such that $\mathcal{E}|\rho\rangle$. This is particularly useful for numerical calculations.

Using this notation we now give some useful quantum operations in the Liouville representation that we use through out this work, with proofs following. Firstly, the channel to trace out (*tr*) the system, and a channel we define to prepare (*prep*: $\text{prep}(1) = \mathbb{1}/d$) a new system in the maximally mixed state

$$\text{tr} = \sqrt{d} \langle \mathbf{X}_0 | \quad \text{and} \quad \text{prep} = |\mathbf{X}_0\rangle / \sqrt{d}. \quad (3.16)$$

This shows that the preparation of the maximally mixed state can be thought of as dual to the trace. As the trace completely discards a system, this strengthens our decision to use the maximally mixed state within the definition of subunitarities.

A direct consequence of the above is that the completely depolarizing channel $\mathcal{D}(\rho) := \mathbb{1}/d$ to the maximally mixed state is given by

$$\mathcal{D} = \mathit{prep} \cdot \mathit{tr} = |\mathbf{X}_0\rangle\langle\mathbf{X}_0|. \quad (3.17)$$

The identity channel ($\mathit{id}(\rho) = \rho$) also allows a very simple form in the Liouville representation: $\mathit{id} = \mathbb{1}^{\otimes 2}$.

Proofs for the preceding equations

Proof. (of equation (3.16)) For the first part we have $\text{tr}[\rho] = \text{tr}[\mathbb{1}\rho] = \sqrt{d} \langle\mathbf{X}_0|\rho\rangle$ as $X_0 = X_0^\dagger$. We can then vectorize both sides and apply the definition of the Liouville representation of a channel $|\text{tr}[\rho]\rangle = \sqrt{d} \langle\mathbf{X}_0|\rho\rangle$ and $\mathit{tr}|\rho\rangle = \sqrt{d} \langle\mathbf{X}_0|\rho\rangle$. Therefore $\mathit{tr} = \sqrt{d} \langle\mathbf{X}_0|$. For the second part, definitionally, $\mathbb{1}/d = X_0/\sqrt{d}$, $\mathit{prep}(1) = X_0/\sqrt{d}$ and the vectorization of 1 leaves it unchanged $|\mathbf{1}\rangle = 1$. Therefore $|\mathit{prep}(\mathbf{1})\rangle = |\mathbf{X}_0\rangle/\sqrt{d}$ and $\mathit{prep}|\mathbf{1}\rangle = |\mathbf{X}_0\rangle/\sqrt{d}|\mathbf{1}\rangle$. As 1 is the only valid state of the trivial system, we read off $\mathit{prep} = |\mathbf{X}_0\rangle/\sqrt{d}$ completing the proof. \square

Proof. (of equation (3.17)) We have $\mathcal{D}|\rho\rangle = |\mathbf{1}/d\rangle = |\mathbf{X}_0\rangle/\sqrt{d}$. As $\langle\mathbf{X}_0|\rho\rangle = 1/\sqrt{d}$ for any quantum state ρ we can write $\mathcal{D} = |\mathbf{X}_0\rangle\langle\mathbf{X}_0|$. \square

3.1.4 Unitarity in the Liouville representation

Using equation (3.14) we can decompose any channel $\mathcal{E} : \mathcal{B}(\mathcal{H}_X) \rightarrow \mathcal{B}(\mathcal{H}_X)$ in the orthonormal basis $X_\mu = (X_0 = \frac{1}{\sqrt{d}}\mathbb{1}, X_i)$ to find the Liouville representation² of any channel:

$$\mathcal{E} = \sum_{\mu=0}^{d^2-1} |\mathcal{E}(X_\mu)\rangle\langle X_\mu|. \quad (3.18)$$

In terms of matrix components we then have that

$$\mathcal{E} = \begin{matrix} & |\mathbf{X}_0\rangle & |\mathbf{X}_j\rangle \\ \begin{matrix} \langle\mathbf{X}_0| \\ \langle\mathbf{X}_i| \end{matrix} & \begin{pmatrix} 1 & \mathbf{0} \\ \mathbf{x} & T \end{pmatrix} \end{matrix}, \quad (3.19)$$

where $\mathcal{E}_{00} = 1$ and $\mathcal{E}_{0j} = \mathbf{0}$ follow from the fact that the channel is a completely positive trace-preserving operation. The $d^2 - 1$ component vector \mathbf{x} corresponds to the generalized Bloch vector of $\mathcal{E}(\mathbb{1}/d)$, which characterizes the degree to which the channel breaks unitarity. This suggests a measure of *non-unitarity* for a quantum channel defined via $x(\mathcal{E}) := \mathbf{x}^\dagger\mathbf{x}$,

²When the basis X_μ is fixed as the Pauli basis then the Liouville representation of a channel is sometimes referred to as the Pauli transfer matrix [121].

with $x = 0$ if and only if the corresponding channel is unital. The matrix block T encodes the remaining features of a channel and from equation (3.19) takes the form

$$T = \sum_{i,j}^{d^2-1} \langle \mathbf{X}_i | \mathcal{E}(\mathbf{X}_j) \rangle | \mathbf{X}_j \rangle \langle \mathbf{X}_i |. \quad (3.20)$$

In this notation, the unitarity of a channel is then given by the simple relation [57]

$$u(\mathcal{E}) := \frac{1}{d^2 - 1} \text{tr}[T^\dagger T]. \quad (3.21)$$

This form gives us further insight into the lower bound of unitarity. We can write $\text{tr}[T^\dagger T] = \|T\|_2^2$ where $\|M\|_2 := \sqrt{\text{tr}[M^\dagger M]}$ is the Schatten 2-norm (or Frobenius norm) of a matrix M [122]. As this is a norm, we have $\text{tr}[T^\dagger T] = \|T\|_2^2 = 0$ if and only if $T = 0$. Therefore the only possible non-zero data in the channel's Liouville representation is the \mathbf{x} vector. This is a completely depolarizing channel to some fixed state. Putting this together, we have that $u(\mathcal{E}) = 0$ if and only if \mathcal{E} is a completely depolarizing channel, as we would expect.

3.2 Generalized subunitarities of bipartite quantum channels

The form given for the unitarity in equation (3.21) will allow us to define all the possible subunitarities of a bipartite channel. We do this by examining how the Liouville representation of a channel extends to bipartite situations.

3.2.1 Liouville decomposition of bipartite quantum channels

We can also compute Liouville representations of bipartite channels, $\mathcal{E}_{AB}: \mathcal{B}(\mathcal{H}_A \otimes \mathcal{H}_B) \rightarrow \mathcal{B}(\mathcal{H}_A \otimes \mathcal{H}_B)$, where we assume for simplicity that the input and output systems are identical.

For subsystem A , we choose an orthonormal basis of operators $X_\mu = (X_0 = \frac{1}{\sqrt{d_A}} \mathbb{1}_A, X_i)$, where d_A is dimension of the subsystem A , and similarly for B a basis $Y_\mu = (Y_0 = \frac{1}{\sqrt{d_B}} \mathbb{1}_B, Y_i)$. Together these provide a basis for the full system which is given in the Liouville representation as ³

$$| \mathbf{X}_\nu \otimes \mathbf{Y}_\mu \rangle := | \mathbf{X}_\nu \rangle \otimes | \mathbf{Y}_\mu \rangle. \quad (3.22)$$

From these definitions we can build bipartite channels, such as the partial trace of subsystem B

$$id_A \otimes tr_B = \sqrt{d_B} id_A \otimes \langle \mathbf{Y}_0 |. \quad (3.23)$$

³Note that the basis $| \mathbf{X} \otimes \mathbf{Y} \rangle$ is a tensor product basis for $(\mathcal{H}_A \otimes \mathcal{H}_A) \otimes (\mathcal{H}_B \otimes \mathcal{H}_B)$ and up to re-ordering of (second and third) Hilbert spaces the same as vectorization of the matrix $X \otimes Y$. As these basis are isomorphic, the Liouville representation will be invariant under such permutations.

where id_A is the Liouville representation of the identity channel on subsystem A . This follows directly from equation (3.16). Similarly, combination of this with the preparation channel on B leads to the complete depolarization channel for the B subsystem

$$id_A \otimes \mathcal{D}_B = id_A \otimes (\text{prep}_B \cdot \text{tr}_B) = id_A \otimes |Y_0\rangle\langle Y_0|. \quad (3.24)$$

Finally we can express the unitary operation, $SWAP : \mathcal{B}(\mathcal{H}_A \otimes \mathcal{H}_B) \rightarrow \mathcal{B}(\mathcal{H}_B \otimes \mathcal{H}_A)$, that swaps the states of both subsystems compactly in the Liouville representation. From definition, we can write any bipartite state in the form $\rho := \sum_{\nu,\mu} \lambda_{\nu\mu} X_\nu \otimes Y_\mu$. The $SWAP$ channel then acts on this state such that $SWAP(\rho) := \sum_{\nu,\mu} \lambda_{\mu\nu} Y_\mu \otimes X_\nu$. Therefore, from inspection, the Liouville representation of the channel is

$$SWAP = \sum_{\nu=0, \mu=0}^{d_A^2-1, d_B^2-1} |Y_\mu \otimes X_\nu\rangle\langle X_\mu \otimes Y_\nu|. \quad (3.25)$$

Having established these explicit forms, we will find they are useful in examining substructures of bipartite channels.

3.2.2 General subunitarities with the Liouville representation

We can further decompose the Liouville representations of bipartite channels, in a manner that leads to a general definition of subunitarities. As $\{|X_\nu \otimes Y_\mu\rangle\}_{\nu,\mu}$ forms a complete orthonormal basis for $\mathcal{H}_A \otimes \mathcal{H}_A \otimes \mathcal{H}_B \otimes \mathcal{H}_B$, the Liouville representation of \mathcal{E}_{AB} corresponds to a matrix \mathcal{E}_{AB} whose entries satisfy

$$\langle X_\nu \otimes Y_\mu | \mathcal{E}_{AB} | X_{\nu'} \otimes Y_{\mu'} \rangle = \text{tr}[X_\nu^\dagger \otimes Y_\mu^\dagger \mathcal{E}_{AB} (X_{\nu'} \otimes Y_{\mu'})]. \quad (3.26)$$

This in turn provides the following matrix decomposition of \mathcal{E}_{AB} ,

$$\mathcal{E}_{AB} = \begin{matrix} \langle X_0 \otimes Y_0 | \\ \langle X_{i_1} \otimes Y_0 | \\ \langle X_{i_1} \otimes Y_{i_2} | \\ \langle X_0 \otimes Y_{i_2} | \end{matrix} \begin{pmatrix} |X_0 \otimes Y_0\rangle & |X_{j_1} \otimes Y_0\rangle & |X_{j_1} \otimes Y_{j_2}\rangle & |X_0 \otimes Y_{j_2}\rangle \\ 1 & \mathbf{0} & \mathbf{0} & \mathbf{0} \\ \mathbf{x}_{A \rightarrow A} & T_{A \rightarrow A} & T_{AB \rightarrow A} & T_{B \rightarrow A} \\ \mathbf{x}_{AB \rightarrow AB} & T_{A \rightarrow AB} & T_{AB \rightarrow AB} & T_{B \rightarrow AB} \\ \mathbf{x}_{B \rightarrow B} & T_{A \rightarrow B} & T_{AB \rightarrow B} & T_{B \rightarrow B} \end{pmatrix} \quad (3.27)$$

where $i_1 = \{1, 2, \dots, (d_A^2 - 1)\}$, $i_2 = \{1, 2, \dots, (d_B^2 - 1)\}$ and similarly for j . Here we break up the entire T matrix of the channel, from equation (3.19), according the subsystem contributions. For example, the term $T_{AB \rightarrow B}$ denotes the mapping of joint degrees of freedom of the input system AB into the B output subsystem.

With this notation in place, we can now define all the possible subunitarities of the bipartite channel.

Definition 3.3. For any quantum channel \mathcal{E}_{AB} on a bipartite system AB a *subunitarity* $u_{X \rightarrow Y}$ of the channel is defined as:

$$u_{X \rightarrow Y}(\mathcal{E}_{AB}) := \alpha_X \operatorname{tr} \left[T_{X \rightarrow Y}^\dagger T_{X \rightarrow Y} \right], \quad (3.28)$$

for any $X, Y \in \{A, B, AB\}$, with $\alpha_A = 1/(d_A^2 - 1)$, $\alpha_B = 1/(d_B^2 - 1)$ and $\alpha_{AB} = \alpha_A \alpha_B$.

Definition 3.3 provides a form for all nine choices of subunitarity. All these subunitarities measure the amount of coherent information that flows from the subsystem X into the subsystem Y . We highlight that Definition 3.3 allows us to construct a $u_{AB \rightarrow AB}$ subunitarity, using the elements of the basis $X_\nu \otimes Y_\mu$ that do not feature the identity on either subsystem (X_0 or Y_0). While $u_{AB \rightarrow AB}$ does not admit a straightforward operational interpretation we will shortly show that it has some useful properties and allows the construction of a correlation measure that is estimatable in practice. We now show that this generalized definition coincides with our previous more operationally defined subunitarities.

Theorem 3.2. For $\mathcal{E}_A(\rho) := \operatorname{tr}_B[\mathcal{E}_{AB}(\rho \otimes \frac{\mathbb{1}_B}{d_B})]$ we have $u(\mathcal{E}_A) = u_{A \rightarrow A}(\mathcal{E}_{AB})$, the unitarity u of the local channel equal to the subunitarity $u_{A \rightarrow A}$ of the full channel.

Proof. From definition the sub-unital block

$$\begin{aligned} T_{A \rightarrow A} &= \langle \mathbf{X}_i \otimes \mathbf{Y}_0 | \mathcal{E}_{AB} | \mathbf{X}_j \otimes \mathbf{Y}_0 \rangle = \operatorname{tr} \left[X_i^\dagger \otimes \frac{\mathbb{1}_B}{\sqrt{d_B}} \mathcal{E}_{AB} \left(X_j \otimes \frac{\mathbb{1}_B}{\sqrt{d_B}} \right) \right], \\ &= \operatorname{tr}_A \left[X_i^\dagger \operatorname{tr}_B \left[\mathcal{E}_{AB} \left(X_j \otimes \frac{\mathbb{1}_B}{d_B} \right) \right] \right] = \operatorname{tr}_A [X_i^\dagger \mathcal{E}_A(X_j)], \end{aligned} \quad (3.29)$$

which gives the unital block T of \mathcal{E}_A . As $T_{A \rightarrow A, \mathcal{E}_{AB}} = T_{\mathcal{E}_A}$ from definition $u_{A \rightarrow A}(\mathcal{E}_{AB}) = u(\mathcal{E}_A)$. Similarly $u(\mathcal{E}_B) = u_{B \rightarrow B}(\mathcal{E}_{AB})$ for $\mathcal{E}_B(\rho) := \operatorname{tr}_A[\mathcal{E}_{AB}(\frac{\mathbb{1}_A}{d_A} \otimes \rho)]$. \square

As these subunitarities of a bipartite channel are the unitaries of local quantum channels between subsystems, we directly inherit useful properties of unitarity as a measure. This includes invariance under local changes of basis (e.g. unitary rotations).

Corollary 3.1. The local subunitarities of any channel $u_{A \rightarrow A}(\mathcal{E})$ $\&$ $u_{B \rightarrow B}(\mathcal{E})$ are invariant under local unitaries.

Proof. This follows directly from Theorem 3.2, as the unitarity of any quantum channel \mathcal{E} is invariant under local unitaries, \mathcal{U} and \mathcal{V} , such that $u(\mathcal{U} \circ \mathcal{E} \circ \mathcal{V}) = u(\mathcal{E})$ [61]. \square

It is straightforward to expand on this property of local subunitarities, and apply it to all subunitarities. Under a local change of bases on the input and output subsystems we have

$$\mathcal{E}_{AB} \rightarrow (\mathcal{V}_A \otimes \mathcal{V}_B) \circ \mathcal{E}_{AB} \circ (\mathcal{U}_A^\dagger \otimes \mathcal{U}_B^\dagger), \quad (3.30)$$

for local unitary channels denoted with \mathcal{V} and \mathcal{U} . These changes of bases transform the submatrices $T_{X \rightarrow Y}$ under multiplication by orthogonal matrices. For example

$$T_{A \rightarrow A} \rightarrow \mathcal{O}_1 T_{A \rightarrow A} \mathcal{O}_2^T, \quad (3.31)$$

for orthogonal matrices $\mathcal{O}_1, \mathcal{O}_2$, with e.g. \mathcal{O}_2 arising from the unitary channel $\mathcal{U}_A(X_i) = \sum_{m=1}^{d_A^2-1} \mathcal{O}_{2;i,m} X_m$. This implies that all the subunitarity terms are invariant under local changes of bases. We formally prove the case $u_{AB \rightarrow AB}$ in Lemma 3.6, and those techniques can be directly applied to the remaining cases.

Summary

Invariance under local change of bases makes subunitarities, $u_{X \rightarrow Y}(\mathcal{E}_{AB})$, well suited to capturing quantum information transfer. This is because we would expect any measure of this resource to be independent of which basis the final measurement was taken in.

The subunitarities relate to the unitarity $u(\mathcal{E}_{AB})$ of the quantum channel \mathcal{E}_{AB} through a weighted sum. Intuitively, the total coherence of a channel can be broken up into the coherence in and between the subsystems of a channel.

Theorem 3.3. *The unitarity of a bipartite channel \mathcal{E}_{AB} is obtained from the weighted sum of its subunitarities:*

$$u(\mathcal{E}_{AB}) = \frac{1}{d_{AB}^2 - 1} \sum_{X,Y \in \{A,B,AB\}} \frac{u_{X \rightarrow Y}(\mathcal{E}_{AB})}{\alpha_X}, \quad (3.32)$$

where $d_{AB} = d_A d_B$ is the dimension of the total system and $\alpha_i = 1/(d_i^2 - 1)$.

Proof. This simply follows from block-matrix multiplication, giving

$\text{tr}[T^\dagger T] = \sum_{n,m=(A,B,AB)} \text{tr}[T_{n \rightarrow m}^\dagger T_{n \rightarrow m}]$. Therefore (see equation (3.21)) the unitarity is $u(\mathcal{E}) = \frac{1}{d^2-1} \sum_{n,m=(A,B,AB)} \text{tr}[T_{n \rightarrow m}^\dagger T_{n \rightarrow m}]$. Rearranging the dimensional constants (see equation (3.28)) completes the proof. \square

A direct consequence of Theorem 3.3 is that estimation of all the non-zero subunitarities of a channel gives an estimation of its total unitarity. We will make use of this property when examining channels with only a small number of non-zero subunitarities.

3.2.3 The subunitarities of product channels

As discussed in Section 3.1, our primary aim in exploring these subunitarities is to use them to construct a measure of correlations in bipartite channels. Towards this we now show that for a product channel $\mathcal{E}_A \otimes \mathcal{E}_B$, the subunitarity $u_{AB \rightarrow AB}$ splits up into the local unitarities, $u_{AB \rightarrow AB}(\mathcal{E}) = u(\mathcal{E}_A)u(\mathcal{E}_B)$.

Lemma 3.1. *For a product channel, $\mathcal{E}_A \otimes \mathcal{E}_B$, the sub-unital block $T_{A \rightarrow A} = T_A \otimes |\mathbf{Y}_0\rangle\langle\mathbf{Y}_0|$ where $T_A := \sum_{i,j} |\mathcal{E}_A(\mathbf{X}_j)\rangle\langle\mathbf{X}_i|$. Similarly $T_{B \rightarrow B} = |\mathbf{X}_0\rangle\langle\mathbf{X}_0| \otimes T_B$ where $T_B := \sum_{i,j} |\mathcal{E}_B(\mathbf{Y}_j)\rangle\langle\mathbf{Y}_i|$.*

Proof. From definition, $T_{A \rightarrow A, ij} = \langle \mathbf{X}_i | \otimes \langle \mathbf{Y}_0 | \mathcal{E}_A \otimes \mathcal{E}_B | \mathbf{X}_j \rangle \otimes | \mathbf{Y}_0 \rangle = \langle \mathbf{X}_i | \mathcal{E}_A | \mathbf{X}_j \rangle \text{tr}[\mathcal{E}_B(\mathbb{1}/d_A)]$. For any trace preserving channel $\text{tr}[\mathcal{E}(\mathbb{1}/d)] = 1$ so $T_{A \rightarrow A} = \sum_{i,j} \langle \mathbf{X}_i | \mathcal{E}_A | \mathbf{X}_j \rangle | \mathbf{X}_i \rangle \langle \mathbf{X}_j | \otimes | \mathbf{Y}_0 \rangle \langle \mathbf{Y}_0 |$. The proof for $T_{B \rightarrow B}$ follows similarly. \square

Lemma 3.2. *For a product channel, $\mathcal{E}_A \otimes \mathcal{E}_B$, we have $T_{AB \rightarrow AB} = T_A \otimes T_B$.*

Proof. From definition, $T_{AB \rightarrow AB} = \sum_{ij}^{d_A^2-1} \sum_{nm}^{d_B^2-1} \langle \mathbf{X}_i | \otimes \langle \mathbf{Y}_n | \mathcal{E}_A \otimes \mathcal{E}_B | \mathbf{X}_j \rangle \otimes | \mathbf{Y}_m \rangle | \mathbf{X}_i \rangle \langle \mathbf{X}_j | \otimes | \mathbf{Y}_n \rangle \langle \mathbf{Y}_m | = \sum_{ij}^{d_A^2-1} \sum_{nm}^{d_B^2-1} | \mathcal{E}_A(\mathbf{X}_j) \rangle \langle \mathbf{X}_i | \otimes | \mathcal{E}_B(\mathbf{Y}_m) \rangle \langle \mathbf{Y}_n | = T_A \otimes T_B$. \square

Theorem 3.4. *For a product channel, $\mathcal{E} = \mathcal{E}_A \otimes \mathcal{E}_B$, we have $u_{AB \rightarrow AB}(\mathcal{E}) = u(\mathcal{E}_A)u(\mathcal{E}_B)$.*

Proof. From Lemma 3.2 we can write $u_{AB \rightarrow AB}(\mathcal{E}) = \alpha_A \cdot \alpha_B \text{tr} \left[T_A^\dagger \otimes T_B^\dagger T_A \otimes T_B \right] = \alpha_A \cdot \alpha_B \text{tr} \left[T_A^\dagger T_A \right] \text{tr} \left[T_B^\dagger T_B \right] = u_{A \rightarrow A}(\mathcal{E})u_{B \rightarrow B}(\mathcal{E})$. As $u(\mathcal{E}_A) = u_{A \rightarrow A}(\mathcal{E})$ and $u(\mathcal{E}_B) = u_{B \rightarrow B}(\mathcal{E})$ for any channel this completes the proof. \square

Putting this all together, we have the first key property of the correlation unitarity measure we first proposed in equation (3.7). Namely, that it vanishes for a product channel.

Corollary 3.2. *The correlation unitarity $u_c(\mathcal{E}) := u_{AB \rightarrow AB}(\mathcal{E}) - u_{A \rightarrow A}(\mathcal{E})u_{B \rightarrow B}(\mathcal{E})$ of a product channel $\mathcal{E}_A \otimes \mathcal{E}_B$ is $u_c(\mathcal{E}_A \otimes \mathcal{E}_B) = 0$.*

Proof. This follows directly from Theorem 3.4. \square

This is a key property for a correlation measure, as it should always be zero for channel that generates no correlations – which is a product channel.

In the following chapter, we shall make use of the above decompositions of unitarity for our benchmarking protocols to estimate local subunitarities and the correlation unitarity. But before discussing the protocol, we first give core properties of our correlation measure that demonstrate its usefulness for assessing the correlation structure of a given channel.

3.3 Correlation unitarity of bipartite quantum channels

The correlation unitarity, $u_c(\mathcal{E}) := u_{AB \rightarrow AB}(\mathcal{E}) - u_{A \rightarrow A}(\mathcal{E})u_{B \rightarrow B}(\mathcal{E})$, has now been fully defined in terms of its constituent subunitarities, and we now address the core properties of this measure. The following result shows that it obeys natural conditions.

Theorem 3.5 (Properties of correlation unitarity). *For any bipartite quantum channel \mathcal{E}_{AB} , the correlation unitarity is bounded as $u_c(\mathcal{E}_{AB}) \leq 1$, and is invariant under local unitary transformations on either the input or output systems. Moreover $u_c(\mathcal{E}_{AB}) = 0$ for product channels and $u_c(\mathcal{E}_{AB}) = 1$ when \mathcal{E}_{AB} is the SWAP channel modulo local unitary changes of bases.*

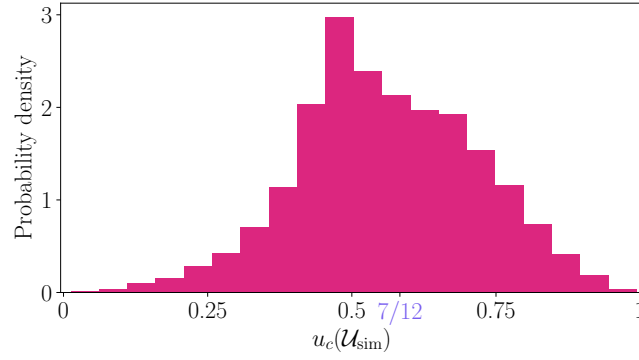


Figure 3.1: Distribution of u_c for 2–qubit unitaries. We plot the histogram of values of $u_c(\mathcal{U}_{\text{sim}})$ for 20,000 random 2 qubit unitaries, \mathcal{U}_{sim} . The correlation unitarities lie between 0 and 1, and must take the value $u_c(\mathcal{E}_A \otimes \mathcal{E}_B) = 0$ for product channels, and $u_c(\text{SWAP}) = 1$ for the *SWAP* channel. The value of u_c is invariant under local unitary changes of basis. The upper bound for 2 qubit separable channels is $u_c^{\text{sep}} \leq 7/12$, and is also shown on the plot. We sampled using the methods of [2] and simulated using QuTip [3].

We have shown that the correlation unitarity vanishes for product channels, $u_c(\mathcal{E}_A \otimes \mathcal{E}_B) = 0$, in Corollary 3.2. Under our measure the *SWAP* channel generates the strongest correlations, which follows from the fact it perfectly transfers all information between the subsystems. Further, the correlation unitarity is invariant under local unitaries on the subsystems. Final rotations on the subsystems do not reduce the correlating effect of a channel, and therefore it is pleasing that such operations do not change the value of the correlation unitarity. Together these properties make u_c a good working measure of the coherence of correlations within a channel, and importantly within Chapter 4 we shall see it is accessible through a randomized benchmarking protocol.

For the remaining properties to be proven, we tackle them individually with the following lemmas.

Lemma 3.3. *The correlation unitarity of a quantum channel, \mathcal{E}_{AB} is bounded as $u_c(\mathcal{E}_{AB}) \leq 1$.*

Proof. Consider the subunitarity $u_{AB \rightarrow AB}(\mathcal{E}_{AB}) = \alpha_{AB} \text{tr} [T_{AB \rightarrow AB}^\dagger T_{AB \rightarrow AB}]$. The matrix $T_{AB \rightarrow AB}$ has dimension $(d_A^2 - 1)(d_B^2 - 1) \times (d_A^2 - 1)(d_B^2 - 1)$. Using Holder’s inequality [123], we can bound this subunitarity as

$$\text{tr} [T_{AB \rightarrow AB}^\dagger T_{AB \rightarrow AB}] \leq \|T_{AB \rightarrow AB}\|_\infty \|T_{AB \rightarrow AB}\|_1 \leq (d_A^2 - 1)(d_B^2 - 1) \quad (3.33)$$

where we have used in the above that the eigenvalues of $T_{AB \rightarrow AB}$ have modulus at most 1 [124], and the rank of $T_{AB \rightarrow AB}$ is at most the number of columns or rows. Therefore we must have $u_{AB \rightarrow AB}(\mathcal{E}_{AB}) \leq 1$. From the non-negativity of the Hilbert-Schmidt inner product, the subunitarities $u_{A \rightarrow A}$ and $u_{B \rightarrow B}$ are strictly non-negative. Putting this together, we have $u_c = u_{AB \rightarrow AB} - u_{A \rightarrow A} \cdot u_{B \rightarrow B} \leq u_{AB \rightarrow AB} \leq 1$, which completes the proof. \square

Lemma 3.4. *The correlation unitarity of the SWAP channel takes a value of $u_c(\text{SWAP}) = 1$*

Proof. From equation (3.25) we have $\text{SWAP} = \sum_{\nu,\mu} |\mathbf{Y}_\nu \otimes \mathbf{X}_\mu\rangle\langle \mathbf{X}_\nu \otimes \mathbf{Y}_\mu|$. This makes the unital block T a matrix with 1 along the minor diagonal and zero everywhere else. We can then simply read off that $u_{AB \rightarrow AB} = u_{A \rightarrow B} = u_{B \rightarrow A} = 1$ and all other subunitarities are zero. The correlation unitarity is then $u_c = u_{AB \rightarrow AB} - u_{A \rightarrow A} \cdot u_{B \rightarrow B} = 1$. \square

Lemma 3.5. *Any channel \mathcal{E} with $u_{AB \rightarrow AB}(\mathcal{E}) = u_{A \rightarrow B}(\mathcal{E}) = u_{B \rightarrow A}(\mathcal{E}) = 1$ is equivalent to the SWAP channel up to local unitaries.*

Proof. From Theorem 3.3 under the given conditions the channel is unitary, and all other subunitarities are zero. We can use that $u_{A \rightarrow B}(\mathcal{E}) = u_{A \rightarrow A}(\text{SWAP} \circ \mathcal{E}) = 1$ and similarly $u_{B \rightarrow B}(\text{SWAP} \circ \mathcal{E}) = 1$. With fixed system dimensions the unitarity equals 1 only for a unitary, therefore we deduce that $\text{SWAP} \circ \mathcal{E} = \mathcal{U}_A \otimes \mathcal{U}_B$, e.g. a product channel of local unitaries on each subsystem. This implies that $\mathcal{E} = \text{SWAP} \circ \mathcal{U}_A \otimes \mathcal{U}_B$, since $\text{SWAP}^2 = \text{id}$. \square

Lemma 3.6. *The correlation unitarity $u_c(\mathcal{E})$ of any quantum channel \mathcal{E} is invariant under local unitaries.*

Proof. Firstly, the local subunitarities of any channel $u_{A \rightarrow A}(\mathcal{E})$ & $u_{B \rightarrow B}(\mathcal{E})$ are invariant under local unitaries from Corollary 3.1. Therefore it remains to prove that u_{AB} is invariant. We can write the Liouville representation of any product unitary in the our basis as $\mathcal{U}_{i,A} \otimes \mathcal{U}_{i,B} = (1 \oplus \mathcal{O}_{i,A}) \otimes (1 \oplus \mathcal{O}_{i,B})$ where $\mathcal{O}_{i,X}$ are unitary matrices of dimension $(d_X^2 - 1) \times (d_X^2 - 1)$ obeying $\mathcal{O}_{i,X} \mathcal{O}_{i,X}^\dagger = \mathbb{1}_{T_X}$. Product channels have the additional property that $T_{AB, \mathcal{U}_i} = T_{A, \mathcal{U}_i} \otimes T_{B, \mathcal{U}_i} = \mathcal{O}_{i,A} \otimes \mathcal{O}_{i,B}$. We define a channel $\mathcal{E}' = \mathcal{U}_{1,A} \otimes \mathcal{U}_{1,B} \circ \mathcal{E} \circ \mathcal{U}_{2,A} \otimes \mathcal{U}_{2,B}$: namely, the channel with product unitaries before and after. The product unitaries will have block diagonal unital blocks which can be seen from considering their only non-zero subunitarities are $u_{A \rightarrow A}$, $u_{B \rightarrow B}$, & $u_{AB \rightarrow AB}$. Because of this simple structure the sub-unital block T_{AB} of \mathcal{E}' is

$$T_{AB, \mathcal{E}'} = T_{AB, \mathcal{U}_1} T_{AB, \mathcal{E}} T_{AB, \mathcal{U}_2} = \mathcal{O}_{1,A} \otimes \mathcal{O}_{1,B} T_{AB, \mathcal{E}} \mathcal{O}_{2,A} \otimes \mathcal{O}_{2,B}. \quad (3.34)$$

We can now calculate the required subunitarity $u_{AB}(\mathcal{E}') = \alpha_{AB} \text{tr} \left[T_{AB, \mathcal{E}'}^\dagger T_{AB, \mathcal{E}'} \right]$. From the cyclical properties of the trace,

$$\begin{aligned} u_{AB}(\mathcal{E}') &= \alpha_{AB} \text{tr} \left[T_{AB, \mathcal{E}}^\dagger T_{AB, \mathcal{E}} \mathcal{O}_{2,A}^\dagger \otimes \mathcal{O}_{2,B}^\dagger \mathcal{O}_{2,A} \otimes \mathcal{O}_{2,B} \right], \\ &= \alpha_{AB} \text{tr} \left[T_{AB, \mathcal{E}}^\dagger T_{AB, \mathcal{E}} \right] = u_{AB}(\mathcal{E}). \end{aligned} \quad (3.35)$$

This implies u_c is invariant under local unitaries. \square

3.3.1 Witness of non-separability

Under our measure, the *SWAP* channel is the farthest from being a product channel, which is consistent with the fact that it perfectly transfers quantum information from one subsystem to the other. However, we can also consider intermediate regimes where no quantum information is transferred, but the channel cannot be written in a product form. This is when the bipartite channel is *separable*, namely it can be written as

$$\mathcal{E}_{AB} = \sum_k p_k \mathcal{E}_k \otimes \mathcal{F}_k, \quad (3.36)$$

for some probability distribution (p_k) , with local channels \mathcal{E}_k and \mathcal{F}_k on A and B respectively. Channels that cannot be written in this form are therefore *non-separable* channels.

The class of separable channels are also known as Local Operations with Shared Randomness (LOSR) [93, 94]. The above definition generalizes that of separable states, and defines a convex subset of channels. It turns out that the correlation unitarity is strictly bounded over separable channels as the following establishes.

Theorem 3.6 (Correlation unitarity is a witness of non-separability). *Given a bipartite quantum system AB with subsystems A and B of dimensions d_A and d_B respectively, for a separable quantum channel, \mathcal{E}_{AB} , we have that*

$$u_c(\mathcal{E}_{AB}) \leq C(d_A, d_B) \leq \frac{17}{24} < 1, \quad (3.37)$$

where

$$C(d_A, d_B) = \beta_A(1 + \beta_B) \left(1 - \frac{1}{\min(d_A^2, d_B^2)}\right) + \frac{1}{4} \quad (3.38)$$

where $\beta_i = \frac{1}{d_i^2 - 1}$ for $d_i = 2$ or $\beta_i = \frac{d_i}{d_i^2 - 1}$ otherwise.

The proof of this bound is non-trivial, and we will provide it directly after this discussion. This bound is not tight in general, and we provide sharper bounds in terms of the subsystem dimensions. The $d_A = d_B = 3$ qutrit case provides the upper bound in $C(d_A, d_B)$ and could be improved, albeit via a non-trivial analysis of qutrit channels.

The consequence of the result is that, if the correlation unitarity can be efficiently estimated, then obtaining values above the upper bound witnesses non-separability in the channel. This provides a practical way to certify quantum information transfer between A and B .

The correlation unitarity, $u_c(\mathcal{E}_{AB})$, is a witness of non-separability as it has a non-trivial value $C(d_A, d_B)$ which cannot be exceeded if the channel \mathcal{E}_{AB} is separable. Therefore, for an unknown channel if we measure $u_c(\mathcal{E}_{AB}) \geq C(d_A, d_B)$, we can guarantee that ‘quantum’ correlations have occurred in the channel, rather than purely ‘classical’ correlating effects.

The bound also relates to recent work on entanglement theory, where the operations most studied are the set of Local Operations and Classical Communication (LOCC). Due to the limitations of LOCC channels when it comes to analysing Bell non-locality [91], it has been argued that LOSR channels provide a more sensible set. However, as LOSR channels are precisely the set of separable channels then any violation of the bound in Theorem 3.6 implies the consumption of a resource state with respect to LOSR.

Proof of correlation unitarity as a witness of non-separability

The proof of the upper bound on correlation unitarity for separable channels turns out to be non-trivial, and relies on bounds on the inner product of T -matrices, the unital portion of quantum channels. We first establish basic ingredients we need for the analysis.

Definition 3.4. For any quantum channel, $\mathcal{E} : \mathcal{B}(\mathcal{H}_X) \rightarrow \mathcal{B}(\mathcal{H}_Y)$, the Choi-Jamiołkowski state $\mathcal{J}(\mathcal{E})$ given by

$$\mathcal{J}(\mathcal{E}) := \mathcal{E} \otimes id(\psi). \quad (3.39)$$

for the input system with dimension d_X , $id : \mathcal{B}(\mathcal{H}_X) \rightarrow \mathcal{B}(\mathcal{H}_X)$ is the identity channel, and the state $\psi = |\psi\rangle\langle\psi|$ is a generalized Bell state, $|\psi\rangle := \frac{1}{\sqrt{d_X}} \sum_i^{d_X} |i\rangle \otimes |i\rangle$ with computational basis states $\{|i\rangle\}$ [32, 61].

The Choi-Jamiołkowski state is clearly a quantum state, as it is simply the output from a bipartite quantum channel, $\mathcal{E} \otimes id$, acting on a valid input state. However the Choi state is also a complete representation of the channel, \mathcal{E} , as it encodes all the information about how the channel acts. We can see this by explicitly substituting in the generalized Bell state, ψ . For any channel, \mathcal{E} , we then have

$$\begin{aligned} \mathcal{J}(\mathcal{E}) &= \frac{1}{d_X} \sum_{i,j}^{d_X} \mathcal{E} \otimes id(|i\rangle\langle j| \otimes |i\rangle\langle j|), \\ &= \frac{1}{d_X} \sum_{i,j}^{d_X} \mathcal{E}(|i\rangle\langle j|) \otimes |i\rangle\langle j|. \end{aligned} \quad (3.40)$$

The set $\{|i\rangle\langle j|\}$ forms a complete basis for the input system. The Choi state tracks how the channel \mathcal{E} acts on each element of this basis, using the second subsystem as an index. Therefore the Choi state, $\mathcal{J}(\mathcal{E})$, captures all possible information about the channel, \mathcal{E} .

The purity of the Choi state can be related to the unitarity, however here we use it for the more abstract goal of bounding the T -matrices of channels. The following lemma relates the Choi state to our favourite basis.

Lemma 3.7. *For any channel $\mathcal{E} : \mathcal{B}(\mathcal{H}_X) \rightarrow \mathcal{B}(\mathcal{H}_Y)$ the Choi-Jamiołkowski state can be expressed in the X_ν basis as*

$$\mathcal{J}(\mathcal{E}) = \frac{1}{d_X} \sum_{\nu=0}^{d_X^2} \mathcal{E}(X_\nu) \otimes X_\nu^*, \quad (3.41)$$

where $X_\mu = (X_0 = \mathbb{1}/\sqrt{d}, X_i)$ is a completely orthonormal basis for \mathcal{H}_X .

Proof. We have $\mathcal{J}(\mathcal{E}) := \mathcal{E} \otimes id(\psi) = \mathcal{E} \otimes id(\frac{1}{d_X} |\mathbf{1}_{d_X}\rangle\langle\mathbf{1}_{d_X}|)$, but one can directly show $|\mathbf{1}_{d_X}\rangle\langle\mathbf{1}_{d_X}| = \sum_\nu X_\nu \otimes X_\nu^*$. This follows from $\text{tr}[X_\nu^\dagger \otimes X_\mu^\dagger |\mathbf{1}_d\rangle\langle\mathbf{1}_d|] = \langle\mathbf{1}|X_\nu^\dagger X_\mu^*\rangle = \text{tr}[X_\nu^\dagger X_\mu^*]$ and therefore $|\mathbf{1}_d\rangle\langle\mathbf{1}_d| = \sum_{\mu,\nu} \text{tr}[X_\nu^\dagger X_\mu^*] X_\nu \otimes X_\mu$. However $\sum_\mu \text{tr}[X_\nu^\dagger X_\mu^*] X_\mu = \sum_\mu \text{tr}[X_\mu^\dagger X_\nu^*] X_\mu = X_\nu^*$ since $\text{tr}[M^T] = \text{tr}[M]$ for any matrix M , and the result follows. \square

We now have the following estimates for the magnitude of the overlap between unital blocks of arbitrary channels. We will then relate this to the unitarity of mixtures of channels which appear when considering separable channels.

Lemma 3.8. *Given two channels \mathcal{E}_1 and \mathcal{E}_2 with unital blocks in the Liouville representation T_1 and T_2 , for the Hilbert-Schmidt inner product between them we have*

$$-d \leq \langle T_1, T_2 \rangle \leq d^2 - 1, \quad (3.42)$$

where d is the dimension of the Hilbert space.

We shall use this lemma to establish the upper bound on correlation unitarity for separable channels. However, we conjecture a stronger result that for any two quantum channels $\mathcal{E}_1, \mathcal{E}_2$ that $\langle T_1, T_2 \rangle \geq -1$. This, for example implies the bound for optimal inversion of the coherence vector of a quantum state [125, 126] as a special case. The analyse to establish this sharper bound appears to be non-trivial. Since it is not essential to our work we leave it as an open problem. We do, however, establish this lower bound for a subset of channels (see Lemma 3.9 below).

Proof. In the Choi representation we have

$$\mathcal{J}(\mathcal{E}_1) = \frac{1}{d} \sum_{\mu}^{d^2} \mathcal{E}_1(X_\mu) \otimes X_\mu^* \quad \text{and} \quad \mathcal{J}(\mathcal{E}_2) = \frac{1}{d} \sum_{\mu}^{d^2} \mathcal{E}_2(X_\mu) \otimes X_\mu^* \quad (3.43)$$

with $X_\mu = (X_0 = \mathbb{1}/\sqrt{d}, X_i)$. Therefore we have that

$$\text{tr}[\mathcal{J}(\mathcal{E}_1)^\dagger \mathcal{J}(\mathcal{E}_2)] = \frac{1}{d^2} \sum_{\mu,\nu}^{d^2} \text{tr}[\mathcal{E}_1(X_\mu)^\dagger \mathcal{E}_2(X_\nu)] \text{tr}[X_\mu^T X_\nu^*]. \quad (3.44)$$

Since Choi matrices are positive semidefinite, then so is the above quantity. Furthermore, $\text{tr}[X_\mu^T X_\nu^*] = \delta_{\mu\nu}$ and so

$$\text{tr}[\mathcal{J}(\mathcal{E}_1)^\dagger \mathcal{J}(\mathcal{E}_2)] = \frac{1}{d^2} \sum_{\mu}^{d^2} \text{tr}[\mathcal{E}_1(X_\mu)^\dagger \mathcal{E}_2(X_\mu)] \geq 0, \quad (3.45)$$

and therefore we have

$$\sum_{\mu}^{d^2} \langle \mathcal{E}_1(\mathbf{X}_{\mu}) | \mathcal{E}_2(\mathbf{X}_{\mu}) \rangle = \sum_{\mu}^{d^2} \text{tr}[\mathcal{E}_1(\mathbf{X}_{\mu})^{\dagger} \mathcal{E}_2(\mathbf{X}_{\mu})] \geq 0. \quad (3.46)$$

Now we look at $\langle T_1, T_2 \rangle = \text{tr}[T_1^{\dagger} T_2]$ and expand with respect to same basis.

$$\begin{aligned} \langle T_1, T_2 \rangle &= \sum_{i=1}^{d^2-1} \langle \mathbf{X}_i | T_1^{\dagger} T_2 | \mathbf{X}_i \rangle = \sum_{i=1}^{d^2-1} \langle \mathcal{E}_1(\mathbf{X}_i) | \mathcal{E}_2(\mathbf{X}_i) \rangle, \\ &= \sum_{\mu}^{d^2} \langle \mathcal{E}_1(\mathbf{X}_{\mu}) | \mathcal{E}_2(\mathbf{X}_{\mu}) \rangle - \langle \mathcal{E}_1(\mathbf{X}_0) | \mathcal{E}_2(\mathbf{X}_0) \rangle. \end{aligned} \quad (3.47)$$

Then it follows that

$$\langle T_1, T_2 \rangle \geq - \langle \mathcal{E}_1(\mathbf{X}_0) | \mathcal{E}_2(\mathbf{X}_0) \rangle. \quad (3.48)$$

However,

$$| \langle \mathcal{E}_1(\mathbf{X}_0) | \mathcal{E}_2(\mathbf{X}_0) \rangle |^2 \leq \langle \mathcal{E}_1(\mathbf{X}_0) | \mathcal{E}_1(\mathbf{X}_0) \rangle \langle \mathcal{E}_2(\mathbf{X}_0) | \mathcal{E}_2(\mathbf{X}_0) \rangle. \quad (3.49)$$

and since $\langle \mathcal{E}_i(\frac{\mathbf{1}}{d}) | \mathcal{E}_i(\frac{\mathbf{1}}{d}) \rangle \leq 1$, we deduce that

$$| \left\langle \mathcal{E}_1 \left(\frac{\mathbf{1}}{\sqrt{d}} \right) \middle| \mathcal{E}_2 \left(\frac{\mathbf{1}}{\sqrt{d}} \right) \right\rangle | \leq d, \quad (3.50)$$

and so we obtain the lower bound of

$$-d \leq \langle T_1, T_2 \rangle. \quad (3.51)$$

The upper bound follows directly from Holder's inequality

$$\langle T_1, T_2 \rangle \leq \|T_1\|_{\infty} \|T_2\|_1 \leq (d^2 - 1) \quad (3.52)$$

where we have used in the above that the eigenvalues of T_1 and T_2 have modulus at most 1, and their rank is at most $d^2 - 1$. \square

Having established bounds on the inner product of two T -matrices for any two arbitrary channels, we now prove an improved bound for two subsets of quantum channels. This will increase the sharpness of our bound for separable channels with lower dimensions.

Lemma 3.9. *Let \mathcal{E}_1 and \mathcal{E}_2 be two quantum channels. If we have that either*

1. *One of the channels is unital,*
2. *The channels are arbitrary $d = 2$ qubit channels,*

then it follows that $-1 \leq \langle T_1, T_2 \rangle \leq d^2 - 1$.

The proof of this is as follows.

Proof. If one of the channels, \mathcal{E}_1 say, is unital then

$$\langle T_1, T_2 \rangle \geq -\langle \mathcal{E}_1(\mathbf{X}_0) | \mathcal{E}_2(\mathbf{X}_0) \rangle = -\langle \mathbf{X}_0 | \mathcal{E}_2(\mathbf{X}_0) \rangle = -\langle \mathbf{X}_0 | \mathbf{X}_0 \rangle = -1, \quad (3.53)$$

where we use the orthonormality $\langle \mathbf{X}_0 | \mathbf{X}_i \rangle$ for all $i = 1, \dots, d^2 - 1$ and the fact that if \mathcal{E}_1 is unital then $\mathcal{E}_1(\mathbf{X}_0) = \mathbf{X}_0$.

Now suppose that both \mathcal{E}_1 and \mathcal{E}_2 are qubit channels. Given any qubit channel \mathcal{E} , the corresponding Choi state take the form

$$\mathcal{J}(\mathcal{E}) = \frac{1}{4}(\mathbb{1} + \mathbf{x} \cdot \boldsymbol{\sigma} \otimes \mathbb{1} + \sum_{i,j} T_{ij} \sigma_i \otimes \sigma_j), \quad (3.54)$$

where $\{\sigma_i\}$ are the Pauli matrices. As shown in [127] it is possible to perform local unitary changes $U_A \otimes U_B$ of basis so that

$$\mathcal{U}_A \otimes \mathcal{U}_B[\mathcal{J}(\mathcal{E})] = \frac{1}{4}(\mathbb{1} + \mathbf{x} \cdot \boldsymbol{\sigma} \otimes \mathbb{1} + \sum_i t_i \sigma_i \otimes \sigma_i), \quad (3.55)$$

and so the channel is described, modulo local choices of basis, by the two vectors \mathbf{x} and $\mathbf{t} = (t_1, t_2, t_3)$. The link between T_{ij} and \mathbf{t} is that $T = O_A \text{diag}(t_1, t_2, t_3) O_B^T$ for orthogonal matrices O_A, O_B corresponding to the local unitary rotations. It can be shown that if $\mathcal{J}(\mathcal{E})$ is a valid quantum state (and so \mathcal{E} a valid quantum channel) the vector \mathbf{x} lies in the Bloch sphere, and \mathbf{t} lies in a particular tetrahedron \mathcal{T} in \mathbf{R}^3 . Moreover, if $\mathbf{x} = \mathbf{0}$ then every $\mathbf{t} \in \mathcal{T}$ corresponds to a valid quantum state. Since \mathbf{x} corresponds to the non-unitality of the quantum channel \mathcal{E} , this implies that if \mathcal{E} is a quantum channel with non-unitality vector \mathbf{x} and T -matrix T then there exists another quantum channel \mathcal{E}_u with the same T -matrix, but which is unital. This implies that for the inner product $\langle T_1, T_2 \rangle$ we can without loss of generality assume that one channel is unital, and thus from the previous part of our proof we obtain $-1 \leq \langle T_1, T_2 \rangle$. The upper bound for $\langle T_1, T_2 \rangle$ is unchanged from the previous lemma. \square

The final component we need before tackling the general bound is a simple form for the correlation unitarity of separable channels.

Lemma 3.10. *For a bipartite separable channel $\mathcal{E} := \sum_i^r p_i \mathcal{E}_{A,i} \otimes \mathcal{E}_{B,i}$ the correlation unitarity $u_c(\mathcal{E})$ can be decomposed as*

$$u_c(\mathcal{E}) = \alpha_A \alpha_B \left(\sum_{i,j}^{r,r} p_i p_j \langle T_A^i, T_A^j \rangle \langle T_B^i, T_B^j \rangle - \sum_{i,j}^{r,r} p_i p_j \langle T_A^i, T_A^j \rangle \sum_{m,n}^{r,r} p_m p_n \langle T_B^m, T_B^n \rangle \right) \quad (3.56)$$

where T_A^i is the unital block in the Liouville representation of $\mathcal{E}_{A,i}$ and T_B^i is the unital block of $\mathcal{E}_{B,i}$.

Proof. From definition the correlation unitarity is

$$u_c(\mathcal{E}) = \alpha_A \alpha_B (\langle T_{AB \rightarrow AB}, T_{AB \rightarrow AB} \rangle - \langle T_{A \rightarrow A}, T_{A \rightarrow A} \rangle \langle T_{B \rightarrow B}, T_{B \rightarrow B} \rangle). \quad (3.57)$$

Since \mathcal{E} is separable, in the Liouville representation linearity implies

$$|\mathcal{E}(\rho)\rangle = \left| \sum_i^r p_i \mathcal{E}_{A,i} \otimes \mathcal{E}_{B,i}(\rho) \right\rangle = \sum_i^r p_i \mathcal{E}_{A,i} \otimes \mathcal{E}_{B,i} |\rho\rangle = \mathcal{E} |\rho\rangle \quad (3.58)$$

therefore it follows that the relevant subunital blocks of the channel are simply the weighted sum of the subunital blocks of each product channel:

$$T_{AB \rightarrow AB} = \sum_i^r p_i T_A^i \otimes T_B^i, \quad T_{A \rightarrow A} = \sum_i^r p_i T_A^i, \quad T_{B \rightarrow B} = \sum_i^r p_i T_B^i, \quad (3.59)$$

where T_A^i is the unital block in the Liouville representation of $\mathcal{E}_{A,i}$ and T_B^i is the unital block in the Liouville representation of $\mathcal{E}_{B,i}$. Thus the correlation unitarity is

$$\begin{aligned} u_c(\mathcal{E}_{AB}) &= \alpha_A \alpha_B \left(\sum_{i,j}^{r,r} p_i p_j \langle T_A^i \otimes T_B^i, T_A^j \otimes T_B^j \rangle - \sum_{i,j}^{r,r} p_i p_j \langle T_A^i, T_A^j \rangle \sum_{m,n}^{r,r} p_m p_n \langle T_B^m, T_B^n \rangle \right), \\ &= \alpha_A \alpha_B \left(\sum_{i,j}^{r,r} p_i p_j \langle T_A^i, T_A^j \rangle \langle T_B^i, T_B^j \rangle - \sum_{i,j}^{r,r} p_i p_j \langle T_A^i, T_A^j \rangle \sum_{m,n}^{r,r} p_m p_n \langle T_B^m, T_B^n \rangle \right). \end{aligned} \quad (3.60)$$

Which completes the proof. \square

With the preceding ingredients, and particularly with the compact form given above for the correlation unitarity of separable channels, we are ready to prove the general bound. We would expect that such a bound would exist, because the correlation unitarity quantifies the strength of the correlations in the channel in terms of quantum information. As separable channels can only produce ‘classical’ correlations they should not saturate the value of the correlation unitarity as the maximally correlating *SWAP* channel does.

The following proof is perhaps the most difficult to follow in this work, as we have stripped away all physics to deal with a probability distribution $\{p_i\}$ and the magnitude of the inner products $t_{ij} = \langle T_A^i, T_A^j \rangle$ and $s_{ij} = \langle T_B^i, T_B^j \rangle$. The correlation unitarity of a separable channel, u_c , is then given by two terms

$$u_c = f(\{p_i\}, \{t_{ij}\}, \{s_{ij}\}) - f(\{p_i\}, \{t_{ij}\}) f(\{p_i\}, \{s_{ij}\}) \quad (3.61)$$

for three non-negative functions $f(\dots)$ with $0 \leq f(\dots) \leq 1$, (i.e. the subunitarities). In order to upper bound u_c overall we need to maximize the first term while minimizing the second.

However, the way the terms interact is subtle. Naively maximizing the first term also

maximizes the second, and vice versa for minimizing the second term. Therefore we have to find a way to bound the first term using the second, and then perform an overall maximization.

We proceed by separating out the contributions to $f(\{p_i\}, \{t_{ij}\}, \{s_{ij}\})$ from when t_{ij} is positive (t_{ii} or $t_{+,ij}$) and negative ($t_{-,ij}$). We then upper bound each of these contributions in terms of just $f(\{p_i\}, \{t_{ij}\})$, the summation $\sum_i p_i^2$ for the probability distribution $\{p_i\}$, and some dimensional factors. This essentially gives us a total upper bound for u_c in terms of $f(\{p_i\}, \{t_{ij}\})$, $f(\{p_i\}, \{s_{ij}\})$ and $\{p_i\}$. This is a lot easier to work with and we find it leads to a non-trivial bound on u_c in terms of the dimensions of the subsystems. Finally we explicitly calculate the value of the upper bound for different dimensions to find an overall numerical upper bound.

Proof. (Of Theorem 3.6) From Lemma 3.10,

$$u_c(\mathcal{E}_{AB}) = \alpha_A \alpha_B \left(\sum_{i,j}^{r,r} p_i p_j \langle T_A^i, T_A^j \rangle \langle T_B^i, T_B^j \rangle - \sum_{i,j}^{r,r} p_i p_j \langle T_A^i, T_A^j \rangle \sum_{m,n}^{r,r} p_m p_n \langle T_B^m, T_B^n \rangle \right) \quad (3.62)$$

where T_A^i is the unital block in the Liouville representation of $\mathcal{E}_{A,i}$ and T_B^i is the unital block of $\mathcal{E}_{B,i}$. To simplify notation we label the normalized inner products

$$t_{ij} := \alpha_A \langle T_A^i, T_A^j \rangle \text{ and } s_{ij} := \alpha_B \langle T_B^i, T_B^j \rangle, \quad (3.63)$$

and define $A := \sum_{i,j}^{r,r} p_i p_j t_{ij}$ and $B := \sum_{i,j}^{r,r} p_i p_j s_{ij}$. In this notation the correlation unitarity of the separable channel is just

$$u_c(\mathcal{E}_{AB}) = \sum_{i,j}^{r,r} p_i p_j t_{ij} s_{ij} - AB. \quad (3.64)$$

From Lemma 3.8 the range of any particular t_{ij} is

$$-\beta_A \leq t_{ij} \leq 1 \quad (3.65)$$

where $\beta_A = d_A \alpha_A$ applies to all channels and $\beta_A = \alpha_A$ holds for the case of qubit channels or if one of the channels is unital. Additionally from the non-negativity of the Hilbert Schmidt inner product $t_i \equiv t_{ii} \geq 0$. Similarly for the B subsystem: $-\beta_B \leq s_{ij} \leq 1$ and $s_i \equiv s_{ii} \geq 0$.

We now bound the first term in equation (3.64) in relation to the second. Out of the r^2 possible terms in the first term there are r terms that are equal to $p_i^2 t_i s_i$ (namely when $i = j$). Now suppose that out of the $r^2 - r$ remaining terms there are k terms where t_{ij} is negative: $t_{-,m}$, ($m = \{0, 1, \dots, k-1, k\}$), and $r^2 - (r + k)$ other terms where t_{ij} is positive: $t_{+,n}$,

($n = \{0, 1, \dots, r^2 - (r+k) - 1, r^2 - (r+k)\}$). We can then write the correlation unitarity as

$$\begin{aligned}
u_c(\mathcal{E}_{AB}) &= \sum_i^r p_i^2 t_i s_i + \sum_{i \neq j}^{r^2-r} p_i p_j t_{ij} s_{ij} - AB, \\
&= \sum_i^r p_i^2 t_i s_i + \sum_{m=(ij), i \neq j}^k p_i p_j t_{-,m} s_m + \sum_{n=(ij), i \neq j}^{r^2-r-k} p_i p_j t_{+,n} s_n - AB, \\
&= \sum_i^r p_i^2 t_i s_i - \sum_{m=(ij), i \neq j}^k p_i p_j |t_{-,m}| s_m + \sum_{n=(ij), i \neq j}^{r^2-r-k} p_i p_j t_{+,n} s_n - AB.
\end{aligned} \tag{3.66}$$

We now bound the summation of positive and negative $t_{i \neq j}$ terms. As all $t_{-,m} \leq 0$ then since $|t_{-,m}| \leq \beta_A$ we can bound the summation of negative terms as

$$\sum_{m=(ij), i \neq j}^k p_i p_j |t_{-,m}| \leq \sum_{m=(ij), i \neq j}^k \beta_A p_i p_j \leq \sum_{i \neq j}^{r^2-r} \beta_A p_i p_j = \beta_A (1 - \sum_i^r p_i^2) \tag{3.67}$$

where we have maximized k to include all $r^2 - r$ possible terms, and used the simple relation that $\sum_i^r p_i^2 + \sum_{i \neq j}^{r^2-r} p_i p_j = 1$. From definition, $A = \sum_i^r p_i^2 t_i + \sum_{i \neq j}^{r^2-r} p_i p_j t_{ij}$ therefore the whole summation of cross terms can be written as

$$\sum_{i \neq j}^{r^2-r} p_i p_j t_{ij} = \sum_{n=(ij), i \neq j}^{r^2-r-k} p_i p_j t_{+,n} - \sum_{m=(ij), i \neq j}^k p_i p_j |t_{-,m}| = A - \sum_i^r p_i^2 t_i. \tag{3.68}$$

From this we can bound the summation of the positive terms using the previous bound in equation (3.67):

$$\begin{aligned}
\sum_{n=(ij), i \neq j}^{r^2-r-k} p_i p_j t_{+,n} &= A - \sum_i^r p_i^2 t_i + \sum_{m=(ij), i \neq j}^k p_i p_j |t_{-,m}|, \\
\sum_{n=(ij), i \neq j}^{r^2-r} p_i p_j t_{+,n} &\leq A - \sum_i^r p_i^2 t_i + \beta_A (1 - \sum_i^r p_i^2).
\end{aligned} \tag{3.69}$$

Since both $t_{+,n} \geq 0$ and $|t_{-,m}| \geq 0$ and all elements $-\min(\beta_B, \sqrt{s_i s_j}) \leq s_{i \neq j} \leq \sqrt{s_i s_j} \leq 1$, then we can bound the summation containing $t_{+,n} s_n$ elements as

$$\sum_{n=(ij), i \neq j}^{r^2-r-k} p_i p_j t_{+,n} s_n \leq \sum_{n=(ij), i \neq j}^{r^2-r-k} p_i p_j t_{+,n} \leq A - \sum_i^r p_i^2 t_i + \beta_A (1 - \sum_i^r p_i^2) \tag{3.70}$$

and the summation containing $t_{-,m} s_m$ elements (assuming $\sqrt{s_i s_j} \geq \beta_B$)

$$- \sum_{m=(ij), i \neq j}^k p_i p_j |t_{-,m}| s_m \leq \beta_B \sum_{m=(ij), i \neq j}^k p_i p_j |t_{-,m}| \leq \beta_B (\beta_A (1 - \sum_i^r p_i^2)). \tag{3.71}$$

Putting all this together we get a bound on the correlation unitarity of

$$\begin{aligned} u_c(\mathcal{E}_{AB}) &\leq \sum_i^r p_i^2 t_i s_i + \beta_B(\beta_A(1 - \sum_i^r p_i^2)) + A - \sum_i^r p_i^2 t_i + \beta_A(1 - \sum_i^r p_i^2) - AB, \\ &\leq \sum_i^r p_i^2 t_i (s_i - 1) + \beta_A(1 + \beta_B)(1 - \sum_i^r p_i^2) + A(1 - B). \end{aligned} \quad (3.72)$$

With no loss of generality we can set $A \leq B$ as A and B are interchangeable. Therefore we have that $A(1 - B) \leq B(1 - B)$. As $0 \leq B \leq 1$, this is maximized when $B = 1/2$. Additionally as $s_i \leq 1$ then $s_i - 1 \leq 0$ and the whole first term is negative. Therefore

$$u_c(\mathcal{E}_{AB}) \leq \beta_A(1 + \beta_B)(1 - \sum_i^r p_i^2) + \frac{1}{4}. \quad (3.73)$$

Further from the Cauchy-Schwartz inequality $\sum_i^r p_i^2 \geq \frac{1}{r} \geq \frac{1}{\min(d_A^2, d_B^2)}$. Putting this together we have:

$$u_c(\mathcal{E}_{AB}) \leq \beta_A(1 + \beta_B)(1 - \frac{1}{\min(d_A^2, d_B^2)}) + \frac{1}{4}, \quad (3.74)$$

where we have $\beta_i = \frac{d_i}{d_i^2 - 1}$ for $d_i > 2$ and $\beta_i = \frac{1}{d_i^2 - 1}$ for $d_i = 2$. Firstly, for $d_A = d_B = 2$ we find that

$$u_c(\mathcal{E}_{AB}) \leq \frac{d_B^2}{(d_A^2 - 1)(d_B^2 - 1)}(1 - \frac{1}{d_B^2}) + \frac{1}{4} = \frac{1}{3} + \frac{1}{4} = \frac{7}{12}. \quad (3.75)$$

We now eliminate the two other cases with a qubit subsystem. Firstly, $(d_A = 2, d_B > 2)$ yields

$$\begin{aligned} u_c(\mathcal{E}_{AB}) &\leq \frac{1}{d_A^2 - 1}(1 + \frac{d_B}{d_B^2 - 1})(1 - \frac{1}{d_A^2}) + \frac{1}{4}, \\ &\leq \frac{1}{3}(1 + \frac{d_B}{d_B^2 - 1})(\frac{3}{4}) + \frac{1}{4}, \end{aligned} \quad (3.76)$$

which is maximised for $d_B = 3$ giving $u_c(\mathcal{E}_{AB}) \leq 17/32 \approx 0.53$. Secondly, $(d_A > 2, d_B = 2)$ yields

$$\begin{aligned} u_c(\mathcal{E}_{AB}) &\leq \frac{d_A}{d_A^2 - 1}(1 + \frac{1}{d_B^2 - 1})(1 - \frac{1}{d_B^2}) + \frac{1}{4}, \\ &\leq \frac{d_A}{d_A^2 - 1}(1 + \frac{1}{3})(\frac{3}{4}) + \frac{1}{4}, \\ &\leq \frac{d_A}{d_A^2 - 1}(\frac{4}{3})(\frac{3}{4}) + \frac{1}{4}, \\ &\leq \frac{d_A}{d_A^2 - 1} + \frac{1}{4}, \end{aligned} \quad (3.77)$$

which is maximised for $d_A = 3$ giving $u_c(\mathcal{E}_{AB}) \leq 5/8 \approx 0.63$.

Now we consider the two broader cases. Firstly, $(d_A, d_B > 2$ with $d_B \geq d_A)$ which yields

$$\begin{aligned} u_c(\mathcal{E}_{AB}) &\leq \frac{d_A}{d_A^2 - 1} \left(1 + \frac{d_B}{d_B^2 - 1}\right) \left(1 - \frac{1}{d_A^2}\right) + \frac{1}{4}, \\ &\leq \frac{1}{d_A} \left(1 + \frac{d_B}{d_B^2 - 1}\right) + \frac{1}{4}, \end{aligned} \quad (3.78)$$

which is maximised for $d_A = d_B = 3$ giving $u_c(\mathcal{E}_{AB}) \leq 17/24 (\approx 0.71)$. Secondly, $(d_A, d_B > 2$ with $d_A > d_B)$ which yields

$$u_c(\mathcal{E}_{AB}) \leq \frac{d_A}{d_A^2 - 1} \left(1 + \frac{d_B}{d_B^2 - 1}\right) \left(1 - \frac{1}{d_B^2}\right) + \frac{1}{4}, \quad (3.79)$$

which is minimised for $d_A = 4, d_B = 3$ giving $u_c(\mathcal{E}_{AB}) \leq 311/540 \approx 0.58$. This completes the proof. \square

We have established the key property that was given in Theorem 3.6 – namely that our correlation measure is a witness of non-separability in quantum channels. We will test to what degree this strictly non-classical effect can be estimated on quantum devices in Chapter 4. However first we explore further properties of correlation unitarity.

3.3.2 Properties of correlation and sub-unitarity for Pauli channels

It is straightforward to compute the correlation unitarity, u_c , for a range of channels. In this section we consider how subunitarities can be decomposed for Pauli channels, and how this leads to a simple form for the correlation unitarity of such channels. This decomposition will be useful when we explore estimation techniques, in the following chapter, as recent research suggests we can cast device noise as a Pauli channel [107].

Throughout this chapter, we have used an orthonormal operator basis, $X_\mu = (X_0 = \mathbb{1}/\sqrt{d_A}, X_i)$, for a d_A dimensional quantum system. This basis can be fixed as the Pauli operators, with the additional constraint that $X_\mu^\dagger = X_\mu$. For a single qubit, these normalized Pauli operators are given by $P_\mu = (\mathbb{1}/\sqrt{2}, X/\sqrt{2}, Y/\sqrt{2}, Z/\sqrt{2})$ for the usual Pauli matrices obeying $X|0\rangle = |1\rangle, X|1\rangle = |0\rangle, Y|0\rangle = -i|1\rangle, Y|1\rangle = i|0\rangle, Z|0\rangle = |0\rangle$ and $Z|1\rangle = -|1\rangle$. A Pauli channel $\mathcal{E} : \mathcal{B}(\mathcal{H}_A) \rightarrow \mathcal{B}(\mathcal{H}_A)$ is then given by

$$\mathcal{E}(\rho) = \sum_{\mu} p_{\mu} P_{\mu} \rho P_{\mu} \quad (3.80)$$

with the condition $\sum_{\mu} p_{\mu} = d_A$. This suggests a simple form for the unital block T of a Pauli channel, and T is in fact diagonal. We now show this leads to a pleasing expression for the unitarity.

Lemma 3.11. Let $\mathcal{E}(\rho) = \sum_{\mu} p_{\mu} P_{\mu} \rho P_{\mu}$ be a Pauli channel with $\sum_{\mu} p_{\mu} = d_A$ acting on a system of dimension d_A , where the Pauli operators, $P_{\mu} = (P_0 = \mathbb{1}/\sqrt{d_A}, P_i)$, are normalized so that $\text{tr}[P_{\mu} P_{\nu}] = \delta_{\mu\nu}$. The unitarity of \mathcal{E} is given by

$$u(\mathcal{E}) = \frac{1}{(d_A^2 - 1)} \left(\left(\sum_{\mu} p_{\mu}^2 \right) - 1 \right). \quad (3.81)$$

Proof. From definition $\langle P_{\mu} | \mathcal{E} | P_{\nu} \rangle = \langle P_{\mu} | \mathcal{E}(P_{\nu}) \rangle = \text{tr}[P_{\mu} \mathcal{E}(P_{\nu})]$. Note that $\langle P_0 | \mathcal{E} | P_0 \rangle = \frac{1}{d} \sum_i p_i = 1$, and $\langle P_0 | \mathcal{E} | P_i \rangle = \langle P_i | \mathcal{E} | P_0 \rangle = 0$ from trace preservation. We can then check directly that

$$\begin{aligned} \text{tr}[P_j \mathcal{E}(P_k)] &= \sum_{\mu} p_{\mu} \text{tr}[P_j P_{\mu} P_k P_{\mu}], \\ &= \frac{1}{d_A} \sum_{\mu} p_{\mu} (-1)^{\eta(P_{\mu}, P_k)} \text{tr}[P_j P_k], \\ &= \frac{1}{d_A} \delta_{jk} \sum_{\mu} p_{\mu} (-1)^{\eta(P_{\mu}, P_k)}. \end{aligned} \quad (3.82)$$

Which gives a diagonal Liouville representation in the Pauli basis. It remains to prove the form of the unitarity. From definition, the unitarity is determined in terms of its unital block $T_{\mathcal{E}}$ as

$$u(\mathcal{E}) = \frac{1}{d_A^2 - 1} \text{tr}[T_{\mathcal{E}}^{\dagger} T_{\mathcal{E}}] \quad (3.83)$$

$$= \frac{1}{d_A^2 - 1} \sum_{j \neq 0} \langle P_j | \mathcal{E} | P_j \rangle^2 = \frac{1}{d_A^2 - 1} \left(\sum_{\mu} \langle P_{\mu} | \mathcal{E} | P_{\mu} \rangle^2 - 1 \right). \quad (3.84)$$

The orthogonality relation $\sum_{\mu} (-1)^{\eta(P_{\omega}, P_{\mu})} (-1)^{\eta(P_{\nu}, P_{\mu})} = d_A^2 \delta_{\omega\nu}$ ensures that

$$\sum_{\mu} \langle P_{\mu} | \mathcal{E} | P_{\mu} \rangle^2 = \frac{1}{d_A^2} \sum_{\mu, \nu, \omega} p_{\nu} p_{\omega} (-1)^{\eta(P_{\nu}, P_{\mu})} (-1)^{\eta(P_{\omega}, P_{\mu})} \quad (3.85)$$

$$= \sum_{\nu} p_{\nu}^2. \quad (3.86)$$

Therefore, we have

$$u(\mathcal{E}) = \frac{1}{(d_A^2 - 1)} \left(\left(\sum_{\nu} p_{\nu}^2 \right) - 1 \right), \quad (3.87)$$

which completes the proof. \square

We now examine the subunitarities of bipartite Pauli channels. For simplicity, we shall consider bipartite systems formed of A and B each of n qubits, so they have dimensions $d_A = d_B = d = 2^n$. A bipartite Pauli channel on two n -qubit systems will take the following form

$$\mathcal{E}(\rho_{AB}) = \sum_{\alpha, \beta} p_{\alpha, \beta} P_{\alpha} \otimes P_{\beta} \rho_{AB} P_{\alpha} \otimes P_{\beta} \quad (3.88)$$

and trace preserving condition requires $\sum_{\alpha,\beta} p_{\alpha,\beta} = 4^n$. The local channel at A is given by

$$\mathcal{E}_A(\rho_A) := \text{tr}_B \circ \mathcal{E}(\rho_A \otimes \mathbb{1}/d) \quad (3.89)$$

$$= \sum_{\alpha} q_{\alpha,0} P_{\alpha} \rho_A P_{\alpha} \quad (3.90)$$

where the $q_{\alpha,0} := \frac{1}{d} \sum_{\beta} p_{\alpha,\beta}$. Similarly at B :

$$\mathcal{E}_B(\rho_B) := \text{tr}_A \circ \mathcal{E}(\mathbb{1}/d \otimes \rho_B) \quad (3.91)$$

$$= \sum_{\alpha} q_{0,\beta} P_{\beta} \rho_B P_{\beta} \quad (3.92)$$

where the $q_{0,\beta} := \frac{1}{d} \sum_{\alpha} p_{\alpha,\beta}$. Note that both local channels are also Pauli channels and therefore inherit the properties of the previous lemma.

The following result links the total unitarity of this bipartite Pauli channel to its subunitarities and therefore the correlation unitarity.

Lemma 3.12. *Consider a bipartite Pauli channel, $\mathcal{E}(\rho_{AB}) = \sum_{\alpha,\beta} p_{\alpha,\beta} P_{\alpha} \otimes P_{\beta} \rho_{AB} P_{\alpha} \otimes P_{\beta}$, with equal subsystem dimensions, $d = d_A = d_B$. We then have that*

$$u_{A \rightarrow A}(\mathcal{E}) = \frac{1}{d^2 - 1} \left(\sum_{\alpha} q_{\alpha,0}^2 - 1 \right), \quad (3.93)$$

$$u_{B \rightarrow B}(\mathcal{E}) = \frac{1}{d^2 - 1} \left(\sum_{\beta} q_{0,\beta}^2 - 1 \right), \quad (3.94)$$

$$u_{AB \rightarrow AB}(\mathcal{E}) = \frac{1}{d^2 - 1} ((d^2 + 1)u(\mathcal{E}) - u_{A \rightarrow A}(\mathcal{E}) - u_{B \rightarrow B}(\mathcal{E})). \quad (3.95)$$

Proof. The relations for $u_{A \rightarrow A}$ and $u_{B \rightarrow B}$ follow directly from Lemma 3.11 with Theorem 3.2. The relation for $u_{AB \rightarrow AB}$ follows from the fact that the Liouville representation of \mathcal{E} is diagonal so that $T_{\mathcal{E}} = T_{A \rightarrow A} \oplus T_{AB \rightarrow AB} \oplus T_{B \rightarrow B}$ and thus

$$\text{tr}[T_{\mathcal{E}}^{\dagger} T_{\mathcal{E}}] = \text{tr}[T_{A \rightarrow A}^{\dagger} T_{A \rightarrow A}] + \text{tr}[T_{B \rightarrow B}^{\dagger} T_{B \rightarrow B}] + \text{tr}[T_{AB \rightarrow AB}^{\dagger} T_{AB \rightarrow AB}]. \quad (3.96)$$

From definition, $u(\mathcal{E}) = \frac{1}{(d^2)^2 - 1} \text{tr}[T_{\mathcal{E}}^{\dagger} T_{\mathcal{E}}]$, so we have

$$\begin{aligned} u(\mathcal{E}) &= \frac{1}{d^4 - 1} (\text{tr}[T_{A \rightarrow A}^{\dagger} T_{A \rightarrow A}] + \text{tr}[T_{B \rightarrow B}^{\dagger} T_{B \rightarrow B}] + \text{tr}[T_{AB \rightarrow AB}^{\dagger} T_{AB \rightarrow AB}]), \\ &= \frac{1}{d^4 - 1} ((d^2 - 1)(u_{A \rightarrow A}(\mathcal{E}) + u_{B \rightarrow B}(\mathcal{E})) + (d^2 - 1)^2(u_{AB \rightarrow AB}(\mathcal{E}))), \\ &= \frac{1}{d^2 + 1} ((u_{A \rightarrow A}(\mathcal{E}) + u_{B \rightarrow B}(\mathcal{E})) + (d^2 - 1)(u_{AB \rightarrow AB}(\mathcal{E}))). \end{aligned} \quad (3.97)$$

Rearranging the dimensional factors completes the proof. \square

Corollary 3.3. Consider a bipartite Pauli channel, $\mathcal{E}(\rho_{AB}) = \sum_{\alpha,\beta} p_{\alpha,\beta} P_\alpha \otimes P_\beta \rho_{AB} P_\alpha \otimes P_\beta$, with equal subsystem dimensions, $d = d_A = d_B$. The correlation unitarity is given by

$$u_c(\mathcal{E}) = \frac{1}{(d^2 - 1)^2} \left(\sum_{\alpha,\beta} p_{\alpha,\beta}^2 - \left(\sum_{\alpha} q_{\alpha,0}^2 \right) \sum_{\beta} q_{0,\beta}^2 \right). \quad (3.98)$$

Proof. Directly from above. \square

Lemma 3.12 proves that the unitarity of a Pauli channel is a weighted sum of three subunitarities. Further, these are exactly the subunitarities we require for correlation unitarity. This suggests that if we have only partial information about the subunitarities of a Pauli channel, then the unitarity may provide additional information about the subunitarities.

Let us make this precise with an example. For a Pauli channel, \mathcal{E} , assume we have access to: the sum of the subunitarities, $X = \sum_{i=(A,B,AB)} u_{i \rightarrow i}(\mathcal{E})$, and the total unitarity, $u(\mathcal{E})$. With just this information, we can identify $u_{AB \rightarrow AB}(\mathcal{E})$ using Lemma 3.12 as

$$u_{AB \rightarrow AB}(\mathcal{E}) = \frac{1}{d^2 - 2} ((d^2 + 1)u(\mathcal{E}) - X). \quad (3.99)$$

However this is more than a mathematical curiosity. As we will find in Chapter 4, this scenario appears within the context of benchmarking Pauli channels on quantum devices, and allows us to estimate the correlation unitarity with increased robustness to SPAM errors.

Summary

For Pauli channels, \mathcal{E} , there are only three non-zero subunitarities: $u_{AB \rightarrow AB}(\mathcal{E})$, $u_{A \rightarrow A}(\mathcal{E})$ and $u_{B \rightarrow B}(\mathcal{E})$. Further, we can write the total unitarity, $u(\mathcal{E})$, as a weighted sum of these terms. This will be useful when we consider benchmarking unknown noise channels.

3.3.3 Further interpretations of the correlation unitarity

There are other families of quantum channels for which the correlation unitarity, u_c , can be decomposed. For example, consider the channel

$$\mathcal{E}_{AB} = \sum_k p_k \mathcal{U}_k \otimes \mathcal{V}_k, \quad (3.100)$$

where $\{\mathcal{U}_i\}_{i=1}^{d_A^2}$ and $\{\mathcal{V}_j\}_{j=1}^{d_B^2}$ are local unitary error bases [128] on A and B respectively, namely unitaries on each subsystem that also form an orthonormal basis with respect to the Hilbert-Schmidt inner product. For this channel, $u_c(\mathcal{E}_{AB})$ then takes the form

$$u_c(\mathcal{E}_{AB}) = \sum_k p_k^2 - \left(\sum_k p_k^2 \right)^2. \quad (3.101)$$

This quantity is maximized for $p_1 = p_2 = 1/2$. Therefore for any \mathcal{E}_{AB} of the form given in equation (3.100) we have $u_c(\mathcal{E}_{AB}) \leq 1/4$. This bound is perhaps not surprising given Theorem 3.6 as the channel is separable.

Further insight into the correlation unitarity can be obtained by formulating it in terms of two-point correlation measures. We define the expectation of an observable O on a state ρ as $\langle O \rangle_\rho := \text{tr}[O^\dagger \rho]$. Now suppose we have local observables O_A and O_B for the subsystems A and B respectively. For any bipartite quantum channel, \mathcal{E} , and bipartite state, ψ_{AB} , we can define the following correlation function

$$F_{O_A, O_B}(\mathcal{E}, \psi_{AB}) := |\langle O_A \otimes O_B \rangle_{\mathcal{E}_{AB}(\psi_{AB})}|^2 - |\langle O_A \rangle_{\mathcal{E}_A(\psi_A)}|^2 |\langle O_B \rangle_{\mathcal{E}_B(\psi_B)}|^2 \quad (3.102)$$

where the channels \mathcal{E}_A and \mathcal{E}_B are local channels on A respectively B defined in Definition 3.1 and the input states ψ_A and ψ_B are the marginals of ψ_{AB} .

The correlation function above becomes related to the covariance of classical random variables when considering classical states embedded in a quantum system. We define the state $\rho_{AB} = \sum_{x,y} p(x,y) |x\rangle\langle x| |y\rangle\langle y|$ for $|x\rangle, |y\rangle$ computational basis states that diagonalize the hermitian operators O_A and O_B and $p(x,y)$ is a joint probability distribution with marginals $p(x)$ and $p(y)$. Then correlation function is

$$\begin{aligned} F_{O_A, O_B}(id, \rho_{AB}) &= |\langle O_A \otimes O_B \rangle_{\rho_{AB}}|^2 - |\langle O_A \rangle_{\rho_A}|^2 |\langle O_B \rangle_{\rho_B}|^2, \\ &= (\langle O_A \otimes O_B \rangle_{\rho_{AB}} - \langle O_A \rangle_{\rho_A} \langle O_B \rangle_{\rho_B}) (\langle O_A \otimes O_B \rangle_{\rho_{AB}} + \langle O_A \rangle_{\rho_A} \langle O_B \rangle_{\rho_B}) \\ &= \text{cov}(O_A, O_B) (\langle O_A \otimes O_B \rangle_{\rho_{AB}} + \langle O_A \rangle_{\rho_A} \langle O_B \rangle_{\rho_B}). \end{aligned} \quad (3.103)$$

where $\text{cov}(O_A, O_B) = \langle O_A \otimes O_B \rangle_{\rho_{AB}} - \langle O_A \rangle_{\rho_A} \langle O_B \rangle_{\rho_B}$ and matches the covariance of classical random variables X, Y .

The correlation unitarity of any bipartite quantum channel, \mathcal{E} , can be expressed using this correlation function as

$$u_c(\mathcal{E}) = \alpha_{AB} d_{AB} \sum_{i,j,m,n} F_{P_i, P_j}(\mathcal{E}, \psi_{m,n}) \quad (3.104)$$

where P_i are the orthonormal traceless Pauli operators on each subsystem, and where $\psi_{m,n} = \frac{P_m \otimes P_n}{\sqrt{d_A d_B}}$ is a ‘‘traceless state’’, that can be statistically prepared via $\psi_{m,n} = \frac{1}{2}(\psi_{+,m,n} - \psi_{-,m,n})$ for the two related quantum states $\psi_{\pm, m, n} = \frac{P_0 \otimes P_0 \pm P_m \otimes P_n}{\sqrt{d_A d_B}}$. We prove this relation in Appendix B.6. This form for the correlation unitarity gives some intuition for how the Liouville representation a channel can be related to Pauli states and measurements.

3.4 Conclusions

We have introduced subunitarities and shown they allow the construction of a correlation measure which is a witness of non-separability in bipartite channels. Overall, the correlation unitarity amounts to a working notion of correlation in a bipartite quantum channel, and we do not delve any further into its theoretical properties. In Appendix B.5, we also compare

$u_c(\mathcal{E}_{AB})$ to a norm measure of correlation. While norm-based measures are mathematically more natural, our aim is to connect to benchmarking protocols, and so ultimately the utility of this measure should be judged by how useful it is in practice. We find that subunitarities arise very naturally in benchmarking protocols.

4

Estimation of coherent correlations and non-separability via benchmarking protocols

And though our separation, it pierced me to the heart,
She still lives inside of me, we've never been apart.

If You See Her, Say Hello

Bob Dylan

In the previous chapter we developed a collection of tools, based around unitarity, to address subsystem features of a quantum channel. The introduction of subunitarities and the correlation unitarity allow us to quantify coherence between subsystems of a bipartite quantum channel in a simple and direct manner. We now turn to the question of how such quantities may be estimated in practice in a protocol that is both efficient in the number of operations required and robust against SPAM errors.

As these quantities are generalizations of the unitarity – which can be efficiently estimated through a benchmarking protocol – it turns out similar methods work for subunitarities. However some complications do arise as we shall discuss.

This chapter is structured as follows. Section 4.1 is an introduction to randomized benchmarking where we give an overview of some key results from the literature. Then in Section 4.2 we summarize the main result of [57] by mathematically deriving how the unitarity of noise appears within a randomized benchmarking protocol. The remainder of the chapter is our original content. In Section 4.3 we extend the unitarity protocol to subsystems and show

that this connects with the subunitarities we defined in Chapter 3. However the estimation of individual subunitarities and our correlation measure require additional steps which we describe in Section 4.4. Finally we show these methods give independent information beyond existing SPAM robust benchmarking methods.

4.1 Randomized Benchmarking Protocols

The certification of quantum devices is a fundamental problem of quantum technologies, such as verifying that a physical device is actually performing with a sufficiently high fidelity. In the context of quantum computing it is desirable to provide a greater abstraction from the underlying physical implementation and talk of benchmarking a logical gateset $\Gamma := \{\mathcal{U}_1, \mathcal{U}_2, \dots, \mathcal{U}_n\}$ of target unitary gates. Using some meaningful quantity, we then wish to measure how ‘far’ the set of physical gates $\tilde{\Gamma} := \{\tilde{\mathcal{U}}_1, \tilde{\mathcal{U}}_2, \dots, \tilde{\mathcal{U}}_n\}$ are from idealised set ¹.

The worst-case error rates are given by the set of diamond norm distances, $\{\|\tilde{\mathcal{U}}_i - \mathcal{U}_i\|_\diamond\}$, which are the relevant physical parameters for the fault tolerance theorem [38, 42]. For two quantum channels \mathcal{E} and \mathcal{F} from a system with dimension d_X to a system with dimension d_Y , diamond norm distance between the channels is given by

$$\|\mathcal{E} - \mathcal{F}\|_\diamond := \max_{\rho} \|\mathcal{E} \otimes id_X(\rho) - \mathcal{F} \otimes id_X(\rho)\|_1 \quad (4.1)$$

where id_X is the identity channel with dimension d_X , the state ρ has dimension d_X^2 , and where $\|M\|_1 := \text{tr} \left[\sqrt{M^\dagger M} \right]$ is the matrix 1-norm for any matrix M .

The diamond norm distance can be directly linked to the maximal probability of distinguishing two known quantum channels with a single measurement, and its calculation can be cast as a semi-definite programme [37]. However, it is not obvious [43] how to estimate the set $\{\|\tilde{\mathcal{U}}_i - \mathcal{U}_i\|_\diamond\}$ directly; or to directly measure the diamond norm distance between two quantum channels of interest. Additionally, estimating each value for the complete gateset of a device will clearly scale very poorly with system size.

To benchmark errors we must therefore consider weaker measures. One such measure is the average fidelity between the idealised unitaries and physical unitaries across the gateset. The average gate infidelity, given in equation (1.4), provides bounds on the diamond distance of the *average* noise associated with the gateset, of the form shown in equation (1.5). The problem with this route is that the bounds cannot be tightened, and for \mathcal{E} corresponding to a non-Pauli error there is a weak link between $r(\mathcal{E})$ and the diamond norm [43, 48, 49].

Randomized benchmarking techniques can be used to estimate $r(\mathcal{E})$ and circumvent the exponential complexity of tomography and the unavoidable SPAM errors. The core components of a randomized benchmarking protocol generally involves the noisy preparation of

¹In this chapter we use the notation $\tilde{(\cdot)}$ to denote the noisy real-world implementation of any idealised operator (\cdot) .

some initial quantum state ρ , which is then subject to a number k of physical gates $\tilde{\mathcal{U}}_i$ that approximate target unitaries $\mathcal{U}_i \in \Gamma$, before a final imperfect measurement is performed for some binary outcome measurement $\{M, \mathbb{1} - M\}$. If the gates applied correspond to a (noisy) unitary 2-design, such as Γ being the Clifford group, then it can be shown that [6] the resulting statistics are exponentially decreasing in k , namely $\mathbb{E}[m(k)] = c_1 + c_2\lambda^k$, for constants c_1 and c_2 that contain the state preparation and measurement details. The decay constant λ is then a measure of the noisiness of the physical gateset $\tilde{\Gamma} = \{\tilde{\mathcal{U}}_i\}$ employed.

In the simplified model of *gate-independent* noise, in which each noisy gate can be decomposed as $\tilde{\mathcal{U}}_i = \mathcal{E} \circ \mathcal{U}_i$ for some \mathcal{E} that is independent of i , then it can be shown that $\lambda \propto 1 - r(\mathcal{E})$, where $r(\mathcal{E})$ is the average gate infidelity of the noise channel \mathcal{E} . In the more realistic case of *gate-dependent* noise the relationship between the decay parameter λ and the physics of the set $\tilde{\Gamma}$ is subtle, due to gauge degrees of freedom in the representation of the physical components [45]. However, despite these details the decay parameter can still be related to the physical gateset and essentially corresponds to the average gateset infidelity [44].

Summary

By averaging over lots of random sequences of gates, an RB scheme simplifies the associated noise channel, \mathcal{E} , down to a single parameter, $r(\mathcal{E})$. This can be readily estimated, as if we increase the length of the sequence, then $r(\mathcal{E})$ can be related to the decay in the value of some observable. This isolates estimation of the gateset noise, \mathcal{E} , from SPAM errors.

At a more abstract level, a randomized benchmarking scheme admits a compact description in terms of convolutions of the channels $\tilde{\mathcal{U}}_i$ with respect to the Clifford group [130]. The decay law is then viewed in a Fourier-transformed basis where the channel compositions become matrix multiplication over different irreps [7]. The resultant protocol then provides a benchmark for the degree to which the physically realized channels $\{\tilde{\mathcal{U}}_i\}$ form an approximate representation of the Clifford group [131, 132].

In the next section we expand on the components of the benchmarking scheme for the case of unitarity benchmarking.

4.2 Unitary 2-designs & Unitarity Benchmarking Protocols

In this section, we now provide an outline of how the unitarity of a quantum channel can be estimated in a benchmarking protocol, as described in [57]. We relegate proofs to the end of the section.

Recall that by \mathcal{U} we denote the Liouville representation of a unitary channel $\mathcal{U}(X) = UXU^\dagger$, and therefore it takes the explicit form, $\mathcal{U} := U \otimes U^*$. A probability measure μ over

the set of unitaries $U(d)$ is called a *unitary 2-design* if we have that

$$\int d\mu(U) \mathbf{u}^{\otimes 2} = \int d\mu_{\text{Haar}}(U) \mathbf{u}^{\otimes 2}, \quad (4.2)$$

where μ_{Haar} is the Haar measure over the group $U(d)$. In practice we are interested in unitary 2-designs which are finite, discrete distributions of unitaries. In particular the uniform distribution over the Clifford group \mathcal{C} of unitaries is a 2-design (in fact it is a 3-design [133]), and therefore

$$\frac{1}{|\mathcal{C}|} \sum_{U \in \mathcal{C}} \mathbf{u}^{\otimes 2} = \int d\mu_{\text{Haar}}(U) \mathbf{u}^{\otimes 2} =: P \quad (4.3)$$

where $|\mathcal{C}|$ is the number of elements in the Clifford group and we denote the resultant operator by P . For the space of bounded operators $\mathcal{B}(\mathcal{H})$ on the Hilbert space \mathcal{H} , this operator acts on the vectorized form of $\mathcal{B}(\mathcal{H} \otimes \mathcal{H})$. It can be shown (see Lemma 4.1) that P is the projector onto the subspace

$$S := \text{span}\{|\mathbf{1}^{\otimes 2}\rangle, |\mathbb{F}\rangle\}, \quad (4.4)$$

where \mathbb{F} is the unitary that transposes vectors in the two subsystems, $|\phi_1\rangle \otimes |\phi_2\rangle \rightarrow |\phi_2\rangle \otimes |\phi_1\rangle$. We now define an orthonormal operator basis $X_\mu = (X_0 = \mathbb{1}/\sqrt{d}, X_i)$ for $\mathcal{B}(\mathcal{H})$ where d is the dimension of the system, in a same way as in Chapter 3. Using this basis, in vectorized form, we can (see Lemma 4.2) decompose the projector P in the following way

$$\begin{aligned} P &= |\mathbf{X}_0\rangle\langle\mathbf{X}_0| \otimes |\mathbf{X}_0\rangle\langle\mathbf{X}_0| + \frac{1}{d^2 - 1} \sum_{i,j}^{d^2-1} |\mathbf{X}_i\rangle\langle\mathbf{X}_j| \otimes |\mathbf{X}_i^\dagger\rangle\langle\mathbf{X}_j^\dagger|, \\ &=: |0\rangle\langle 0| + |1\rangle\langle 1|, \end{aligned} \quad (4.5)$$

where $\{|0\rangle, |1\rangle\}$ forms an orthonormal basis of the subspace S .

For a quantum channel, $\mathcal{E} : \mathcal{B}(\mathcal{H}) \rightarrow \mathcal{B}(\mathcal{H})$, the projector P can be directly related to the unitarity. From Theorem 4.1, as

$$P\mathcal{E}^{\otimes 2}P = |0\rangle\langle 0| + u(\mathcal{E})|1\rangle\langle 1| + \frac{x(\mathcal{E})}{\sqrt{d^2 - 1}}|1\rangle\langle 0| \quad (4.6)$$

where $x(\mathcal{E})$ is a measure of non-unitality of the channel such that $x(\mathcal{E}) = 0$ if and only if \mathcal{E} is unital, meaning that $\mathcal{E}(\mathbb{1}) = \mathbb{1}$.

Summary

We have the projector, P , induced by averaging over two copies of the unitary group. When applied $P\mathcal{E}^{\otimes 2}P$ this *twirls* any channel \mathcal{E} into a simpler form based purely on the values of the two parameters: unitarity, $u(\mathcal{E})$ and non-unitality, $x(\mathcal{E})$.

Further, if we consider placing this construction to a power, say k , we find that the unitarity scales with k while the other factors remain constant such that

$$\begin{aligned} (P\mathcal{E}^{\otimes 2}P)^k &= |0\rangle\langle 0| + u(\mathcal{E})^k|1\rangle\langle 1| + \frac{x(\mathcal{E})(u(\mathcal{E})^k - 1)}{\sqrt{d^2 - 1}}|1\rangle\langle 0|, \\ &= |0\rangle\langle 0| - \frac{x(\mathcal{E})}{\sqrt{d^2 - 1}}|1\rangle\langle 0| + u(\mathcal{E})^k(|1\rangle\langle 1| + \frac{x(\mathcal{E})}{\sqrt{d^2 - 1}}|1\rangle\langle 0|). \end{aligned} \quad (4.7)$$

This scaling and the previous link between sampling from the Clifford group and the unitarity of a quantum channel will be key to benchmarking protocol.

For the physical Clifford group gateset, $\tilde{\Gamma} = \{\tilde{\mathcal{U}}_i\}$, we now define an effective noise channel \mathcal{E} via $\mathcal{E} := \mathcal{U}^\dagger \circ \tilde{\mathcal{U}}$. Moreover in what follows we shall assume for simplicity that each gate $\mathcal{U} \in \Gamma$ is subject to the same effective noise channel (but again this assumption can be weakened and gate-dependent noise can be assessed [44]).

The unitarity of the noise channel, \mathcal{E} , can then be estimated in the following way. We prepare a quantum state ρ and now define

$$\mathcal{U}_s := \mathcal{U}_{(s_1, s_2, \dots, s_k)} := \mathcal{U}_{s_1} \circ \mathcal{U}_{s_2} \circ \dots \circ \mathcal{U}_{s_k}, \quad (4.8)$$

where $\mathcal{U}_{s_i} \in \Gamma$ for all i in the Clifford group gateset, and s_i labels the particular choice of unitary. We also denote by $\tilde{\mathcal{U}}_s$ the corresponding noisy implementation of the above sequence $s = (s_1, s_2, \dots, s_k)$ of k unitaries. For any sequence s and some hermitian observable M we estimate the quantity

$$m(s) := \text{tr} \left[M \tilde{\mathcal{U}}_s(\rho) \right], \quad (4.9)$$

and then randomly sample over the Clifford group for each step in the sequence to estimate $\mathbb{E}_s[m(s)^2] := \frac{1}{|\Gamma|^k} \sum_s m(s)^2$. By exploiting the fact that the Clifford group is a 2-design, and specifically equations (4.3) and (4.4), it was shown in [57] that

$$\mathbb{E}_s[m(s)^2] = c_1 + c_2 u(\mathcal{E})^{k-1}, \quad (4.10)$$

for constants c_1 and c_2 that contain any errors due to state-preparation or measurement. Therefore, by repeating this estimation for sequences of varying length we may extract an estimation of $u(\mathcal{E})$ as a decay constant for the quantity in an efficient and SPAM-robust manner.

To derive equation (4.10), we essentially expand every term in the estimation until we obtain the form given in equation (4.6). The following sketches this process out, and will be

covered in more detail for the original protocols presented in the following section:

$$\begin{aligned}
\mathbb{E}_s[m(s)^2] &:= \frac{1}{|\Gamma|^k} \sum_s m(s)^2 = \frac{1}{|\Gamma|^k} \sum_s (\text{tr}[M\tilde{U}_s(\rho)])^2, \\
&= \frac{1}{|\Gamma|^k} \sum_s \langle \tilde{M} | \tilde{u}_{s_k} \tilde{u}_{s_{k-1}} \dots \tilde{u}_{s_1} | \rho \rangle^2, \\
&= \frac{1}{|\Gamma|^k} \sum_s \langle \tilde{M} | (\mathcal{E}u_{s_k})(\mathcal{E}u_{s_{k-1}}) \dots (\mathcal{E}u_{s_1}) | \rho \rangle^2, \\
&= \frac{1}{|\Gamma|^k} \sum_s \langle \tilde{M} |^{\otimes 2} (\mathcal{E}^{\otimes 2} u_{s_k}^{\otimes 2})(\mathcal{E}^{\otimes 2} u_{s_{k-1}}^{\otimes 2}) \dots (\mathcal{E}^{\otimes 2} u_{s_1}^{\otimes 2}) | \rho \rangle^{\otimes 2}, \\
&= \langle \tilde{M} \mathcal{E}^\dagger |^{\otimes 2} \left(\frac{1}{|\Gamma|} \sum_{i_k} u_{i_k}^{\otimes 2} \right) (\mathcal{E}^{\otimes 2})_{k-1} \left(\frac{1}{|\Gamma|} \sum_{i_{k-1}} u_{i_{k-1}}^{\otimes 2} \right) \dots (\mathcal{E}^{\otimes 2})_1 \left(\frac{1}{|\Gamma|} \sum_{i_1} u_{i_1}^{\otimes 2} \right) | \rho \rangle^{\otimes 2}, \\
&= \langle \tilde{M} \mathcal{E}^\dagger |^{\otimes 2} P (\mathcal{E}^{\otimes 2})_{k-1} P \dots (\mathcal{E}^{\otimes 2})_1 P | \rho \rangle^{\otimes 2}, \\
&= \langle \tilde{M} |^{\otimes 2} (P \mathcal{E}^{\otimes 2} P)^{k-1} | \rho \rangle^{\otimes 2}, \\
&= \langle \tilde{M} |^{\otimes 2} (|0\rangle\langle 0| + u(\mathcal{E}) |1\rangle\langle 1| + \frac{x(\mathcal{E})}{\sqrt{d^2-1}} |1\rangle\langle 0|)^{k-1} | \rho \rangle^{\otimes 2}, \\
&= \langle \tilde{M} |^{\otimes 2} (|0\rangle\langle 0| - \frac{x(\mathcal{E})}{\sqrt{d^2-1}} |1\rangle\langle 0| + u(\mathcal{E})^{k-1} (|1\rangle\langle 1| + \frac{x(\mathcal{E})}{\sqrt{d^2-1}} |1\rangle\langle 0|)) | \rho \rangle^{\otimes 2}.
\end{aligned} \tag{4.11}$$

Note we have absorbed the final error channel into the noise of the measurement. As the unitarity decays exponentially, $u(\mathcal{E})^{k-1}$, with the length of the sequence, while the other factors remain constant, we can isolate and estimate the unitarity independently. This allows the constants c_1 and c_2 to be read off.

Summary

By averaging over lots of random sequences of gates, a unitarity RB scheme simplifies the associated noise channel, \mathcal{E} , down to two parameters, $u(\mathcal{E})$ and $x(\mathcal{E})$. The unitarity, $u(\mathcal{E})$, can then be readily estimated, as if we increase the length of the sequence, $u(\mathcal{E})$ can be related to the exponential decay in the square of the value of some observable. This isolates estimation of the gateset noise, \mathcal{E} , from SPAM errors.

Proofs for the unitarity benchmarking protocol

First we show that a unitarity 2-design produces a projector into a subspace spanned by two vectors which we can identify.

Lemma 4.1. *The operator*

$$P := \int d\mu_{\text{Haar}}(U) \mathbf{u}^{\otimes 2} = \int d\mu_{\text{Haar}}(U) (U \otimes U^*)^{\otimes 2}, \tag{4.12}$$

on $\mathcal{H}^{\otimes 4} = V \oplus V^\perp$ is a projector into the subspace $V = \text{span}(|\mathbf{1}^{\otimes 2}\rangle, |\mathbb{F}\rangle)$, where \mathbb{F} is the Flip operator on the subsystems, and therefore $P = 0$ on V^\perp .

Proof. For any finite or compact group G with a representation V , averaging over all elements of the group gives a projector,

$$P = \int V(g) dg, \quad (4.13)$$

onto the invariant subspace $\{|\psi\rangle : V(g)|\psi\rangle = |\psi\rangle \forall g \in G\}$. Therefore for $V(U) = (U \otimes U^*)^{\otimes 2}$, according to the above definition of an invariant subspace, we must find X such that

$$V(U)|\mathbf{X}\rangle = |\mathbf{X}\rangle, \quad (4.14)$$

or equivalently $[X, U \otimes U] = 0$.

We can decompose $U \otimes U$ into irreducible representations of $U(d)$. There are 2 of them: the symmetric subspace and the alternating subspace. This is related to the fact that symmetric group on two elements has two irreducible representations: the trivial one ($\mathbb{1}$) and the alternating one (\mathbb{F}).

Using Schur's lemma² the operator X must be a multiple of the identity when restricted to either of these two subspaces. Putting everything together, the invariant subspace is then spanned by $|\mathbf{1}^{\otimes 2}\rangle$ and $|\mathbb{F}\rangle$, which completes the proof. \square

An alternative line for the above proof is to invoke Schur-Weyl duality to give an exact form for P in terms of the permutation operators ($\mathbb{1}, \mathbb{F}$) [134, 135].

Now we show that the unitary 2-design projector can be decomposed into the same basis we used when examining the unitarity of quantum channels in the Liouville representation (see Chapter 3).

Lemma 4.2. *The operator $P = \int d\mu_{\text{Haar}}(U) \mathbf{U}^{\otimes 2}$ can be decomposed as $P = |0\rangle\langle 0| + |1\rangle\langle 1|$ where*

$$\begin{aligned} |0\rangle &= |\mathbf{X}_0\rangle \otimes |\mathbf{X}_0\rangle, \\ |1\rangle &= \frac{1}{\sqrt{d^2 - 1}} \sum_{k=1}^{d^2 - 1} |\mathbf{X}_k\rangle \otimes |\mathbf{X}_k^\dagger\rangle, \end{aligned} \quad (4.15)$$

with $X_\mu = (X_0 = \mathbb{1}/\sqrt{d}, X_i)$.

Proof. The operator P is a projector into the invariant vector space $V = \text{span}(|\mathbf{1}^{\otimes 2}\rangle, |\mathbb{F}\rangle)$. Therefore, if we find an orthonormal basis for V , we can write the operator P using a linear combination of basis elements such that $P^2 = P$.

We define the tensor product of two vectorized matrices as: $|\mathbf{A} \otimes \mathbf{B}\rangle := |\mathbf{A}\rangle \otimes |\mathbf{B}\rangle$. Applying this definition to the first vector that spans the space $|\mathbf{1}^{\otimes 2}\rangle = |\mathbf{1}\rangle \otimes |\mathbf{1}\rangle = d|\mathbf{X}_0\rangle \otimes |\mathbf{X}_0\rangle$. Normalizing, the first eigenvector is therefore $|0\rangle := |\mathbf{X}_0\rangle \otimes |\mathbf{X}_0\rangle$.

²Schur's Lemma states that the only matrices that commute with all elements of an irreducible representation of a group are scalar multiples of $\mathbb{1}$.

The Flip operator in our basis is given by considering the permutation of computational basis states:

$$\mathbb{F} := \sum_{i,j}^{d,d} |j\rangle\langle i| \otimes |i\rangle\langle j| = \sum_{i,j}^{d,d} |j\rangle\langle i| \otimes (|j\rangle\langle i|)^\dagger = \sum_{\mu}^{d^2} X_{\mu} \otimes X_{\mu}^\dagger \quad (4.16)$$

up to a dimensional factor. Therefore $|\mathbb{F}\rangle = \sum_{\mu=0}^{d^2-1} |\mathbf{X}_{\mu}\rangle \otimes |\mathbf{X}_{\mu}^\dagger\rangle$. From inspection, the second normalized eigenvector that spans this subspace is

$$|1\rangle = \frac{1}{\sqrt{d^2-1}} \sum_{k=1}^{d^2-1} |\mathbf{X}_{\mathbf{k}}\rangle \otimes |\mathbf{X}_{\mathbf{k}}^\dagger\rangle. \quad (4.17)$$

It is easily checked that $\langle i|j\rangle = \delta_{ij}$.

We can now write the decomposition of the projector $P = |0\rangle\langle 0| + |1\rangle\langle 1|$ as

$$P = |\mathbf{X}_0\rangle\langle \mathbf{X}_0| \otimes |\mathbf{X}_0\rangle\langle \mathbf{X}_0| + \frac{1}{d^2-1} \sum_{i,j}^{d^2-1} |\mathbf{X}_i\rangle\langle \mathbf{X}_j| \otimes |\mathbf{X}_i^\dagger\rangle\langle \mathbf{X}_j^\dagger|. \quad (4.18)$$

This completes the proof. \square

Finally we prove that, when applied to a quantum channel, the unitary 2-design projector averages the channel such that unitarity of the channel can be isolated.

Theorem 4.1. *Consider the operator $P = \int d\mu_{\text{Haar}}(U) \mathbf{U}^{\otimes 2} = |0\rangle\langle 0| + |1\rangle\langle 1|$ decomposed in the basis $X_{\mu} = (X_0 = \mathbb{1}/\sqrt{d}, X_i)$. For a quantum channel \mathcal{E} , with fixed system dimension d we have*

$$P\mathcal{E}^{\otimes 2}P = |0\rangle\langle 0| + u(\mathcal{E})|1\rangle\langle 1| + \frac{x(\mathcal{E})}{\sqrt{d^2-1}}|1\rangle\langle 0|. \quad (4.19)$$

where $u(\mathcal{E})$ is the unitarity of the channel, and $x(\mathcal{E})$ is the non-unitarity of the channel.

Proof. We simply need to calculate each $\langle i|\mathcal{E}^{\otimes 2}|j\rangle$ as $P\mathcal{E}^{\otimes 2}P = \sum_{i,j=(0,1)} \langle i|\mathcal{E}^{\otimes 2}|j\rangle |i\rangle\langle j|$. Firstly, we have $\langle 0|\mathcal{E}^{\otimes 2}|0\rangle = \langle \mathbf{X}_0|\mathcal{E}|\mathbf{X}_0\rangle^2 = \text{tr}[\mathbb{1}\mathcal{E}(\mathbb{1}/d)]^2 = 1$. Secondly, we have

$$\begin{aligned} \langle 0|\mathcal{E}^{\otimes 2}|1\rangle &= \frac{1}{\sqrt{d^2-1}} \sum_i^{d^2-1} \langle \mathbf{X}_0|\mathcal{E}|\mathbf{X}_i\rangle \langle \mathbf{X}_0|\mathcal{E}|\mathbf{X}_i^\dagger\rangle, \\ &= \frac{1}{\sqrt{d^2-1}} \sum_i^{d^2-1} \langle \mathbf{X}_0|\mathcal{E}|\mathbf{X}_i\rangle \langle \mathbf{X}_i|\mathcal{E}^\dagger|\mathbf{X}_0\rangle. \end{aligned} \quad (4.20)$$

However $\langle \mathbf{X}_0|\mathcal{E}|\mathbf{X}_i\rangle = 0$ for all i for a trace preserving channel. Therefore $\langle 0|\mathcal{E}^{\otimes 2}|1\rangle = 0$. For the third element we have

$$\begin{aligned} \langle 1|\mathcal{E}^{\otimes 2}|0\rangle &= \frac{1}{\sqrt{d^2-1}} \sum_i^{d^2-1} \langle \mathbf{X}_i|\mathcal{E}|\mathbf{X}_0\rangle \langle \mathbf{X}_i^\dagger|\mathcal{E}|\mathbf{X}_0\rangle, \\ &= \frac{1}{\sqrt{d^2-1}} \sum_i^{d^2-1} \langle \mathbf{X}_i|\mathcal{E}|\mathbf{X}_0\rangle \langle \mathbf{X}_0|\mathcal{E}^\dagger|\mathbf{X}_i\rangle = \frac{1}{\sqrt{d^2-1}}x(\mathcal{E}). \end{aligned} \quad (4.21)$$

Finally, we have

$$\begin{aligned} \langle 1 | \mathcal{E}^{\otimes 2} | 1 \rangle &= \frac{1}{d^2 - 1} \sum_{i,j}^{d^2-1} \langle \mathbf{X}_i | \mathcal{E} | \mathbf{X}_j \rangle \langle \mathbf{X}_i^\dagger | \mathcal{E} | \mathbf{X}_j^\dagger \rangle, \\ &= \frac{1}{d^2 - 1} \sum_i^{d^2-1} \langle \mathbf{X}_i | \mathcal{E} | \mathbf{X}_j \rangle \langle \mathbf{X}_j | \mathcal{E}^\dagger | \mathbf{X}_j \rangle = u(\mathcal{E}). \end{aligned} \quad (4.22)$$

As this exhausts all the options so we have an exact form for $P\mathcal{E}^{\otimes 2}P$. \square

This completes our discussion of benchmarking of the total unitarity of a noise channel. Now we will extend the core protocol to allow for the subunitarities of noise to be estimated.

4.3 Bipartite channel subunitarities via local twirls

The unitarity arose from considering a global twirl using a 2-design, it turns out that the subunitarities arise in a similar fashion, but now by considering local twirls for a bipartite quantum system. Specifically, we now have a bipartite quantum system AB with local gatesets Γ_A and Γ_B , which we assume are unitary 2-designs, and a global gateset Γ_{AB} .

For simplicity, we consider fixed subsystem dimensions, with d_A and d_B for subsystems A and B respectively. The Hilbert space for the system takes the form, $\mathcal{H}_A \otimes \mathcal{H}_B$, where \mathcal{H}_A and \mathcal{H}_B are the spaces associated with each subsystem. Bipartite quantum channels, \mathcal{E} , on the whole system act on the space of bounded operators $\mathcal{E} : \mathcal{B}(\mathcal{H}_A \otimes \mathcal{H}_B) \rightarrow \mathcal{B}(\mathcal{H}_A \otimes \mathcal{H}_B)$. We now define the tensor product of two vectorized matrices as: $|\mathbf{A} \otimes \mathbf{B}\rangle := |\mathbf{A}\rangle \otimes |\mathbf{B}\rangle$. For the Liouville representation, \mathcal{E} , of a bipartite channel, this reorders tensor product of the Hilbert spaces; such that \mathcal{E} acts on $\mathcal{B}(\mathcal{H}_A \otimes \mathcal{H}_A \otimes \mathcal{H}_B \otimes \mathcal{H}_B)$. This reordering is a powerful ‘trick’, and we believe it makes the following calculations easier to follow.

4.3.1 Local twirls of a bipartite system

We now examine independent twirls on each subsystem, $\mathcal{C} \times \mathcal{C}$. In the Liouville representation we have

$$\begin{aligned} P_{AB} &:= \int d\mu_{\text{Haar}}(U_A) \int d\mu_{\text{Haar}}(U_B) \mathbf{u}_A^{\otimes 2} \otimes \mathbf{u}_B^{\otimes 2}, \\ &= \frac{1}{|\Gamma_A||\Gamma_B|} \sum_{U_A \in \Gamma_A, U_B \in \Gamma_B} \mathbf{u}_A^{\otimes 2} \otimes \mathbf{u}_B^{\otimes 2}. \end{aligned} \quad (4.23)$$

Since the integrals are independent, it is readily seen that $P_{AB} = P_A \otimes P_B$ where P_A and P_B are local projections at A and B onto subspaces S_A and S_B , with

$$S_A = \text{span}\{|\mathbf{1}_A \otimes \mathbf{1}_{A'}\rangle, |\mathbf{F}_{AA'}\rangle\}, \quad (4.24)$$

where A' is isomorphic to A , and we have a similar expression for S_B . The next step is to decompose P_{AB} as we did for P in equation (4.5).

We define two orthonormal operator bases for each subsystem, in the same manner as in Chapter 3. Firstly for subsystem A , we choose $X_\mu = (X_0 = \frac{1}{\sqrt{d_A}}\mathbb{1}_A, X_i)$, where d_A is dimension of the subsystem A , and $\text{tr}[X_\mu^\dagger X_\nu] = \delta_{\mu\nu}$. Similarly for B , an orthonormal basis $Y_\mu = (Y_0 = \frac{1}{\sqrt{d_B}}\mathbb{1}_B, Y_i)$. Together these provide a basis for the full system which is given in the Liouville representation as $|\mathbf{X}_\nu \otimes \mathbf{Y}_\mu\rangle := |\mathbf{X}_\nu\rangle \otimes |\mathbf{Y}_\mu\rangle$. Following from the tensor structure in Lemma 4.2, simply

$$P_{AB} = P_A \otimes P_B = \sum_{i,j=(0,1)} |i\rangle\langle i|_A \otimes |j\rangle\langle j|_B \quad (4.25)$$

where we have

$$\begin{aligned} |0\rangle_A \otimes |0\rangle_B &= |\mathbf{X}_0\rangle \otimes |\mathbf{X}_0\rangle \otimes |\mathbf{Y}_0\rangle \otimes |\mathbf{Y}_0\rangle, \\ |1\rangle_A \otimes |0\rangle_B &= \sqrt{\alpha_A} \sum_{n=1}^{d_A^2-1} |\mathbf{X}_n\rangle \otimes |\mathbf{X}_n^\dagger\rangle \otimes |\mathbf{Y}_0\rangle \otimes |\mathbf{Y}_0\rangle, \\ |0\rangle_A \otimes |1\rangle_B &= \sqrt{\alpha_B} \sum_{m=1}^{d_B^2-1} |\mathbf{X}_0\rangle \otimes |\mathbf{X}_0\rangle \otimes |\mathbf{Y}_m\rangle \otimes |\mathbf{Y}_m^\dagger\rangle, \\ |1\rangle_A \otimes |1\rangle_B &= \sqrt{\alpha_A \alpha_B} \sum_{n,m=1}^{d_A^2-1, d_B^2-1} |\mathbf{X}_n\rangle \otimes |\mathbf{X}_n^\dagger\rangle \otimes |\mathbf{Y}_m\rangle \otimes |\mathbf{Y}_m^\dagger\rangle, \end{aligned} \quad (4.26)$$

with $\alpha_i = 1/(d_i^2 - 1)$. In what follows we will drop the subscript subsystem labels and always have A as the first subsystem and B as the second.

Summary

Applying two local twirls simultaneously over the Clifford group, $\mathcal{C} \times \mathcal{C}$, gives a projector P_{AB} that contains ‘local’ terms describing the twirl on each subsystem, $|1\rangle_A \otimes |0\rangle_B$ and $|0\rangle_A \otimes |1\rangle_B$, while tracing out the other subsystem; and also a further ‘non-local’ term $|1\rangle_A \otimes |1\rangle_B$. These terms will directly connect with the subunitarities of a channel.

4.3.2 The matrix of subunitarities for local twirls

The projector P_{AB} appears naturally within settings where local twirls are performed on a device, such as in randomized benchmarking protocols. Therefore, we should consider the structure of $P_{AB} \mathcal{E}^{\otimes 2} P_{AB}$, where $\mathcal{E} : \mathcal{B}(\mathcal{H}_A \otimes \mathcal{H}_B) \rightarrow \mathcal{B}(\mathcal{H}_A \otimes \mathcal{H}_B)$ is a bipartite quantum channel. We will see that it relates to the *subunitarities* of \mathcal{E} , the measures of coherence within and between subsystems of a channel introduced in Chapter 3.

More precisely, we now show that the operator $P_{AB} \mathcal{E}^{\otimes 2} P_{AB}$ can be viewed as encoding the quadratic order invariants of the quantum channel, and in particular the traceless components form a 3×3 *matrix of subunitarities* \mathcal{S} for the bipartite quantum channel. We then

examine how things simplify for particular important classes of quantum channels. Finally, we study the structure of $(P_{AB}\mathcal{E}^{\otimes 2}P_{AB})^k$ where k is some positive integer. This object is key, as it appears prominently within protocols for estimating subunitarities.

We now calculate the matrix elements of $P_{AB}\mathcal{E}^{\otimes 2}P_{AB}$ in the basis defined in the previous section. There are two mathematical properties that make use of liberally. Firstly, for each subsystem, as the $\mu = 0$ elements are proportional to the identity we have $X_0^\dagger = X_0$ & $Y_0^\dagger = Y_0$. Secondly, as the channel \mathcal{E} is a CPTP map, we have that $\mathcal{E}((X_\mu \otimes Y_\nu)^\dagger) = (\mathcal{E}(X_\mu \otimes Y_\nu))^\dagger$ for any elements of the basis, and so

$$\begin{aligned} \langle \mathbf{X}_\mu^\dagger \otimes \mathbf{Y}_\nu^\dagger | \mathcal{E} | \mathbf{X}_\sigma^\dagger \otimes \mathbf{Y}_\omega^\dagger \rangle &= \text{tr}[(X_\mu^\dagger \otimes Y_\nu^\dagger)^\dagger \mathcal{E}(X_\sigma^\dagger \otimes Y_\omega^\dagger)], \\ &= \text{tr}[\mathcal{E}^\dagger(X_\sigma^\dagger \otimes Y_\omega^\dagger) X_\mu \otimes Y_\nu], \\ &= \text{tr}[\mathcal{E}(X_\sigma \otimes Y_\omega)^\dagger X_\mu \otimes Y_\nu], \\ &= \langle \mathcal{E}(X_\sigma \otimes Y_\omega) | | \mathbf{X}_\mu \otimes \mathbf{Y}_\nu \rangle, \\ &= \langle \mathbf{X}_\sigma \otimes \mathbf{Y}_\omega | \mathcal{E}^\dagger | \mathbf{X}_\mu \otimes \mathbf{Y}_\nu \rangle, \end{aligned} \quad (4.27)$$

where \mathcal{E}^\dagger corresponds to the adjoint of \mathcal{E} that is defined via $\text{tr}[A\mathcal{E}(B)] = \text{tr}[\mathcal{E}^\dagger(A)B]$. Furthermore note that if the non-unital block of \mathcal{E} is T , then the non-unital block of \mathcal{E}^\dagger is T^\dagger .

We can now calculate the 16 possible combinations $\langle a | \mathcal{E}^{\otimes 2} | b \rangle$. One element is simply equivalent to the trace preserving property of a quantum channel

$$\langle 00 | \mathcal{E}^{\otimes 2} | 00 \rangle = \left(\text{tr} \left[\frac{\mathbb{1}}{\sqrt{d}} \mathcal{E} \left(\frac{\mathbb{1}}{\sqrt{d}} \right) \right] \right)^2 = 1. \quad (4.28)$$

The remaining elements can be divided into 3 sub-blocks to be defined, such that

$$P_{AB}\mathcal{E}^{\otimes 2}P_{AB} = \begin{array}{cc} & \begin{array}{c} |00\rangle \\ |ij\rangle \end{array} \\ \begin{array}{c} \langle 00| \\ \langle ij| \end{array} & \begin{pmatrix} 1 & \mathbf{0} \\ \mathbf{x} & \mathcal{S} \end{pmatrix} \end{array} \text{ where } ij \in \{10, 11, 01\}. \quad (4.29)$$

For the definition of subunitarities in the Liouville representation, we refer the reader to Definition 3.3.

Consider a diagonal $\langle 10 | \mathcal{E}^{\otimes 2} | 10 \rangle$ element in the matrix \mathcal{S} , from the above properties it follows that

$$\begin{aligned} \langle 10 | \mathcal{E}^{\otimes 2} | 10 \rangle &= \alpha_A \sum_{i,j=1}^{d_A^2-1} (\langle \mathbf{X}_i | \otimes \langle \mathbf{X}_i^\dagger | \otimes \langle \mathbf{Y}_0 | \otimes \langle \mathbf{Y}_0 |) \mathcal{E}^{\otimes 2} (| \mathbf{X}_j \rangle \otimes | \mathbf{X}_j^\dagger \rangle \otimes | \mathbf{Y}_0 \rangle \otimes | \mathbf{Y}_0 \rangle), \\ &= \alpha_A \sum_{i,j=1}^{d_A^2-1} \langle \mathbf{X}_i \otimes \mathbf{Y}_0 | \mathcal{E} | \mathbf{X}_j \otimes \mathbf{Y}_0 \rangle \langle \mathbf{X}_j \otimes \mathbf{Y}_0 | \mathcal{E}^\dagger | \mathbf{X}_i \otimes \mathbf{Y}_0 \rangle, \\ &= \alpha_A \text{tr} [T_{A \rightarrow A} T_{A \rightarrow A}^\dagger] = \alpha_A \text{tr} [T_{A \rightarrow A}^\dagger T_{A \rightarrow A}] = u_{A \rightarrow A}(\mathcal{E}), \end{aligned} \quad (4.30)$$

where care must be taken with the ordering of the spaces. Similarly, we have $\langle 01 | \mathcal{E}^{\otimes 2} | 01 \rangle = u_{B \rightarrow B}(\mathcal{E})$ and $\langle 11 | \mathcal{E}^{\otimes 2} | 11 \rangle = u_{AB \rightarrow AB}(\mathcal{E})$.

Off diagonal elements in \mathcal{S} can be calculated with an additional dimensional factor. For example, following the same line

$$\begin{aligned} \langle 01 | \mathcal{E}^{\otimes 2} | 10 \rangle &= \sqrt{\alpha_A \alpha_B} \sum_{i,j=1}^{(d_B^2-1)(d_A^2-1)} \langle \mathbf{X}_0 \otimes \mathbf{Y}_i | \mathcal{E} | \mathbf{X}_j \otimes \mathbf{Y}_0 \rangle \langle \mathbf{X}_j \otimes \mathbf{Y}_0 | \mathcal{E}^\dagger | \mathbf{X}_0 \otimes \mathbf{Y}_i \rangle, \\ &= \sqrt{\alpha_A \alpha_B} \text{tr} \left[T_{A \rightarrow B} T_{A \rightarrow B}^\dagger \right] = \sqrt{\frac{\alpha_B}{\alpha_A}} u_{A \rightarrow B}(\mathcal{E}). \end{aligned} \quad (4.31)$$

Further, we have elements such as

$$\begin{aligned} \langle 11 | \mathcal{E}^{\otimes 2} | 10 \rangle &= \alpha_A \sqrt{\alpha_B} \sum_{k,j,n=1}^{(d_A^2-1)(d_B^2-1)} \langle \mathbf{X}_j \otimes \mathbf{Y}_n | \mathcal{E} | \mathbf{X}_k \otimes \mathbf{Y}_0 \rangle \langle \mathbf{X}_k \otimes \mathbf{Y}_0 | \mathcal{E}^\dagger | \mathbf{X}_j \otimes \mathbf{Y}_n \rangle, \\ &= \alpha_A \sqrt{\alpha_B} \text{tr} \left[T_{A \rightarrow AB}^\dagger T_{A \rightarrow AB} \right] = \sqrt{\alpha_B} u_{A \rightarrow AB}(\mathcal{E}) \end{aligned} \quad (4.32)$$

and $\langle 10 | \mathcal{E}^{\otimes 2} | 11 \rangle = \alpha_A \sqrt{\alpha_B} \text{tr} \left[T_{AB \rightarrow A}^\dagger T_{AB \rightarrow A} \right] = \frac{1}{\sqrt{\alpha_B}} u_{AB \rightarrow A}(\mathcal{E})$. The remaining elements of \mathcal{S} can be found by swapping the labeling of the subsystems. Putting this together we have the full matrix of subunitarities given by,

$$\mathcal{S} = \begin{matrix} & \begin{matrix} |10\rangle & |11\rangle & |01\rangle \end{matrix} \\ \begin{matrix} \langle 10| \\ \langle 11| \\ \langle 01| \end{matrix} & \begin{pmatrix} u_{A \rightarrow A}(\mathcal{E}) & \frac{1}{\sqrt{\alpha_B}} u_{AB \rightarrow A}(\mathcal{E}) & \sqrt{\frac{\alpha_A}{\alpha_B}} u_{B \rightarrow A}(\mathcal{E}) \\ \sqrt{\alpha_B} u_{A \rightarrow AB}(\mathcal{E}) & u_{AB \rightarrow AB}(\mathcal{E}) & \sqrt{\alpha_A} u_{B \rightarrow AB}(\mathcal{E}) \\ \sqrt{\frac{\alpha_B}{\alpha_A}} u_{A \rightarrow B}(\mathcal{E}) & \frac{1}{\sqrt{\alpha_A}} u_{AB \rightarrow B}(\mathcal{E}) & u_{B \rightarrow B}(\mathcal{E}) \end{pmatrix} \end{matrix}. \quad (4.33)$$

Pleasingly, every subunitarity of a bipartite channel is represented in \mathcal{S} . We highlight that the diagonal elements of \mathcal{S} are of particular interest as they are exactly the components of correlation unitarity, as previously defined.

The three elements $\langle ij | \mathcal{E}^{\otimes 2} | 00 \rangle$ with $ij \in \{01, 10, 11\}$ quantify the *non-unitarity* of the channel for each subsystem to quadratic order, through the H-S inner product of the generalized Bloch vector \mathbf{x} for each subsystem. We can define $x_A := \mathbf{x}_{A \rightarrow A}^\dagger \mathbf{x}_{A \rightarrow A}$ and similarly for B and AB . Therefore we have

$$\begin{aligned} \langle 10 | \mathcal{E}^{\otimes 2} | 00 \rangle &= \sqrt{\alpha_A} \sum_{i=1}^{d_A^2-1} \langle \mathbf{X}_i \otimes \mathbf{Y}_0 | \mathcal{E} | \mathbf{X}_0 \otimes \mathbf{Y}_0 \rangle \langle \mathbf{X}_0 \otimes \mathbf{Y}_0 | \mathcal{E}^\dagger | \mathbf{X}_i \otimes \mathbf{Y}_0 \rangle, \\ &= \sqrt{\alpha_A} \mathbf{x}_{A \rightarrow A}^\dagger \mathbf{x}_{A \rightarrow A} = \sqrt{\alpha_A} x_A, \end{aligned} \quad (4.34)$$

similarly $\langle 11 | \mathcal{E}^{\otimes 2} | 00 \rangle = \sqrt{\alpha_A \alpha_B} x_{AB}$, $\langle 01 | \mathcal{E}^{\otimes 2} | 00 \rangle = \sqrt{\alpha_B} x_B$. We group these together into the vector $\mathbf{x}^T = (\sqrt{\alpha_A} x_A, \sqrt{\alpha_A \alpha_B} x_{AB}, \sqrt{\alpha_B} x_B)$ to get the form of equation (4.29).

The final three elements $\langle 00 | \mathcal{E}^{\otimes 2} | ij \rangle$ with $ij \in \{01, 10, 11\}$ are required to be zero from the trace preserving properties of a quantum channel. For example, considering $\langle 00 | \mathcal{E}^{\otimes 2} | 10 \rangle$ for \mathcal{E} to be a valid TP map we must have $\langle \mathbf{X}_0 \otimes \mathbf{Y}_0 | \mathcal{E} | \mathbf{X}_i \otimes \mathbf{Y}_0 \rangle = 0$ for all i . Therefore

$$\langle 00 | \mathcal{E}^{\otimes 2} | 10 \rangle = \sqrt{\alpha_A} \sum_{i=1}^{d_A^2-1} \langle \mathbf{X}_0 \otimes \mathbf{Y}_0 | \mathcal{E} | \mathbf{X}_i \otimes \mathbf{Y}_0 \rangle \langle \mathbf{X}_i \otimes \mathbf{Y}_0 | \mathcal{E}^\dagger | \mathbf{X}_0 \otimes \mathbf{Y}_0 \rangle = 0. \quad (4.35)$$

Through the same argument $\langle 00 | \mathcal{E}^{\otimes 2} | 01 \rangle = \langle 00 | \mathcal{E}^{\otimes 2} | 11 \rangle = 0$.

Finally, putting all elements together, labeling $P_{AB} \mathcal{E}^{\otimes 2} P_{AB} = (\star)$ we get,

$$(\star) = \begin{matrix} & |00\rangle & |10\rangle & |11\rangle & |01\rangle \\ \begin{matrix} \langle 00| \\ \langle 10| \\ \langle 11| \\ \langle 01| \end{matrix} & \begin{pmatrix} 1 & 0 & 0 & 0 \\ \sqrt{\alpha_A} x_A & u_{A \rightarrow A}(\mathcal{E}) & \frac{1}{\sqrt{\alpha_B}} u_{AB \rightarrow A}(\mathcal{E}) & \sqrt{\frac{\alpha_A}{\alpha_B}} u_{B \rightarrow A}(\mathcal{E}) \\ \sqrt{\alpha_A \alpha_B} x_{AB} & \sqrt{\alpha_B} u_{A \rightarrow AB}(\mathcal{E}) & u_{AB \rightarrow AB}(\mathcal{E}) & \sqrt{\alpha_A} u_{B \rightarrow AB}(\mathcal{E}) \\ \sqrt{\alpha_B} x_B & \sqrt{\frac{\alpha_B}{\alpha_A}} u_{A \rightarrow B}(\mathcal{E}) & \frac{1}{\sqrt{\alpha_A}} u_{AB \rightarrow B}(\mathcal{E}) & u_{B \rightarrow B}(\mathcal{E}) \end{pmatrix} \end{matrix}. \quad (4.36)$$

Comparing this with decomposition of the Liouville representation of a bipartite channel \mathcal{E} in equation (3.27), we see that P_{AB} produces the normalized purity of every sub-block of \mathcal{E} . As subunitarities are the normalized purity of sub-blocks of the unital block T , these values are extracted, as well as the absolute value of the non-unital vector for both subsystems.

Summary

Two local twirls, $\mathcal{C} \times \mathcal{C}$, produces a projector, P_{AB} , that averages a bipartite channel on a subsystem level to produce a matrix of the all the subunitarities of the channel, \mathcal{S} .

Using the form of the top row of $P_{AB} \mathcal{E}^{\otimes 2} P_{AB}$, it is easily seen that

$$\det(P_{AB} \mathcal{E}^{\otimes 2} P_{AB} - \lambda \mathbb{1}) = (1 - \lambda) \det(\mathcal{S} - \lambda \mathbb{1}) \quad (4.37)$$

and therefore for any channel \mathcal{E} the 4 eigenvalues of $P_{AB} \mathcal{E}^{\otimes 2} P_{AB}$ will be $\lambda_0 = 1$ and the 3 eigenvalues of \mathcal{S} . Within a subunitarity randomized benchmarking protocol, we would expect to encounter the object $(P_{AB} \mathcal{E}^{\otimes 2} P_{AB})^m$ for an integer m similar to the total unitarity protocol. Before tackling the general case of decomposing this matrix, we first consider a simpler case.

4.3.3 The matrix components for separable channels

For a product channel $\mathcal{E}_A \otimes \mathcal{E}_B$ the subunitarity matrix \mathcal{S} takes a particularly simple form. Since the channel is separable quantum information does not flow between A and B and Theorem 3.4 tells us that $u_{A \rightarrow B}(\mathcal{E}_A \otimes \mathcal{E}_B) = u_{B \rightarrow A}(\mathcal{E}_A \otimes \mathcal{E}_B) = 0$ and $u_{AB \rightarrow AB}(\mathcal{E}_A \otimes \mathcal{E}_B) =$

$u_{A \rightarrow A}(\mathcal{E}_A \otimes \mathcal{E}_B) \cdot u_{B \rightarrow B}(\mathcal{E}_A \otimes \mathcal{E}_B)$. Thus, for a product channel $\mathcal{E} = \mathcal{E}_A \otimes \mathcal{E}_B$ we have

$$P_{AB} \mathcal{E}^{\otimes 2} P_{AB} = \begin{array}{l} \langle 00| \\ \langle 10| \\ \langle 11| \\ \langle 01| \end{array} \begin{pmatrix} |00\rangle & |10\rangle & |11\rangle & |01\rangle \\ 1 & 0 & 0 & 0 \\ \sqrt{\alpha_A} x_A & u(\mathcal{E}_A) & 0 & 0 \\ \sqrt{\alpha_A \alpha_B} x_A x_B & \sqrt{\alpha_B} u(\mathcal{E}_A) x_B & u(\mathcal{E}_A) u(\mathcal{E}_B) & \sqrt{\alpha_A} u(\mathcal{E}_B) x_A \\ \sqrt{\alpha_B} x_B & 0 & 0 & u(\mathcal{E}_B) \end{pmatrix}. \quad (4.38)$$

From this it is readily seen that the eigenvalues are $\{1, u(\mathcal{E}_A), u(\mathcal{E}_B), u(\mathcal{E}_A)u(\mathcal{E}_B)\}$. More generally, for the case of a *separable* channel, $\mathcal{E}_{AB} = \sum_i p_i \mathcal{E}_{A,i} \otimes \mathcal{E}_{B,i}$, from Lemmas B.2 & B.3 we find instead that, again labeling $P_{AB} \mathcal{E}^{\otimes 2} P_{AB} = (\star)$,

$$(\star) = \begin{array}{l} \langle 00| \\ \langle 10| \\ \langle 11| \\ \langle 01| \end{array} \begin{pmatrix} |00\rangle & |10\rangle & |11\rangle & |01\rangle \\ 1 & 0 & 0 & 0 \\ \sqrt{\alpha_A} x_A & u_{A \rightarrow A}(\mathcal{E}_{AB}) & 0 & 0 \\ \sqrt{\alpha_A \alpha_B} x_{AB} & \sqrt{\alpha_B} u_{A \rightarrow AB}(\mathcal{E}_{AB}) & u_{AB \rightarrow AB}(\mathcal{E}_{AB}) & \sqrt{\alpha_A} u_{B \rightarrow AB}(\mathcal{E}_{AB}) \\ \sqrt{\alpha_B} x_B & 0 & 0 & u_{B \rightarrow B}(\mathcal{E}_{AB}) \end{pmatrix} \quad (4.39)$$

and so now the eigenvalues are $\{1, u_{A \rightarrow A}(\mathcal{E}_{AB}), u_{B \rightarrow B}(\mathcal{E}_{AB}), u_{AB \rightarrow AB}(\mathcal{E}_{AB})\}$. Therefore in both these cases, $(P_{AB} \mathcal{E}^{\otimes 2} P_{AB})^m$, will have eigenvalues

$$\{\lambda_i\} = \{1, u_{A \rightarrow A}(\mathcal{E}_{AB})^m, u_{B \rightarrow B}(\mathcal{E}_{AB})^m, u_{AB \rightarrow AB}(\mathcal{E}_{AB})^m\}. \quad (4.40)$$

We will see shortly that this exact form appears within a randomized benchmarking protocol, and that for separable (and product) channels the decay constants are simply the above three subunitarities.

More generally, we do not have such a simple link between the eigenvalues and subunitarities. Indeed, it may be the case that the matrix cannot be diagonalized fully, and so one must instead use a Jordan decomposition to determine the decay law for the associated protocol. We provide these details in the next section.

4.3.4 Jordan decomposition for arbitrary bipartite channels

For a general bipartite channel \mathcal{E} we can use the Jordan normal form of the matrix $P_{AB} \mathcal{E}^{\otimes 2} P_{AB}$ to study the structure scales with a power, $(P_{AB} \mathcal{E}^{\otimes 2} P_{AB})^m$. This will be critical for estimating the subunitarities of channels where we have no knowledge about their structure.

Definition 4.1. *Using the Jordan matrix decomposition of any square matrix M , we can find the Jordan normal form such that*

$$M = S^{-1} J S, \quad (4.41)$$

where S is a invertible matrix, and J is a block diagonal matrix of Jordan blocks [122].

This gives a very simple scaling law.

Corollary 4.1. *The Jordan matrix decomposition of a square matrix M to the power n follows*

$$M^n = S^{-1} J^n S. \quad (4.42)$$

Proof. This follows from definition as $SS^{-1} = \mathbb{1}$. \square

The above imply that if write $P_{AB}\mathcal{E}^{\otimes 2}P_{AB}$, in a Jordan normal form, J , then the decay law of $(P_{AB}\mathcal{E}^{\otimes 2}P_{AB})^m$ will be determined entirely by J^m . There are 3 possibilities that could occur:

$$J = \begin{pmatrix} 1 & 0 & 0 & 0 \\ 0 & \lambda_1 & 0 & 0 \\ 0 & 0 & \lambda_3 & 0 \\ 0 & 0 & 0 & \lambda_2 \end{pmatrix}, J = \begin{pmatrix} 1 & 0 & 0 & 0 \\ 0 & \lambda_1 & 1 & 0 \\ 0 & 0 & \lambda_1 & 0 \\ 0 & 0 & 0 & \lambda_2 \end{pmatrix}, J = \begin{pmatrix} 1 & 0 & 0 & 0 \\ 0 & \lambda_1 & 1 & 0 \\ 0 & 0 & \lambda_1 & 1 \\ 0 & 0 & 0 & \lambda_1 \end{pmatrix}, \quad (4.43)$$

where λ_i are the eigenvalues of the block \mathcal{S} . Which form the Jordan decomposition takes depends on the degeneracy of λ_i and whether the geometric and algebraic multiplicities of each λ_i coincide [122].

For J diagonal, we have that

$$(P_{AB}\mathcal{E}^{\otimes 2}P_{AB})^m = S^{-1} J^m S = S^{-1} \begin{pmatrix} 1 & 0 & 0 & 0 \\ 0 & \lambda_1^m & 0 & 0 \\ 0 & 0 & \lambda_3^m & 0 \\ 0 & 0 & 0 & \lambda_2^m \end{pmatrix} S, \quad (4.44)$$

where $\{\lambda_i\}$ are the eigenvalues of \mathcal{S} . Therefore,

$$(P_{AB}\mathcal{E}^{\otimes 2}P_{AB})^m = S^{-1}(|00\rangle\langle 00| + \lambda_1^m |10\rangle\langle 10| + \lambda_2^m |01\rangle\langle 01| + \lambda_3^m |11\rangle\langle 11|)S \quad (4.45)$$

where S is some invertible matrix.

If the Jordan decomposition of $P_{AB}\mathcal{E}^{\otimes 2}P_{AB}$ is not completely diagonal, then the object $(P_{AB}\mathcal{E}^{\otimes 2}P_{AB})^m$ still scales with the eigenvalues of \mathcal{S} but in a slightly more complex manner. From above, the 2 remaining options are

$$(P_{AB}\mathcal{E}^{\otimes 2}P_{AB})^m = S^{-1} \begin{pmatrix} 1 & 0 & 0 & 0 \\ 0 & \lambda_1 & 1 & 0 \\ 0 & 0 & \lambda_1 & 0 \\ 0 & 0 & 0 & \lambda_2 \end{pmatrix}^m S = S^{-1} \begin{pmatrix} 1 & 0 & 0 & 0 \\ 0 & \lambda_1^m & m\lambda_1^{m-1} & 0 \\ 0 & 0 & \lambda_1^m & 0 \\ 0 & 0 & 0 & \lambda_2^m \end{pmatrix} S, \quad (4.46)$$

and

$$(P_{AB}\mathcal{E}^{\otimes 2}P_{AB})^m = S^{-1} \begin{pmatrix} 1 & 0 & 0 & 0 \\ 0 & \lambda_1 & 1 & 0 \\ 0 & 0 & \lambda_1 & 1 \\ 0 & 0 & 0 & \lambda_1 \end{pmatrix}^m S = S^{-1} \begin{pmatrix} 1 & 0 & 0 & 0 \\ 0 & \lambda_1^m & \lambda_1^{m-1} & \frac{m(m-1)}{2}\lambda_1^{m-2} \\ 0 & 0 & \lambda_1^m & \lambda_1^{m-1} \\ 0 & 0 & 0 & \lambda_1^m \end{pmatrix} S. \quad (4.47)$$

1. **Prepare** the system in a state ρ .
2. **Select** a sequence of length k of simultaneous random noisy Clifford gates locally on subsystems A and B , starting with $k = 1$. E.g. for each gate $\mathcal{U}_{AB,i} = \mathcal{U}_{A,i_1} \otimes \mathcal{U}_{B,i_2}$.
3. **Estimate** the square $(m)^2$ of an expectation value of an observable M , for this particular sequence of gates.
4. **Repeat 1, 2 & 3** for many random sequences \mathbf{s} of the same length, finding the average estimation $\mathbb{E}_s[m(s)^2]$ of $(m)^2$.
5. **Repeat 1, 2, 3 & 4** increasing the length of the sequence k by 1.
6. **Fit** each value of $\mathbb{E}_s[m(s)^2]$ against the corresponding k and obtain decay parameters as in equation (4.55).

Protocol 1: **SPAM robust subunitarity estimation** ($\mathcal{C} \times \mathcal{C}$)

Therefore, in this more general scenario the decay law behaviour of $(P_{AB}\mathcal{E}^{\otimes 2}P_{AB})^m$ is still described by the constants $\{\lambda_i\}$.

This gives us all the tools we require to define a novel unitarity benchmarking protocol that we can relate to the subunitarities of a quantum channel.

4.3.5 Analysis of a local twirl unitarity benchmarking protocol

We now introduce a unitarity benchmarking protocol, Protocol 1, and prove that it allows the eigenvalues of the matrix of subunitarities \mathcal{S} to be estimated SPAM robustly, under the assumption of gate-independent noise associated to the gateset $\Gamma_A \otimes \Gamma_B$. We do not assume the noise is local to each subsystem and it is therefore described by some bipartite channel.

The protocol implements a local twirling on each subsystem of the associated bipartite noise, similar to the total twirl we encountered in the total unitarity protocol. We now prove this result analytically, and show that it gives us object $(P_{AB}\mathcal{E}^{\otimes 2}P_{AB})^m$ that we have been examining in the previous section.

Lemma 4.3. *Over all sequences \mathbf{s} , and for a gate-independent noise channel \mathcal{E} , the expectation value of a observable \tilde{M} squared can be written as:*

$$\mathbb{E}_s[m(s)^2] = \left\langle \tilde{M} \right\rangle^{\otimes 2} (P_{AB}\mathcal{E}^{\otimes 2}P_{AB})^{k-1} |\rho\rangle^{\otimes 2}. \quad (4.48)$$

with circuit of depth k , and sequences indexed via $\mathbf{s} = (s_A, s_B)$ with $s_A = (a_1, a_2, \dots, a_k)$ and $s_B = (b_1, b_2, \dots, b_k)$ specifying the particular target unitary in each of the local gatesets $\Gamma_{AB} = \Gamma_A \otimes \Gamma_B$.

Proof. From equation (4.9), over all sequences we have

$$\begin{aligned}
\mathbb{E}_s[m(s)^2] &:= \frac{1}{|\Gamma_{AB}|^k} \sum_s m(s)^2 = \frac{1}{|\Gamma_{AB}|^k} \sum_s (\text{tr}[M\tilde{\mathcal{U}}_s(\rho)])^2 \\
&= \frac{1}{|\Gamma_{AB}|^k} \sum_s \langle \mathbf{M} | \tilde{\mathcal{U}}_s(\rho) \rangle^2 = \frac{1}{|\Gamma_{AB}|^k} \sum_s \langle \mathbf{M} | \tilde{\mathcal{U}}_s | \rho \rangle^2, \\
&= \frac{1}{|\Gamma_{AB}|^k} \sum_s \langle \mathbf{M} | \tilde{\mathcal{U}}_{s_k} \tilde{\mathcal{U}}_{s_{k-1}} \dots \tilde{\mathcal{U}}_{s_1} | \rho \rangle^2, \\
&= \frac{1}{|\Gamma_{AB}|^k} \sum_s \langle \mathbf{M} | (\boldsymbol{\varepsilon} \mathbf{u}_{s_k})(\boldsymbol{\varepsilon} \mathbf{u}_{s_{k-1}}) \dots (\boldsymbol{\varepsilon} \mathbf{u}_{s_1}) | \rho \rangle^2.
\end{aligned} \tag{4.49}$$

Which we can write equivalently as a bipartite system,

$$\mathbb{E}_s[m(s)^2] = \frac{1}{|\Gamma_{AB}|^k} \sum_s \langle \mathbf{M} |^{\otimes 2} (\boldsymbol{\varepsilon}^{\otimes 2} \mathbf{u}_{s_k}^{\otimes 2})(\boldsymbol{\varepsilon}^{\otimes 2} \mathbf{u}_{s_{k-1}}^{\otimes 2}) \dots (\boldsymbol{\varepsilon}^{\otimes 2} \mathbf{u}_{s_1}^{\otimes 2}) | \rho \rangle^{\otimes 2}. \tag{4.50}$$

For each gate up to k , we can substitute the summation over \mathcal{U}_{s_k} , such that

$$\begin{aligned}
\mathbb{E}_s[m(s)^2] &= \langle \mathbf{M} |^{\otimes 2} \left(\frac{1}{|\Gamma_{AB}|} \sum_{U_{s_k} \in \Gamma_{AB}} \boldsymbol{\varepsilon}^{\otimes 2} \mathbf{u}_{s_k}^{\otimes 2} \right) \\
&\quad \left(\frac{1}{|\Gamma_{AB}|} \sum_{U_{s_{k-1}} \in \Gamma_{AB}} \boldsymbol{\varepsilon}^{\otimes 2} \mathbf{u}_{s_{k-1}}^{\otimes 2} \right) \\
&\quad \dots \left(\frac{1}{|\Gamma_{AB}|} \sum_{U_{s_1} \in \Gamma_{AB}} \boldsymbol{\varepsilon}^{\otimes 2} \mathbf{u}_{s_1}^{\otimes 2} \right) | \rho \rangle^{\otimes 2},
\end{aligned} \tag{4.51}$$

recalling that $\mathcal{U}_s = \mathcal{U}_{s_A} \otimes \mathcal{U}_{s_B}$ and the sequences expand as $\sum_s^{k^2} = \sum_{s_A, s_B}^{k, k}$. We now have the form to use the property that the whole gateset forms a unitarity 2-design on each subsystem. Namely, from equations (4.3) and (4.23), we have

$$\frac{1}{|\Gamma_{AB}|} \sum_{U_{s_i} \in \Gamma_{AB}} \boldsymbol{\varepsilon}^{\otimes 2} \mathbf{u}_{s_i}^{\otimes 2} = \int d\mu_{\text{Haar}}(U_A) \int d\mu_{\text{Haar}}(U_B) \boldsymbol{\varepsilon}^{\otimes 2} (\mathbf{u}_A \otimes \mathbf{u}_B)^{\otimes 2} \tag{4.52}$$

for any index in the sequence up to k . Substituting this into equation (4.51) reduces the summation to k identical integrals over U_A and U_B . So we can write

$$\mathbb{E}_s[m(s)^2] = \langle \mathbf{M} |^{\otimes 2} (\boldsymbol{\varepsilon}^{\otimes 2} \int d\mu_{\text{Haar}}(U_A) \int d\mu_{\text{Haar}}(U_B) (\mathbf{u}_A \otimes \mathbf{u}_B)^{\otimes 2})^k | \rho \rangle^{\otimes 2}. \tag{4.53}$$

This is just the projector $P_{AB} = P_A \otimes P_B$ as decomposed in Section 4.3.1. Therefore with a final substitution we can find desired form

$$\begin{aligned}
\mathbb{E}_s[m(s)^2] &= \langle \mathbf{M} |^{\otimes 2} (\boldsymbol{\varepsilon}^{\otimes 2} P_{AB})^k | \rho \rangle^{\otimes 2}, \\
&= \langle \mathbf{M} |^{\otimes 2} \boldsymbol{\varepsilon}^{\otimes 2} (P_{AB} \boldsymbol{\varepsilon}^{\otimes 2} P_{AB})^{k-1} | \rho \rangle^{\otimes 2}, \\
&= \langle \boldsymbol{\varepsilon}^{-1}(\mathbf{M}) |^{\otimes 2} (P_{AB} \boldsymbol{\varepsilon}^{\otimes 2} P_{AB})^{k-1} | \rho \rangle^{\otimes 2}, \\
&= \langle \tilde{\mathbf{M}} |^{\otimes 2} (P_{AB} \boldsymbol{\varepsilon}^{\otimes 2} P_{AB})^{k-1} | \rho \rangle^{\otimes 2},
\end{aligned} \tag{4.54}$$

where we have absorbed the final noise channel to the noisy measurement of the system. This completes the proof. \square

It remains to give the final relation between the twirled error channel and the eigenvalues of the associated matrix of subunitarities. The following result connects the benchmarking protocol given in Protocol 1 to the matrix of subunitarities, \mathcal{S} .

Theorem 4.2 (Derivation of subunitarity estimation protocol). *Over all sequences s with circuit of depth k , and for a gate-independent noise channel \mathcal{E} , the expectation value of a observable \tilde{M} squared can be written as:*

$$\mathbb{E}_s[m(s)^2] = c_{00} + c_{10} \lambda_1^{k-1} + c_{01} \lambda_2^{k-1} + c_{11} \lambda_3^{k-1}, \quad (4.55)$$

where $\{c_{ij}\}$ are constants related to SPAM errors and $\{\lambda_i\}$ are the eigenvalues of the matrix of subunitarities for the channel \mathcal{E} given as

$$\mathcal{S} = \begin{pmatrix} u_{A \rightarrow A}(\mathcal{E}) & \frac{1}{\sqrt{\alpha_B}} u_{AB \rightarrow A}(\mathcal{E}) & \sqrt{\frac{\alpha_A}{\alpha_B}} u_{B \rightarrow A}(\mathcal{E}) \\ \sqrt{\alpha_B} u_{A \rightarrow AB}(\mathcal{E}) & u_{AB \rightarrow AB}(\mathcal{E}) & \sqrt{\alpha_A} u_{B \rightarrow AB}(\mathcal{E}) \\ \sqrt{\frac{\alpha_B}{\alpha_A}} u_{A \rightarrow B}(\mathcal{E}) & \frac{1}{\sqrt{\alpha_A}} u_{AB \rightarrow B}(\mathcal{E}) & u_{B \rightarrow B}(\mathcal{E}) \end{pmatrix}. \quad (4.56)$$

Proof. From Section 4.3.4, if the Jordan decomposition is diagonal we have

$$(P_{AB} \mathcal{E}^{\otimes 2} P_{AB})^{k-1} = S^{-1} (|00\rangle\langle 00| + \lambda_1^{k-1} |10\rangle\langle 10| + \lambda_2^{k-1} |01\rangle\langle 01| + \lambda_3^{k-1} |11\rangle\langle 11|) S, \quad (4.57)$$

where λ_i are the eigenvalues of the matrix \mathcal{S} . Therefore from Lemma 4.3 we can write

$$\begin{aligned} \mathbb{E}_s[m(s)^2] &= \left\langle \tilde{M} \right|^{\otimes 2} (P_{AB} \mathcal{E}^{\otimes 2} P_{AB})^{k-1} |\rho\rangle^{\otimes 2}, \\ &= \left\langle \tilde{M} \right|^{\otimes 2} S^{-1} J^{k-1} S |\rho\rangle^{\otimes 2}, \\ &= \left\langle \tilde{M} \right|^{\otimes 2} S^{-1} (|00\rangle\langle 00| + \lambda_1^{k-1} |10\rangle\langle 10| + \lambda_2^{k-1} |01\rangle\langle 01| + \lambda_3^{k-1} |11\rangle\langle 11|) S |\rho\rangle^{\otimes 2}. \end{aligned} \quad (4.58)$$

The transformation matrix S can be absorbed into the initial state of the system and the final measurement such that

$$\begin{aligned} \mathbb{E}_s[m(s)^2] &= \left\langle S^{-1\dagger} (\tilde{M}^{\otimes 2}) \right| 00 \rangle \langle 00 | S(\rho^{\otimes 2}) \rangle \\ &\quad + \lambda_1^{k-1} \left\langle S^{-1\dagger} (\tilde{M}^{\otimes 2}) \right| 10 \rangle \langle 10 | S(\rho^{\otimes 2}) \rangle \\ &\quad + \lambda_2^{k-1} \left\langle S^{-1\dagger} (\tilde{M}^{\otimes 2}) \right| 01 \rangle \langle 01 | S(\rho^{\otimes 2}) \rangle \\ &\quad + \lambda_3^{k-1} \left\langle S^{-1\dagger} (\tilde{M}^{\otimes 2}) \right| 11 \rangle \langle 11 | S(\rho^{\otimes 2}) \rangle. \end{aligned} \quad (4.59)$$

Or simply,

$$\mathbb{E}_s[m(s)^2] = c_{00} + c_{10} \lambda_1^{k-1} + c_{01} \lambda_2^{k-1} + c_{11} \lambda_3^{k-1}. \quad (4.60)$$

So if a channel \mathcal{E} produces a diagonal Jordan decomposition J , the protocol will produce a fit of this form where λ_i are the eigenvalues of \mathcal{S} .

If any eigenvalues are degenerate the Jordan decomposition will not be diagonal, and can take two forms. Firstly,

$$J^{k-1} = \begin{pmatrix} 1 & 0 & 0 & 0 \\ 0 & \lambda_1^{k-1} & (k-1)\lambda_1^{k-2} & 0 \\ 0 & 0 & \lambda_1^{k-1} & 0 \\ 0 & 0 & 0 & \lambda_2^{k-1} \end{pmatrix}, \quad (4.61)$$

where the fit will take the following form: $\mathbb{E}_s[m(s)^2] = c_0 + c_1 \lambda_1^{k-1} + c_2 \lambda_2^{k-1}$, where λ_i are the degenerate eigenvalues of \mathcal{S} , and constants c_i are dependent on M, ρ, S, S^{-1} & \mathbf{x} . However, with simple rearrangement we can get the required form of equation (4.60), such as with $c_2 \lambda_2^{k-1} = (c_{01} + c_{11}) \lambda_2^{k-1}$. Secondly,

$$J^{k-1} = \begin{pmatrix} 1 & 0 & 0 & 0 \\ 0 & \lambda_1^{k-1} & \lambda_1^{k-2} & \frac{(k-1)(k-2)}{2} \lambda_1^{k-3} \\ 0 & 0 & \lambda_1^{k-1} & \lambda_1^{k-2} \\ 0 & 0 & 0 & \lambda_1^{k-1} \end{pmatrix}, \quad (4.62)$$

where the fit will take the following form: $\mathbb{E}_s[m(s)^2] = c_0 + c_1 \lambda_1^{k-1}$, where λ_1 is the degenerate eigenvalue of \mathcal{S} , and for different constants c_i dependent on M, ρ, S, S^{-1} and \mathbf{x} . Again, with simple rearrangement we can get the required form of equation (4.60). This completes the proof. \square

This completes the connection between Protocol 1 and the subunitarities of a channel.

Summary

We have established that the subunitarities, $u_{X \rightarrow Y}(\mathcal{E})$, of a bipartite channel, \mathcal{E} , appear naturally through the local twirling, $\mathcal{C} \times \mathcal{C}$, of a novel randomized benchmarking protocol. However the connection is non-trivial as the three decay parameters estimated through Protocol 1 are the eigenvalues, $\{\lambda_i\}$ of a matrix, \mathcal{S} , of *all* subunitarities.

Our ultimate goal is to access individual subunitarities such as, $u_{A \rightarrow A}(\mathcal{E})$, and the correlation unitarity, $u_c(\mathcal{E})$, as these quantities have operational interpretations and useful properties as discussed in Chapter 3. In the following section, we summarize how Protocol 1 can be used in practice to estimate particular subunitarities.

4.4 SPAM robust estimation of subunitarities for device noise

In the context of benchmarking we have the problem of determining the *addressability* of qubits and the existence of *crossstalk* between qubits. For example, we want to implement

some target unitary $\mathcal{U}_i \otimes id$ on one qubit, while leaving all others unaffected. However, in reality the physical channel performed $\tilde{\mathcal{U}}_i$ will involve an effective noise channel \mathcal{E} that does not factorize neatly with noise only on the target qubit. Instead, the noise channel will act non-trivially on each subsystem of the bipartite split and could involve correlations that include the leakage of quantum information. Learning the subunitarities and correlation unitarity of \mathcal{E} would therefore give independent information beyond existing techniques. We now discuss under which circumstances such quantities can be estimated SPAM robustly for device noise.

4.4.1 Estimation of subunitarities through local & global protocols

In what follows we again consider the averaged noise channel over the gateset, and so at the simplest level of analysis assume that we have gate-independent noise. A more general analysis involving gate-dependent noise should be possible by following perturbative approaches such as in [44, 136] and by making use of interleaved benchmarking [82].

We also note that the channel under consideration need not be a noise channel in such a scheme, but could be a target channel on which we wish to do robust tomography. For this context it would be possible to exploit recent methods that make use of randomized benchmarking to do tomography of quantum channels such as in [4]. We leave this kind of analysis for later investigation in Chapter 5.

Under this average noise model assumption, we now perform a unitarity benchmarking scheme by randomly sampling from $\Gamma_A \otimes \Gamma_B$ and obtain a circuit of depth k , with sequence indexed via $s = (s_A, s_B)$ with $s_A = (a_1, a_2, \dots, a_k)$ and $s_B = (b_1, b_2, \dots, b_k)$ specifying the particular target unitary in the local gatesets. As before, we estimate the quantity $m(s) := \text{tr} \left[M \tilde{\mathcal{U}}_s(\rho) \right]$ and also $\mathbb{E}_s[m(s)^2]$ for circuits of depth k . However, for these local twirls, this quantity now has a different decay profile. As we have shown in Section 4.3.5 this quantity behaves as

$$\mathbb{E}_s[m(s)^2] = c_{00} + c_{01}\lambda_1^{k-1} + c_{10}\lambda_2^{k-1} + c_{11}\lambda_3^{k-1}, \quad (4.63)$$

where $(\lambda_1, \lambda_2, \lambda_3)$ are the eigenvalues³ of the matrix of subunitarities

$$\mathcal{S} = \begin{pmatrix} u_{A \rightarrow A}(\mathcal{E}) & \frac{1}{\sqrt{\alpha_B}} u_{AB \rightarrow A}(\mathcal{E}) & \sqrt{\frac{\alpha_A}{\alpha_B}} u_{B \rightarrow A}(\mathcal{E}) \\ \sqrt{\alpha_B} u_{A \rightarrow AB}(\mathcal{E}) & u_{AB \rightarrow AB}(\mathcal{E}) & \sqrt{\alpha_A} u_{B \rightarrow AB}(\mathcal{E}) \\ \sqrt{\frac{\alpha_B}{\alpha_A}} u_{A \rightarrow B}(\mathcal{E}) & \frac{1}{\sqrt{\alpha_A}} u_{AB \rightarrow B}(\mathcal{E}) & u_{B \rightarrow B}(\mathcal{E}) \end{pmatrix}, \quad (4.64)$$

with $\alpha_X = \frac{1}{d_X^2 - 1}$, and the constants c_{00}, \dots, c_{11} contain the SPAM-errors. Therefore, the subunitarities arise in the context of this benchmarking, albeit in a more non-trivial form to

³This implicitly assumes a non-degenerate form of a Jordan matrix decomposition. However degenerate cases give rise to similar expressions. See Section 4.3.4 for details.

the global protocol. For example, we have that

$$\mathrm{tr}[\mathcal{S}] = \sum_i \lambda_i = u_{A \rightarrow A}(\mathcal{E}) + u_{AB \rightarrow AB}(\mathcal{E}) + u_{B \rightarrow B}(\mathcal{E}), \quad (4.65)$$

with similar relations existing for the other coefficients of the characteristic polynomial of \mathcal{S} [122]. Note that $\sum_i \lambda_i = 3$ if and only if \mathcal{E} is a product of unitaries, $\mathcal{E} = \mathcal{U}_A \otimes \mathcal{U}_B$, and so this sum of eigenvalues gives a blunt handle on how much \mathcal{E} deviates from this regime.

By estimating the decay constants in equation (4.63) it is possible to obtain an estimate of channel correlations that coincides with the correlation unitarity for a family of channels. It is easily checked that for a product noise channel $\mathcal{E} = \mathcal{E}_A \otimes \mathcal{E}_B$ we have the matrix of subunitarities given by

$$\mathcal{S} = \begin{pmatrix} u(\mathcal{E}_A) & 0 & 0 \\ \sqrt{\alpha_B} u(\mathcal{E}_A) x_B & u(\mathcal{E}_A) u(\mathcal{E}_B) & \sqrt{\alpha_A} u(\mathcal{E}_B) x_A \\ 0 & 0 & u(\mathcal{E}_B) \end{pmatrix}, \quad (4.66)$$

where x_A and x_B are constants related to deviations from unitality (see Section 4.3.3). This implies that eigenvalues of \mathcal{S} are given by

$$\{\lambda_i\} = \{u(\mathcal{E}_A), u(\mathcal{E}_B), u(\mathcal{E}_A)u(\mathcal{E}_B)\}. \quad (4.67)$$

It can be checked that this simple link with subunitarities extends to arbitrary *separable* channels, for which $\lambda_1, \lambda_2, \lambda_3$ are exactly equal to the subunitarities $u_{A \rightarrow A}, u_{B \rightarrow B}, u_{AB \rightarrow AB}$. This provides a way to compute the correlation unitarity. More precisely, given $\lambda_1 \geq \lambda_2 \geq \lambda_3$, we may compute the quantity

$$C = \lambda_3 - \lambda_1 \cdot \lambda_2, \quad (4.68)$$

where we use the fact that subunitarities are upper bounded by one to distinguish λ_3 from the other two. For a separable channel we have $C = u_c$ and therefore get an estimate of the correlation unitarity in a SPAM robust manner from Protocol 1.

Summary

For separable noise channels, \mathcal{E} , we can estimate the correlation unitarity, $u_c(\mathcal{E})$, in a completely SPAM robust manner. However for an unknown channel (which might be non-separable) we cannot guarantee the decay parameters are exactly the subunitarities. Therefore we require additional information to estimate the correlation unitarity.

Beyond separable channels, while in general equation (4.68) is not equal to the correlation unitarity, we could use C as a witness to non-separability in the following way. For a two qubit channel, we have shown in Theorem 3.6 that $u_c(\mathcal{E}_{AB}) > 7/12$ means that \mathcal{E}_{AB} is non-separable. As we have $C = u_c$ for a separable channel, this implies that a value of $C > 7/12$ means the corresponding channel must be non-separable. Therefore C is a witness to non-separability. However the problem with this approach is that, for channels far from separable, the measure C is typically small or even negative. For example, for the *SWAP* channel

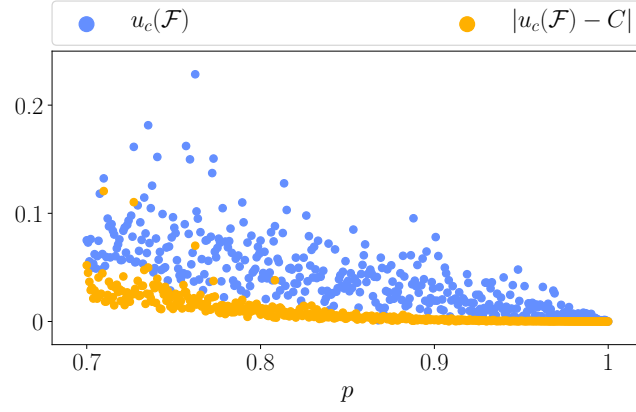


Figure 4.1: **SPAM error robust estimation of u_c for generic quantum channels.** The convergence of the values of correlation unitarity and C as gate noise takes a product form, for a 2 qubit simulation. We show $|u_c - C|$ over p , where $\mathcal{F} = p\mathcal{E}_A \otimes \mathcal{E}_B + (1-p)\mathcal{G}$. The channels \mathcal{E}_A , \mathcal{E}_B and \mathcal{G} are sampled using the methods of [2] and simulated using QuTip [3].

we get $C = -2$. This means that, in practice, using C on its own is not a particularly useful measure for non-separable channels.

For non-separable channels the deviation of the eigenvalues from each of the subunitarities can be bounded by using the Girshgorin Circle Theorem or Brauer's Theorem [122]. For example, we obtain the bounds

$$|\lambda_1 - u_{A \rightarrow A}(\mathcal{E})| \leq \frac{1}{\sqrt{\alpha_B}} u_{AB \rightarrow A}(\mathcal{E}) + \sqrt{\frac{\alpha_A}{\alpha_B}} u_{B \rightarrow A}(\mathcal{E}). \quad (4.69)$$

Using identities for subunitarities, we can further show that

$$|\lambda_1 - u_{A \rightarrow A}(\mathcal{E})| \leq \frac{1}{\sqrt{\alpha_B}} [1 - u_{A \rightarrow A}(\mathcal{E})]. \quad (4.70)$$

These two inequalities are generally weak, due to the factors of α_B and α_A , but they do imply that the approximation is very good when either the off-diagonal elements are small or when the local unitarities are large. In such regimes Protocol 1 will return a good estimate of the correlation unitarity as $C \approx u_c$. We demonstrate this with simulations in Figure 4.1.

Estimation of the three decay constants requires fitting noisy multi-exponential data. This is non-trivial, but a range of methods have been developed to tackle this problem [7]. To assist with fitting, and moreover identify the subunitarity $u_{AB \rightarrow AB}$, we may supplement the local twirling with a global estimate of unitarity, and then make use of the decomposition of unitarity into subunitarities. Specifically, for the case of *unital* separable channels, with $d_A = d_B = d$, we have that

$$u(\mathcal{E}) = \frac{u_{A \rightarrow A}(\mathcal{E}) + u_{B \rightarrow B}(\mathcal{E}) + (d^2 - 1)u_{AB \rightarrow AB}(\mathcal{E})}{d^2 + 1}, \quad (4.71)$$

and therefore we have the relation

$$u_{AB \rightarrow AB}(\mathcal{E}) = \frac{(d^2 + 1)u(\mathcal{E}) - \sum_i \lambda_i}{d^2 - 2}. \quad (4.72)$$

This means that separate estimations of $u(\mathcal{E})$ and the decay constants (λ_i) provide an estimate of $u_{AB \rightarrow AB}(\mathcal{E})$, and so provides additional independent information on the terms entering the correlation unitarity. In practice, this will require careful consideration as the average noise channel associated with global gateset, Γ , (employed in the estimation of unitarity) might be different than that associated with $\Gamma_A \otimes \Gamma_B$.

4.4.2 Black box noise estimation with randomized compiling

We note that by using *randomized compiling* [107, 137] for the implementation of a quantum circuit we may reduce the noise channel to being a Pauli channel.

For Pauli channels, the decay constants (λ_i) exactly coincide with the three subunitarities required for the correlation unitarity, in a similar manner to equation (4.66). However we lack the information to assign each decay constant to a particular subunitarity. We showed in Chapter 3 that equation (4.72) holds for Pauli channels. Therefore, we can identify $u_{AB \rightarrow AB}(\mathcal{E})$ assuming access to $u(\mathcal{E})$. The remaining two subunitarities do not need to be individually identified to calculate $u_{A \rightarrow A}(\mathcal{E}) \cdot u_{B \rightarrow B}(\mathcal{E})$, and we have an estimate of $u_c(\mathcal{E})$.

Putting this together, assuming the same noise is associated with the global and local gatesets as discussed above, with randomized compiling we have a SPAM-robust estimation of the correlation unitarity, $u_c(\mathcal{E})$.

Summary

Recent research indicates we may be able to reduce device noise to a Pauli channel, \mathcal{E} . Then, if the noise is the same for the local and global gatesets, we can estimate the correlation unitarity, $u_c(\mathcal{E})$ of device noise, \mathcal{E} , with complete SPAM robustness.

Alternatively, since a general noise channel will not have λ_i coinciding precisely with the subunitarities, by running the local twirling protocol with and without randomized compiling one could witness the presence of non-Pauli noise.

4.5 Estimation of local subunitarities with resetting errors

While the local twirling protocol provides a means to estimate the correlation unitarity in the case of any separable or Pauli channel, we would like to be able to estimate such correlations for general non-separable channels. The obstacle here is to determine subunitarities such as $u_{A \rightarrow A}(\mathcal{E}_{AB})$. However, this requires preparing the maximally mixed state on subsystem B and benchmarking the unitarity of the effective channel output on A . This presents a problem of how accurately such a reset can be performed. Current devices, including ion-traps [138] and IBM's superconducting qubits [139], allow for mid-circuit measurements and resets. These dynamical circuits capabilities can be accessed through hardware-agnostic SDKs [140, 141].

1. **Prepare** the system in the state ρ .
2. **Select** a sequence of length k of random noisy Clifford gates on subsystem A , starting with $k = 1$. E.g. for each gate $\mathcal{U}_{A,i} \otimes id_B$
3. **Estimate** the square $(m_A)^2$, of the expectation value of an observable M_A on subsystem A for this particular sequence of gates, while performing a **reset** $\mathcal{D}_B(\rho_B) := \frac{\mathbb{1}}{d_B}$ of the B subsystem after every gate.
4. **Repeat 1, 2 & 3** for many random sequences of the same length, finding the average estimation $\mathbb{E}[(m_A)^2]$ of $(m_A)^2$.
5. **Repeat 1, 2, 3 & 4** increasing the length of the sequence k by 1.
6. **Fit** the data $\mathbb{E}[(m_A)^2]$ against k and obtain decay parameters as in equation (4.10).

Protocol 2: **SPAM effected subunitarity estimation** ($\mathcal{C} \times 1$)

4.5.1 Estimation while utilizing the maximally mixed state

The local subunitarities $u_{A \rightarrow A}(\mathcal{E}_{AB})$ and $u_{B \rightarrow B}(\mathcal{E}_{AB})$ of any bipartite channel \mathcal{E}_{AB} are measures of interest in their own right. However the exact estimation of the subunitarity of gate noise through unitarity benchmarking requires the repeated preparation of the maximally mixed state on the ancillary subsystem. As shown in [54], this introduces additional noise from the imperfect depolarization.

While challenging to do in a fully SPAM-robust way, from the form of equation (3.2) we see that if it is possible to do a resetting of subsystem close to the maximally mixed state then one can obtain an estimate of the subunitarity $u_{A \rightarrow A}(\mathcal{E}_{AB})$, and similarly for other single-subsystem cases, by estimating the unitarity of the marginal channel $\mathcal{E}_A = \text{tr}_B \circ \mathcal{E}_{AB} \circ \mathcal{D}_B$, where $\mathcal{D}_B(\rho) = \frac{1}{d} \mathbb{1}_B$ for a completely depolarizing channel to the maximally mixed state. Within the benchmarking circuit this would mean performing a noisy reset $\tilde{\mathcal{D}}_B$ on B after each $\tilde{\mathcal{U}}_i$ on A , with the aim of having $\tilde{\mathcal{D}}_B \approx \mathcal{D}_B$. This is a non-trivial assumption, and so in general the protocol will not be fully robust against reset errors. However, if these errors are substantially smaller than the addressability errors one wishes to estimate then the protocol returns an approximate estimate.

The manner in which the induced error is modelled determines the accuracy of the predicted estimate of the subunitarity. Consider the case where we model the noisy reset channel $\tilde{\mathcal{D}}_B$ as

$$\tilde{\mathcal{D}}_B = \mathcal{E}_P \circ (id_A \otimes \mathcal{D}_B) \circ \mathcal{E}_M, \quad (4.73)$$

where \mathcal{D}_B is the exact reset, and where \mathcal{E}_M and \mathcal{E}_P are SPAM errors on whole system related to the imperfect reset of the subsystem B . Then it is straightforward⁴ to show that Protocol

⁴The proof follows from considering unitarity benchmarking protocol with the above channels interleaved.

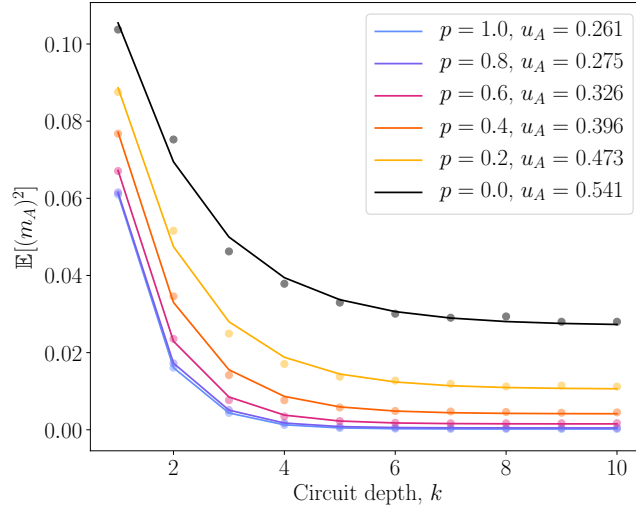


Figure 4.2: **Subunitarity estimation with reset error.** Shown is a simulation of Protocol 2 to estimate the subunitarity $u_A \equiv u_{A \rightarrow A}(\mathcal{E}_{AB})$, modelling the reset error associated B as in equation (4.75). This reset error is shown for different levels of depolarization p , including $p = 0$ i.e. no reset. The channel \mathcal{E}_{AB} in this case has a theoretical value of $u_{A \rightarrow A}(\mathcal{E}_{AB}) = 0.261$. The protocol returns an estimate of the subunitarity accurate to $\sim 90\%$ for reset errors up to $\sim 20\%$.

2 allows the estimation of the subunitarity of the combined channel

$$\mathbb{E}_{s_A}[m(s_A)^2] = c_1 + c_2 u_{A \rightarrow A}(\mathcal{E}_M \circ \mathcal{E} \circ \mathcal{E}_P)^{k-1} \quad (4.74)$$

for a sequence of length k where \mathcal{E} is the noise channel associated to the gateset. The constants c_1 & c_2 depend on the initial and final SPAM and non-unitality of the channel \mathcal{E} .

Given approximate estimates of $u_{A \rightarrow A}(\mathcal{E}_{AB})$ and $u_{B \rightarrow B}(\mathcal{E}_{AB})$ we may then exploit the fact that $\sum_i \lambda_i = u_{A \rightarrow A}(\mathcal{E}_{AB}) + u_{B \rightarrow B}(\mathcal{E}_{AB}) + u_{AB \rightarrow AB}(\mathcal{E}_{AB})$ to infer the value of $u_{AB \rightarrow AB}(\mathcal{E}_{AB})$ and thus compute the correlation unitarity for the channel \mathcal{E}_{AB} . Therefore, under the assumption of sufficiently small resetting errors we may estimate the correlation unitarity for an arbitrary channel. Note that in the context of the local Clifford gatesets the effective channel need not be the same in each protocol since Protocol 2 uses a different gateset. However, we can use the same gateset in Protocol 2 as in 1, since the application of non-trivial Clifford gates on B does not change matters if $\tilde{\mathcal{D}}_B \approx \mathcal{D}_B$.

We can numerically test how sensitive the above protocol is to coherent resetting errors. For example, one can model such reset errors as partially depolarizing with

$$\tilde{\mathcal{D}}_B = id_A \otimes (p\mathcal{D}_B + (1-p)id_B), \quad (4.75)$$

where $p \in [0, 1]$. In Figure 4.2, we plot the benchmarking decay curves and find that for resetting errors up to $\sim 20\%$ the protocol returns an estimate of the subunitarity $u_{A \rightarrow A}(\mathcal{E})$ accurate to $\sim 90\%$.

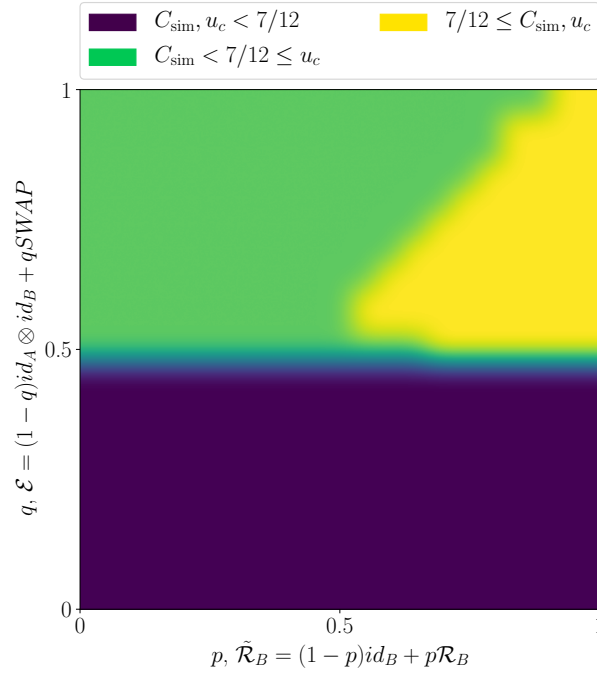


Figure 4.3: **Witnessing channel non-separability.** Given a quantum channel \mathcal{E}_{AB} we consider the ability to efficiently witness its non-separability via correlation unitarity in the presence of resetting noise. This could be realized, for example, in the context of robust tomography using randomized benchmarking [4]. We consider a 1-parameter family of 2-qubit channels obtained from a convex combination of the maximally non-separable *SWAP* channel and the identity channel (a product channel). The contour plot compares the true value of correlation unitarity $u_c(\mathcal{E}_{AB})$ with the correlation measure $C_{\text{sim}} \approx C$ estimating equation (4.68) in the presence of reset errors. For two qubits, non-separability occurs if $u_c(\mathcal{E}_{AB}) > 7/12$. We simulate both Protocol 1 and 2, and we find that for a wide range of reset errors we may witness non-separability for $p, q \gtrsim 0.5$. The region of green where $p, q \geq 1/2$ is an artifact of our particular method, and with a more refined algorithm we expect detection of non-separability also in this region.

Summary

For general non-separable channels, to estimate the correlation unitarity we require an additional protocol which is not fully SPAM robust. However, we find in practice that it works reasonably well.

Note that the channel in equation (4.75) will not in general destroy correlations between A and B , in contrast to a stronger, more simplistic error model of

$$\tilde{\mathcal{D}}_B(\rho_{AB}) = \rho_A \otimes \left(\frac{1}{2}(\mathbf{1} + \mathbf{b} \cdot \boldsymbol{\sigma}) \right), \quad (4.76)$$

where one assumes a reset to a local qubit state with non-zero Bloch vector \mathbf{b} . Under this stronger model assumption a simulation shows that such a scenario returns a good estimate for the subunitarity for $|\mathbf{b}| \leq 0.2$.

4.5.2 Estimation while utilizing computational basis states

There are further variants around the above protocol. For example, if resetting to states other than the maximally mixed state have very low errors then this provides another means to estimate $u_{A \rightarrow A}(\mathcal{E}_{AB})$. For example, we will show shortly that if a low-error reset to the pair of states $\frac{1}{2}(\mathbb{1} \pm \mathbf{b} \cdot \boldsymbol{\sigma})$ is possible for some \mathbf{b} then it can be shown that the average unitarity of the output on A over the pair is always an upper bound on $u_{A \rightarrow A}(\mathcal{E}_{AB})$, and so would provide a lower bound on the correlation unitarity. Therefore, this would allow witnessing of non-separability under the preceding assumptions.

Recall the notation we introduced in Chapter 3 for quantum channels in the Liouville representation. Protocol 2 requires the preparation of the maximally mixed state ($|\mathbf{Y}_0\rangle / \sqrt{d_B}$ in our notation) on subsystem B , albeit noisily. However, consider an alternative line, where we randomly reset to one of the computational basis states. For two qubits, in the Liouville representation we define the preparation channel

$$\mathit{prep}_{B,\pm Z} := \mathit{id}_A \otimes (|\mathbf{Y}_0\rangle / \sqrt{2} \pm |\mathbf{Y}_Z\rangle / \sqrt{2}), \quad (4.77)$$

which prepares the state $|0\rangle\langle 0| = \frac{1}{2}(\mathbb{1}_B \pm Z)$ on subsystem B . For a bipartite channel \mathcal{E} , the related channel \mathcal{E}_{+Z} on qubit A is defined as

$$\mathcal{E}_{+Z} := \mathit{tr}_B \cdot \mathcal{E} \cdot \mathit{prep}_{B,+Z} = (\mathit{id}_A \otimes \langle \mathbf{Y}_0 |) \mathcal{E} (\mathit{id}_A \otimes (|\mathbf{Y}_0\rangle + |\mathbf{Y}_Z\rangle)), \quad (4.78)$$

and similarly $\mathcal{E}_{-Z} := \mathit{tr}_B \cdot \mathcal{E} \cdot \mathit{prep}_{B,-Z}$.

We can calculate the structure of the unitarity of these channels using the Liouville representation. The definition of unitarity can be written in our basis as

$$u(\mathcal{E}_A) = \frac{1}{d^2 - 1} \sum_{ij} \langle \mathbf{X}_i | \mathcal{E}^\dagger | \mathbf{X}_j \rangle \langle \mathbf{X}_j | \mathcal{E} | \mathbf{X}_i \rangle, \quad (4.79)$$

for some channel \mathcal{E}_A that maps $\mathcal{B}(\mathcal{H}_A) \rightarrow \mathcal{B}(\mathcal{H}_A)$. The unitarity of the channel \mathcal{E}_{+Z} can then be related to the local subunitarity of the channel \mathcal{E} as

$$\begin{aligned} u(\mathcal{E}_{+Z}) = u_{A \rightarrow A}(\mathcal{E}) + \frac{1}{3} \sum_{ij} & \langle \mathbf{X}_i \otimes \mathbf{Y}_Z | \mathcal{E}^\dagger | \mathbf{X}_j \otimes \mathbf{Y}_0 \rangle \langle \mathbf{X}_j \otimes \mathbf{Y}_0 | \mathcal{E} | \mathbf{X}_i \otimes \mathbf{Y}_Z \rangle \\ & + \langle \mathbf{X}_i \otimes \mathbf{Y}_Z | \mathcal{E}^\dagger | \mathbf{X}_j \otimes \mathbf{Y}_0 \rangle \langle \mathbf{X}_j \otimes \mathbf{Y}_0 | \mathcal{E} | \mathbf{X}_i \otimes \mathbf{Y}_0 \rangle \\ & + \langle \mathbf{X}_i \otimes \mathbf{Y}_0 | \mathcal{E}^\dagger | \mathbf{X}_j \otimes \mathbf{Y}_0 \rangle \langle \mathbf{X}_j \otimes \mathbf{Y}_0 | \mathcal{E} | \mathbf{X}_i \otimes \mathbf{Y}_Z \rangle, \end{aligned} \quad (4.80)$$

and similarly

$$\begin{aligned} u(\mathcal{E}_{-Z}) = u_{A \rightarrow A}(\mathcal{E}) + \frac{1}{3} \sum_{ij} & \langle \mathbf{X}_i \otimes \mathbf{Y}_Z | \mathcal{E}^\dagger | \mathbf{X}_j \otimes \mathbf{Y}_0 \rangle \langle \mathbf{X}_j \otimes \mathbf{Y}_0 | \mathcal{E} | \mathbf{X}_i \otimes \mathbf{Y}_Z \rangle \\ & - \langle \mathbf{X}_i \otimes \mathbf{Y}_Z | \mathcal{E}^\dagger | \mathbf{X}_j \otimes \mathbf{Y}_0 \rangle \langle \mathbf{X}_j \otimes \mathbf{Y}_0 | \mathcal{E} | \mathbf{X}_i \otimes \mathbf{Y}_0 \rangle \\ & - \langle \mathbf{X}_i \otimes \mathbf{Y}_0 | \mathcal{E}^\dagger | \mathbf{X}_j \otimes \mathbf{Y}_0 \rangle \langle \mathbf{X}_j \otimes \mathbf{Y}_0 | \mathcal{E} | \mathbf{X}_i \otimes \mathbf{Y}_Z \rangle. \end{aligned} \quad (4.81)$$

This follows from expansion of the definitions of the channels and the Liouville definition of unitarity. By taking the mean of the unitarity of these two channels we find

$$\frac{1}{2}(u(\mathcal{E}_{+Z}) + u(\mathcal{E}_{-Z})) = u_{A \rightarrow A}(\mathcal{E}) + \frac{1}{3} \sum_{ij} \langle \mathbf{X}_i \otimes \mathbf{Y}_Z | \mathcal{E}^\dagger | \mathbf{X}_j \otimes \mathbf{Y}_0 \rangle \langle \mathbf{X}_j \otimes \mathbf{Y}_0 | \mathcal{E} | \mathbf{X}_i \otimes \mathbf{Y}_Z \rangle. \quad (4.82)$$

As the 2nd term in equation 4.82 is strictly non-negative we can use this measure to bound the subunitarity of the target channel. Therefore, if we can better reset to one of the computational basis states, then we can bound the subunitarity $u_{A \rightarrow A}$ via the following:

$$u_{A \rightarrow A}(\mathcal{E}) \leq \frac{1}{2}(u(\mathcal{E}_{+Z}) + u(\mathcal{E}_{-Z})) \quad (4.83)$$

where $\mathcal{E}_{+Z}(\rho) = \text{tr}_B[\mathcal{E}(\rho \otimes |0\rangle\langle 0|)]$ and $\mathcal{E}_{-Z}(\rho) = \text{tr}_B[\mathcal{E}(\rho \otimes |1\rangle\langle 1|)]$. This bound reaches equality for a product channel, $\mathcal{E} = \mathcal{E}_A \otimes \mathcal{E}_B$, as the 2nd term in equation (4.82) always contains the element $\langle \mathbf{Y}_0 | \mathcal{E}_B | \mathbf{Y}_i \rangle$, which must be zero for a valid CPTP map.

Additionally, it can be shown that the bound holds for any two orthogonal initial states on qubit B , replacing Z with a general Bloch vector on qubit B . If we then minimize over all orthogonal states we get

$$u_{A \rightarrow A}(\mathcal{E}) \leq \min \left[\frac{1}{2}(u(\mathcal{E}_{+b}) + u(\mathcal{E}_{-b})) \right], \quad (4.84)$$

where $\mathcal{E}_{\pm b}(\rho) = \text{tr}_B[\mathcal{E}(\rho \otimes \frac{1}{2}(\mathbb{1}_B \pm \mathbf{b} \cdot \boldsymbol{\sigma}))]$. However it is not obvious how this minimization could be performed efficiently (i.e. without many rounds of estimation with different settings).

However, under the assumption that computational basis states induce fewer errors when prepared compared to the maximally mixed state, then estimating $u(\mathcal{E}_{+Z})$ and $u(\mathcal{E}_{-Z})$ with a RB protocol allows an upper bound to be placed on the local subunitarity $u_{A \rightarrow A}(\mathcal{E})$, where \mathcal{E} is the noisy channel associated with the target gateset.

In such a case, the RB protocol would simply entail two experiments: firstly performing unitarity RB on qubit A with a reset of qubit B to $|0\rangle$, and then secondly with a reset to $|1\rangle$. If we assume the reset is performed completely incoherently, but with bipartite SPAM errors we have for the 1st experiment will produce a fit of the form

$$\mathbb{E}_{s_A}[m(s_A)^2] = c_1 + c_2 u(\mathcal{E}_{+Z,M} \circ \mathcal{E}_{+Z} \circ \mathcal{E}_{+Z,P})^{k-1}, \quad (4.85)$$

where $\Lambda_{+Z,M}$ & $\Lambda_{+Z,P}$ are the bipartite SPAM errors associated with the noisy reset of qubit B to $|0\rangle$. Similarly the 2nd experiment will produce a fit of the form

$$\mathbb{E}_{s_A}[m(s_A)^2] = c_1 + c_2 u(\mathcal{E}_{-Z,M} \circ \mathcal{E}_{-Z} \circ \mathcal{E}_{-Z,P})^{m-1}, \quad (4.86)$$

where $\mathcal{E}_{\pm Z,M}$ & $\mathcal{E}_{\pm Z,P}$ are the bipartite SPAM errors associated with the noisy reset of qubit B . Such a modification could then be used when the preparation of a maximally mixed state

is significantly noisier compared to computational basis state preparation and reset which would detrimentally affect estimation of $u_{A \rightarrow A}(\mathcal{E})$. In the case when $\mathcal{E}_{\pm Z, M, P} \approx id$ an upper bound could be estimated as shown above.

4.5.3 Benchmarking non-local subunitarities directly

In theory, another source of information that could be exploited is the unitarity of the channel from AB to A , given by

$$\mathcal{E}_{AB \rightarrow A}(\rho) = \text{tr}_B \circ \mathcal{E}_{AB}(\rho). \quad (4.87)$$

In terms of subunitarities this quantity can be decomposed as

$$u(\mathcal{E}_{AB \rightarrow A}) = \frac{1}{(d_A d_B)^2 - 1} \left(\frac{1}{\alpha_A} u_{A \rightarrow A}(\mathcal{E}_{AB}) + \frac{1}{\alpha_B} u_{B \rightarrow A}(\mathcal{E}_{AB}) + \frac{1}{\alpha_A \alpha_B} u_{AB \rightarrow A}(\mathcal{E}_{AB}) \right). \quad (4.88)$$

However, while this provides an expression in terms of subunitarities without requiring resetting, the standard benchmarking protocol will not work here due to the input and output systems being of different dimensions, and therefore a more involved protocol would be required.

4.6 Conclusions

4.6.1 Comparison with addressability of qubits

Several methods have recently been developed for detection [142], characterization [56, 143] and mitigation [144] of unwanted correlations between subsystems (specifically cross-talk) in a quantum device from a hardware-agnostic and model independent perspective. Our work adds to this toolkit new methods to characterize non-separable correlations and provides information about noise channels that is independent from features captured by previous works.

Simultaneous randomized benchmarking [56] compares the increase in error rates when both subsystems are simultaneously and independently driven vs when one subsystem is driven and the other is kept idle. This quantifies the amount of new errors experienced by a subsystem as a result of simultaneously applying Clifford gates on the other. As it is the case for Protocol 2, due to the local independent Clifford twirl on one subsystem, simultaneous RB is also affected by SPAM, and strong errors may be detected by deviations from exponential decay [56].

To compare with the information obtained from subunitarities, a quantity to detect correlations can be determined from the simultaneous Clifford twirl as in [56]. We denote this quantity by

$$a(\mathcal{E}_{AB}) := e_{AB} - e_A \cdot e_B. \quad (4.89)$$

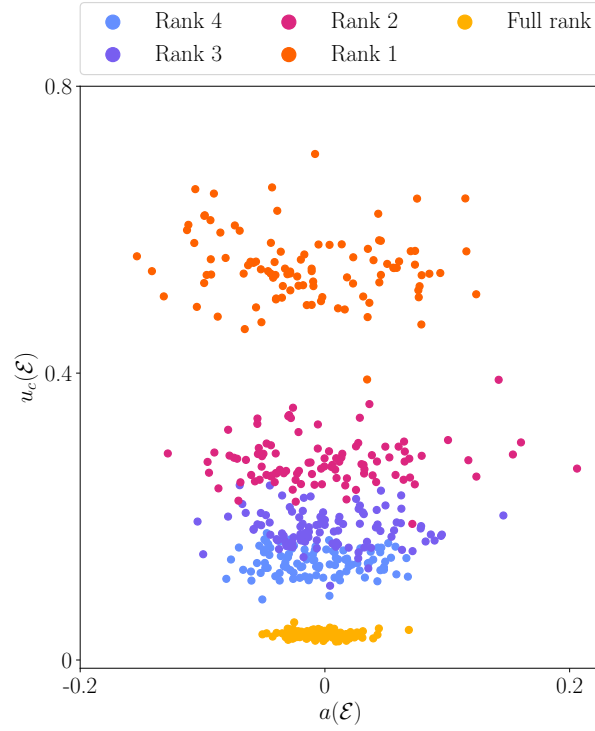


Figure 4.4: **Correlation unitarity vs. addressability.** Correlation unitarity is largely independent from existing addressability measures, while Kraus rank is a better indicator of the value of u_c , which is consistent with it capturing the non-separable correlations between subsystems. This suggests the measure might be suitable for benchmarking 2-qubit gates where the unitary transfer of quantum information between subsystems is required. The above plot is for random channels of different ranks from the distributions of Bruzda *et al.* and simulated using QuTip [2, 3].

where \mathcal{E}_{AB} is an effective noise channel associated to the Clifford gateset acting locally on each subsystem A and B . The three decay parameters e_{AB} , e_A and e_B are extracted from the randomized benchmarking protocol that applies simultaneous local Clifford gates to subsystems A and B and are given in terms of the Liouville data for the channel as

$$\begin{aligned}
 e_A &= \alpha_A \operatorname{tr}[T_{A \rightarrow A}], \\
 e_B &= \alpha_B \operatorname{tr}[T_{B \rightarrow B}], \\
 e_{AB} &= \alpha_A \alpha_B \operatorname{tr}[T_{AB \rightarrow AB}],
 \end{aligned} \tag{4.90}$$

with the coefficients α_X as defined earlier.

For a product channel, $T_{AB \rightarrow AB} = T_{A \rightarrow A} \otimes T_{B \rightarrow B}$ and therefore $a(\mathcal{E}_A \otimes \mathcal{E}_B) = 0$. In this manner, any deviation of $a(\mathcal{E})$ from zero is taken as detection of correlated behaviour. Note that in contrast to subunitarities, these measures are not invariant under local basis changes which makes it more problematic to interpret as a strict correlation measure.

It is easy to verify that the correlation unitarity provides independent information to a simultaneous RB protocol. For example, the CNOT gate is undetected by the addressabil-

ity correlation measure; however it is detected by correlation unitarity. Figure 4.4 shows that this independence is generic for bipartite channels, and we find that there are regions where the addressability correlation measure is zero or close to it, but the correlation unitarity varies greatly.

4.6.2 Overview

Our starting point in Chapter 3 was to develop simple, yet effective measures of correlations in quantum channels and means to assess sub-structures of such channels. The approach was motivated and guided by the idea of introducing measures that can be both efficiently estimated through RB-type of techniques and interpreted operationally as to quantify non-separable correlations, as we have shown in this chapter.

Certain subunitarities of a general bipartite channel can be interpreted as unitarities of locally acting channels induced by state preparation and discarding on one subsystem. We showed that they satisfy a set of inequalities that express an information-disturbance relation. This opens up new directions to analyse non-classical features of quantum channels directly from their robust tomographic description [4].

In the context of benchmarking of quantum devices, it will be of interest to develop hardware implementations of the protocols here and determine how effective and useful they are in practice. Such analysis will closely investigate the effects of reset errors for the subsystem unaddressed by target gates. Our simulations show that our second protocol, while not fully robust can still allow small reset errors to estimate magnitudes of correlated noise, but ultimately whether this is a reasonable assumption must be assessed for the system at hand.

Efficient and robust verification of quantum no-go theorems

Fear them not therefore: for there is nothing covered, that shall not be revealed; and hid, that shall not be known.

King James Bible
Matthew 10:26

Within Chapter 2 we established a framework to capture the incompatibility of channels for both quantum and classical theories, based around sets of Compatible Unitarity Pairs (CUP-sets). For quantum theory, we showed that CUP-sets capture both the no-cloning and no-hiding theorems, as well as broader quantum incompatibility. Having established this relationship, we now turn to the estimation of quantum CUP-sets (both isometric and reversible) on noisy quantum devices. As we based our framework on ideas from benchmarking our ultimate goal is to produce robust schemes, however we should also test the effectiveness of simpler techniques.

We therefore take two approaches here. For the first, we apply a ‘direct’ approach where we construct the minimal possible circuits to estimate points on a CUP-set. To do this we employ a SWAP test, a standard quantum circuit primitive to measure the purity of quantum states, that we can relate to CUPs. However, these techniques do not differentiate between noise in the channels generating a CUP-set and the preparation of the SWAP test itself. Therefore to achieve more accuracy we move to more involved techniques.

Our second approach is to consider ideas from device benchmarking such as randomized benchmarking and spectral methods [57, 83]. We show that, with some assumptions, both

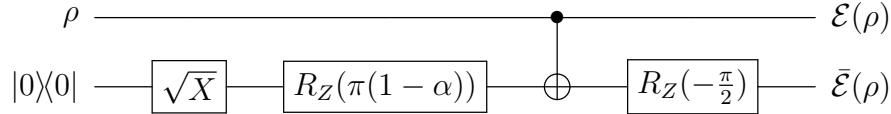


Figure 5.1: **Circuit decomposition in IBM gateset for lower right isometric CUP-set surface.** Circuit for 2 qubit isometry $CNOT_{AB}^\alpha(\rho \otimes |0\rangle\langle 0|)$, and complementary channels \mathcal{E} & $\bar{\mathcal{E}}$ for the lower right surface of the CUP-set are shown. The final R_Z rotation is optional but aids in the estimation of CUPs through spectral techniques.

the simplest isometric and reversible quantum CUP-sets can be estimated more accuracy and with robustness to some SPAM errors. The randomized benchmarking protocols we introduce are different to those in Chapter 4, specifically because we now interleave a target unitary but require less advanced mid-circuit measurements.

We test the performance of both approaches through simulations of a noisy IBMQ quantum device. We then discuss to what degree we can infer that current devices obey the limits of quantum theory.

5.1 Initial considerations

In this section we discuss some considerations that apply to all the methods we use.

5.1.1 Decomposition with device gatesets

Our simulations using IBMQ focus on two qubit systems as this allows for the smallest non-trivial quantum CUP-set. This was the isometric quantum CUP-set with $d_X = d_A = d_B = 2$. Any method for estimating a point (u, \bar{u}) in the CUP-set will require the preparation of the associated channels $(\mathcal{E}, \bar{\mathcal{E}})$. We have shown in Figure 2.3 that any pair can be generated with two CNOTs and two single qubit rotations about the Pauli Y axis. However a device will have a specific gateset of operations, and so for any experimental relation we should ensure $(\mathcal{E}, \bar{\mathcal{E}})$ can be decomposed efficiently. This is particularly important in the current era devices when noise prohibits circuits of even modest depth.

For a typical IBM device, the native gateset is given by the single qubit operations $R_Z(\theta)$, \sqrt{X} and X , along with the two qubit $CNOT$ gate. In Figures 5.2 and 5.1, we give the minimal circuits generating the boundary of the isometric quantum CUP-set in this gateset. As the channels $(\mathcal{E}, \bar{\mathcal{E}})$ can be efficiently decomposed this opens the path to estimation on a current noisy IBM device.

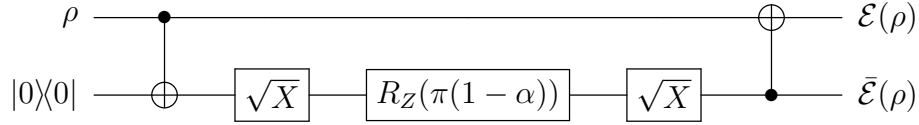


Figure 5.2: **Circuit decomposition in IBM gateset for lower left isometric CUP-set surface.** Circuit for 2 qubit isometry $CNOT_{BA}^\alpha \circ CNOT_{AB}(\rho \otimes |0\rangle\langle 0|)$, and complementary channels \mathcal{E} & $\bar{\mathcal{E}}$ for the lower left surface of the CUP-set are shown.

5.1.2 Effects of noise

The methods for estimating CUP-sets we employ can be separated into two stages: (i) the preparation of the channels that generate the CUP-set, (ii) the estimation of the prepared channel's unitarity. There will be errors associated with both (i) and (ii). The errors in (i) are our primary interest as they place a limit on the device's performance at estimating CUPs. However for the direct methods introduced shortly we cannot easily distinguish between these errors, so refer to a noisy version, $(\cdot)_N$, of the whole process (u_N, \bar{u}_N) for estimating (u, \bar{u}) .

The simplest way to model how noise affects CUP-sets is through a depolarizing channel given by

$$\mathcal{D}_p := (1 - p)id + p\mathcal{D} \quad (5.1)$$

where $id(\rho) = \rho$ & $\mathcal{D}(\rho) = \sigma$, for σ another fixed quantum state. Given $u(id \circ \mathcal{E}) = u(\mathcal{E} \circ id) = u(\mathcal{E})$ and $u(\mathcal{D} \circ \mathcal{E}) = u(\mathcal{E} \circ \mathcal{D}) = u(\mathcal{D}) = 0$ then for any CUP-set we have

$$\begin{aligned} (u_N, \bar{u}_N) &= (u(\mathcal{D}_{p_A} \circ \mathcal{E}), u(\mathcal{D}_{p_B} \circ \bar{\mathcal{E}})), \\ &= ((1 - p_A)^2 u, (1 - p_B)^2 \bar{u}). \end{aligned} \quad (5.2)$$

Therefore by varying p_A & p_B independently a CUP-set can be projected towards either axis, or towards the origin. We illustrate this process in Figure 5.3. As this allows us to reach any point in the full CUP-set (\mathcal{C}_*), we will use depolarization as a crude way to quantify how 'noisy' an estimated CUP-set is (\mathcal{C} or \mathcal{C}_r).

We have shown that the channels generating the border of the simplest quantum CUP-set can be efficiently decomposed into the gateset of a real device. Further, as the CUP-set deforms in a simple way for depolarizing noise, we can use such noise as a blunt way to compare the noisiness of experimental CUP-sets.

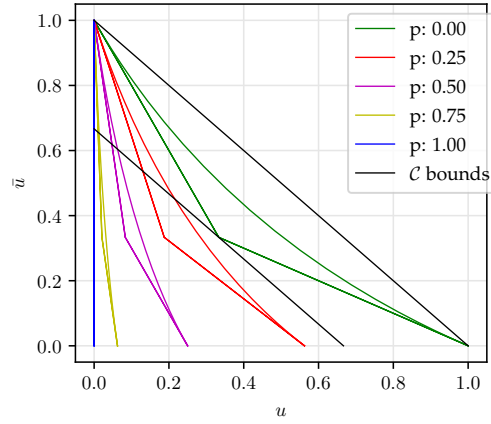


Figure 5.3: **CUP-set deformation through depolarization.** The simplest quantum CUP-set \mathcal{C} is shown when one output is depolarized, $(u(\mathcal{D}_p \circ \mathcal{E}), u(\bar{\mathcal{E}}))$ for different values of p .

5.2 Direct CUP-set estimation through state purity measurements

In this section, we use formulations of unitarity in terms of quantum state purities to construct simple circuits to estimate CUPs. We use these to estimate a representative selection of points on the perimeter of the CUP-set using a simulation of an IBMQ device.

Summary We designed our framework of CUP-sets with SPAM robust methods in mind. However we should first test the performance of more elementary techniques with lower experimental overheads.

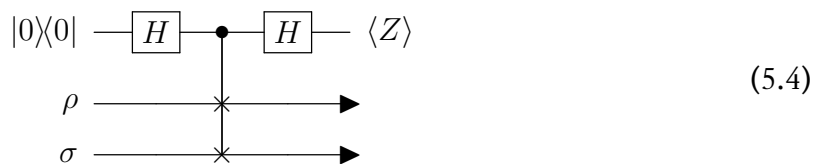
5.2.1 Estimation through complementarity formulation

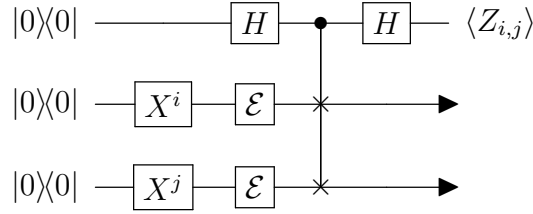
For any quantum channel, \mathcal{E} , (with input dimension d_X) we can express the unitarity in terms of purities as

$$u(\mathcal{E}) = \frac{d_X}{d_X^2 - 1} \left(d_X \gamma(\tilde{\mathcal{E}}(\frac{\mathbb{1}}{d_X})) - \gamma(\mathcal{E}(\frac{\mathbb{1}}{d_X})) \right), \tag{5.3}$$

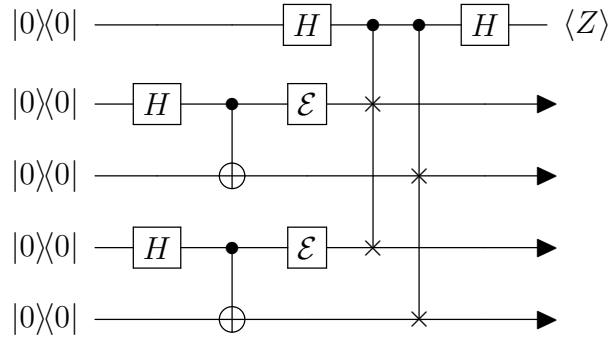
where $\tilde{\mathcal{E}}$ is any channel complementary to \mathcal{E} [61]. For the isometric CUP-set, \mathcal{C} , any compatible pair of channels $(\mathcal{E}, \bar{\mathcal{E}})$ will be complementary to each other. Therefore, by estimating the two purity terms in equation (5.3) we get the point (u, \bar{u}) .

The purity of a quantum state can be estimated through a SWAP test [32]. For two unknown quantum states, ρ & σ , the following circuit performs a SWAP test of the states





(a) For $X^1 = X$ & $X^0 = id$, the above circuit gives an estimation of $\gamma(\mathcal{E}(\mathbb{1}/2))$ through the relation $\frac{1}{4}(\langle Z_{0,0} \rangle + \langle Z_{0,1} \rangle + \langle Z_{1,0} \rangle + \langle Z_{1,1} \rangle) = \gamma(\mathcal{E}(\mathbb{1}/2))$.



(b) The above circuit gives an estimation of the Choi state purity with $\langle Z \rangle = \gamma(\mathcal{J}(\mathcal{E}))$.

Figure 5.4: **Unitarity estimation with state purities.** Circuits for estimation of unitarity $u(\mathcal{E})$ of single qubit channel \mathcal{E} through SWAP test and state purity relations.

giving $\langle Z \rangle = \text{tr}[\rho\sigma]$, for the expectation value of Pauli Z measured on the first qubit. The central gate is the controlled *SWAP* (or Fredkin) gate.

With $\rho = \sigma = \mathcal{E}(\mathbb{1}/2)$ or $\rho = \sigma = \bar{\mathcal{E}}(\mathbb{1}/2)$ (restricting to the case $d_X = d_A = d_B = 2$), we can use the SWAP test circuit on a quantum device to get direct, albeit noisy, estimation (u_N, \bar{u}_N) of a point (u, \bar{u}) of the CUP-set. This however requires the preparation of the maximally mixed state, which we discuss in Section 5.2.3.

5.2.2 Estimation through Choi state formulation

For the reversible CUP-set, \mathcal{C}_r , the resulting compatible pair of channels $(\mathcal{E}, \bar{\mathcal{E}})$ are not necessarily complementary to each other. While it is straightforward to derive complementary channels for the families of channels we consider, the number of purity terms to be estimated from equation (5.3) doubles compared to \mathcal{C} . Further, these new complementary channels will necessarily have a larger dimension, thereby increasing the complexity of the SWAP test. However equivalently, and perhaps more naturally, we can formulate an approach using only the channels $(\mathcal{E}, \bar{\mathcal{E}})$ through the Choi-Jamiołkowski isomorphism.

For any quantum channel \mathcal{E} (with input dimension d_X) we have

$$u(\mathcal{E}) = \frac{d_X}{d_X^2 - 1} (d_X \gamma(\mathcal{J}(\mathcal{E})) - \gamma(\mathcal{E}(\frac{\mathbb{1}}{d_X}))) \quad (5.5)$$

where $\mathcal{J}(\mathcal{E})$ is the Choi-Jamiołkowski state of the channel (see Definition 3.4) which is given by

$$\mathcal{J}(\mathcal{E}) := \mathcal{E} \otimes id(\psi). \quad (5.6)$$

The state $\psi = |\psi\rangle\langle\psi|$ is a generalized Bell state, $|\psi\rangle := \frac{1}{\sqrt{d_X}} \sum_i^{d_X} |i\rangle \otimes |i\rangle$, which has dimension d_X^2 [32, 61].

Restricting to $d_X = d_A = d_B = 2$, from equation (5.4) we can estimate the first purity by preparing two copies of the Choi state e.g. $\rho = \sigma = \mathcal{J}(\mathcal{E})$. For a channel with dimension d , the Choi state has dimension d^2 , therefore the number of target qubits in the controlled *SWAP* for \mathcal{C}_r is doubled compared to estimating \mathcal{C} . The second term in equation (5.4) can be obtained from $\rho = \sigma = \mathcal{E}(\mathbb{1}/2)$. As this process must be repeated for $u(\bar{\mathcal{E}})$, estimating points on \mathcal{C}_r will generally require twice the number of experiments of \mathcal{C} .

Summary

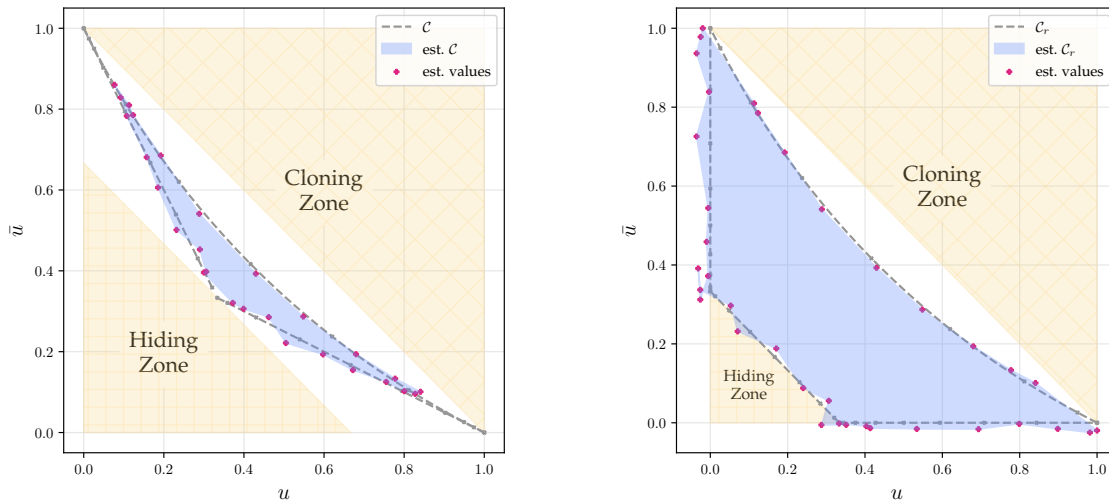
For any channel \mathcal{E} , we can relate the purity of certain states (such as the Choi state, $\mathcal{J}(\mathcal{E})$) to the unitarity, $u(\mathcal{E})$. For the channels that generate the CUP-set we can then estimate these purities directly through very simple quantum circuits.

5.2.3 Preparation of the maximally mixed state and experimental results

Both of the above methods require the preparation of the maximally mixed state. With a unitary circuit, we can do this (i) statistically, by averaging the results of experiments performed on computational basis states, or (ii) by discarding information about a prepared pure state (e.g. a marginal state of a Bell state). The former method requires more experiments while the later introduces further uncertainty into the estimation.

We use (i) to estimate the isometric CUP-set \mathcal{C} using complementarity formulation, as it requires a smaller system size. The exact circuits for the complete purity estimations are given in Figure 5.4(a). We then experimentally estimate a range of CUPs on the surface of the CUP-set \mathcal{C} on a simulated IBM device. The results of this experiment are shown in Figure 5.5(a) where a partially depolarizing model has been fitted to each surface.

Then we pair (ii) with estimation through the Choi state. The exact circuits for this method are given in Figure 5.4(b). We again estimate a range of CUPs on the surface of the reversible CUP-set \mathcal{C}_r . The results of this experiment are shown in Figure 5.5 (b) where a partially depolarizing model has been fitted to each surface.



(a) Isometric CUP-set (\mathcal{C}), estimated with complementary channel method.

(b) Reversible CUP-set (\mathcal{C}_r), estimated with Choi state method.

Figure 5.5: Direct estimation of quantum CUP-sets. The two simplest quantum CUP-sets are experimentally estimated directly through SWAP test schemes. A best fit depolarising noise model has been applied to each surface (see Table 5.2).

5.2.4 Discussion of direct methods

The direct methods we have implemented have a few sources of errors. For any estimated CUP, (u_N, \bar{u}_N) , the largest error, in terms of the size of intended operation, will be on the controlled SWAP gate(s). Secondly, as the SWAP test relies upon the final measurement being taken in the correct basis, the direct methods are sensitive to even small final SPAM errors.

Examining Figure 5.5 we observe variance in the data, even after a round of averaging over 100 experimental runs has been performed. The lack of robustness to SPAM errors, means that we cannot ascribe this variance to one source – it may come primarily from SPAM ($u_N \approx u_N(\mathcal{E})$) or it may occur in the preparation of the channel itself ($u_N \approx u(\mathcal{E}_N)$). This is the main weakness with the direct methods, compared to methods we discuss in the following section. However, we note that even after the depolarizing fit is applied, for both \mathcal{C} and \mathcal{C}_r the noisy estimated CUP-set is found strictly below the no-cloning upper bound, and therefore in the full CUP-set \mathcal{C}_* .

Summary

The direct methods work reasonably well, however we cannot separate the errors occurring in the experimental procedure (the SWAP test) from the more fundamental errors in the target channels (\mathcal{E} and $\bar{\mathcal{E}}$). We therefore will need more advanced techniques to better isolate the latter errors which are truly the limits of the device.

The size of parameters needed for the depolarizing fit let us compare between the estimation of \mathcal{C} and \mathcal{C}_r . From Table 5.2, the estimated depolarization is two to three times higher

for \mathcal{C}_r . As the channels required to generate \mathcal{C}_r are very similar to \mathcal{C} , we can prescribe this increase directly to the larger overhead and complexity of the protocol for \mathcal{C}_r .

Finally, we note that the direct methods rely on a SWAP test(s), and are therefore not efficiently scalable in number of qubits. From Figure 5.4 we can extrapolate that for $(\mathcal{E}, \bar{\mathcal{E}})$ being n qubit channels we would require a system of $4n + 1$ qubits. However these methods are quite efficient in the number of runs required as detailed in Table 5.1.

5.3 SPAM robust CUP-set estimation through RB

With the direct method of the previous section, we make no distinction between errors in the implementation of the target channel, and errors in the estimation protocol including initial state preparation and final measurement SPAM errors. This severely limits the usefulness of the direct method as a measure of whether a device obeys the CUP-set's informational bounds. For example, in the extreme, we could imagine a device that implements any quantum channel perfectly but has SPAM errors such that it applies a final Hadamard transform on all qubits before measurement. With the direct SWAP test method, this would only generate the point $(0, 0)$ on the CUP-set diagram. From this we might conclude the device is not acting as a closed quantum system – when in fact, prior to measurement, it was performing perfectly.

With the above in mind, in this section we consider protocols to estimate quantum CUP-sets that are robust to SPAM errors. However will see that the SPAM robust protocols come with a cost of much larger operational overheads, and introduce different sources of potential noise compared to the direct methods.

5.3.1 Estimation through randomized benchmarking

Through randomized benchmarking (RB) [57] we can estimate the unitarity $u(\Lambda_C)$ of the average error channel Λ_C induced by a computational gateset $\{\mathcal{U}_C\}$ generating the Clifford group. Here we use the notation Λ for noise channels to avoid confusion with the specific channels that generate the CUP-set, $(\mathcal{E}, \bar{\mathcal{E}})$.

If we interleave the target channel, \mathcal{E} , (of fixed dimension) between rounds of random Clifford unitaries in the RB protocol, we can estimate the unitarity of the joint channel $u(\mathcal{E} \circ \Lambda_C)$. Therefore in the limit $\Lambda_C = id$ the interleaved RB protocol returns an exact estimation of $u(\mathcal{E})$. More generally, as unitarity is proportional to the Hilbert-Schmidt norm of the channel's matrix representation we also have the relation $u(\mathcal{E} \circ \Lambda_C) \leq u(\mathcal{E}) \|\Lambda_C\|_\infty$, where $\|\Lambda_C\|_\infty$ corresponds to the largest singular value of the average noisy Clifford gateset channel. This may also be determined, for example via spectral methods as in Section 5.4 to obtain more precise bounds for $u(\mathcal{E})$ in the presence of noisy Clifford operations.

1. **Prepare** the system in the state $\rho_A \otimes |0\rangle\langle 0|_B$.
2. **Select** a sequence of length k of random elements of the Clifford group, $\{\mathcal{U}_{C,i}\}$, on subsystem A , starting with $k = 1$, while performing a reset on subsystem B after every gate. E.g. for each gate $\mathcal{U}_{C,i} \otimes \mathcal{D}$
3. **Interleave** the bipartite unitary \mathcal{U}_{AB} after every Clifford gate (such that the final gate is a Clifford gate).
4. **Estimate** the square $(m_A)^2$, of the expectation value of an observable M_A on subsystem A for this particular sequence of gates.
5. **Repeat 1, 2, 3 & 4** for many random sequences of the same length, finding the average estimation $\mathbb{E}_\rho[(m_A)^2]$ of $(m_A)^2$.
6. **Repeat 1, 2, 3, 4 & 5** increasing the length of the sequence k by 1.
7. **Fit** the data $\mathbb{E}_\rho[(m_A)^2] = c_0 + c_1 s^{k-1}$ where c_0, c_1 are real constants, and find the estimated unitarity, s .

Protocol 3: **Interleaved unitarity RB** for marginal channel $\mathcal{E}(\rho) := \text{tr}_B \circ \mathcal{U}_{AB}(\rho \otimes |0\rangle\langle 0|)$.

Applying interleaved RB to an estimation of the CUP-set follows from the above. However, in addition, it involves an interleaved implementation of \mathcal{E} using an ancilla initialisation, the global unitary \mathcal{U}_{AB} and a partial trace. We require the additional assumption that we can perform mid-circuit resets, $\mathcal{D}(\rho) := |0\rangle\langle 0|$, and that the noisy version of these resets are incoherent – in that none of the state ρ is carried through even if \mathcal{D} induces some larger error on the device. This allows us to include the error \mathcal{D} in Λ_C .

Through interleaved RB we can estimate the unitarity of the following channel in a SPAM robust manner

$$\mathcal{E}_N(\rho) = \text{tr}_B \circ \Lambda_{AB} \circ \mathcal{U}_{AB} \circ \Lambda_C(\rho \otimes |0\rangle\langle 0|), \quad (5.7)$$

where Λ_{AB} is the noise channel we want to probe associated with the experimental implementation of $(\mathcal{E}, \bar{\mathcal{E}})$, the channels generating the (isometric) CUP-set. In the noiseless limit $\Lambda_C = \Lambda_{AB} = id$, Protocol 3 returns exactly $u(\mathcal{E})$ in the isometric CUP-set \mathcal{C} .

Protocol 3 gives the decay parameter that estimates $s = u(\mathcal{E}_N)$ for the noisy channel \mathcal{E}_N which includes the device errors from preparation of the channel \mathcal{E} , but also protocol-specific errors coming from the noisy random Cliffords.

The protocol for $\bar{\mathcal{E}}$ is very similar but requires an additional *SWAP* operation which we can absorb into the interleaved unitary, $\mathcal{U}'_{AB} = \text{SWAP} \circ \mathcal{U}_{AB}$ but this may have some resource costs associated with it. Allowing us to estimate $u(\bar{\mathcal{E}}_N)$ for

$$\bar{\mathcal{E}}_N(\rho) = \text{tr}_A \circ \Lambda_{AB} \circ \mathcal{U}_{AB} \circ \Lambda_C(\rho \otimes |0\rangle\langle 0|). \quad (5.8)$$

Proofs showing that the above protocols indeed produce estimates of CUP-sets can be found

shortly in Section 5.3.2. An examination of how the protocols behave under gate independent noise is given in after this, in Section 5.3.3.

Summary

With the (physically unrealistic) assumption there are no errors associated with the gate-set or mid-circuit resets, $\Lambda_C = id$, an interleaved unitarity RB protocol returns an exact estimation of a point (u, \bar{u}) in the noisy CUP-set. This applies even in the presence of initial and final SPAM errors.

We implement these protocols on a simulated version of the IBM BELEM device, in an efficient manner (see Protocol 4) [5]. The results of the experiment for \mathcal{C} are shown in Figure 5.6(a), and for \mathcal{C}_r in Figure 5.6(b) where a depolarization model has been fitted to each surface.

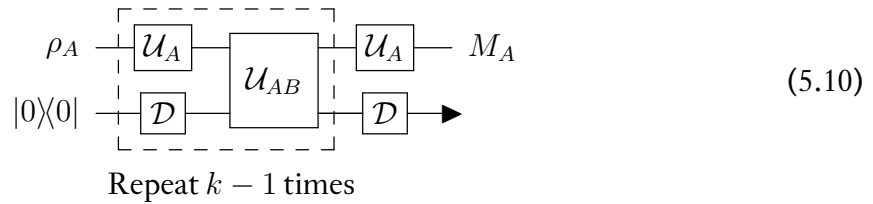
5.3.2 Interleaved unitarity protocol for $(\mathcal{E}, \bar{\mathcal{E}})$ without noise

We now give a pictographic sketch of the proof for Protocol 3 without noise, showing that it reduces to the form of a unitarity benchmarking protocol as discussed in Chapter 3.

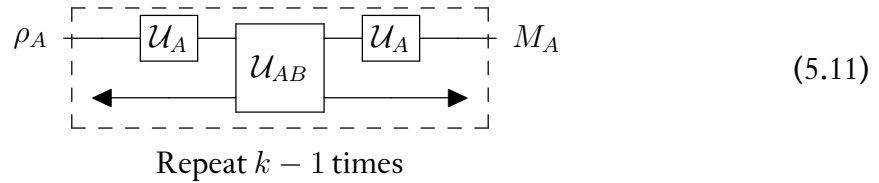
Define the elements of the Clifford group on qubit A to be $\{\mathcal{U}_{A,i}\}$. We define channel induced by averaging over many Clifford unitaries as

$$\mathcal{U}_A := \frac{1}{N} \sum_i^N \mathcal{C}_{A,i}. \quad (5.9)$$

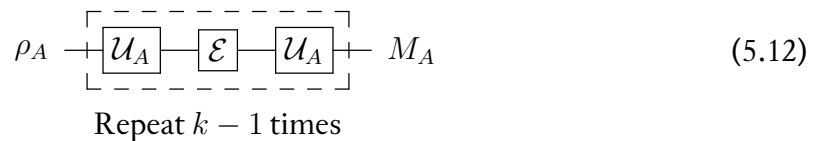
In the case $\Lambda = \Lambda_C = id$, the circuit diagram representation of Protocol 3 is



where \blacktriangleleft indicates the channel preparing $|0\rangle\langle 0|$ and \blacktriangleright the trace operation. As $\blacktriangleright\blacktriangleleft = \mathcal{D}$, the circuit reduces to



which further reduces to



Which is exactly the right form for the circuit to estimate $u(\mathcal{E})$. The decay parameter e_1 in Protocol 3 is then exactly $u(\mathcal{E})$ in this idealised case.

The protocol to estimate $u(\bar{\mathcal{E}})$ is the same as for $u(\mathcal{E})$ replacing \mathcal{U}_{AB} with $SWAP \circ \mathcal{U}_{AB}$. This follows from the fact that

$$\bar{\mathcal{E}}(\rho) := \text{tr}_A \circ \mathcal{U}_{AB}(\rho \otimes |0\rangle\langle 0|) = \text{tr}_B \circ SWAP \circ \mathcal{U}_{AB}(\rho \otimes |0\rangle\langle 0|). \quad (5.13)$$

or as a circuit diagram



$$\boxed{\bar{\mathcal{E}}} = \boxed{\mathcal{U}_{AB}} \quad (5.14)$$

where we implicitly assume $d_A = d_B$, which is appropriate in this two qubit case.

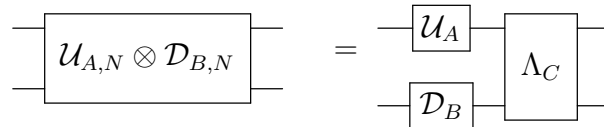
Therefore, in the noise free limit, see how the protocols average the channels $(\mathcal{E}, \bar{\mathcal{E}})$ over the Clifford group and produce an estimate of any point (u, \bar{u}) . However, of more importance is the behaviour of the protocol under device noise, which we shall explore now.

5.3.3 Interleaved unitarity protocol for $(\mathcal{E}, \bar{\mathcal{E}})$ with noise

In this section we set out the minimum assumptions required to produce interleaved unitarity RB circuits, where all operations are assumed to be noisy. We then show how this effects the estimation of CUP-sets. For channels, states, functions, any X , we write the noisy version X_N .

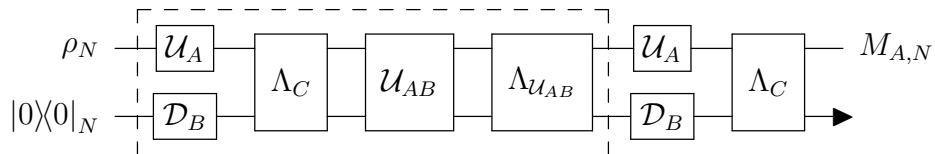
For a two qubit system when we implement any gate or mid-circuit measurement, the noise associated with the process may effect the whole device. Therefore we should model errors as bipartite quantum channels. We make two simplifying assumptions about these errors. Firstly, we consider the noise to be fixed across the Clifford group gateset, such that $\Lambda_{C,i} = \Lambda_C$ for all \mathcal{U}_i . E.g. $\mathcal{U}_{i,N} = \Lambda_C \circ \mathcal{U}_i \otimes id_B$. Secondly, we assume the reset of a qubit is perfectly incoherent, but potentially noisy. Therefore the total channel can be written as $\mathcal{D}_{B,N} = \Lambda_D \circ id_A \otimes \mathcal{D}_B$, with a general bipartite error channel Λ_D .

A direct consequence of these two assumptions is that we can write the noisy version of the summation of Clifford unitaries $\mathcal{U}_{A,N}$ and the reset operation as



$$\boxed{\mathcal{U}_{A,N} \otimes \mathcal{D}_{B,N}} = \begin{array}{c} \boxed{\mathcal{U}_A} \\ \boxed{\mathcal{D}_B} \end{array} \rightarrow \boxed{\Lambda_C} \quad (5.15)$$

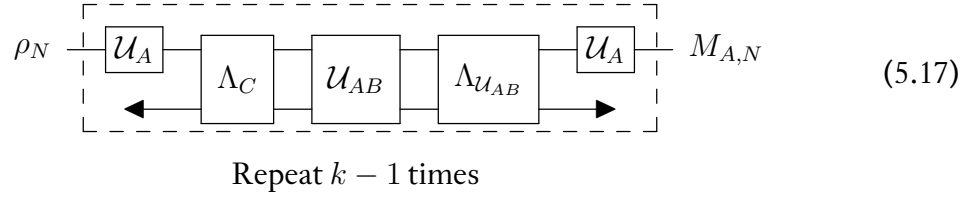
where Λ_C is an error channel associated with the operations together. Putting this together with a noisy version of the interleaved unitary $\mathcal{U}_{AB,N} = \mathcal{U}_{AB} \circ \Lambda_{AB}$ we can write a noisy version of the circuit for Protocol 3:



$$\begin{array}{c} \rho_N \\ |0\rangle\langle 0|_N \end{array} \rightarrow \begin{array}{c} \boxed{\mathcal{U}_A} \\ \boxed{\mathcal{D}_B} \end{array} \rightarrow \boxed{\Lambda_C} \rightarrow \boxed{\mathcal{U}_{AB}} \rightarrow \boxed{\Lambda_{\mathcal{U}_{AB}}} \rightarrow \begin{array}{c} \boxed{\mathcal{U}_A} \\ \boxed{\mathcal{D}_B} \end{array} \rightarrow \boxed{\Lambda_C} \rightarrow M_{A,N} \quad (5.16)$$

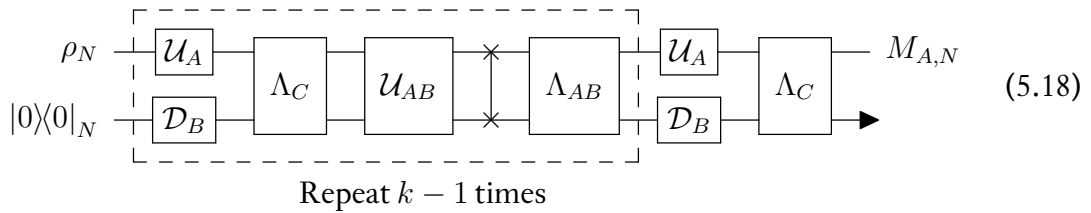
Repeat $k - 1$ times

Further we can write the reset operations as trace and preparation operations in our notation and absorb the initial and final error channels as SPAM errors in the A subsystem. This leaves us with:

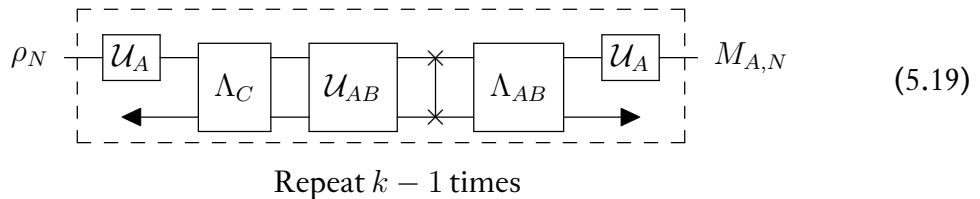


As the protocol is SPAM robust, we get an estimation of the unitarity $u(\mathcal{E}_N)$ of the channel $\mathcal{E}_N(\rho) := tr_B \circ \Lambda_{AB} \circ \mathcal{U}_{AB} \circ \Lambda_C(\rho \otimes |0\rangle\langle 0|)$.

When we implement the protocol for $\bar{\mathcal{E}}$ we will have an additional required operation, $SWAP$, which we absorb into the joint unitary, $\mathcal{U}'_{AB} = SWAP \circ \mathcal{U}_{AB}$, but there may be additional noise associated with it. We can write the noisy version of this in full generality with $\mathcal{U}'_{AB,N} = SWAP_N \circ \mathcal{U}_{AB,N} = \Lambda_{AB} \circ SWAP \circ \mathcal{U}_{AB}$. This leads to a noisy circuit of the form



Finally, absorbing the initial and final error channels as SPAM errors in the A subsystem leaves us with:



Giving an exact estimation of the unitarity $u(\bar{\mathcal{E}}_N)$ for the channel $\bar{\mathcal{E}}_N(\rho) := tr_A \circ \Lambda_{AB} \circ \mathcal{U}_{AB} \circ \Lambda_C(\rho \otimes |0\rangle\langle 0|)$.

Putting this together we have considered the gateset noise to be fixed across the gateset, Λ_{AB} , and have assumed the reset of a qubit is perfectly incoherent (but potentially noisy). Under such circumstances the interleaved unitarity RB protocol estimates the unitarity, $u(\mathcal{E}_N)$ of a joint quantum channel for a process \mathcal{E}_N which contains the target process \mathcal{E} and the above error channels.

Summary With some assumptions on the nature of device noise, the interleaved unitarity RB protocol still returns an estimation of a point (u, \bar{u}) in the CUP-set, however there will be contributions from errors in the gateset and mid-circuit resets. However, it remains to see how these techniques perform compared to the direct methods.

1. **Select** a random sequence, $\mathcal{U}_k := \mathcal{U}_k \circ \mathcal{E} \circ \mathcal{U}_{k-1} \circ \mathcal{E} \circ \dots \circ \mathcal{U}_2 \circ \mathcal{E} \circ \mathcal{U}_1$, of random Clifford gates interleaved with target channel \mathcal{E} .
2. **Prepare** the system in the state $\rho_{\pm,i} := \frac{1}{d}(\mathbb{1} \pm P_i)$ for all non-identity elements P_i , of the Pauli group $P \neq \mathbb{1}$. In the single qubit input and output case, the states $\rho_{\pm,i}$ are pure states given by $\rho_{\pm,i} = \{|+\rangle, |-\rangle, |+i\rangle, |-i\rangle, |0\rangle, |1\rangle\}$.
3. **Estimate** the average purity of the sequence across all possible traceless input and output Pauli operators:

$$q_k = \frac{1}{d^2 - 1} \sum_{i,j}^{d^2-1} (\text{tr}[P_j \mathcal{C}_k(\rho_{+,i})] - \text{tr}[P_j \mathcal{C}_k(\rho_{-,i})])^2.$$

4. **Repeat 1, 2 & 3** for N_k random sequences of length k , finding the average estimation $\mathbb{E}[q_k] := \frac{1}{N_k} \sum_k^{N_k} q_k$.
5. **Repeat 1, 2, 3 & 4** increasing the length of the sequence, e.g. $k = k + 1$.
6. **Fit** the data with $\mathbb{E}[q_k] = c_1 s^{k-1}$, to find s the estimated value of $u(\mathcal{E})$.

Protocol 4: **Efficient interleaved unitarity RB** for single qubit channel \mathcal{E} , adapted from [5].

5.3.4 Efficient implementation of protocols

In the experiments for the SPAM robust CUP-set, we perform an *efficient* unitarity RB protocol, as introduced in [5]. Here we mean efficient in the sense that the protocol is optimal rather than it scales linearly with system size. The protocol is particularly useful as it allows for rigorous bounds on the variance in the associated decay curve, and therefore the value of unitarity extracted ¹. Protocol 4 summarizes the efficient unitarity RB protocol given in [5] applied to our methods here, where we consider interleaving a single qubit channel.

Efficiency, in the sense of a linear scaling of operational costs with system size, can be achieved in a unitarity benchmarking protocol if one has access to two copies of the system [5, 107]. However this approach requires the assumptions that: the local errors on each system are identical, that entangled states across both systems can be created, and that there are no unwanted (noise) correlations between the systems. These assumptions are extremely unlikely to hold outside of a fault tolerant device. Therefore for our simulations using IBM BELEM we use the single system protocol given above.

5.3.5 Discussion of SPAM robust methods

We now discuss the limitations of the interleaved randomized benchmarking technique we give for estimating CUP-sets. While the protocol is robust to initial and final SPAM errors, it

¹This scheme could be straightforwardly applied to the subunitarity protocols given in Chapter 4.

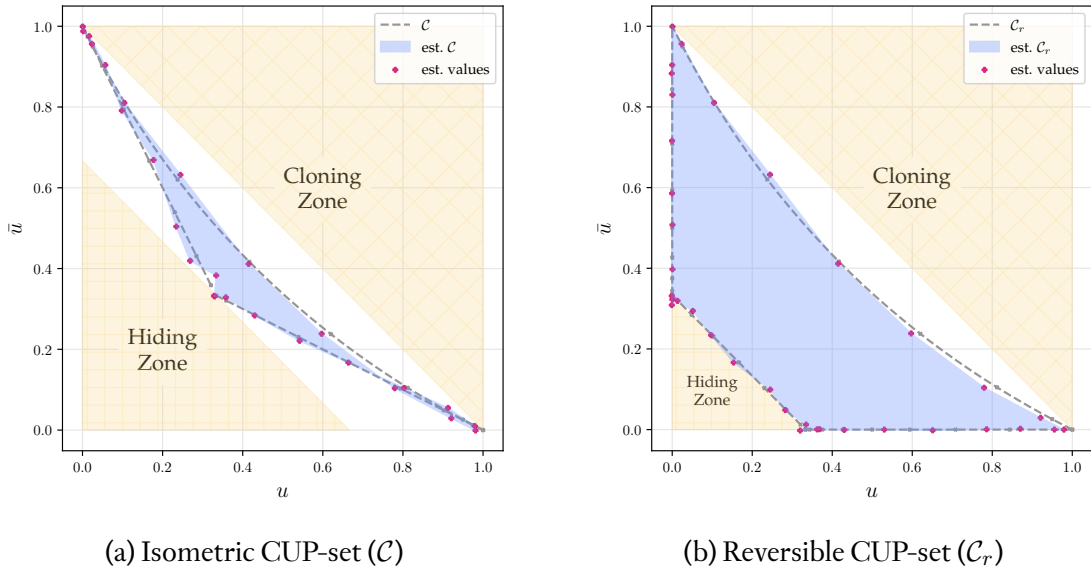


Figure 5.6: **SPAM robust estimation of quantum CUP-sets.** The simplest quantum CUP-sets are experimentally estimated through an interleaved unitarity randomized benchmarking scheme. A best fit depolarising noise model has been fitted to each surface (see Table 5.2), where each surface is produced from 9 pairs of experimental values.

relies on mid-circuit measurements to perform resets which must be incoherent (but can be noisy). Under this assumption, the decay parameter of the protocol gives a robust estimation of the unitarity of the given channel, $s = u(\mathcal{E}_N)$. If, as we might expect on a NISQ device, the reset allows some coherent information through, then the decay parameter can no longer be directly related to the unitarity, e.g. $s = u_N(\mathcal{E}_N)$. For further discussion see Section 5.3.3.

For the channels $(\mathcal{E}_N, \bar{\mathcal{E}}_N)$ to be close (in terms of unitarity) to the channels that generate the CUP-set $(\mathcal{E}, \bar{\mathcal{E}})$, we need the error Λ_C on one qubit Clifford unitaries to be small. As the error preparing $(\mathcal{E}, \bar{\mathcal{E}})$ should be of similar size to Λ_C , then we expect that the approximately half of the depolarizing fit required in Figure 5.6 can be attributed to the preparation of $(\mathcal{E}, \bar{\mathcal{E}})$.

5.3.6 Comparison with direct methods

While the SPAM robust methods require an additional assumption about the nature of resets on the device, this is a vast improvement over the direct methods of Section 5.2, where errors arising in the protocol and in the channel preparation could not be separated. Further, the estimation of each CUP-set obtained through interleaved RB is significantly better in terms of the required depolarizing fit than the direct methods (see Table 5.2). The variance in the data points is also significantly lower for interleaved RB, even when performing an additional round of averaging for the direct methods. However the number of individual runs required for each data point is higher as shown in Table 5.1.

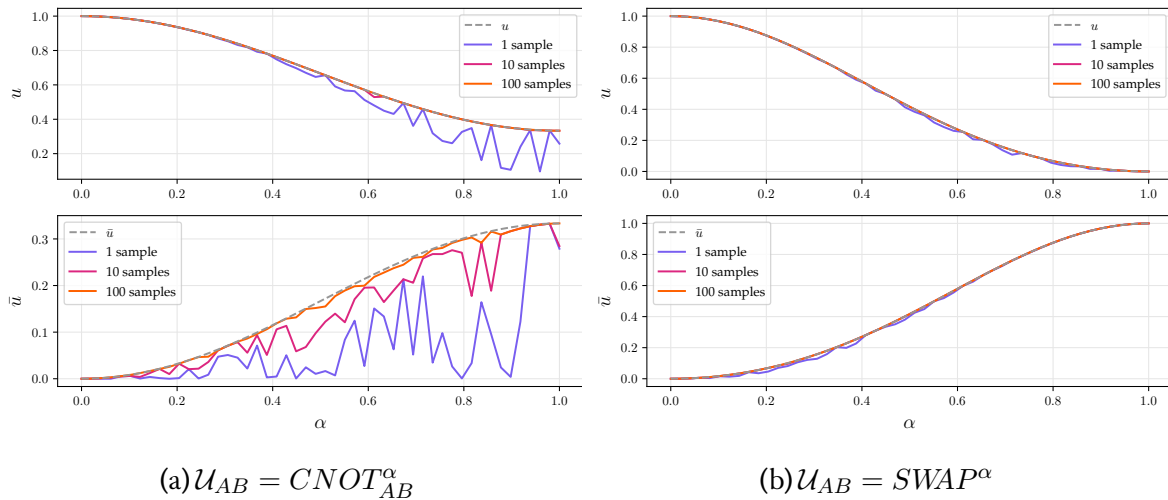


Figure 5.7: Bound on CUP-set through random unitaries. For two surfaces of the isometric CUP-set \mathcal{C} (for a range of 50 discrete values of $0 \leq \alpha \leq 1$) we can test how quickly the lower bound given in Lemma 5.1 converges towards the actual unitarity given in Theorem 5.1. Roughly, we observe, for bound within 1% of the unitarity we need 1 random setting if $u > 2/3$, and at most 100 random settings for lower values.

Summary

By adapting randomized benchmarking methods designed for SPAM-robust estimation of device noise, we achieve a much better estimation of a CUP-set that more accurately reflects the limits of the quantum device. This improves our ability to test whether quantum devices obey the limits of quantum theory.

Additionally, we see that the interleaved RB protocol is very good at estimating points where u or $\bar{u} = 0$, especially compared to the direct methods. This is likely due to the fact that, for the direct methods, these points require the estimation of two non-zero purities for any value of u , whereas the SPAM robust methods estimate a single decay parameter.

5.4 Estimation through spectral methods

We next discuss if spectral methods (that estimate eigenvalues of a channel) are an alternative SPAM robust path to estimate CUP-sets. We include two results that link unitarity to quantities estimable through spectral tomography [83] which may be of independent interest.

5.4.1 Unitarity and channel eigenvalues

Any quantum channel $\mathcal{E}: \mathcal{B}(\mathcal{H}) \rightarrow \mathcal{B}(\mathcal{H})$ on a system \mathcal{H} of dimension d has a (Liouville) representation as a $d^2 \times d^2$ matrix. Its non-unital $d^2 - 1 \times d^2 - 1$ block $T_{\mathcal{E}}$ has eigenvalues $\{\lambda_i(\mathcal{E})\}$ that are real or come in complex conjugate pairs [146]. Further, we can relate the

singular values, $\{\sigma_i(\mathcal{E})\}$, of $T_{\mathcal{E}}$ to the unitarity via [83]

$$u(\mathcal{E}) = \frac{1}{d^2 - 1} \sum_{i=1}^{d^2-1} \sigma_i(\mathcal{E})^2. \quad (5.20)$$

The set $\{\lambda_i(\mathcal{E})\}$ can in theory be estimated SPAM robustly for some noisy target process through spectral tomography [83]. Bounding the unitarity of a channel using its eigenvalues may provide a route to estimating points on the CUP-set.

The following holds for all quantum channels of fixed dimension, and allows us to lower bound the unitarity of a channel in terms of the eigenvalues of the channel under changes of basis.

Lemma 5.1. *For any quantum channel \mathcal{E} , of fixed dimension d and unitary channels \mathcal{U}_i and \mathcal{U}_j we have*

$$u(\mathcal{E}) \geq \sum_{k=1}^{d^2-1} \frac{|\lambda_k(\mathcal{U}_i \circ \mathcal{E} \circ \mathcal{U}_j)|^2}{d^2 - 1}. \quad (5.21)$$

Proof. For any quantum channel \mathcal{F} , $T_{\mathcal{F}}$ is real matrix [147]. From Weyl's Majorant Theorem [148], $\sum_k^{d^2-1} |\lambda_k(\mathcal{F})|^2 \leq \sum_k^{d^2-1} \sigma_k(\mathcal{F})^2$, where $\lambda_k(\mathcal{F})$ denote eigenvalues and $\sigma_k(\mathcal{F})$ singular values of $T_{\mathcal{F}}$. With $\mathcal{F} = \mathcal{U}_i \circ \mathcal{E} \circ \mathcal{U}_j$ for unitary channels \mathcal{U}_i & \mathcal{U}_j it follows that

$$\sum_k^{d^2-1} |\lambda_k(\mathcal{U}_i \circ \mathcal{E} \circ \mathcal{U}_j)|^2 \leq \sum_k^{d^2-1} \sigma_k(\mathcal{U}_i \circ \mathcal{E} \circ \mathcal{U}_j)^2. \quad (5.22)$$

Further more

$$\sum_k^{d^2-1} \sigma_k(\mathcal{U}_i \circ \mathcal{E} \circ \mathcal{U}_j)^2 = \sum_k^{d^2-1} \sigma_k(\mathcal{E})^2 = (d^2 - 1) u(\mathcal{E}) \quad (5.23)$$

from the invariance of singular values under unitary rotations, which completes the proof. \square

Further, for a single qubit channel, we can always saturate the above bound.

Theorem 5.1 (Variational formulation of unitarity). *For any single qubit quantum channel \mathcal{E} , maximising over all single qubit unitary channels $\{\mathcal{U}_i\}$ and $\{\mathcal{U}_j\}$ gives*

$$u(\mathcal{E}) = \max_{\mathcal{U}_i, \mathcal{U}_j} \sum_{k=1}^3 \frac{|\lambda_k(\mathcal{U}_i \circ \mathcal{E} \circ \mathcal{U}_j)|^2}{3}. \quad (5.24)$$

Proof. From the previous lemma we have $\sum_k^3 |\lambda_k(\mathcal{U}_i \circ \mathcal{E} \circ \mathcal{U}_j)|^2 \leq \sum_k^3 \sigma_k(\mathcal{U}_i \circ \mathcal{E} \circ \mathcal{U}_j)^2$ for all \mathcal{U}_i & \mathcal{U}_j . However for a single qubit channel, \mathcal{E} , we can always find [47] two specific uni-

aries \mathcal{U}_1 & \mathcal{U}_2 such that $T_{\mathcal{U}_1 \circ \mathcal{E} \circ \mathcal{U}_2}$ is a diagonal matrix, and therefore the eigenvalues and singular values are equal $\{\lambda_i(\mathcal{U}_1 \circ \mathcal{E} \circ \mathcal{U}_2)\} = \{\sigma_i(\mathcal{U}_1 \circ \mathcal{E} \circ \mathcal{U}_2)\}$ and

$$\sum_k^3 |\lambda_k(\mathcal{U}_1 \circ \mathcal{E} \circ \mathcal{U}_2)|^2 = \sum_k^3 \sigma_k(\mathcal{U}_1 \circ \mathcal{E} \circ \mathcal{U}_2)^2, \quad (5.25)$$

saturating the inequality. Therefore over the complete set of single qubit unitary channels $\{\mathcal{U}_i\}$ and $\{\mathcal{U}_j\}$, from the above two equations

$$\max_{\mathcal{U}_i, \mathcal{U}_j} \sum_k^3 |\lambda_k(\mathcal{U}_i \circ \mathcal{E} \circ \mathcal{U}_j)|^2 = \sum_k^3 \sigma_k(\mathcal{U}_1 \circ \mathcal{E} \circ \mathcal{U}_2)^2 \quad (5.26)$$

which completes the proof. \square

The practical application of Theorem 5.1 to the channels that generate the simplest CUP-set (when $(\mathcal{E}, \bar{\mathcal{E}})$ are both single qubit channels) is shown in Figure 5.7. We now consider how these results could be used if one has access to channel eigenvalues through benchmarking protocol.

5.4.2 Estimation of CUP-set through spectral tomography

Putting this together, a spectral protocol to estimate a CUP-set would require the following steps. For any point, estimate the eigenvalues of the channel $\mathcal{U}_i \circ \mathcal{E} \circ \mathcal{U}_j$ through spectral tomography for M different randomly chosen \mathcal{U}_i & \mathcal{U}_j . From Lemma 5.1, the set of estimated eigenvalues provide a lower bound on $u(\mathcal{E}_N)$ where \mathcal{E}_N is a noisy experimental implementation of $\mathcal{U}_i \circ \mathcal{E} \circ \mathcal{U}_j$. Repeat for $\bar{\mathcal{E}}$ to obtain a lower bound on $u(\bar{\mathcal{E}}_N)$ similarly. For $M \rightarrow \infty$, and in practice for at most $M \approx 100$ (see Figure 5.7), from Theorem 5.1 the estimated lower bound becomes an estimation of exactly the required unitarities.

We performed the above sequence of spectral tomographic experiments on a simulated version of the IBMQ device, IBM BELEM. However, using a similar number of resources to the interleaved RB protocol, we were unable to extract eigenvalues accurately from the tomographic data. For state vector simulations with a fixed gateset error (and without sampling) we were able to extract eigenvalues correctly. Therefore we suspect that the gate-dependence of errors or issues with the finite sampling of expectation values impede the estimation process. While increasing the number of shots may help with the later, the experimental overhead would be greatly increased compared to the other techniques we consider.

Alternative SPAM robust methods to estimate the CUP-set with a lower experimental overhead would be desirable. Here we gave several results for how spectral tomography could be used but were unable to extract CUPs with this method in practice. We leave as future work the implementation of other techniques which may allow for the robust estimation of CUP-sets, such as randomized measurements [149].

5.5 Conclusions

Quantum CUP-sets are simple and geometrical tools for analyzing the incompatibility of channels under quantum theory. We have developed methods to estimate the simplest quantum CUP-sets through direct purity relations, but also – with some assumptions – in a SPAM robust way through interleaved randomized benchmarking of unitarity. We then tested the effectiveness of these methods with simulations of an IBM device. In doing so we completed our aim of testing quantum theory using current quantum devices – where noise is a major obstacle to producing reliable tests.

As quantum CUP-sets encapsulate quantum incompatibility they may be used as a tool for benchmarking quantum devices. While estimating many points on the CUP-set may not be an efficient method of benchmarking, the extremal points of the isometric CUP-set (given for the qubit case by $(0, 1)$, $(1, 0)$ and $(1/3, 1/3)$), requires just 6 experiments. The extremal points capture both the core CUP-set geometry and the unitarity-based information-disturbance relation given in Theorem 2.1, and therefore are a natural minimal set.

Future work will focus on implementing the estimation methods for CUP-set on different quantum hardware. In particular, we may also consider randomized measurements [149] for direct purity estimation, which would give an additional method to produce the CUP-set, with minimal implementation overhead.

Technique	# of qubits (C)	# of qubits (C_r)	States	Measurements	Sequences	Repetitions	Shots	Total Runs
Complementarity SWAP	5	7	4	1	1	100	200	80000
Choi SWAP	7	9	1	1	1	100	200	20000
Spectral tomography	2	3	2	3	40	10	200	480000
Interleaved RB	2	3	6	3	10	10	200	360000

Table 5.1: **Operational overhead of CUP-set estimation.** Comparison of total number of experiments undertaken for the estimation of a point on the CUP distribution. For each technique, an experimental scheme was run on a simulation of a quantum device, with device noise imported from IBM Q via qiskit.

	Upper	\mathcal{C} Left	\mathcal{C} Right	\mathcal{C}_r Left	\mathcal{C}_r Middle	\mathcal{C}_r Right
Interleaved RB	(0.063,0.137)	(0.032,0.125)	(0.095,0.159)	(0,0.015)	(0.047,0.107)	(0,0)
SWAP test	(0.165,0.147)	(0.073,0.160)	(0.084,0.153)	(0,0.562)	(0.365,0.337)	(0.253,0)

Table 5.2: **Depolarization fits for noisy CUP-sets.** For each experimental estimation of the quantum CUP-sets \mathcal{C} & \mathcal{C}_r we fit a depolarising noise model $(u_N, \bar{u}_N) = ((1 - p_A)^2 u, (1 - p_B)^2 \bar{u})$ to each surface (see Section 5.1.2). Best fit values for (p_A, p_B) are tabulated here.

Concluding remarks

In the dime stores and bus stations,
People talk of situations,
Read books, repeat quotations,
Draw conclusions on the wall.

Love Minus Zero

Bob Dylan

Our overarching research question in this work was whether tools from the benchmarking of quantum devices could capture fundamental features of quantum theory. The unitarity of a quantum channel is measure of coherence for the channel that appears naturally within randomized benchmarking protocols. To answer our research question we developed a range of results building on the unitarity and connecting with foundational ideas such as quantum no-go theorems and strictly non-classical effects like non-separability in quantum channels. We chose our research question because we could relate it to three useful goals. These were:

- (1) To test the limits of quantum theory using current noisy quantum devices,
- (2) To gain independent information about the nature of device noise,
- (3) To provide efficient and robust certification of non-classical effects.

We now briefly summarize how we approached these goals, and whether we achieved them. Following this, we examine how the ideas we have presented relate to other areas of research and they could be built upon in future.

6.1 Summary of results

Within Chapter 2, we extended the unitarity of quantum channels to channels in other probability theories. Then we used this generalised measure to establish a framework for capturing quantum incompatibility based around sets of compatible unitarity pairs – CUP-sets. We showed these CUP-sets encode no-cloning and no-hiding and allow for a simple geometrical comparison with classical theory.

Having taken an ‘outward’ looking approach in the first chapter, we turned ‘inwards’ in Chapter 3. Namely, we considered how unitarity can be extended to subsystems within a channel. We defined subunitarities which capture the coherence in and between subsystems within a channel. We showed that these measures have nice properties for quantifying subsystem information transfer and lead to a measure for the coherence of correlations in a channel – the correlation unitarity – which is a witness to a strictly non-classical effect, non-separability.

While the results we obtained in the first two chapters are of independent interest, as they connect with foundational ideas, to complete our goals we had to devise methods for estimation on quantum devices. Therefore in Chapter 4 we proved that, with some assumptions, subunitarities and the correlation unitarity can be estimated for device noise through randomized benchmarking protocols. These protocols were efficient and robust to initial and final errors in state preparation and measurements, however in general we required mid-circuit resets which reduced robustness. When device noise can be assumed to be a Pauli channel, through randomized compiling, we could estimate the correlation unitarity with complete robustness. Further, we showed that our techniques work well in practice if the reset errors are small. Finally, we showed that these methods give independent information beyond existing benchmarking techniques namely in the form of a novel measure of coherent correlations which we proved witnesses non-separability and can be estimated in practice. In this way, we achieved goals (2) and (3).

We then turned to the estimation of CUP-sets in Chapter 5, where we showed that the simplest quantum CUP-sets can be estimated on current devices. We gave straightforward methods of estimation and more involved methods based on randomized benchmarking. These latter methods gave improved performance, as we could separate some of the errors in the preparation of the experiment itself from errors in the target quantum process we were trying to probe. As we gave an estimation of CUP-sets for a simulation of a real device, we come close to realizing goal (1). We hope to implement the same experimental procedures on a physical quantum device in the near future.

6.2 Outlook

We now give some opinions on how our work could be improved or built upon, and how it may be connected to other areas of active research.

Our primary protocol for subunitarity estimation relies on fitting a multi-exponential decay to noisy data. In general this is a hard problem, and there will be many fits that will approximate the decay curve. The protocol could be substantially improved by exploiting recent statistical techniques [151] or algorithms for multi-exponential fitting [7, 152].

Throughout this work we have considered the error induced by a computational gateset to be time-independent and gate-independent and averaged for the gateset considered. As such, relaxing these constraints would be a natural line to develop [44, 153, 154].

Recently, many theoretical results have analysed how the effect of noise on quantum algorithms results in a computation that can be efficiently simulated classically [155]. This behaviour remains even for quantum advantage experiments [156]. Similarly, we have seen that noise affects the quantum CUP-set by shifting it towards regions that exhibit classical behaviour such as hiding. An interesting future direction would be to connect these two aspects and determine if device benchmarking via CUP-sets can provide additional information to bound finite size classical simulability of quantum circuits in the presence of noise.

While we expect classical devices to perform a perfect estimation of the isometric CUP-set, the reversible classical CUP-set relies on a source of randomness to perform perfect hiding. The accuracy of the estimated CUP-set can then be directly related to the bias in the randomness. Therefore the CUP-set formulation could conceivably provide a means of assessing the quality of a source of randomness.

Finally, in this work we primarily considered two theories, classical theory and quantum theory, however CUP-sets can be derived for more general physical theories. It would be interesting to see how the structure of CUP-sets varies between different theories.

A

Material related to CUP-sets

This section contains proofs and technical statements that were omitted from the discussion in Chapter 2.

A.1 Convexity of unitarity

The following properties of unitarity are utilized within the proof of an upper bound on reversible quantum CUP-sets. They may be of independent interest.

Lemma A.1. *For any convex combination of channels $\mathcal{E} = \sum_i^r p_i \mathcal{E}_i$, the respective unital matrix, $T_{\mathcal{E}}$, has the form: $T_{\mathcal{E}} = \sum_i^r p_i T_{\mathcal{E}_i}$.*

Proof. $T_{\mathcal{E}} = \sum_{j,k}^{d_X^2-1, d_Y^2-1} \langle y_k | \mathcal{E}(x_j) \rangle |y_k\rangle \langle x_j| = \sum_{j,k}^{d_X^2-1, d_Y^2-1} \langle y_k | \sum_i^r p_i \mathcal{E}_i(x_j) \rangle |y_k\rangle \langle x_j|$. However as quantum channels are linear, this is $\sum_i^r p_i \sum_{j,k}^{d_X^2-1, d_Y^2-1} \langle y_k | \mathcal{E}_i(x_j) \rangle |y_k\rangle \langle x_j| = \sum_i^r p_i T_{\mathcal{E}_i}$. \square

Lemma A.2. *The unitarity $u(\mathcal{E})$ is a convex function of any quantum channel \mathcal{E} .*

Proof. From Lemma A.1, for any convex combination of channels $\mathcal{E} = \sum_i^r p_i \mathcal{E}_i$ the corresponding $T_{\mathcal{E}}$ matrix is the convex combination of each individual term, $T_{\mathcal{E}} = \sum_i^r p_i T_{\mathcal{E}_i}$. All norms are convex non-negative functions, including the l_2 norm, $\|\cdot\|$ [122]. Further, if $f(x)$ is convex and non-negative function of x then $f(x)^2$ is also convex. Therefore $\|T_{\mathcal{E}}\|^2$ is a convex function of $T_{\mathcal{E}}$. Putting this together with the appropriate dimension factor we have

$$u(\mathcal{E}) = \alpha \left\| \sum_i^r p_i T_{\mathcal{E}_i} \right\|^2 \leq \sum_i^r p_i \alpha \|T_{\mathcal{E}_i}\|^2 = \sum_i^r p_i u(\mathcal{E}_i) \quad (\text{A.1})$$

which completes the proof. \square

A.2 Analytical form for quantum CUP-set surfaces

We now calculate the unitarity of several channels analytically. This gives us the mathematical form for the surfaces of the (isometric) quantum CUP-set.

A.2.1 Upper surface ($SWAP^\alpha$)

Lemma A.3. *For the isometry $\mathcal{V}_\alpha(\rho) := SWAP^\alpha(\rho \otimes |0\rangle\langle 0|)$ where $0 \leq \alpha \leq 1$, we define the marginals $\mathcal{E}_\alpha(\rho) := \text{tr}_B[\mathcal{V}(\rho)_\alpha]$ and $\bar{\mathcal{E}}_\alpha(\rho) := \text{tr}_A[\mathcal{V}(\rho)_\alpha]$. The unitarities of each marginal are*

$$u(\mathcal{E}_\alpha) = \frac{(1-s)(3-s)}{3} \quad (\text{A.2})$$

and

$$u(\bar{\mathcal{E}}_\alpha) = 1 - \frac{(1-s)(3+s)}{3} \quad (\text{A.3})$$

respectively, where $s = \sin^2(\frac{\pi\alpha}{2})$.

If we consider the sum of the marginals from Lemma A.3 we have

$$u(\mathcal{E}_\alpha) + u(\bar{\mathcal{E}}_\alpha) = 1 - \frac{2s(1-s)}{3} \quad (\text{A.4})$$

with $0 \leq s \leq 1$ and produce a tighter bound on the marginals, namely for any isometry with $d_X = d_A = d_B = 2$, for a given $u(\mathcal{E})$ we have

$$u(\bar{\mathcal{E}}) \leq 3 + u(\mathcal{E}) - 2\sqrt{1 + 3u(\mathcal{E})}. \quad (\text{A.5})$$

Proof. (of Lemma A.3) First we must obtain a useful analytical form for $SWAP^\alpha$. As $SWAP$ is a unitary channel to derive the analytical form it is sufficient to find the unitary matrix U that transforms the two qubit pure state $|\psi\rangle \otimes |\phi\rangle$ such that

$$U |\psi\rangle \otimes |\phi\rangle = |\phi\rangle \otimes |\psi\rangle. \quad (\text{A.6})$$

From this definition we can write

$$\begin{aligned} U &= |00\rangle\langle 00| + |10\rangle\langle 01| + |01\rangle\langle 10| + |11\rangle\langle 11|, \\ &= \frac{1}{2}(\mathbb{1}^{\otimes 2} + X^{\otimes 2} + Y^{\otimes 2} + Z^{\otimes 2}), \end{aligned} \quad (\text{A.7})$$

where $\{\mathbb{1}, X, Y, Z\}$ are the Pauli matrices on 1 qubit. Defining the Bell states as $|\Phi_\pm\rangle := \frac{1}{\sqrt{2}}(|00\rangle \pm |11\rangle)$ and $|\Psi_\pm\rangle := \frac{1}{\sqrt{2}}(|01\rangle \pm |10\rangle)$, we can diagonalise this unitary as

$$\begin{aligned} U &= |\Phi_+\rangle\langle \Phi_+| + |\Phi_-\rangle\langle \Phi_-| + |\Psi_+\rangle\langle \Psi_+| - |\Psi_-\rangle\langle \Psi_-|, \\ &= |\Phi_+\rangle\langle \Phi_+| + |\Phi_-\rangle\langle \Phi_-| + |\Psi_+\rangle\langle \Psi_+| + e^{i\pi} |\Psi_-\rangle\langle \Psi_-|. \end{aligned} \quad (\text{A.8})$$

As $SWAP^\alpha(\rho) = U^\alpha \rho (U^\alpha)^\dagger$, up to a global phase we can find [157]

$$U^\alpha = |\Phi_+\rangle\langle\Phi_+| + |\Phi_-\rangle\langle\Phi_-| + |\Psi_+\rangle\langle\Psi_+| + e^{i\pi\alpha} |\Psi_-\rangle\langle\Psi_-|, \quad (\text{A.9})$$

and through careful expansion

$$\begin{aligned} U^\alpha &= |00\rangle\langle 00| + |11\rangle\langle 11| \\ &\quad + \frac{1}{2}(1 + e^{i\pi\alpha})(|01\rangle\langle 01| + |10\rangle\langle 10|) \\ &\quad + \frac{1}{2}(1 - e^{i\pi\alpha})(|01\rangle\langle 10| + |10\rangle\langle 01|), \\ &= \frac{1}{2}(\mathbb{1}^{\otimes 2} + Z^{\otimes 2}) + \frac{1}{4}(1 + e^{i\pi\alpha})(\mathbb{1}^{\otimes 2} - Z^{\otimes 2}) + \frac{1}{4}(1 - e^{i\pi\alpha})(X^{\otimes 2} + Y^{\otimes 2}), \\ &= \frac{1}{2}(1 + e^{i\pi\alpha})\mathbb{1}^{\otimes 2} + \frac{1}{4}(1 - e^{i\pi\alpha})(\mathbb{1}^{\otimes 2} + X^{\otimes 2} + Y^{\otimes 2} + Z^{\otimes 2}), \\ &= \frac{1}{2}(1 + e^{i\pi\alpha})\mathbb{1}^{\otimes 2} + \frac{1}{2}(1 - e^{i\pi\alpha})U. \end{aligned} \quad (\text{A.10})$$

If we now expand the isometry definition we have

$$\begin{aligned} \mathcal{V}(\rho)_\alpha &= U^\alpha \rho \otimes |0\rangle\langle 0| (U^\alpha)^\dagger, \\ &= \left(\frac{1}{2}(1 + e^{i\pi\alpha})\mathbb{1}^{\otimes 2} + \frac{1}{2}(1 - e^{i\pi\alpha})U\right) \\ &\quad (\rho \otimes |0\rangle\langle 0|) \\ &\quad \left(\frac{1}{2}(1 + e^{-i\pi\alpha})\mathbb{1}^{\otimes 2} + \frac{1}{2}(1 - e^{-i\pi\alpha})U^\dagger\right), \\ &= \cos\left(\frac{\pi\alpha}{2}\right)^2 \mathbb{1}^{\otimes 2} (\rho \otimes |0\rangle\langle 0|) \mathbb{1}^{\otimes 2} + \sin\left(\frac{\pi\alpha}{2}\right)^2 U (\rho \otimes |0\rangle\langle 0|) U^\dagger \\ &\quad + \frac{i}{2} \sin(\pi\alpha) \mathbb{1}^{\otimes 2} (\rho \otimes |0\rangle\langle 0|) U^\dagger - \frac{i}{2} \sin(\pi\alpha) U (\rho \otimes |0\rangle\langle 0|) \mathbb{1}^{\otimes 2}, \\ &= \cos\left(\frac{\pi\alpha}{2}\right)^2 \rho \otimes |0\rangle\langle 0| + \sin\left(\frac{\pi\alpha}{2}\right)^2 |0\rangle\langle 0| \otimes \rho \\ &\quad + \frac{i}{2} \sin(\pi\alpha) \mathbb{1}^{\otimes 2} (\rho \otimes |0\rangle\langle 0|) U^\dagger - \frac{i}{2} \sin(\pi\alpha) U (\rho \otimes |0\rangle\langle 0|) \mathbb{1}^{\otimes 2}. \end{aligned} \quad (\text{A.11})$$

From this point it is relatively straightforward to show that the unital block T for the 1 qubit channels \mathcal{E}_α & $\bar{\mathcal{E}}_\alpha$ will be

$$T_{\mathcal{E},\alpha} = \begin{array}{c} |X/\sqrt{2}\rangle \\ |Y/\sqrt{2}\rangle \\ |Z/\sqrt{2}\rangle \end{array} \left(\begin{array}{ccc} |X/\sqrt{2}\rangle & |Y/\sqrt{2}\rangle & |Z/\sqrt{2}\rangle \\ \cos\left(\frac{\pi\alpha}{2}\right)^2 & \frac{1}{2} \sin(\pi\alpha) & 0 \\ -\frac{1}{2} \sin(\pi\alpha) & \cos\left(\frac{\pi\alpha}{2}\right)^2 & 0 \\ 0 & 0 & \cos\left(\frac{\pi\alpha}{2}\right)^2 \end{array} \right), \quad (\text{A.12})$$

and

$$T_{\bar{\mathcal{E}},\alpha} = \begin{array}{c} |X/\sqrt{2}\rangle \\ |Y/\sqrt{2}\rangle \\ |Z/\sqrt{2}\rangle \end{array} \left(\begin{array}{ccc} |X/\sqrt{2}\rangle & |Y/\sqrt{2}\rangle & |Z/\sqrt{2}\rangle \\ \sin\left(\frac{\pi\alpha}{2}\right)^2 & -\frac{1}{2} \sin(\pi\alpha) & 0 \\ \frac{1}{2} \sin(\pi\alpha) & \sin\left(\frac{\pi\alpha}{2}\right)^2 & 0 \\ 0 & 0 & \sin\left(\frac{\pi\alpha}{2}\right)^2 \end{array} \right), \quad (\text{A.13})$$

respectively. Therefore the unitarity of \mathcal{E}_α is given by

$$u(\mathcal{E}_\alpha) = \frac{1}{3} \operatorname{tr} [T_{\mathcal{E},\alpha}^\dagger T_{\mathcal{E},\alpha}] = \cos\left(\frac{\pi\alpha}{2}\right)^4 + \frac{1}{6} \sin(\pi\alpha)^2 = \frac{1}{6} \cos\left(\frac{\pi\alpha}{2}\right)^2 (5 + \cos(\pi\alpha)). \quad (\text{A.14})$$

For the other marginal, the unitarity of $\bar{\mathcal{E}}_\alpha$ is given by

$$u(\bar{\mathcal{E}}_\alpha) = \frac{1}{3} \operatorname{tr} [T_{\bar{\mathcal{E}},\alpha}^\dagger T_{\bar{\mathcal{E}},\alpha}] = \sin\left(\frac{\pi\alpha}{2}\right)^4 + \frac{1}{6} \sin(\pi\alpha)^2 = \frac{1}{6} \sin\left(\frac{\pi\alpha}{2}\right)^2 (5 - \cos(\pi\alpha)). \quad (\text{A.15})$$

This completes the proof. \square

A.2.2 Lower right surface ($CNOT_{AB}^\alpha$)

Lemma A.4. *For the isometry $\mathcal{V}(\rho)_\alpha := CNOT_{AB}^\alpha(\rho \otimes |0\rangle\langle 0|)$ where $0 \leq \alpha \leq 1$, we define the marginals $\mathcal{E}_\alpha(\rho) := \operatorname{tr}_B[\mathcal{V}(\rho)_\alpha]$ and $\bar{\mathcal{E}}_\alpha(\rho) := \operatorname{tr}_A[\mathcal{V}(\rho)_\alpha]$. The unitarities of each marginal are*

$$u(\mathcal{E}_\alpha) = 1 - \frac{2s}{3} \quad (\text{A.16})$$

and

$$u(\bar{\mathcal{E}}_\alpha) = \frac{s}{3} \quad (\text{A.17})$$

respectively, where $s = \sin^2(\frac{\pi\alpha}{2})$.

If we consider the sum of the marginals from Lemma A.4 we have

$$u(\mathcal{E}_\alpha) + u(\bar{\mathcal{E}}_\alpha) = 1 - \frac{s}{3} \quad (\text{A.18})$$

with $0 \leq s \leq 1$.

Proof. (of Lemma A.4) The proof follows in a similar way to the $SWAP^\alpha$ case. For the given $CNOT_{AB}$ channel we use the notation $CNOT_{AB}(\rho) = U\rho U^\dagger$, to clarify that we mean the unitary matrix U itself. We can diagonalise U with respect to the computational basis by applying a hadamard transform $H = (Z + X)/\sqrt{2}$ on the target qubit before and after such that the sandwiched unitary is the controlled phase gate:

$$\begin{aligned} U &= \frac{1}{2}(\mathbb{1} \otimes \mathbb{1} + Z \otimes \mathbb{1} + \mathbb{1} \otimes X - Z \otimes X), \\ &= \frac{1}{2}(\mathbb{1} \otimes H\mathbb{1}H + Z \otimes H\mathbb{1}H + \mathbb{1} \otimes HZH - Z \otimes HZH), \\ &= (\mathbb{1} \otimes H) \frac{1}{2}(\mathbb{1} \otimes \mathbb{1} + Z \otimes \mathbb{1} + \mathbb{1} \otimes Z - Z \otimes Z)(\mathbb{1} \otimes H), \\ &= (\mathbb{1} \otimes H)(|00\rangle\langle 00| + |01\rangle\langle 01| + |10\rangle\langle 10| - |11\rangle\langle 11|)(\mathbb{1} \otimes H), \\ &= (\mathbb{1} \otimes H)(|00\rangle\langle 00| + |01\rangle\langle 01| + |10\rangle\langle 10| + e^{i\pi} |11\rangle\langle 11|)(\mathbb{1} \otimes H). \end{aligned} \quad (\text{A.19})$$

Therefore we have

$$\begin{aligned} U^\alpha &= (\mathbb{1} \otimes H)(|00\rangle\langle 00| + |01\rangle\langle 01| + |10\rangle\langle 10| + e^{i\pi\alpha} |11\rangle\langle 11|)(\mathbb{1} \otimes H), \\ &= |0\rangle\langle 0| \otimes \mathbb{1} + \frac{1}{2}(1 + e^{i\pi\alpha})(|1\rangle\langle 1| \otimes \mathbb{1}) + \frac{1}{2}(1 - e^{i\pi\alpha})(|1\rangle\langle 1| \otimes X). \end{aligned} \quad (\text{A.20})$$

From the isometry definition we have $\mathcal{V}(\rho)_\alpha = U^\alpha \rho \otimes |0\rangle\langle 0| (U^\alpha)^\dagger$, substituting in the definition of U^α we can show that the unital block T for the 1 qubit channels \mathcal{E}_α & $\bar{\mathcal{E}}_\alpha$ will be

$$T_{\mathcal{E},\alpha} = \begin{array}{c} |X/\sqrt{2}\rangle \\ |Y/\sqrt{2}\rangle \\ |Z/\sqrt{2}\rangle \end{array} \left(\begin{array}{ccc} \cos^2(\frac{\pi\alpha}{2}) & \frac{1}{2} \sin(\pi\alpha) & 0 \\ -\frac{1}{2} \sin(\pi\alpha) & \cos^2(\frac{\pi\alpha}{2}) & 0 \\ 0 & 0 & 1 \end{array} \right), \quad (\text{A.21})$$

and

$$T_{\bar{\mathcal{E}},\alpha} = \begin{array}{c} |X/\sqrt{2}\rangle \\ |Y/\sqrt{2}\rangle \\ |Z/\sqrt{2}\rangle \end{array} \left(\begin{array}{ccc} 0 & 0 & 0 \\ 0 & 0 & 0 \\ 0 & \frac{1}{2} \sin(\pi\alpha) & \sin^2(\frac{\pi\alpha}{2}) \end{array} \right), \quad (\text{A.22})$$

respectively. Therefore, with some multiplication, the unitarity of \mathcal{E}_α is given by $u(\mathcal{E}_\alpha) = 1 - \frac{2}{3} \sin^2(\frac{\alpha\pi}{2})$ and the unitarity of $\bar{\mathcal{E}}_\alpha$ is given by $u(\bar{\mathcal{E}}_\alpha) = \frac{1}{3} \sin^2(\frac{\alpha\pi}{2})$. This completes the proof. \square

A.2.3 Lower left surface ($CNOT_{BA}^\alpha \circ CNOT_{AB}$)

Lemma A.5. For the isometry $\mathcal{V}(\rho)_\alpha := CNOT_{BA}^\alpha \circ CNOT_{AB}(\rho \otimes |0\rangle\langle 0|)$ where $0 \leq \alpha \leq 1$, we define the marginals $\mathcal{E}_\alpha(\rho) := \text{tr}_B[\mathcal{V}(\rho)_\alpha]$ and $\bar{\mathcal{E}}_\alpha(\rho) := \text{tr}_A[\mathcal{V}(\rho)_\alpha]$. The unitarities of each marginal are

$$u(\mathcal{E}_\alpha) = \frac{1}{3}(1 - s) \quad (\text{A.23})$$

and

$$u(\bar{\mathcal{E}}_\alpha) = 1 - \frac{2}{3}(1 - s) \quad (\text{A.24})$$

respectively, where $s = \sin^2(\frac{\pi\alpha}{2})$.

If we consider the sum of the marginals from Lemma A.5 we have

$$u(\mathcal{E}_\alpha) + u(\bar{\mathcal{E}}_\alpha) = 1 - \frac{1}{3}(1 - s) \quad (\text{A.25})$$

with $0 \leq s \leq 1$.

Proof. (of Lemma A.5) Proof follows in the same way as the previous two lemmas. From the previous lemma we can write the unitary matrix for the channel $CNOT_{BA}(\rho) := U_{BA}\rho U_{BA}^\dagger$ as

$$U_{BA} = (H \otimes \mathbf{1})(|00\rangle\langle 00| + |01\rangle\langle 01| + |10\rangle\langle 10| + e^{i\pi} |11\rangle\langle 11|)(H \otimes \mathbf{1}), \quad (\text{A.26})$$

and therefore

$$\begin{aligned} U_{BA}^\alpha &= (H \otimes \mathbf{1})(|00\rangle\langle 00| + |01\rangle\langle 01| + |10\rangle\langle 10| + e^{i\pi\alpha} |11\rangle\langle 11|)(H \otimes \mathbf{1}), \\ &= \mathbf{1} \otimes |0\rangle\langle 0| + \frac{1}{2}(1 + e^{i\pi\alpha})(\mathbf{1} \otimes |1\rangle\langle 1|) + \frac{1}{2}(1 - e^{i\pi\alpha})(X \otimes |1\rangle\langle 1|). \end{aligned} \quad (\text{A.27})$$

The unitary matrix for the channel $CNOT_{AB}(\rho) := U_{AB}\rho U_{AB}^\dagger$ is given in the Pauli basis as

$$U_{AB} = \frac{1}{2}(\mathbb{1} \otimes \mathbb{1} + Z \otimes \mathbb{1} + \mathbb{1} \otimes X - Z \otimes X), \quad (\text{A.28})$$

therefore from the isometry definition $\mathcal{V}(\rho)_\alpha = U_{BA}^\alpha U_{AB}\rho \otimes |0\rangle\langle 0| U_{AB}^\dagger (U_{BA}^\alpha)^\dagger$ we can show that the unital block T for the 1 qubit channels \mathcal{E}_α & $\bar{\mathcal{E}}_\alpha$ will be

$$T_{\mathcal{E},\alpha} = \begin{array}{c} |X/\sqrt{2}\rangle \\ |Y/\sqrt{2}\rangle \\ |Z/\sqrt{2}\rangle \end{array} \left(\begin{array}{ccc} \langle X/\sqrt{2}| & \langle Y/\sqrt{2}| & \langle Z/\sqrt{2}| \\ 0 & 0 & 0 \\ 0 & 0 & 0 \\ 0 & -\frac{1}{2}\sin(\pi\alpha) & \cos^2(\frac{\pi\alpha}{2}) \end{array} \right), \quad (\text{A.29})$$

and

$$T_{\bar{\mathcal{E}},\alpha} = \begin{array}{c} |X/\sqrt{2}\rangle \\ |Y/\sqrt{2}\rangle \\ |Z/\sqrt{2}\rangle \end{array} \left(\begin{array}{ccc} \langle X/\sqrt{2}| & \langle Y/\sqrt{2}| & \langle Z/\sqrt{2}| \\ \sin^2(\frac{\pi\alpha}{2}) & -\frac{1}{2}\sin(\pi\alpha) & 0 \\ \frac{1}{2}\sin(\pi\alpha) & \sin^2(\frac{\pi\alpha}{2}) & 0 \\ 0 & 0 & 1 \end{array} \right), \quad (\text{A.30})$$

respectively. Therefore, with some multiplication, the unitarity of \mathcal{E}_α is given by $u(\mathcal{E}_\alpha) = \frac{1}{3}\cos^2(\frac{\alpha\pi}{2})$ and the unitarity of $\bar{\mathcal{E}}_\alpha$ is given by $u(\bar{\mathcal{E}}_\alpha) = 1 - \frac{2}{3}\cos^2(\frac{\alpha\pi}{2})$. This completes the proof. \square

A.3 Compatible fidelity pairs

As we discussed in Chapter 1, the unitarity appears when considering the variance of an observable for an RB sequence. The prototypical measure estimated through RB is the average gate fidelity of noise, which can be estimated more straightforwardly. Fidelity RB scales better with system size [5] than unitarity RB and rigorous analysis has been completed examining the gate dependence in noise for fidelity RB. Overall, average gate fidelity would seem an easier SPAM robust tool to use compared to unitarity. It is therefore reasonable to ask if fidelity can be used instead of unitarity in the analysis we have undertaken throughout this work.

In this section, we illustrate that fidelity cannot be used to capture the no-hiding and no-cloning theorems in the same manner as unitarity, as discussed in Chapter 2. The arguments could be extended to non-separability as discussed in Chapter 4.

For a fixed dimension d , consider the average gate fidelity, $f(\mathcal{E})$, of a quantum channel, \mathcal{E} , is defined via $f(\mathcal{E}) = 1 - r(\mathcal{E})$ for the average gate infidelity given in equation (1.4) [48]. The fidelity is bounded $\frac{1}{d+1} \leq f(\mathcal{E}) \leq 1$ and takes the value $f(\mathcal{E}) = 1$ if and only if $\mathcal{E} = id$ [52]. The fidelity of a channel is upper bounded by its unitarity [83] with

$$\left(\frac{df(\mathcal{E}) - 1}{d - 1}\right)^2 \leq u(\mathcal{E}). \quad (\text{A.31})$$

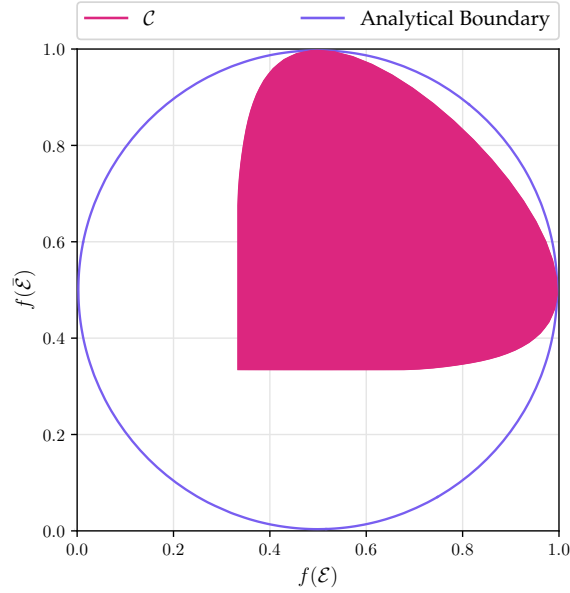


Figure A.1: **Compatible Fidelity Pairs.** The simplest non-trivial set, \mathcal{C} , of compatible average gate fidelity pairs, $(f(\mathcal{E}), f(\bar{\mathcal{E}}))$, are shown. The bound given in equation (A.32) constrains the set to within the unit circle.

These bounds are tight as they hold exactly for a partially depolarizing channel.

Let us consider splitting quantum information between subsystems using quantum channels. This was discussed in detail in Chapter 2. For simplicity, we will consider single qubit channels. For the isometry, $\mathcal{V}(\rho) := \mathcal{U}_{AB}(\rho \otimes |0\rangle\langle 0|)$, from one qubit to two qubits, we define a pair of complementarity channels. These are the single qubit marginal channels $\mathcal{E} := \text{tr}_B \circ \mathcal{V}$ and $\bar{\mathcal{E}} := \text{tr}_A \circ \mathcal{V}$. By ranging over all unitaries, \mathcal{U}_{AB} , we generate all compatible channels, $(\mathcal{E}, \bar{\mathcal{E}})$, and we can examine possible ways to divide quantum information between two parties.

Now let us consider pairs of compatible fidelities given by any tuple, $(f(\mathcal{E}), f(\bar{\mathcal{E}}))$ for a pair of compatible channels, $(\mathcal{E}, \bar{\mathcal{E}})$. The set of all fidelity pairs will capture some of properties of the set of all compatible channels. For example, the no-cloning theorem excludes the channels $\mathcal{E} = \bar{\mathcal{E}} = id$ from the set compatible channels, as $f(\mathcal{E}) = 1$ if and only if $\mathcal{E} = id$, then the point $(1, 1)$ must be excluded from the set of compatible fidelity pairs.

We can also more broadly constrain the set of fidelities analytically. Applying Theorem 2.1 to the bound in equation (A.31), and we immediately have

$$(2f(\mathcal{E}) - 1)^2 + (2f(\bar{\mathcal{E}}) - 1)^2 \leq u(\mathcal{E}) + u(\bar{\mathcal{E}}) \leq 1. \quad (\text{A.32})$$

Rather pleasingly, these bounds constrain the set of compatible fidelity pairs to be within the unit circle. Through the general circuit decomposition given in Figure 2.2 we can generate the complete set of compatible fidelity pairs, which is shown in Figure A.1. We observe the bounds are tight at the points $(1, 1/2)$ and $(1/2, 1)$.

We now discuss the limitations of using fidelity to quantify incompatibility between channels. First, we note that the fidelity of a completely depolarizing channel, \mathcal{D} , is $f(\mathcal{D}) = \frac{1}{2}$. Fidelity is not invariant under local changes of basis, and the fidelity of a unitary channel, \mathcal{U} , can be anywhere in the full range of $\frac{1}{3} \leq f(\mathcal{U}) \leq 1$. Given this, an experimental value of $f(\mathcal{E}) = \frac{1}{2}$ can correspond to the complete loss of the input state ($\mathcal{E} = \mathcal{D}$) or complete recoverability ($\mathcal{E} = \mathcal{U}$). For partial loss of information, we can extend this argument across all values of $f(\mathcal{E})$. This makes it difficult for fidelity to capture information-disturbance in terms of recoverability, as a final unitary change of basis can give same fidelity as completely discarding the input.

A direct consequence of the above is that the set of compatible fidelity pairs cannot easily capture the no-hiding theorem. In terms of compatible channels, (see Chapter 4) the no-hiding theorem states that if $\mathcal{E} = \mathcal{D}$ then we must have $\bar{\mathcal{E}} = \mathcal{U}$. Given $f(\mathcal{D}) = \frac{1}{2}$, if we examine the points $(\frac{1}{2}, x)$ in Figure A.1, we find x can take any value. Therefore we cannot relate the loss of information at one marginal to the complete recovery of information at the other. A similar argument applies to the no-cloning theorem, as for the point $(1, x)$ while we must have $x = \frac{1}{2}$, this does not uniquely identify a corresponding channel.

Putting this all together, while the average gate fidelity of a quantum channel is a highly useful measure in the context of benchmarking, it doesn't allow for the same expression of incompatibility as our analysis using unitarity.

A.4 Interpretation of unitarity and reversibility

Our intuitive understanding of unitarity is that it measures how well a channel preserves quantum information. However mathematically, the unitarity captures how close a channel is to an isometry. As we shall show shortly, for channels with equal input and output dimensions these statements are equivalent – unitary channels are the only channels which can be deterministically reversed for all input states. When we consider quantum channels with differing input and output dimensions then we must be more careful. In this section we consider what the unitarity of information preserving channels can tell us in general.

When we consider all quantum channels, the set of channels that perfectly preserve quantum information are *reversible* channels. We discussed these channels at length in Chapter 2. Recall, that a reversible channel \mathcal{R} is defined as quantum channel for which there exists another quantum channel \mathcal{R}' such that for all quantum states ρ we have

$$\mathcal{R}' \circ \mathcal{R}(\rho) = \rho. \quad (\text{A.33})$$

It can be shown [158] that this definition is equivalent to the following statement:

$$\langle \mathcal{R}(\sigma), \mathcal{R}(\rho) \rangle = c \langle \sigma, \rho \rangle \quad (\text{A.34})$$

for some constant $c > 0$ and for any two quantum states σ & ρ .

If we label the input system the dimension d_X and the output system the dimension d_Y , then \mathcal{R} can always be written [158] in the following form:

$$\mathcal{R}(\rho) = \mathcal{U}(\rho \otimes \tau) \quad (\text{A.35})$$

where τ is a (potentially mixed) quantum state with dimension d_Y/d_X and \mathcal{U} is a unitary on the output system. Therefore when $d_X = d_Y$ the set of reversible channels is equal to the set of unitaries on the system. Putting the above together with equation (A.34), we have $c = \text{tr}[\tau^2]$, meaning the constant c captures the purity of the auxiliary system introduced by the channel. Maximizing and minimizing this purity gives us the following bounds

$$\frac{d_X}{d_Y} \leq c \leq 1. \quad (\text{A.36})$$

Let us see how these properties relate to the unitarity.

Lemma A.6. *The unitarity $u(\mathcal{R})$ of a reversible channel \mathcal{R} is given by*

$$u(\mathcal{R}) = c \quad (\text{A.37})$$

where $c = \frac{\langle \sigma, \rho \rangle}{\langle \mathcal{R}(\sigma), \mathcal{R}(\rho) \rangle}$ for any input states σ & ρ .

Proof. We give the input system for \mathcal{R} the dimension d . With $\psi = |\psi\rangle\langle\psi|$, from definition

$$\begin{aligned} u(\mathcal{R}) &= \frac{d}{d-1} \int d\psi \langle \mathcal{R}(\psi), \mathcal{R}(\psi) \rangle - \langle \mathcal{R}(\mathbf{1}/d), \mathcal{R}(\mathbf{1}/d) \rangle, \\ &= \frac{d}{d-1} \int d\psi c \langle \psi, \psi \rangle - c \langle \mathbf{1}/d, \mathbf{1}/d \rangle = c u(id). \end{aligned} \quad (\text{A.38})$$

As $u(id) = 1$, this completes the proof. \square

Combining this result with equation (A.36), for any reversible channel, \mathcal{R} , from an input system with dimension d_X to an output system with dimension d_Y must obey

$$\frac{d_X}{d_Y} \leq u(\mathcal{R}) \leq 1. \quad (\text{A.39})$$

A direct consequence of this is that unitarity can be used to witness non-reversible behaviour in a unknown quantum channel. Consider a channel, \mathcal{E} , from a one qubit system to a two qubits system. From the above bounds, if $u(\mathcal{E}) < \frac{1}{2}$, the channel cannot be reversible.

To conclude, the unitarity of a channel is a measure of how close it is from being isometric. Therefore – outside of fixed dimensions – cannot be directly interpreted as quantifying quantum information transfer. However we have shown that, even in the general case, it can be used to bound how much quantum information has be preserved in terms of reversibility. To be exact, we have shown unitarity can act as a witness to the reversibility of a process, thereby extending its usefulness.

B

Material related to subunitarities and correlation unitarity

B.1 Review of notation

Throughout this appendix, we consistently use the same notation as in Chapter 3, which we review here.

We consider an open bipartite quantum system with an associated Hilbert space $\mathcal{H}_A \otimes \mathcal{H}_B$ and dimension $d = d_A d_B$. Quantum channels act on the system such that $\mathcal{E}_{AB}: \mathcal{B}(\mathcal{H}_A \otimes \mathcal{H}_B) \rightarrow \mathcal{B}(\mathcal{H}_A \otimes \mathcal{H}_B)$, and unless otherwise stated we assume for simplicity that the input and output systems are identical. We denote all vectorized quantities in boldface, $|\mathbf{M}\rangle := |\text{vec}(M)\rangle$ for any operator $M \in \mathcal{B}(\mathcal{H}_A \otimes \mathcal{H}_B)$ and similarly, we denote the Liouville representation $\mathcal{E}_{AB} := \mathcal{L}(\mathcal{E}_{AB})$ for any channel \mathcal{E}_{AB} , as detailed in the main text.

For subsystem A , we choose an orthonormal basis of operators $X_\mu = (X_0 = \frac{1}{\sqrt{d_A}} \mathbb{1}_A, X_i)$, where d_A is dimension of the subsystem A , and $\text{tr}[X_\mu^\dagger X_\nu] = \delta_{\mu\nu}$. Similarly for B an orthonormal basis $Y_\mu = (Y_0 = \frac{1}{\sqrt{d_B}} \mathbb{1}_B, Y_i)$. Together these provide a basis for the full system which is given in the Liouville representation as

$$|\mathbf{X}_\nu \otimes \mathbf{Y}_\mu\rangle := |\mathbf{X}_\nu\rangle \otimes |\mathbf{Y}_\mu\rangle. \quad (\text{B.1})$$

For simplicity, where there is no ambiguity on the local labels μ and ν we will sometimes use a single-label notation $|\mathbf{Z}_\omega\rangle = |\mathbf{X}_\nu \otimes \mathbf{Y}_\mu\rangle$. In particular, we denote $|\mathbf{Z}_0\rangle = |\mathbf{X}_0\rangle \otimes |\mathbf{Y}_0\rangle$.

B.2 General definition of separability

Consider a quantum channel $\mathcal{E}_{AB \rightarrow A'B'} : \mathcal{B}(\mathcal{H}_A \otimes \mathcal{H}_B) \rightarrow \mathcal{B}(\mathcal{H}_{A'} \otimes \mathcal{H}_{B'})$. We define a *product channel* as one that takes the form

$$\mathcal{E}_{AB \rightarrow A'B'} = \mathcal{E}_{A \rightarrow A'} \otimes \mathcal{E}_{B \rightarrow B'}, \quad (\text{B.2})$$

for channels $\mathcal{E}_{A \rightarrow A'} : \mathcal{B}(\mathcal{H}_A) \rightarrow \mathcal{B}(\mathcal{H}_{A'})$ and $\mathcal{E}_{B \rightarrow B'} : \mathcal{B}(\mathcal{H}_B) \rightarrow \mathcal{B}(\mathcal{H}_{B'})$. The choice of labeling of the output subsystems is for convenience, as a joint channel of the form $\mathcal{E}_{A \rightarrow B'} \otimes \mathcal{E}_{B \rightarrow A'}$ can be cast in the above form simply by relabeling $A' \leftrightarrow B'$. A *separable channel* is defined as a convex combination of product channels, namely

$$\mathcal{E}_{AB \rightarrow A'B'} = \sum_k p_k \mathcal{E}_{A \rightarrow A'}^k \otimes \mathcal{E}_{B \rightarrow B'}^k, \quad (\text{B.3})$$

for some distribution p_k and local channels between (A, A') and (B, B') . A channel that is not separable is defined to be *non-separable*.

B.3 Properties of the subunitarities of product channels

Lemma B.1. *The subunitarity $u_{A \rightarrow AB}(\mathcal{E}_A \otimes \mathcal{E}_B)$ for a bipartite product channel $\mathcal{E}_A \otimes \mathcal{E}_B$, decomposes as*

$$u_{A \rightarrow AB}(\mathcal{E}_A \otimes \mathcal{E}_B) = u_{A \rightarrow A}(\mathcal{E}_A \otimes \mathcal{E}_B)x_B, \quad (\text{B.4})$$

where $x_B := \mathbf{x}_{B \rightarrow B}^\dagger \mathbf{x}_{B \rightarrow B}$ for the non-unital vector of the subsystem B of the channel \mathcal{E}_B .

Proof. From the definition of $u_{A \rightarrow AB}$ we have

$$\begin{aligned} u_{A \rightarrow AB}(\mathcal{E}_A \otimes \mathcal{E}_B) &= \alpha_A \sum_{k,j,n=1}^{(d_A^2-1)(d_B^2-1)} \langle \mathbf{X}_j \otimes \mathbf{Y}_n | \mathcal{E} | \mathbf{X}_k \otimes \mathbf{Y}_0 \rangle \langle \mathbf{X}_k \otimes \mathbf{Y}_0 | \mathcal{E}^\dagger | \mathbf{X}_j \otimes \mathbf{Y}_n \rangle, \\ &= \alpha_A \sum_{k,j,n=1}^{(d_A^2-1)(d_B^2-1)} \langle \mathbf{X}_k | \mathcal{E}_A^\dagger | \mathbf{X}_j \rangle \langle \mathbf{X}_j | \mathcal{E}_A | \mathbf{X}_k \rangle \langle \mathbf{Y}_0 | \mathcal{E}_B^\dagger | \mathbf{Y}_n \rangle \langle \mathbf{Y}_n | \mathcal{E}_B | \mathbf{Y}_0 \rangle, \\ &= u_{A \rightarrow A}(\mathcal{E}_A \otimes \mathcal{E}_B) \sum_{n=1}^{d_B^2-1} \langle \mathbf{Y}_0 | \mathcal{E}_B^\dagger | \mathbf{Y}_n \rangle \langle \mathbf{Y}_n | \mathcal{E}_B | \mathbf{Y}_0 \rangle, \\ &= u_{A \rightarrow A}(\mathcal{E}_A \otimes \mathcal{E}_B)x_B \end{aligned} \quad (\text{B.5})$$

which completes the proof. \square

Swapping the subsystem labels we also have $u_{B \rightarrow AB}(\mathcal{E}_A \otimes \mathcal{E}_B) = u_{B \rightarrow B}(\mathcal{E}_A \otimes \mathcal{E}_B)x_A$, where $x_A := \mathbf{x}_{A \rightarrow A}^\dagger \mathbf{x}_{A \rightarrow A}$ for the non-unital vector of the subsystem A of the channel.

B.4 Properties of the subunitarities of separable channels

Lemma B.2. *The subunitarity $u_{AB \rightarrow A}(\mathcal{E})$ for a bipartite separable channel $\mathcal{E} := \sum_i^r p_i \mathcal{E}_{A,i} \otimes \mathcal{E}_{B,i}$ is zero.*

Proof. From the definition of $u_{AB \rightarrow A}$ we have

$$\begin{aligned}
u_{AB \rightarrow A}(\mathcal{E}) &= \alpha_A \alpha_B \operatorname{tr} \left[T_{AB \rightarrow A}^\dagger T_{AB \rightarrow A} \right], \\
&= \alpha_A \alpha_B \sum_{k,j,n=1}^{(d_A^2-1)(d_B^2-1)} \langle \mathbf{X}_j \otimes \mathbf{Y}_n | \mathcal{E}^\dagger | \mathbf{X}_k \otimes \mathbf{Y}_0 \rangle \langle \mathbf{X}_k \otimes \mathbf{Y}_0 | \mathcal{E} | \mathbf{X}_j \otimes \mathbf{Y}_n \rangle, \\
&= \alpha_A \alpha_B \sum_{k,j,n=1}^{(d_A^2-1)(d_B^2-1)} \sum_{i,j}^r p_i p_j \langle \mathbf{X}_j | \mathcal{E}_{A,i}^\dagger | \mathbf{X}_k \rangle \langle \mathbf{X}_k | \mathcal{E}_{A,j} | \mathbf{X}_j \rangle \\
&\quad \langle \mathbf{Y}_n | \mathcal{E}_{B,i}^\dagger | \mathbf{Y}_0 \rangle \langle \mathbf{Y}_0 | \mathcal{E}_{B,j} | \mathbf{Y}_n \rangle.
\end{aligned} \tag{B.6}$$

For the channel to be trace preserving we must have $\langle \mathbf{Y}_0 | \mathcal{E}_{B,j} | \mathbf{Y}_n \rangle = 0$ for all n & j . Therefore $u_{AB \rightarrow A}(\mathcal{E}) = 0$. \square

Additionally, swapping the subsystem labels, $u_{AB \rightarrow B}(\mathcal{E}) = 0$ for any separable bipartite channel \mathcal{E} .

Lemma B.3. *The subunitarity $u_{A \rightarrow B}(\mathcal{E})$ for a bipartite separable channel $\mathcal{E} := \sum_i^r p_i \mathcal{E}_{A,i} \otimes \mathcal{E}_{B,i}$ is zero.*

Proof. From definition

$$\begin{aligned}
u_{A \rightarrow B}(\mathcal{E}) &= \alpha_A \operatorname{tr} \left[T_{A \rightarrow B}^\dagger T_{A \rightarrow B} \right], \\
&= \alpha_A \sum_{k,j=1}^{(d_A^2-1)(d_B^2-1)} \langle \mathbf{X}_j \otimes \mathbf{Y}_0 | \mathcal{E}^\dagger | \mathbf{X}_0 \otimes \mathbf{Y}_k \rangle \langle \mathbf{X}_0 \otimes \mathbf{Y}_k | \mathcal{E} | \mathbf{X}_j \otimes \mathbf{Y}_0 \rangle, \\
&= \alpha_A \sum_{k,j=1}^{(d_A^2-1)(d_B^2-1)} \sum_{i,j}^r p_i p_j \langle \mathbf{X}_j | \mathcal{E}_{A,i}^\dagger | \mathbf{X}_0 \rangle \langle \mathbf{X}_0 | \mathcal{E}_{A,j} | \mathbf{X}_j \rangle \\
&\quad \langle \mathbf{Y}_0 | \mathcal{E}_{B,i}^\dagger | \mathbf{Y}_k \rangle \langle \mathbf{Y}_k | \mathcal{E}_{B,j} | \mathbf{Y}_0 \rangle.
\end{aligned} \tag{B.7}$$

For the channel to be trace preserving we must have $\langle \mathbf{X}_0 | \mathcal{E}_{A,j} | \mathbf{X}_j \rangle = 0$ for all j . Therefore $u_{A \rightarrow B}(\mathcal{E}) = 0$. \square

Additionally, swapping the subsystem labels, $u_{B \rightarrow A}(\mathcal{E}) = 0$ for any separable bipartite channel \mathcal{E} .

Lemma B.4. *For a unital bipartite separable channel $\mathcal{E} := \sum_i^r p_i \mathcal{E}_{A,i} \otimes \mathcal{E}_{B,i}$ where $\mathcal{E}_{X,i}$ are local unital channels, the subunitarity $u_{A \rightarrow AB}(\mathcal{E})$ is zero.*

Proof. From the definition of $u_{A \rightarrow AB}$ we have

$$\begin{aligned}
u_{A \rightarrow AB}(\mathcal{E}) &= \alpha_A \operatorname{tr} \left[T_{A \rightarrow AB}^\dagger T_{A \rightarrow AB} \right], \\
&= \alpha_A \sum_{k,j,n=1}^{(d_A^2-1)(d_B^2-1)} \langle \mathbf{X}_k \otimes \mathbf{Y}_0 | \mathcal{E}^\dagger | \mathbf{X}_j \otimes \mathbf{Y}_n \rangle \langle \mathbf{X}_j \otimes \mathbf{Y}_n | \mathcal{E} | \mathbf{X}_k \otimes \mathbf{Y}_0 \rangle, \\
&= \alpha_A \sum_{k,j,n=1}^{(d_A^2-1)(d_B^2-1)} \sum_{i,j}^r p_i p_j \langle \mathbf{X}_k | \mathcal{E}_{A,j}^\dagger | \mathbf{X}_j \rangle \langle \mathbf{X}_j | \mathcal{E}_{A,i} | \mathbf{X}_k \rangle \\
&\quad \langle \mathbf{Y}_0 | \mathcal{E}_{B,j}^\dagger | \mathbf{Y}_n \rangle \langle \mathbf{Y}_n | \mathcal{E}_{B,i} | \mathbf{Y}_0 \rangle.
\end{aligned} \tag{B.8}$$

For the channel to be unital we must have $\langle \mathbf{Y}_n | \mathcal{E}_{B,i} | \mathbf{Y}_0 \rangle = 0$ for all n . Therefore $u_{A \rightarrow AB}(\mathcal{E}) = 0$. \square

Additionally, swapping the subsystem labels, $u_{B \rightarrow AB}(\mathcal{E}) = 0$ for any unital separable bipartite channel \mathcal{E} .

B.5 Comparison of correlation unitarity with norm measures

We can compare the choice of definition for correlation unitarity with a norm, which sheds light on its structure and limitations. Consider the Hilbert-Schmidt norm (e.g. Schatten 2-norm or Frobenius norm) given by $\|M\| := \sqrt{\langle M, M \rangle} = \sqrt{\operatorname{tr}[M^\dagger M]}$ for a matrix M [122], which is the square root of the Hilbert-Schmidt inner product of the matrix with itself. We have the following expression

$$\Delta^2 := \|T_{AB} - T_A \otimes T_B\|^2 \tag{B.9}$$

where for the unital block we write $T_{AB} \equiv T_{AB \rightarrow AB}$ and similarly for T_A and T_B . As this is a norm we have $\Delta = 0$ if and only if $T_{AB} = T_A \otimes T_B$, namely if and only if the channel is a product channel. We can expand this expression in terms of the inner product to obtain

$$\begin{aligned}
\Delta^2 &= \langle T_{AB} - T_A \otimes T_B, T_{AB} - T_A \otimes T_B \rangle \\
&= \langle T_{AB}, T_{AB} \rangle + \langle T_A \otimes T_B, T_A \otimes T_B \rangle - \langle T_{AB}, T_A \otimes T_B \rangle - \langle T_A \otimes T_B, T_{AB} \rangle \\
&= \|T_{AB}\|^2 + \|T_A\|^2 \|T_B\|^2 - 2 \operatorname{Re} [\langle T_{AB}, T_A \otimes T_B \rangle] \\
&= \|T_{AB}\|^2 + \|T_A\|^2 \|T_B\|^2 - 2 \|T_{AB}\| \|T_A\| \|T_B\| \cos \theta \\
\Delta^2 &= t_{AB}^2 + t_A^2 t_B^2 - 2 t_{AB} t_A t_B \cos \theta,
\end{aligned}$$

where we have defined an angular variable θ via the inner product between T_{AB} and $T_A \otimes T_B$ and replaced the norm values with t_{AB}, t_A, t_B in the obvious way. Now the correlation unitarity is given by $u_c = \alpha_{AB} (t_{AB}^2 - t_A^2 t_B^2)$, with the dimensional prefactor $\alpha_{AB} = \frac{1}{(d_A^2-1)(d_B^2-1)}$. Substituting for t_{AB} into Δ^2 we have that

$$\Delta^2 = \frac{u_c}{\alpha_{AB}} + 2(t_A t_B)^2 - 2 \sqrt{\frac{u_c}{\alpha_{AB}} + (t_A t_B)^2} (t_A t_B) \cos \theta. \tag{B.10}$$

This implies a few things. Firstly, for $u_c = 0$ we have

$$\Delta^2 = 2(t_A t_B)^2(1 - \cos \theta), \quad (\text{B.11})$$

and so we see that u_c vanishing does not imply a product channel unless one of the t_A, t_B vanishes or if $\theta = 0$. The expression also implies that θ is an independent parameter that will in general vary the norm distance. Note that the benchmarking protocol gives us both $(t_A t_B)$ and u_c but does not give us θ . Therefore our existing benchmarking does not return enough to determine the norm distance measure.

The above highlights relevant data at quadratic order that our approach is not sensitive to, but note that the $\cos \theta$ term is bounded and so it still is the case that u_c is acting as a “distance” from being a product channel. Specifically, we have

$$\frac{u_c}{\alpha_{AB}} + 2(t_A t_B)^2 - 2\sqrt{\frac{u_c}{\alpha_{AB}} + (t_A t_B)^2(t_A t_B)} \leq \Delta^2 \quad (\text{B.12})$$

and

$$\Delta^2 \leq \frac{u_c}{\alpha_{AB}} + 2(t_A t_B)^2 + 2\sqrt{\frac{u_c}{\alpha_{AB}} + (t_A t_B)^2(t_A t_B)}. \quad (\text{B.13})$$

This implies that estimating u_c and $t_A t_B$ allows us to estimate the norm distance Δ .

B.6 Expression for correlation unitarity using an operational function

Finally, in this section we give the proof that the correlation unitarity of a channel can be expressed using an operational function, $F_{P_i, P_j}(\mathcal{E}, \psi_{m,n})$ given in Section 3.3.3. This was defined in the following way. For the expectation of an observable O on a state ρ we have $\langle O \rangle_\rho := \text{tr}[O^\dagger \rho]$. Now suppose we have local observables O_A and O_B for the subsystems A and B respectively. For any bipartite quantum channel, \mathcal{E} , we can define the following correlation function

$$F_{O_A, O_B}(\mathcal{E}, \psi_{AB}) := |\langle O_A \otimes O_B \rangle_{\mathcal{E}_{AB}(\psi_{AB})}|^2 - |\langle O_A \rangle_{\mathcal{E}_A(\psi_A)}|^2 |\langle O_B \rangle_{\mathcal{E}_B(\psi_B)}|^2 \quad (\text{B.14})$$

where the channels \mathcal{E}_A and \mathcal{E}_B are local channels on A respectively B defined in Definition 3.1 and the input states ψ_A and ψ_B are the marginals of ψ_{AB} .

We now connect this function with the correlation unitarity of a bipartite channel.

Proof. (Of equation (3.104)) Using the Pauli basis we can show how the correlation unitarity is related to the correlation function given in Section 3.3.3. We define the orthonormal Pauli basis $P_\mu = (P_0 = \mathbb{1}/\sqrt{d_A}, P_i)$ for subsystem A and (with slight abuse of notion) equivalently

for subsystem B . Starting from the correlation unitarity we have

$$\begin{aligned}
u_c(\mathcal{E}_{AB}) &= \alpha_{AB} \left(\text{tr} \left[T_{AB \rightarrow AB}^\dagger T_{AB \rightarrow AB} \right] - \text{tr} \left[T_{A \rightarrow A}^\dagger T_{A \rightarrow A} \right] \text{tr} \left[T_{B \rightarrow B}^\dagger T_{B \rightarrow B} \right] \right) \\
&= \alpha_{AB} \left(\sum_{i,j,m,n \neq 0} |\langle \mathbf{P}_i \otimes \mathbf{P}_j | T_{AB \rightarrow AB} | \mathbf{P}_m \otimes \mathbf{P}_n \rangle|^2 \right. \\
&\quad \left. - |\langle \mathbf{P}_i | T_{A \rightarrow A} | \mathbf{P}_m \rangle|^2 |\langle \mathbf{P}_j | T_{B \rightarrow B} | \mathbf{P}_n \rangle|^2 \right) \\
&= \alpha_{AB} \left(\sum_{i,j,m,n \neq 0} |\text{tr}[P_i \otimes P_j \mathcal{E}_{AB}(P_m \otimes P_n)]|^2 \right. \\
&\quad \left. - |\text{tr}[P_i \mathcal{E}_A(P_m)]|^2 |\text{tr}[P_j \mathcal{E}_B(P_n)]|^2 \right), \tag{B.15} \\
&= \alpha_{AB} d_{AB} \left(\sum_{i,j,m,n \neq 0} |\text{tr}[P_i \otimes P_j \mathcal{E}_{AB}(\psi_{m,n})]|^2 \right. \\
&\quad \left. - |\text{tr}[P_i \mathcal{E}_A(\text{tr}_B[\psi_{m,n}])]|^2 |\text{tr}[P_j \mathcal{E}_B(\text{tr}_B[\psi_{m,n}])]|^2 \right), \\
&= \alpha_{AB} d_{AB} \sum_{i,j,m,n} F_{P_i, P_j}(\mathcal{E}, \psi_{m,n}).
\end{aligned}$$

Which completes the proof. \square

Bibliography

- [1] Farrokh Vatan and Colin Williams. Optimal quantum circuits for general two-qubit gates. *Physical Review A*, 69(3):032315, 2004.
- [2] Wojciech Bruzda, Valerio Cappellini, Hans-Jürgen Sommers, and Karol Życzkowski. Random quantum operations. *Physics Letters A*, 373(3):320–324, 2009.
- [3] J.R. Johansson, P.D. Nation, and Franco Nori. Qutip 2: A python framework for the dynamics of open quantum systems. *Computer Physics Communications*, 184(4): 1234–1240, 2013. ISSN 0010-4655.
- [4] Shelby Kimmel, Marcus P da Silva, Colm A Ryan, Blake R Johnson, and Thomas Ohki. Robust extraction of tomographic information via randomized benchmarking. *Physical Review X*, 4(1):011050, 2014.
- [5] Bas Dirkse, Jonas Helsen, and Stephanie Wehner. Efficient unitarity randomized benchmarking of few-qubit clifford gates. *Physical Review A*, 99(1):012315, 2019.
- [6] Martin Kliesch and Ingo Roth. Theory of quantum system certification. *PRX Quantum*, 2(1):010201, 2021.
- [7] Jonas Helsen, Ingo Roth, Emilio Onorati, Albert H Werner, and Jens Eisert. A general framework for randomized benchmarking. *arXiv preprint arXiv:2010.07974*, 2020.
- [8] Timothy J Proctor, Arnaud Carignan-Dugas, Kenneth Rudinger, Erik Nielsen, Robin Blume-Kohout, and Kevin Young. Direct randomized benchmarking for multiqubit devices. *Physical review letters*, 123(3):030503, 2019.
- [9] John P Gaebler, Adam M Meier, Ting Rei Tan, Ryan Bowler, Yiheng Lin, David Hanneke, John D Jost, JP Home, Emanuel Knill, Dietrich Leibfried, et al. Randomized benchmarking of multiqubit gates. *Physical review letters*, 108(26):260503, 2012.
- [10] Alexander Erhard, Joel J Wallman, Lukas Postler, Michael Meth, Roman Stricker, Esteban A Martinez, Philipp Schindler, Thomas Monz, Joseph Emerson, and Rainer

- Blatt. Characterizing large-scale quantum computers via cycle benchmarking. *Nature communications*, 10(1):1–7, 2019.
- [11] Jens Eisert, Dominik Hangleiter, Nathan Walk, Ingo Roth, Damian Markham, Rhea Parekh, Ulysse Chabaud, and Elham Kashefi. Quantum certification and benchmarking. *Nature Reviews Physics*, 2(7):382–390, 2020.
- [12] Ellen Derbyshire, Rawad Mezher, Theodoros Kapourniotis, and Elham Kashefi. Randomized benchmarking with stabilizer verification and gate synthesis. *arXiv preprint arXiv:2102.13044*, 2021.
- [13] John Preskill. Sufficient condition on noise correlations for scalable quantum computing. *arXiv preprint arXiv:1207.6131*, 2012.
- [14] Naomi H Nickerson and Benjamin J Brown. Analysing correlated noise on the surface code using adaptive decoding algorithms. *Quantum*, 3:131, 2019.
- [15] Joseph K Iverson and John Preskill. Coherence in logical quantum channels. *New Journal of Physics*, 22(7):073066, 2020.
- [16] John Preskill. Quantum computing in the nisq era and beyond. *Quantum*, 2:79, 2018.
- [17] William K Wootters and Wojciech H Zurek. A single quantum cannot be cloned. *Nature*, 299(5886):802–803, 1982.
- [18] Horace P Yuen. Amplification of quantum states and noiseless photon amplifiers. *Physics Letters A*, 113(8):405–407, 1986.
- [19] Howard Barnum, Jonathan Barrett, Matthew Leifer, and Alexander Wilce. Generalized no-broadcasting theorem. *Physical review letters*, 99(24):240501, 2007.
- [20] Howard Barnum, Carlton M Caves, Christopher A Fuchs, Richard Jozsa, and Benjamin Schumacher. Noncommuting mixed states cannot be broadcast. *Physical Review Letters*, 76(15):2818, 1996.
- [21] Dennis Kretschmann, Dirk Schlingemann, and Reinhard F Werner. The information-disturbance tradeoff and the continuity of stinespring’s representation. *IEEE transactions on information theory*, 54(4):1708–1717, 2008.
- [22] Teiko Heinosaari, Takayuki Miyadera, and Mário Ziman. An invitation to quantum incompatibility. *Journal of Physics A: Mathematical and Theoretical*, 49(12):123001, 2016.

- [23] Andreas Bluhm, Anna Jenčová, and Ion Nechita. Incompatibility in general probabilistic theories, generalized spectrahedra, and tensor norms. *Communications in Mathematical Physics*, 393(3):1125–1198, 2022.
- [24] Anna Jenčová. Incompatible measurements in a class of general probabilistic theories. *Physical Review A*, 98(1):012133, 2018.
- [25] Bas Hensen, Hannes Bernien, Anaïs E Dréau, Andreas Reiserer, Norbert Kalb, Machiel S Blok, Just Ruitenberg, Raymond FL Vermeulen, Raymond N Schouten, Carlos Abellán, et al. Loophole-free bell inequality violation using electron spins separated by 1.3 kilometres. *Nature*, 526(7575):682–686, 2015.
- [26] Marissa Giustina, Marijn AM Versteegh, Sören Wengerowsky, Johannes Handsteiner, Armin Hochrainer, Kevin Phelan, Fabian Steinlechner, Johannes Kofler, Jan-Åke Larsson, Carlos Abellán, et al. Significant-loophole-free test of bell’s theorem with entangled photons. *Physical review letters*, 115(25):250401, 2015.
- [27] Lynden K Shalm, Evan Meyer-Scott, Bradley G Christensen, Peter Bierhorst, Michael A Wayne, Martin J Stevens, Thomas Gerrits, Scott Glancy, Deny R Hamel, Michael S Allman, et al. Strong loophole-free test of local realism. *Physical review letters*, 115(25):250402, 2015.
- [28] Jharana Rani Samal, Arun K Pati, and Anil Kumar. Experimental test of the quantum no-hiding theorem. *Physical review letters*, 106(8):080401, 2011.
- [29] Huixia Gao, Lei Xiao, Kunkun Wang, Dengke Qu, Quan Lin, and Peng Xue. Experimental verification of trade-off relation for coherence and disturbance. *New Journal of Physics*, 24(7):073011, 2022.
- [30] Héctor Bombín. Single-shot fault-tolerant quantum error correction. *Physical Review X*, 5(3):031043, 2015.
- [31] Yasunari Suzuki, Suguru Endo, Keisuke Fujii, and Yuuki Tokunaga. Quantum error mitigation as a universal error reduction technique: Applications from the nisq to the fault-tolerant quantum computing eras. *PRX Quantum*, 3(1):010345, 2022.
- [32] Michael A Nielsen and Isaac L Chuang. *Quantum Computation and Quantum Information*. Cambridge University Press, 2010.
- [33] Ibm quantum device calibration data (ibmq belem). https://quantum-computing.ibm.com/services/resources?system=ibmq_belem, 2023. Accessed: 2023/09/20.
- [34] Simanraj Sadana, Lorenzo Maccone, and Urbasi Sinha. Testing quantum foundations with quantum computers. *Physical Review Research*, 4(2):L022001, 2022.

- [35] G. M. D'Ariano and P. Lo Presti. Quantum tomography for measuring experimentally the matrix elements of an arbitrary quantum operation. *Physical review letters*, 86(19): 4195, 2001.
- [36] Daniel Greenbaum. Introduction to quantum gate set tomography. *arXiv preprint arXiv:1509.02921*, 2015.
- [37] Martin Kliesch and Ingo Roth. Theory of quantum system certification. *PRX Quantum*, 2(1):010201, 2021.
- [38] John Watrous. *The theory of quantum information*. Cambridge University Press, 2018.
- [39] John Preskill. Lecture notes for physics 229: Quantum information and computation. <http://theory.caltech.edu/~preskill/ph229/>, 1998. Accessed: 2023/09/20.
- [40] David Jennings. Lecture notes for advanced quantum information. Unpublished, 2022.
- [41] Jeongwan Haah, Robin Kothari, Ryan O'Donnell, and Ewin Tang. Query-optimal estimation of unitary channels in diamond distance. *arXiv preprint arXiv:2302.14066*, 2023.
- [42] Aleksei Yur'evich Kitaev. Quantum computations: algorithms and error correction. *Uspekhi Matematicheskikh Nauk*, 52(6):53–112, 1997.
- [43] Richard Kueng, David M Long, Andrew C Doherty, and Steven T Flammia. Comparing experiments to the fault-tolerance threshold. *Physical review letters*, 117(17): 170502, 2016.
- [44] Joel J Wallman. Randomized benchmarking with gate-dependent noise. *Quantum*, 2: 47, 2018.
- [45] Timothy Proctor, Kenneth Rudinger, Kevin Young, Mohan Sarovar, and Robin Blume-Kohout. What randomized benchmarking actually measures. *Physical review letters*, 119(13):130502, 2017.
- [46] Mark M Wilde. *Quantum information theory*. Cambridge University Press, 2013.
- [47] Ingemar Bengtsson and Karol Życzkowski. *Geometry of quantum states: an introduction to quantum entanglement*. Cambridge university press, 2017.
- [48] Arnaud Carignan-Dugas, Joel J Wallman, and Joseph Emerson. Bounding the average gate fidelity of composite channels using the unitarity. *New Journal of Physics*, 21(5): 053016, 2019.

- [49] Joel J Wallman and Steven T Flammia. Randomized benchmarking with confidence. *New Journal of Physics*, 16(10):103032, 2014.
- [50] Dorit Aharonov and Michael Ben-Or. Fault-tolerant quantum computation with constant error rate. *SIAM Journal on Computing*, 2008.
- [51] Robin Harper and Steven T Flammia. Fault-tolerant logical gates in the ibm quantum experience. *Physical review letters*, 122(8):080504, 2019.
- [52] Yoshifumi Nakata, Da Zhao, Takayuki Okuda, Eiichi Bannai, Yasunari Suzuki, Shiro Tamiya, Kentaro Heya, Zhiguang Yan, Kun Zuo, Shuhei Tamate, Yutaka Tabuchi, and Yasunobu Nakamura. Quantum circuits for exact unitary t -designs and applications to higher-order randomized benchmarking, 2021.
- [53] Jonas Helsen, Xiao Xue, Lieven MK Vandersypen, and Stephanie Wehner. A new class of efficient randomized benchmarking protocols. *npj Quantum Information*, 5(1):1–9, 2019.
- [54] Joshua Combes, Christopher Granade, Christopher Ferrie, and Steven T Flammia. Logical randomized benchmarking. *arXiv preprint arXiv:1702.03688*, 2017.
- [55] Ellen Derbyshire, J Yago Malo, AJ Daley, Elham Kashefi, and Petros Wallden. Randomized benchmarking in the analogue setting. *Quantum Science and Technology*, 5(3):034001, 2020.
- [56] Jay M Gambetta, AD Córcoles, Seth T Merkel, Blake R Johnson, John A Smolin, Jerry M Chow, Colm A Ryan, Chad Rigetti, S Poletto, Thomas A Ohki, et al. Characterization of addressability by simultaneous randomized benchmarking. *Physical review letters*, 109(24):240504, 2012.
- [57] Joel Wallman, Chris Granade, Robin Harper, and Steven T Flammia. Estimating the coherence of noise. *New Journal of Physics*, 17(11):113020, 2015.
- [58] Ryszard Kukulski, Ion Nechita, Łukasz Paweł, Zbigniew Puchała, and Karol Życzkowski. Generating random quantum channels. *arXiv preprint arXiv:2011.02994*, 2020.
- [59] Neereja Sundaresan, Isaac Lauer, Emily Pritchett, Easwar Magesan, Petar Jurcevic, and Jay M Gambetta. Reducing unitary and spectator errors in cross resonance with optimized rotary echoes. *PRX Quantum*, 1(2):020318, 2020.
- [60] Kamil Korzekwa, Stanisław Czachórski, Zbigniew Puchała, and Karol Życzkowski. Coherifying quantum channels. *New Journal of Physics*, 20(4):043028, 2018.

- [61] Cristina Cîrstoiu, Kamil Korzekwa, and David Jennings. Robustness of noether's principle: Maximal disconnects between conservation laws and symmetries in quantum theory. *Physical Review X*, 10(4):041035, 2020.
- [62] Joel J Wallman. Bounding experimental quantum error rates relative to fault-tolerant thresholds. *arXiv preprint arXiv:1511.00727*, 2015.
- [63] Claudio Carmeli, Teiko Heinosaari, Takayuki Miyadera, and Alessandro Toigo. Witnessing incompatibility of quantum channels. *Journal of Mathematical Physics*, 60(12):122202, 2019.
- [64] Claudio Carmeli, Teiko Heinosaari, and Alessandro Toigo. Quantum incompatibility witnesses. *Physical review letters*, 122(13):130402, 2019.
- [65] Mark Girard, Martin Plávala, and Jamie Sikora. Jordan products of quantum channels and their compatibility. *Nature communications*, 12(1):1–6, 2021.
- [66] Qing-Hua Zhang and Ion Nechita. A fisher information-based incompatibility criterion for quantum channels. *Entropy*, 24(6):805, 2022.
- [67] Dennis Kretschmann, Dirk Schlingemann, and Reinhard F Werner. A continuity theorem for stinespring's dilation. *Journal of Functional Analysis*, 255(8):1889–1904, 2008.
- [68] Erkkka Haapasalo. Robustness of incompatibility for quantum devices. *Journal of Physics A: Mathematical and Theoretical*, 48(25):255303, 2015.
- [69] Sébastien Designolle, Máté Farkas, and Jędrzej Kaniewski. Incompatibility robustness of quantum measurements: a unified framework. *New Journal of Physics*, 21(11):113053, 2019.
- [70] Samuel L Braunstein and Arun K Pati. Quantum information cannot be completely hidden in correlations: implications for the black-hole information paradox. *Physical review letters*, 98(8):080502, 2007.
- [71] Steven B Giddings. The black hole information paradox. *arXiv preprint hep-th/9508151*, 1995.
- [72] Juan Maldacena. Black holes and quantum information. *Nature Reviews Physics*, 2(3):123–125, 2020.
- [73] Kavan Modi, Arun Kumar Pati, Aditi Sen, Ujjwal Sen, et al. Masking quantum information is impossible. *Physical review letters*, 120(23):230501, 2018.

- [74] Huangjun Zhu. Hiding and masking quantum information in complex and real quantum mechanics. *Physical Review Research*, 3(3):033176, 2021.
- [75] Arun Kumar Pati and Samuel L Braunstein. Impossibility of deleting an unknown quantum state. *Nature*, 404(6774):164–165, 2000.
- [76] Amolak Ratan Kalra, Navya Gupta, Bikash K Behera, Shiroman Prakash, and Prasanta K Panigrahi. Demonstration of the no-hiding theorem on the 5-qubit ibm quantum computer in a category-theoretic framework. *Quantum Information Processing*, 18:1–13, 2019.
- [77] Giulio Chiribella and Robert W Spekkens. *Quantum theory: informational foundations and foils*. Springer, 2016.
- [78] Martin Plávala. General probabilistic theories: An introduction. *arXiv preprint arXiv:2103.07469*, 2021.
- [79] Howard Barnum, Jonathan Barrett, Matthew Leifer, and Alexander Wilce. Cloning and broadcasting in generic probabilistic theories. *arXiv preprint quant-ph/0611295*, 2006.
- [80] Michał Horodecki, Paweł Horodecki, and Ryszard Horodecki. General teleportation channel, singlet fraction, and quasidistillation. *Physical Review A*, 60(3):1888, 1999.
- [81] Emanuel Knill, Dietrich Leibfried, Rolf Reichle, Joe Britton, R Brad Blakestad, John D Jost, Chris Langer, Roee Ozeri, Signe Seidelin, and David J Wineland. Randomized benchmarking of quantum gates. *Physical Review A*, 77(1):012307, 2008.
- [82] Easwar Magesan, Jay M. Gambetta, B. R. Johnson, Colm A. Ryan, Jerry M. Chow, Seth T. Merkel, Marcus P. da Silva, George A. Keefe, Mary B. Rothwell, Thomas A. Ohki, Mark B. Ketchen, and M. Steffen. Efficient measurement of quantum gate error by interleaved randomized benchmarking. *Physical review letters*, 109(8):080505, 2012.
- [83] Jonas Helsen, Francesco Battistel, and Barbara M Terhal. Spectral quantum tomography. *npj Quantum Information*, 5(1):1–11, 2019.
- [84] Harry Buhrman, Richard Cleve, John Watrous, and Ronald De Wolf. Quantum fingerprinting. *Physical Review Letters*, 87(16):167902, 2001.
- [85] Gus Gutoski. Properties of local quantum operations with shared entanglement. *arXiv preprint arXiv:0805.2209*, 2008.

- [86] Julio I De Vicente. On nonlocality as a resource theory and nonlocality measures. *Journal of Physics A: Mathematical and Theoretical*, 47(42):424017, 2014.
- [87] Joshua Geller and Marco Piani. Quantifying non-classical and beyond-quantum correlations in the unified operator formalism. *Journal of Physics A: Mathematical and Theoretical*, 47(42):424030, 2014.
- [88] Rodrigo Gallego and Leandro Aolita. Nonlocality free wirings and the distinguishability between bell boxes. *Physical Review A*, 95(3):032118, 2017.
- [89] Denis Rosset, David Schmid, and Francesco Buscemi. Characterizing nonclassicality of arbitrary distributed devices. *arXiv preprint arXiv:1911.12462*, 2019.
- [90] David Schmid, Denis Rosset, and Francesco Buscemi. The type-independent resource theory of local operations and shared randomness. *Quantum*, 4:262, 2020.
- [91] David Schmid, Thomas C Fraser, Ravi Kunjwal, Ana Belen Sainz, Elie Wolfe, and Robert W Spekkens. Why standard entanglement theory is inappropriate for the study of bell scenarios. *arXiv preprint arXiv:2004.09194*, 2020.
- [92] Elie Wolfe, David Schmid, Ana Belén Sainz, Ravi Kunjwal, and Robert W Spekkens. Quantifying bell: The resource theory of nonclassicality of common-cause boxes. *Quantum*, 4:280, 2020.
- [93] Chung-Yun Hsieh, Matteo Lostaglio, and Antonio Acín. Entanglement preserving local thermalization. *Physical Review Research*, 2(1):013379, 2020.
- [94] Gus Gutoski. Properties of local quantum operations with shared entanglement, 2009.
- [95] Gilad Gour and Carlo Maria Scandolo. Dynamical entanglement. *Physical Review Letters*, 125(18):180505, 2020.
- [96] Stefan Bäuml, Siddhartha Das, Xin Wang, and Mark M Wilde. Resource theory of entanglement for bipartite quantum channels. *arXiv preprint arXiv:1907.04181*, 2019.
- [97] David Poulin, Angie Qarry, Rolando Somma, and Frank Verstraete. Quantum simulation of time-dependent hamiltonians and the convenient illusion of hilbert space. *Physical review letters*, 106(17):170501, 2011.
- [98] Jens Eisert. Entanglement and tensor network states. *Modeling and Simulation* 3, 520, 2013.
- [99] Alexandre Dumas. *The Count of Monte Cristo*. Wordsworth Classics, 1997.

- [100] Martin Müller-Lennert, Frédéric Dupuis, Oleg Szehr, Serge Fehr, and Marco Tomamichel. On quantum rényi entropies: A new generalization and some properties. *Journal of Mathematical Physics*, 54(12):122203, 2013.
- [101] Ashwin Nayak and Pranab Sen. Invertible quantum operations and perfect encryption of quantum states. *arXiv preprint quant-ph/0605041*, 2006.
- [102] Chris Heunen and Robin Kaarsgaard. Bennett and stinespring, together at last. *arXiv preprint arXiv:2102.08711*, 2021.
- [103] Charles H Bennett. Logical reversibility of computation. *IBM journal of Research and Development*, 17(6):525–532, 1973.
- [104] Scott Aaronson, Daniel Grier, and Luke Schaeffer. The classification of reversible bit operations. *arXiv preprint arXiv:1504.05155*, 2015.
- [105] Holger Bock Axelsen and Robert Glück. What do reversible programs compute? In *International Conference on Foundations of Software Science and Computational Structures*, pages 42–56. Springer, 2011.
- [106] Claude E Shannon. Communication theory of secrecy systems. *The Bell system technical journal*, 28(4):656–715, 1949.
- [107] Joel J Wallman and Joseph Emerson. Noise tailoring for scalable quantum computation via randomized compiling. *Physical Review A*, 94(5):052325, 2016.
- [108] Margarita A Man’ko and Vladimir I Man’ko. Deformed subadditivity condition for qudit states and hybrid positive maps. *Journal of Russian Laser Research*, 35(5):509–517, 2014.
- [109] Alexander S Holevo. Complementary channels and the additivity problem. *Theory of Probability & Its Applications*, 51(1):92–100, 2007.
- [110] Michele Mosca, Alain Tapp, and Ronald de Wolf. Private quantum channels and the cost of randomizing quantum information. *arXiv preprint quant-ph/0003101*, 2000.
- [111] Kirill Dubovitskii and Yuriy Makhlin. Partial randomized benchmarking. *Scientific Reports*, 12(1):1–10, 2022.
- [112] Giulio Chiribella, Giacomo Mauro D’Ariano, and Paolo Perinotti. Probabilistic theories with purification. *Physical Review A*, 81(6):062348, 2010.
- [113] Teiko Heinosaari and Takayuki Miyadera. Incompatibility of quantum channels. *Journal of Physics A: Mathematical and Theoretical*, 50(13):135302, 2017.

- [114] Peter Janotta and Hye Hinrichsen. Generalized probability theories: what determines the structure of quantum theory? *Journal of Physics A: Mathematical and Theoretical*, 47(32):323001, 2014.
- [115] Jonathan Barrett. Information processing in generalized probabilistic theories. *Physical Review A*, 75(3):032304, 2007.
- [116] Lucien Hardy. Quantum theory from five reasonable axioms. *arXiv preprint quant-ph/0101012*, 2001.
- [117] Scott Aaronson. *Quantum computing since Democritus*. Cambridge University Press, 2013.
- [118] Chung-Yun Hsieh, Matteo Lostaglio, and Antonio Acín. Quantum channel marginal problem, 2021.
- [119] Horace P Yuen. Amplification of quantum states and noiseless photon amplifiers. *Physics Letters A*, 113(8):405–407, 1986.
- [120] Howard Barnum, Jonathan Barrett, Matthew Leifer, and Alexander Wilce. Generalized no-broadcasting theorem. *Physical review letters*, 99(24):240501, 2007.
- [121] Christopher J Wood, Jacob D Biamonte, and David G Cory. Tensor networks and graphical calculus for open quantum systems. *arXiv preprint arXiv:1111.6950*, 2011.
- [122] Roger A Horn and Charles R Johnson. *Matrix analysis*. Cambridge university press, second edition, 2012.
- [123] Yurii D Burago and Viktor A Zalgaller. *Geometric inequalities*, volume 285. Springer Science & Business Media, 2013.
- [124] Michael M Wolf. Quantum channels and operations-guided tour. <https://mediatum.ub.tum.de/doc/1701036/document.pdf/>, 2012. Accessed: 2023/09/20.
- [125] Mark S Byrd and Navin Khaneja. Characterization of the positivity of the density matrix in terms of the coherence vector representation. *Physical Review A*, 68(6):062322, 2003.
- [126] Pranaw Rungta, Vladimir Bužek, Carlton M Caves, Mark Hillery, and Gerard J Milburn. Universal state inversion and concurrence in arbitrary dimensions. *Physical Review A*, 64(4):042315, 2001.
- [127] Ryszard Horodecki et al. Information-theoretic aspects of inseparability of mixed states. *Physical Review A*, 54(3):1838, 1996.

- [128] Emanuel Knill. Non-binary unitary error bases and quantum codes. *arXiv preprint quant-ph/9608048*, 1996.
- [129] Bob Dylan. *Blood on the tracks*. Columbia Records, 1975.
- [130] Seth T Merkel, Emily J Pritchett, and Bryan H Fong. Randomized benchmarking as convolution: Fourier analysis of gate dependent errors. *arXiv preprint arXiv:1804.05951*, 2018.
- [131] William Timothy Gowers and Omid Hatami. Inverse and stability theorems for approximate representations of finite groups. *Sbornik: Mathematics*, 208(12):1784, 2017.
- [132] Daniel Stilck França and AK Hashagen. Approximate randomized benchmarking for finite groups. *Journal of Physics A: Mathematical and Theoretical*, 51(39):395302, 2018.
- [133] Huangjun Zhu. Multiqubit clifford groups are unitary 3-designs. *Physical Review A*, 96(6):062336, 2017.
- [134] Daniel A Roberts and Beni Yoshida. Chaos and complexity by design. *Journal of High Energy Physics*, 2017(4):1–64, 2017.
- [135] Senrui Chen, Wenjun Yu, Pei Zeng, and Steven T Flammia. Robust shadow estimation. *PRX Quantum*, 2(3):030348, 2021.
- [136] Kristine Boone. *Concepts and methods for benchmarking quantum computers*. University of Waterloo, 2021.
- [137] Akel Hashim, Ravi K Naik, Alexis Morvan, Jean-Loup Ville, Bradley Mitchell, John Mark Kreikebaum, Marc Davis, Ethan Smith, Costin Iancu, Kevin P O’Brien, et al. Randomized compiling for scalable quantum computing on a noisy superconducting quantum processor. *arXiv preprint arXiv:2010.00215*, 2020.
- [138] Juan M Pino, Jennifer M Dreiling, Caroline Figgatt, John P Gaebler, Steven A Moses, MS Allman, CH Baldwin, M Foss-Feig, D Hayes, K Mayer, et al. Demonstration of the qccd trapped-ion quantum computer architecture. *arXiv preprint arXiv:2003.01293*, 2020.
- [139] Antonio D Corcoles, Maika Takita, Ken Inoue, Scott Lekuch, Zlatko K Mineev, Jerry M Chow, and Jay M Gambetta. Exploiting dynamic quantum circuits in a quantum algorithm with superconducting qubits. *arXiv preprint arXiv:2102.01682*, 2021.
- [140] Seyon Sivarajah, Silas Dilkes, Alexander Cowtan, Will Simmons, Alec Edgington, and Ross Duncan. Tket: a retargetable compiler for nisq devices. *Quantum Science and Technology*, 6(1):014003, 2020.

- [141] Qiskit: An open-source framework for quantum computing, 2019.
- [142] Mohan Sarovar, Timothy Proctor, Kenneth Rudinger, Kevin Young, Erik Nielsen, and Robin Blume-Kohout. Detecting crosstalk errors in quantum information processors. *Quantum*, 4:321, 2020.
- [143] David C McKay, Andrew W Cross, Christopher J Wood, and Jay M Gambetta. Correlated randomized benchmarking. *arXiv preprint arXiv:2003.02354*, 2020.
- [144] Adam Winick, Joel J Wallman, and Joseph Emerson. Simulating and mitigating crosstalk. *arXiv preprint arXiv:2006.09596*, 2020.
- [145] King James Version. *The Holy Bible*. Cambridge Edition, 1769.
- [146] Michael M Wolf and David Perez-Garcia. The inverse eigenvalue problem for quantum channels. *arXiv preprint arXiv:1005.4545*, 2010.
- [147] Matthew Girling, Cristina Cîrstoiu, and David Jennings. Estimation of correlations and nonseparability in quantum channels via unitarity benchmarking. *Physical Review Research*, 4(2):023041, 2022.
- [148] Rajendra Bhatia. *Matrix analysis*, volume 169. Springer Science & Business Media, 2013.
- [149] Andreas Elben, Steven T Flammia, Hsin-Yuan Huang, Richard Kueng, John Preskill, Benoît Vermersch, and Peter Zoller. The randomized measurement toolbox. *Nature Reviews Physics*, pages 1–16, 2022.
- [150] Bob Dylan. *Bringing It All Back Home*. Columbia Records, 1965.
- [151] Robin Harper, Ian Hincks, Chris Ferrie, Steven T Flammia, and Joel J Wallman. Statistical analysis of randomized benchmarking. *Physical Review A*, 99(5):052350, 2019.
- [152] X Xue, TF Watson, J Helsen, Daniel R Ward, Donald E Savage, Max G Lagally, Susan N Coppersmith, MA Eriksson, S Wehner, and LMK Vandersypen. Benchmarking gate fidelities in a si/sige two-qubit device. *Physical Review X*, 9(2):021011, 2019.
- [153] Harrison Ball, Thomas M Stace, Steven T Flammia, and Michael J Biercuk. Effect of noise correlations on randomized benchmarking. *Physical Review A*, 93(2):022303, 2016.
- [154] Jiaan Qi and Hui Khoon Ng. Randomized benchmarking in the presence of time-correlated dephasing noise. *Physical Review A*, 103(2):022607, 2021.

- [155] Daniel Stilck França and Raul Garcia-Patron. Limitations of optimization algorithms on noisy quantum devices. *Nature Physics*, 17(11):1221–1227, 2021.
- [156] Dorit Aharonov, Xun Gao, Zeph Landau, Yunchao Liu, and Umesh Vazirani. A polynomial-time classical algorithm for noisy random circuit sampling. *arXiv preprint arXiv:2211.03999*, 2022.
- [157] Heng Fan, Vwani Roychowdhury, and Thomas Szkopek. Optimal two-qubit quantum circuits using exchange interactions. *Physical Review A*, 72(5):052323, 2005.
- [158] Maksim E Shirokov. Reversibility conditions for quantum channels and their applications. *Sbornik: Mathematics*, 204(8):1215, 2013.